THE ROLE OF PLATELET ACTIVATING FACTOR IN TUMOUR PROGRESSION AND NEURODEGENERATION

Steffany Ann Larwill Bennett

Thesis submitted to the Department of Biochemistry in partial fulfillment of the requirements for the degree Doctor of Philosophy

University of Ottawa
Ottawa, Ontario, Canada
January, 1995

ABSTRACT

Tumourigenesis is the result of *increased* cell number. Progressive neurodegenerative disorders are characterized by *decreased* cell number. These illnesses emphasize the life-threatening consequences of disrupting the delicate balance between cell growth, cell differentiation, and cell death. Exposure to chronic inflammation is a recognized risk factor for a variety of human cancers and progressive neurodegenerative diseases. This thesis represents an attempt to determine whether one endogenous proinflammatory agent, platelet activating factor (PAF), may participate in tumourigenesis and/or neurodegeneration. Data are presented to indicate that PAF is capable of inducing sustained alterations in both the rate of cell growth *and* the rate of cell death in non-inflammatory cells. This ability can be characterized as follows: (1) Brief stimulation (<1 hr) of rodent and human fibroblasts and epithelial cells cultured *in vitro* induced PAF receptor activation, PKC activity, phosphorylation of proteins on tyrosine residues, oxyradical production, and *de novo* gene expression of the proto-oncogene c-*fos* and the active cell death (ACD)-related gene clusterin. (2) Transient stimulation (1-6 hr) elicited long-term growth enhancement (60-80 days) characterized by increased focus formation, saturation density, autonomous cell growth, and AI growth in the absence of further ligand exposure. Cell proliferation was, apparently, mediated by increases in intracellular PAF concentrations triggering the synthesis and release of mitogenic factors. Growth enhancement was accompanied by induction of clusterin and urokinase plasminogen activator gene expression. (3) Prolonged exposure (72 hr) to PAF induced ACD when cells were cultured in the absence of excess growth factors. ACD was determined by changes in nuclear and cytoplasmic morphology and by DNA analysis. (4) The kinetics of these responses to PAF could be altered by introduction of an activated *ras* oncogene into cells. Transient exposure to PAF under suboptimal growth conditions was sufficient to elicit a defined period of cell loss in *ras*-transformed fibroblasts followed by growth enhancement in surviving cells. (5) Increased PAFR expression was associated with chronic neurodegenerative lesions and cell death *in vivo* using a kainic acid model of myoclonic epilepsy. In summary, PAF, was shown to be capable of disrupting the delicate balance between cell growth and cell death. In this manner, PAF may contribute to tumour progression and progressive neurodegenerative disorders.

DEDICATIONS

This thesis is dedicated to Clifford Larwill, Lulu Larwill, Shirley Larwill Bennett, Jim Bennett, and Stephen Fai. Six years is a long time - not necessarily in terms of an academic degree but certainly in terms of a family and in the dedication of that family to the support of one member. I cannot thank each of you enough for your support, your brilliance, your patience, and your heart-felt interest in my never-ending stream of consciousness. For my grandfather, who explained to me the meaning of strength. For my grandmother, who taught me about tomorrow's beauty. For my mother and father, in the name of everything that can't be said, especially love. You are my best friends and my most cherished parents. And for Stephen, because the only thing I can adequately say is that I love you more than ever before.

Six years ago I read an article on PAF that would change my way of thinking. It now seems curious that one single piece of writing could have this effect but it did just the same. I was lucky enough to share what I thought were full-fledged ideas with three very special people. These people actually supported my naive conviction and gently (and sometimes not-so gently) shaped my endeavours into science. I would like to humbly thank these friends who opened my eyes to a larger world. These people, in their own way, dedicated part of themselves to my welfare and it is with great appreciation that I acknowledge Dave Roberts, Bill Staines, and Chaim Birnboim. I owe a huge debt of gratitude to you. This is especially true of Chaim. Thanks immensely.

Finally, for trying to keep me from running headlong into a very large wall and for laughing with (and at) me continually, I would like to thank Cai-Ying Zhou, Jia-hua Chen, Diana Wilkinson, Randy Cowling, Amy Yamazaki, Mike DeVouge, Jaqdeep Sandhu, Paula Genik, Rick Pilon, Tina Raynor, Chantal Couture, and all of the members, past and present, of the Birnboim lab. Their humour, (their financial support of my artistic endeavours), and their willingness to participate in the ritual of the social drink goes way beyond the call of duty. Thanks guys.

Finally, and most importantly, this thesis and my life is dedicated to my God with love.

TABLE OF CONTENTS

I
ABBREVIATIONS

Terms are defined when they first appear in text. The following acronyms are used upon subsequent citation.

10x SSC	1.5M NaCl, 0.15M Na Citrate
6-TG	6-thioguanine
6-TGMP	6-thioguanine 5'monophosphate
AA	arachidonic acid
AAGPC	alkylacylglycerophosphocholine
ACD	active cell death
AI	anchorage independent
ALS	amyotrophic lateral sclerosis
AMP	adenosine 5' monophosphate
APP	amyloid precursor protein
APRL	antihypertensive polar renal lipid
BCIP	bromocholorindoyl phosphate
BSA	bovine serum albumin
CAM	cell adhesion molecule
CCS	1 mM Na Citrate, 1 mM CDTA, 0.1% SDS, pH 6.8
CDTA	trans-1,2,-diamine-cyclohexane-NNN'N',-tetraacetic acid
CNS	central nervous system
DAG	diacylglycerol
DMEM	Dulbecco's minimal essential medium
DMF	dimethylformamide
DMSO	dimethyl sulfoxide
DNA	deoxyribonucleic acid
ECM	extracellular matrix
EDTA	ethylenediamine tetraacetic acid
FCS	fetal calf serum
FGF	basic fibroblast growth factor
GAP	GTPase activating protein
GAPDH	glyceraldehyde-3-phosphate-dehydrogenase
GFAP	glial fibrillary acidic protein
GMP	guanosine 5'-monophosphate
GTP	guanosine 5'-trisphosphate
FLI	*fos*-like immunoreactivity
HAT	hypoxanthine + aminopterin + thymidine
HF	human fibroblast
HPRT	hypoxanthine-guanine phosphoribosyltransferase
HT	hypoxanthine + thymidine
ICAM	intracellular adhesion molecule (CD54)
IP	intraperitoneal
LFA	lymphocyte function associated antigen (CD18)
LTR	long terminal repeat
LPS	lipopolysaccaride
MAC	membrane attack complex
MAP	mitogen associated protein
MHC	major histocompatability complex
MoMuLV	Moloney murine leukemia virus
NBT	nitroblue tetrazolium
Neo	Tn (10) neomycin resistance gene
NO	nitric oxide
NO_2	nitric dioxide
O_2^-	superoxide anion
$OH^·$	hydroxyl radical
$ONOO^-$	peroxynitrite
PAF	platelet activating factor (1-*O*-alkyl-2-acetyl-*sn*-glycero-3-phosphocholine)
PAFR	platelet activating factor receptor
PAS	periodic acid Schiff
PAS-D	PAS-dimedone
PBS	phosphate buffered saline
PECAM	platelet endothelial cell adhesion molecule-1
PKC	protein kinase C
PIP	phosphoinositide
PLA	phospholipase A
PLC	phospholipase C
PNS	peripheral nervous system
PrP^{sc}	prion protein-scrapie
REC	rat embryo cell
RES	RNA extraction solution
RNA	ribonucleic acid
SDS	sodium doedcyl sulfate
SOD	superoxide dismutase
TGFβ	transforming growth factor β
TIS-1	12-*O*-tetradecanoyl-phorbol-13-acetate inducible sequence
TNFα	tumour necrosis factor α
TPA	12-*O*-tetradecanoyl-phorbol-13-acetate
UPA	urokinase plasminogen activator

II

INTRODUCTION

1. Preface

Cell number in multicellular organisms is determined by the rate of cell growth, cell differentiation, and cell death. The ability of an animal to sustain life depends upon a tight regulation of these processes and any prolonged alteration in the integrity of this balance can have devastating consequences. For example, cancers arise as a result of an anomalous *increase* in cell proliferation or, conversely, from an inappropriate *decrease* in the rate of cell death. Accelerations in either process can lead to the replacement of normal tissue with growth-deregulated cells (tumour formation). A benign tumour may then become malignant and metastasize if it acquires five distinct phenotypic characteristics: (1) the ability to degrade extracellular matrix (ECM) and invade neighbouring tissue, (2) the ability to enter and survive in the circulatory system, (3) the ability to exit the circulation and encroach upon foreign tissue, (4) the ability to sustain cell proliferation in an unfamiliar environment in order to successfully colonize secondary tumours, and (5) the ability to induce angiogenesis and sufficient vascularization of the growing tumour mass to ensure sustenance. This 'malignant transformation' is thought to require a series of successive genetic alterations within proliferating cells that promote the ability to survive within a hostile environment. However, an analogous process is perpetuated on almost a daily basis. Activated white blood cells, endothelial cells, and participating non-inflammatory cell types respond to physical insult by (1) increasing vascular supply to the site of injury, (2) sustaining cell proliferation to mediate wound closure, (3) permitting circulating phagocytes to exit the blood stream and extravasate through basal lamina and connective tissue, (4) inducing ECM degradation to facilitate the rapid chemotaxis of cells through intact tissue, and (5) ensuring the functional activation of phagocytes within the hostile environment of a wound or infection. Transient induction of the inflammatory response is a necessary component of wound healing. Sustained induction of the 'inflammatory phenotype' results in pathophysiological conditions such as rheumatoid arthritis, Crohn's disease, ulcerative colitis, and atrophic gastritis. Many of these disorders have been associated with an increased predisposition to the development of solid tumours suggesting that the role of proinflammatory agents in mediating cell proliferative disorders should be evaluated.

Tumourigenesis is the result of *increased* cell number. However, the inflammatory response is characterized not only by sustained cell proliferation but also by increases in the rate of cell death as irreparably damaged cells are targeted for phagocytosis and are replaced by healthy tissue. Similar dynamics are observed *in vivo* in established tumours. Increased cell proliferation is localized to the periphery of the tumour mass while protracted cell death is noted within the necrotic core. In malignant tumours, the rate of cell growth exceeds the rate of cell death permitting tumour cell expansion. Such alterations are only possible in tissues capable of compensating for a reduction in overall cell number. What effect, then, does chronic inflammation have on cells incapable of continued proliferation? Progressive neurodegenerative disorders are characterized by a sustained *reduction* in cell number due to the fact that terminally differentiated neurons, once generated, do not replicate. This fact renders the central nervous system (CNS) uniquely susceptible to cell ablation due to injury. Recent ground-breaking research has indicated that aberrant inflammatory responses may play a role in the pathogenesis of a wide variety of neurodegenerative disorders including Alzheimer's Disease, Downs Syndrome, Amyotrophic Lateral Sclerosis (ALS), Pick's Disease, Parkinson's Disease, Myoclonic Epilepsy, and prion-related disorders. These conditions are characterized by increases in phagocytic (glial) cell growth, neuronal cell death, and deposition of non-degradable elements in CNS parenchyma. The neurodegenerative lesions, specific to each disorder, trigger variable degrees of inflammatory reactions, increasing both local and often systemic concentrations of proinflammatory mediators. However, the role of inflammatory agents in mediating progressive neurodegenerative disorders has only begun to be systematically evaluated.

Do endogenous inflammatory agents participate in tumour progression and provoke progressive neurodegeneration? Certainly chronic inflammatory conditions have been associated with an increased predisposition both to the development and progression of cancer (clonal expansion of growth-deregulated cells) and to the exacerbation of progressive neurodegenerative disorders (accelerated cell dystrophy and dysfunction). This thesis represents an attempt to assess the contribution of one such endogenous proinflammatory mediator, platelet activating factor (PAF: 1-*O*-alkyl-2-acetyl-*sn*-glycero-3-phosphocholine), to tumourigenesis and neurodegeneration and to elucidate some of the mechanisms underlying PAF's putative effects.

2. The Inflammatory Response

This section provides a brief, descriptive overview of the inflammatory environment in order to define terms and place in context the hypothesis that PAF plays a role in exacerbating malignant transformation and neurodegeneration. The review is based on the following references (74,135,175,187,192,193).

Inflammatory and non-inflammatory cell types

If the body is wounded, a series of defensive reactions are initiated that, together, constitute inflammation. Two, arbitrarily defined, cell groups are involved: inflammatory and non-inflammatory cell types (Figure 1). The first group refers to those cells that actively migrate into a site of injury in order to contain toxic agents, promote angiogenesis, kill invading microbes, remove damaged tissue, and facilitate wound repair. These cells include platelets, lymphocytes, monocytes/macrophages, neutrophils, and endothelial cells. In the CNS, this list is further extended to include astrocytes and microglia - two cell types unique to the brain and spinal cord. The second group refers to non-inflammatory cells that, upon injury, release proinflammatory mediators in order to attract and activate inflammatory cells, elicit cell death in damaged or contaminated tissue, and induce cell proliferation in neighbouring cells. Needless to say, the division between inflammatory and non-inflammatory cells is somewhat arbitrary. All of the cell

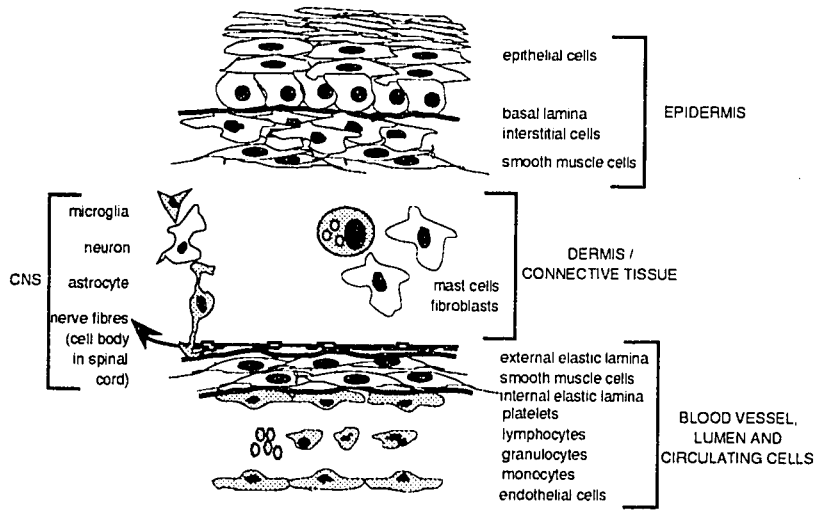

Figure 1. Inflammatory and non-inflammatory cell networks

Schematic section through vasculature, connective tissue and epidermis. CNS cells are included for comparison. Inflammatory cell types are indicated in grey.

types depicted in Figure 1 are capable of releasing cytokines, chemotactic agents, and other proinflammatory signalling molecules. Furthermore, to some extent, each cell type is capable of limited phagocytosis (with the possible exception of CNS neurons) facilitating the removal of damaged tissue from a site of injury. However, only inflammatory cell types migrate over long distances and across tissue barriers.

Inflammation

The inflammatory response consists of acute and chronic phases. Upon injury, irritation, or infection, non-inflammatory cells release a wide variety of proinflammatory agents that initiate the acute response. Acute inflammation is characterized by (1) vasodilation and enhanced vascular permeability, (2) *de novo* angiogenesis, and (3) infiltration of damaged tissue by activated platelets and polymorphonuclear leukocytes (Figure 2). This reaction is considered to be non-specific in that similar responses are generated by diverse sources of irritation or injury. The intensity of each

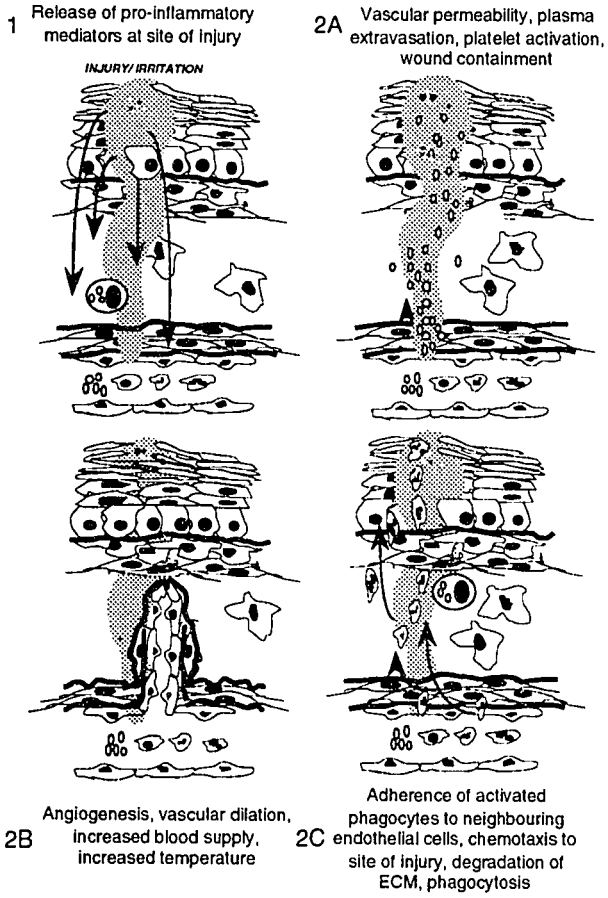

Figure 2. Acute inflammatory responses

Schematic section through the vasculature, connective tissue/dermis, and epidermis. Cell types are as in Figure 1. Upon injury, irritation, or infection, non-inflammatory cells release a myriad of proinflammatory agents that diffuse through neighbouring tissue establishing a concentration gradient of inflammatory activators (1). These agents induce a non-specific cascade of responses that include edema and platelet activation (2A), angiogenesis and vascular dilation (2B), and activation and infiltration of circulating phagocytes (2C). Such responses underly the four primary characteristics of acute inflammation - heat, redness, swelling and pain.

reaction is determined by the concentration gradient of proinflammatory agents present at the site of injury. High concentrations of inflammatory mediators (ie. in and around the core of the injury) promote inflammatory cell activation and generate feedback loops that maintain elevated cytokine production. Low concentrations of cytokines (ie. at the periphery of damaged tissue) and/or specific proinflammatory agents stimulate cells to produce inflammatory inhibitors. This response serves to localize the inflammatory response and regulate its duration.

Chronic inflammatory reactions are triggered by a decrease in the number of injured non-inflammatory cells as the result of successful phagocytosis. This response also depends upon the elaboration of immune molecules at the site of injury that stimulate specific, secondary inflammatory cell types (Figure 3). Production and accumulation of neutrophils diminishes and macrophages and lymphocytes emerge in larger numbers at the site of injury. Macrophages are specialized cells derived from circulating monocytes that, upon infiltration of connective tissue, undergo terminal differentiation and achieve functional specificity. This phenomenon also occurs in the CNS where antigenically distinct monocytes are permitted limited entry into the perivascular space before differentiating into phagocytic microglia. Both macrophages and microglia elaborate and process antigen targeting the release of lytic enzymes and directing the phagocytosis of dead leukocytes and cellular debris. These cells also produce agents that stimulate non-inflammatory cells to synthesize and release ECM components in order to stabilize the surrounding matrix and generate scar tissue.

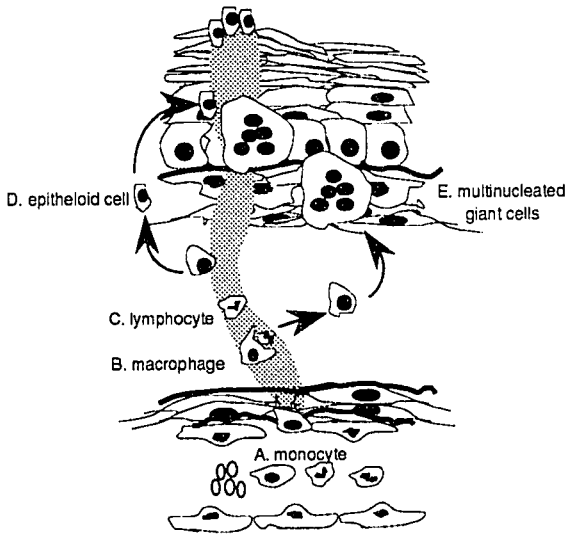

Figure 3. Chronic inflammatory responses

Schematic section through the vasculature, connective tissue/dermis, and epidermis in and around damaged tissue. Unlabelled cell types are as in Figure 1. Acute inflammation progresses to chronic inflammation with the activation of macrophages (B) and lymphocytes (C). Both of these cells elaborate and process antigen that direct the cells to perform specific functions (ie. targeted cell lysis and phagocytosis). Macrophages (B) are derived from circulating monocytes (A) that differentiate upon migration into damaged tissue. These cells are also capable of further transformation into epitheloid cells (D) and fusion into multinucleated giant cells (E). These latter cell types contribute to wound containment, matrix stabilization, and generation of scar tissue.

Immune modulation of the inflammatory response.

One additional consideration important to the discussion of PAF and cell regulative disorders affecting cell number is the role of complement in promoting inflammation. Complement is a general term denoting an entire series of immunological serum (and cerebral) proteins that undergo a cascade of proteolytic reactions when activated by antibody-antigen complexes or microorganisms. Different products of these reactions enhance the response of phagocytic cells to injury, facilitate blood vessel dilation and plasma extravasation, and form membrane attack complexes (MACs) that bind to and permeabilize invading microorganisms. In this fashion, complement serves as both a recognition and an effecter system of humoral immunity determining 'self' from 'non-self' and amplifying the actions of both antibody and proinflammatory agents.

Complement consists of approximately 30 interacting proteins synthesized and released predominantly by the liver and, to a lesser extent, by the brain. Liver-derived components are released systemically; brain-derived products are retained locally. Two mechanisms are available for activation of the complement cascade - the classical and alternative pathways (Figure 4). Functional components, designated C1-C9, factor B, and factor D, regulate assembly of MACs. Regulatory factors control the specificity of the complement response by inactivating reactive fragments that bind to autologous tissue ('self') and by enhancing the attachment of these same proteins to invading organisms ('non-self'). These latter agents will be discussed in more detail in Chapter II, Section 4 with respect to the cerebral complement cascade. In addition to the formation of MAC, complement C3a, C3b, and C5a also directly modulate the inflammatory response. C3b binds to specific receptor proteins on macrophages and neutrophils thereby promoting the interaction between inflammatory cell and microorganism and facilitating phagocytosis. C3a and C5a increase smooth muscle contraction and stimulate mast cell and basophil secretion of histamine through induction of intermediate signalling molecule, PAF (74,23). Both PAF and histamine induce vasculature permeability contributing to the extravasation of plasma and circulating cells into the site of injury. In addition, PAF, synthesized in response to complement activation, plays a pivotal role in modulating the response of both inflammatory and non-inflammatory cells during each phase of inflammation (Chapter II, Section 5).

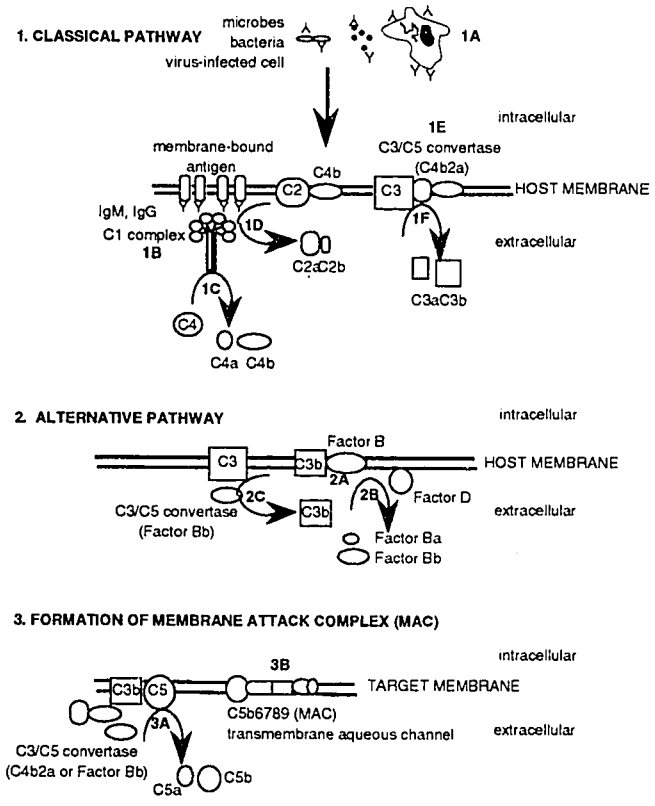

Figure 4. Complement activation: classical and alternative pathways

The *classical pathway* is activated by IgG or IgM antibodies associated with antigens on the surface of an invading microorganism or on an infected antigen-presenting host cell (1A). Circulating C1 complex binds to the constant region of these antibodies (1B). Binding activates C1's proteolytic capabilities enabling the complex to cleave C4 into two smaller fragments, C4a and C4b (1C). C4b binds covalently to the cell membrane and interacts with C2. Once bound, C2 can also be cleaved by active C1 complex (1D). The larger product of this reaction, C2a, remains bound to C4b forming the C4b2a complex or the classical pathway's C3/C5 convertase which can be retained or released locally. C3/C5 convertase cleaves C3, forming C3a and C3b (1E). C3b is released and rapidly binds to neighbouring cell membranes. Regulatory complement proteins (not shown) immediately inactivate the C3b bound to host tissue. Invading organisms lack these proteins and are unable to degrade C3b complement. C3b binds circulating C5. Once bound, C5 is cleaved by C3/C5 convertase into C5a and C5b (3A). C5b combines with C6 to initiate assembly of the membrane attack complex (C5b6789) (3B). MACs are transmembrane pores that permeabilize target membranes and destroy the organism or cell to which it is bound. In the *alternative pathway*, polysaccharides in the cell envelopes of invading microorganisms attenuate the inactivation of spontaneously produced C3b. This active membrane-bound C3b interacts with circulating factor B (2A). Once bound, factor B is cleaved by factor D (which is constitutively active in blood) into factor Ba and factor Bb (2B). Factor Bb is a C3/C5 convertase capable of generating further C3b (2C) and activating C5 (3A) leading to the assembly of MAC (3B).

3. Cancer and Inflammation

How does the inflammatory response relate to tumour progression? As indicated in Table 1, chronic infection, injury, and inflammation are recognized risk factors for a variety of human cancers. It is postulated that agents generated in chronically inflamed tissue promote the malignant conversion of cells through stimulation of prolonged cell replication and/or induction of deoxyribonucleic acid (DNA) damage. Most of the proinflammatory agents implicated in tumourigenesis are believed to exert both a physiological and pathophysiological effect depending upon the circumstances of exposure. At low concentrations or with limited exposure, they act as

Table 1. Increase in cancer incidence in patients with chronic inflammatory conditions[a]

	Inflammatory Disorder	Characteristics	Associated cancer site	Implicated inflammatory mediators	Mechanism of action
1.	Parasitic infection	Schistosomiasis *Opisthorchis viverrini* *Clonorchis sinensis* Malaria	bladder liver colorectal	nitrosamines oxyradicals	Chromosomal abnormalities DNA damage ↑ cell proliferation
2.	Bacterial infection	H*elicobacter pylori* Urinary infection Tuberculosis	stomach bladder lung	oxyradicals	Chromosomal abnormalities DNA damage ↑ cell proliferation
3.	Viral infection	Hepatitis Human papilloma Herpes simplex type 2 Cytomegalovirus	liver cervix	nitrosamines oxyradicals	DNA damage
4.	Ulcerative colitis	Diffuse inflammation of mucous membranes	colorectal	oxyradicals	DNA damage ↑ cell proliferation
5.	Crohn's disease	Nonspecific inflammation of the ileum with granuloma	colorectal	PAF oxyradicals	DNA damage ↑ cell proliferation
6.	Atrophic gastritis	Inflammation of the stomach with atrophy of mucosa and glands	stomach	oxyradicals	DNA damage ↑ cell proliferation
8.	Chronic exposure to particulates (ie. asbestos, silica dust)	Irritation and inflammation of exposed tissue	lung	oxyradicals nitrosamines	Chromosomal abnormalities DNA damage ↑ cell proliferation
9.	Chronic injury (ie. burns, heat, smoking)	Repeated abrasion Recurrent cystitis Chronic skin ulcers	skin throat lung bladder	oxyradicals	Chromosomal abnormalities DNA damage ↑ cell proliferation

[a] Summary is based on the following references (4,11,15,49,51,57,69,94,175,185,191,192,205,210).

essential signalling molecules facilitating wound healing and containment of harmful irritants. At high concentrations or with extended exposure they can stimulate prolonged cell replication within a potentially harmful environment and/or act as endogenous mutagens.

Chronic inflammatory disorders associated with cancers

A large number of chronic inflammatory disorders are also associated with tumour progression (Table 1). These conditions are characterized by repeated exposure to proinflammatory agents synthesized and released by invading macrophages, leukocytes, lymphocytes, capillary endothelial cells, basal epithelial cells, and stromal fibroblasts located both within and around the site of chronic irritation. Under normal circumstances, inflammation is transient, progressing through acute and chronic phases before dissipating. Successful resolution of the response is signalled by the attenuation of proinflammatory mediator (and inhibitor) release, the cessation of inflammatory cell movement into recovering tissue, and the regression of the superfluous blood vessels. The end of the response occurs when the entire complex of activated inflammatory and proliferating non-inflammatory cells, their blood supply, and the secreted glycoproteins and proteoglycans that comprise inflamed (granulation) tissue is replaced by collagenous scar tissue. However, under pathological circumstances, the stimulus responsible for activating the inflammatory response fails to be eradicated from granulation tissue and the entire cycle is perpetuated and/or exacerbated. For example, in the case of parasitic infections such as schistosomiasis, larvae (cercariae or metacercariae), capable of penetrating both the skin and digestive track of a human host, migrate through blood capillaries to the liver and colon. Upon maturation, male and female worms mate and travel together through the blood system to the bladder where the female sheds her eggs in the epithelial cell lining of the bladder. The eggs can either penetrate the mucosa to be released in the urine or become trapped in the bladder lining. At each point of contact, the parasitic infiltration incites an inflammatory reaction. If the larvae are not completely obliterated, the cycle is perpetuated (94,175,192). It is this prolonged non-productive response that is associated with increased risk of tumour development (94,175,192). Similar cycles appear to be incited by sustained irritation with particulate matter, bacterial contamination, viral infection, persistent injury, or during idiopathic inflammatory disorders such as ulcerative

colitis, Crohn's disease, and atrophic gastritis (Table 1).

Proinflammatory agents and cell proliferation

The mechanisms by which chronic inflammation may contribute to cancer are unclear. Tumourigenesis requires the clonal expansion of a single cell with one or more genetic abnormalities. Within the inflammatory environment, proinflammatory agents stimulate cell growth in order to facilitate wound healing, angiogenesis, and white blood cell activation and induce DNA damage in order to destroy invading organisms and infected host cells. Sustained augmentation of cell proliferation within the inflammatory environment may contribute to tumour progression in four ways: (1) Clonal expansion is a fundamental requirement for tumourigenesis; (2) Prolonged cell division increases the likelihood of mutagenic events occurring by repeatedly altering the structural configuration of nucleic acids rendering DNA more susceptible to interaction with carcinogens; (3) Accelerated cell doubling rates reduce the amount of time cells spend in growth arrest and, consequently, increase the probability of errors in DNA repair prior to mitosis; (4) Many genetic alterations depend upon cell division and cannot occur in quiescent cells (ie. chromosome loss, duplication, and translocation. *In vitro* evidence supports the hypothesis that enhanced cell proliferation induced by proinflammatory agents such as oxyradicals, interleukins, and PAF mediates tumour progression. Heritable morphological alterations, decreases in cell doubling time, induction of anchorage independent (AI) growth, increases in autonomous cell growth (growth in low serum containing medium), and *in vivo* tumourgenicity of cells transformed *in vitro* have been elicited in normal epithelial cells and fibroblasts by co-culture with 12-*O*-tetradecanoyl-phorbol-13-acetate (TPA)-activated phagocytes or by exposure to oxyradicals generated by xanthine and xanthine oxidase (175,234,244). In addition to exogenous exposure, many tumour lines demonstrate constitutive autocrine production of inflammatory mediators when cultured *in vitro*. Autocrine PAF stimulation has been shown to be responsible for the sustained cell proliferation observed in HEC-1A adenocarcinoma cells (143). Cooperation between inflammatory cytokines and oncogenes has also been observed to increase cell growth. For example, transfection of *ras*-transformed pre-B cells with an activated interleukin-6 construct enhances clonal expansion and yields highly tumourigenic lymphoid cell lines (47).

As indicated by the effect of PAF on HEC-1A cells, some tumour lines may actually depend upon proinflammatory agents to sustain their own malignant growth. In fact, these effects are often counter-intuitive. For example, transforming growth factor β (TGFβ) is an inflammatory agent characterized in normal cells to act as a negative growth regulator. Surprisingly, TGFβ potentiates *in vitro* cell growth in a variety of transformed lines while eliciting growth arrest in normal parental cells (108). In another example, the inflammatory cytokine tumour necrosis factor α (TNFα) induces cell death in non-inflammatory cells. Although increases in the p55 and p75 TNF receptors have been demonstrated in a number of tumour lines, stimulation with the TNFα ligand elicits proliferation rather than cytotoxicity (73,154). Such phenotypic changes presumably depend upon genetic mutations in key signal transduction molecules regulating the normal cell responses to inflammatory ligands. One such molecule is the human CL100 gene product and its mouse homolog JCH134. Expression of CL100 is significantly increased in fibroblasts cultured in the presence of either oxyradicals or cytokines. The CL100 protein is a dual-specificity serine/threonine/tyrosine phosphatase that dephosphorylates mitogen-associated protein (MAP) kinase thus limiting the duration of the kinase-mediated proliferative signal. Overexpression of CL100 has even been shown to suppress the continual activation of MAP kinase elicited by oncogenic Ha-*ras* subsequently reducing the clonal expansion of *ras*-transformed cells. Mutation of the cysteine residue within the phosphatase's active site restores the ability of activated *ras* to induce autonomous cell growth. In normal cells, overexpression of the CL100 mutant results in enhanced cell proliferation when cultures are stimulated with sub-threshold concentrations of endogenous growth factors (3). Analogous mutations in other regulatory genes may be responsible for the sustained tumour cell growth observed upon exposure to proinflammatory agents.

Proinflammatory agents and mutagenesis

It has also been hypothesized that chronic inflammation might predispose a cell to genetic damage *in vivo* given that many proinflammatory agents have been shown to be mutagenic *in vitro*. For example, nitric oxide (NO) is a highly reactive endogenous gas that acts as a cell

signalling molecule in a variety of tissues by activating guanylate cyclase (167,175). Its reactive products, peroxynitrite ($ONOO^-$), hydroxyl radicals ($OH^\cdot$), nitric dioxide (NO_2), singlet oxygen, and nitrosamines, are highly mutagenic, capable of inducing chromosomal aberrations, DNA breaks, deamination, and base-pair mutations (27,168,175,192). Furthermore, exposure of non-inflammatory cells to TPA-activated neutrophils results in chromosomal abnormalities on chromosome 11 (a chromosome commonly altered in bladder cancer) and oxidative damage to DNA bases (formation of thymine glycol, 5-hydroxymethyl uracil, 8-hydroxy-2'-deoxyguanosine) (42,72,161,175,200). The mechanisms underlying this damage are, as yet, unclear. DNA damage may be induced during the respiratory burst by hydrogen peroxide (H_2O_2). H_2O_2 moves through target cell and nuclear membranes to interact with DNA and is believed to form $OH^\cdot$ in a metal catalyzed Haber-Weiss reaction that appears to result in DNA base oxidation and strand breaks (72). Other clastogenic inflammatory compounds include arachidonic acid (AA) metabolites and oxidative products of structural cell membrane lipids. AA is released during an inflammatory response as the result of phospholipase A_2 and phospholipase C lipid membrane remodelling and is metabolized by either the cyclooxygenase pathway to prostaglandins and thromboxanes or the lipooxygenase pathway to eicosanoids and leukotrienes. Several intermediates of this latter pathway, including hydroxy- and hydroperoxy-eicosatetraneonic acids, have been shown to elicit DNA strand breal and double-minute chromosomes *in vitro* (174). Oxidation of cell membrane unsaturated fatty acids generates lipid hydroperoxides and their breakdown products, aldehydes and epoxides. These latter agents can cause DNA base mutations and cross linking *in vitro* (83). Finally, leukocytes themselves may inadvertently synthesize DNA-damaging agents. Activated phagocytes have been shown to be uniquely capable of metabolizing a variety of exogenous procarcinogens into genotoxic agents (111,175).

Proinflammatory agents and tumour invasion

A possible role for proinflammatory agents in malignant transformation can be further inferred from studies of tumour cell lines and characterization of tumour biopsies. Many phenotypic features exhibited by cells during an inflammatory response are recapitulated by

transformed cells during the metastatic process. For example, elevated levels of PAF, TNFα, the p55 and p75 TNF receptors, intracellular adhesion molecule (ICAM)-1, -2, and -3, platelet endothelial cell adhesion molecule (PECAM)-1, and lymphocyte function associated antigen (LFA)-1 have been demonstrated in the colon carcinoma lines HT-29, DLD-1, and CaCo-2 (52,60,70,138), in the adenocarcinoma line HEC-1A (16,143), and in primary colon carcinomas (60), prostatic carcinomas (78), nasopharygeneal carcinomas (78), leukemias (78), melanomas (120,230), lymphomas (63), associated metastatic lesions (78,120) and in colonic mucosa cells of patients suffering from ulcerative colitis and Crohn's disease (57,69,190,210). With respect to the cell adhesion molecules (CAMs), expression of these glycoproteins on non-inflammatory cells represents a gain of function not normally observed in non-inflamed tissue. CAMs mediate contact between vascular endothelial cells and activated inflammatory cells by acting as receptors for the cell surface ligands expressed on inflammatory cells. The ICAMs, for example, interact with their ligand, LFA-1. Stimulation of receptor with ligand facilitates the adherence of circulating phagocytes to those vascular endothelial cells in closest proximity to granulation tissue, mediates chemotaxis, and elicits the production of additional proinflammatory agents (29,112). Under normal circumstances, these molecules are predominantly expressed on hematopoietic and endothelial cells. However, as indicated above, many tumour cells are also capable of CAM expression. This gain of function in transformed cells could, conceivably, facilitate tumour cell interaction, promote chemotaxis of inflammatory cells to tumour sites, and assist in the migration of transformed cells into and out of the circulatory system during metastasis. In fact, *in vitro* evidence indicates that the inflammatory reactions elicited in host tissue in response to invading tumour cells would acutally facilitate rather than impede this process. Exposure to proinflammatory cytokines elicits additional increases in the already elevated expression levels of CAMs in a variety of tumour lines cultured *in vitro* emphasizing, once again, the self-perpetuating feedback loop that appears to regulate both inflammation and tumour progression (6,52,60,136).

Proinflammatory agents also promote the synthesis and release of degradative enzymes. The net effect of this action is to facilitate the invasion of activated phagocytes and, by analogy, transformed cells through basement membrane. TNFα, for example, mediates release of

plasminogen activators (208,235) while PAF induces collagenase expression (20) in epithelial cells suggesting that the role of proinflammatory agents in tumour progression is not only confined to growth deregulation but also encompasses other features of the metastatic process.

Overview

This brief review suggests a variety of mechanisms by which inflammatory agents may influence the development of human cancers. Figure 5 depicts a basic schematic. Activated inflammatory cells migrate to areas of injury or irritation in response to proinflammatory chemotactic agents released from cells in and around the damaged tissue (Figure 5A). This process requires that inflammatory cells exit the circulation at an appropriate site proximal to the injured tissue (via interaction between CAMs), cross the endothelial cell lining and basal lamina of the blood vessel, extravasate and survive in a new environment, burrow through foreign tissues to reach the injured site (via induction of degradative enzymes), mount an inflammatory response, and promote neighbouring cell proliferation in an attempt to replace irreversibly damaged cells within the injured tissue. It is of note that, in many respects, these activities are reminiscent of the metastatic process. To disseminate throughout the body, solid tumour cells must degrade surrounding tissue and extravasate through the underlying stroma until they reach a blood or lymphatic vessel (Figure 5B). At this point, transformed cells must cross the basal lamina and endothelial lining of vasculature, enter and survive the circulatory environment, exit the vessel at an appropriate location, and proliferate in a new environment in the absence of familiar growth factors. Coincidentally, these same transformed cells are presumed to face repeated stimulation with proinflammatory mediators synthesized and released by surrounding cells as part of an inflammatory reaction to the tumour cell invasion. It is suggested that exposure to the inflammatory environment may influence cell proliferative rates and/or play a role in the multi-step process of genetic alterations characteristic of tumour progression. Putative mechanisms by which these agents could mediate *de novo* tumourigenesis and facilitate tumour cell growth *in vivo* based on *in vitro* evidence are summarized in Figure 5C.

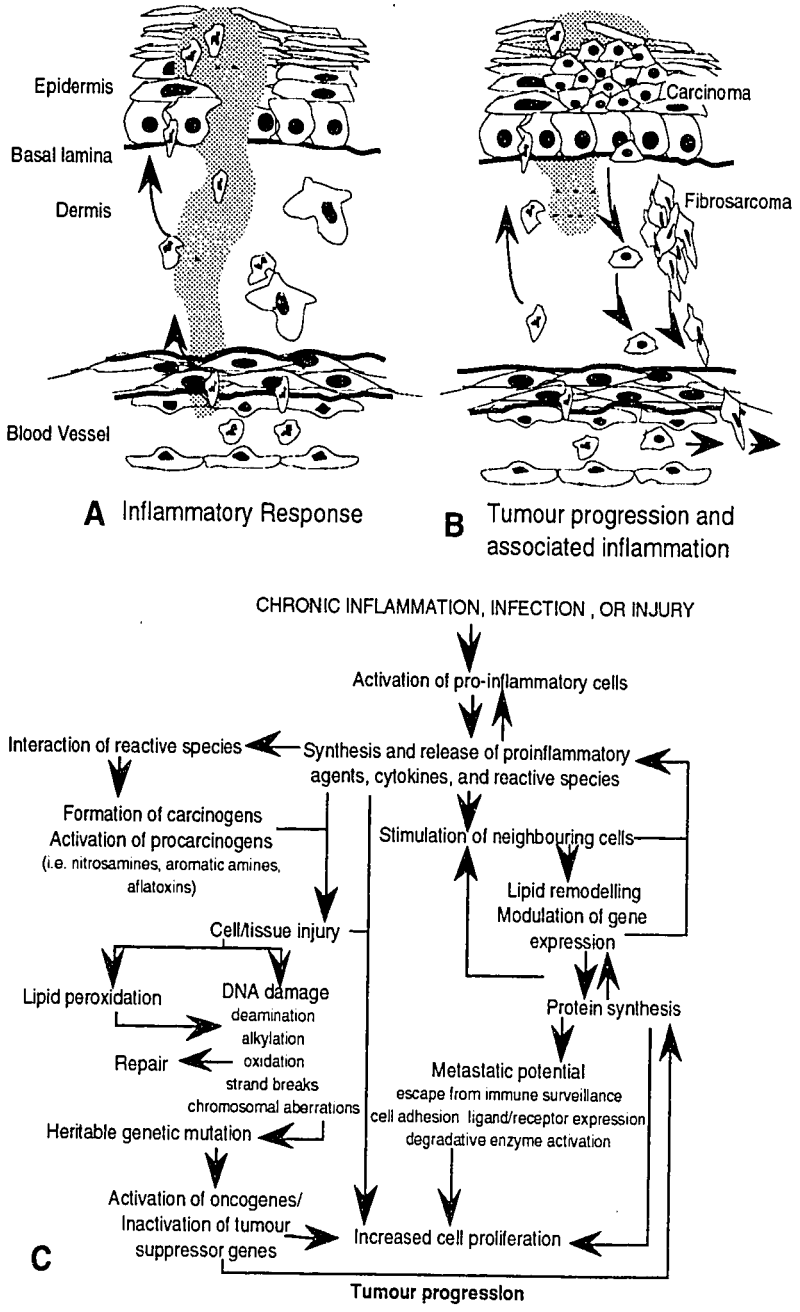

Figure 5. Hypothetical role of chronic inflammation in tumourigenesis and tumour progression

Schematic section through a blood vessel, dermis, and epidermis. Cell types as in Figure 1. (A) The inflammatory response elicits migration of activated phagocytes out of the circulation, chemotaxis of inflammatory cells through connective tissue, degradation of the surrounding ECM, and enhanced cell proliferation of both activated inflammatory and neighbouring non-inflammatory cells. (B) Irritation of resident fibroblasts and epithelial cells by expanding dysplastic cells induces chronic inflammation associated with tumour progression. (C) Possible biochemical mechanisms by which proinflammatory agents may mediate *de novo* tumourigenesis and/or facilitate tumour progression.

4. Neurodegeneration and Inflammation

Cell regulative disorders affecting cell number encompass not only growth deregulation but also uncontrolled cell ablation. The consequences of these disruptions are nowhere so evident as in the CNS. Most progressive neurodegenerative disorders are defined by substantial increases in both the rate of glial cell growth and the rate of neuronal cell death. In the conditions listed in Table 2, pathological alterations in cell number are invariably accompanied by the accumulation of non-degradable proteinaceous and carbohydrate-containing lesions and, as such, are the site of chronic inflammation (Table 2). The source of this inflammation has been hotly debated. Traditionally, the CNS was considered to be immunologically privileged, isolated from peripheral inflammatory cell involvement by the blood-brain barrier. Cerebral inflammation associated with

Table 2. Inflammatory mechanisms implicated in progressive neurodegenerative disorders[a]

	Syndrome	Characteristic Abnormalities	Common Pathologies	Increased Cell Number	Inflammatory Mediator Increase
1.	Alzheimer's Disease Senile dementia of the Alzheimer's type	Senile plaques Neurofibrillary tangles Cereb. amyloid angiopathy	Neuronal loss Gliosis Periodic Acid Schiff (PAS)$^+$ deposits	microglia astrocytes	complement acute phase proteins macrophage col. stim. factor
2.	Down Syndrome	Trisomy 21		microglia astrocytes	
3.	Pick's Disease	Pick bodies + cells		astrocytes	complement acute phase proteins
4.	Diffuse Lewy Body Disease	Cortical Lewy bodies		microglia astrocytes	
5.	Creutzveldt-Jacob Gerstmann-Straussler-Scheinker Syndromes	Prion protein (Prp^{sc}) Spongiform encephalopathy Diffuse amyloidosis		astrocytes microglia	complement acute phase proteins leuk. common antigen
6.	Parkinson's Disease	Nigral Cell Loss Lewy bodies		microglia astrocytes	acute phase proteins TNFα
7.	Amyotrophic Lateral Sclerosis	Motor neuron degeneration		macrophages microglia	macrophage col. stim. factor
8.	Hereditary Cerebral Hemorrhage with Amyloidosis	Cerebral amyloid angiopathy Diffuse plaques		microglia	acute phase proteins
9.	Myoclonic Epilepsy	Sustained neuronal depolarization Diffuse amyloidosis			

[a]Summary is based on the following references (2,65,110,121,122,129,141,158,236).

neurodegeneration was attributed to a loss in blood-brain barrier integrity resulting in extravasation of circulating immune cells and proinflamamtory agents into CNS parenchyma. The presence of these markers in diseased brain was considered to be a non-specific later-stage development of diverse disorders without relevance to early disease etiology. However, the recent development of specific antibodies to subsets of lymphocytes and macrophages/monocytes, major histocompatability (MHC) antigens, complement, and acute phase proteins has permitted a reevaluation of this principle. Remarkably, the brain has been shown to be capable of mounting its own immunological and inflammatory defences in response to injury, synthesizing endogenous proinflammatory and immune agents (including PAF), and activating distinct CNS inflammatory cell types. Although these reactions can occur transiently without recourse to peripheral cell involvement or blood-brain barrier breakdown, such pathologies often accompany chronic cerebral inflammation.

What role do proinflammatory agents play in mediating chronic neurodegeneration? The relative importance of cerebral inflammation is open to speculation. Due to the fact that investigations of diseased human brain are necessarily descriptive in nature, it is unclear whether induction of inflammatory response molecules in the CNS precedes the formation of neurodegenerative lesions and, in fact, contributes to their development and/or whether exposure to the non-degradable elements of these lesions (ie. β amyloid, periodic acid Schiff $(PAS)^+$ deposits, aberrant prion protein (PrP^{sc})) induces chronic inflammation and exacerbates the preexisting disorder. Both hypotheses are supported by recent data.

Inflammatory and non-inflammatory cell types in CNS

Two distinct types of cells are found in the CNS, glia and neurons, corresponding to the inflammatory and non-inflammatory cells of the peripheral nervous system (PNS). However, unlike the PNS cell types, glial cells are the *only* CNS cell type capable of continued proliferation and, consequently, are susceptible to the same sorts of genetic disorders and inflammatory influences reviewed in Chapter II, Section 3 with reference to gliomas. Neurons, however, are unique. Mature cells do not divide. Adult neurons are terminally differentiated lacking a stem cell

population or even a committed progenitor precursor capable of additional cell growth. Immature neurons do retain a limited capacity for cell division and pathological alterations in proliferative potential can result in childhood neuroblastomas. Mature cells, however, have yet to be shown to 'de-differentiate' in order to undergo cell replication. Consequently, there are no adult 'neuromas.' Neurons can, however, be induced to die. This distinctive phenotype renders the CNS uniquely susceptible to increases in the rate of neuronal cell death.

Two types of glia, astrocytes and microglia, respond to CNS injury. Astrocytes are analogous to PNS leukocytes. They react to immediate injury by sustained proliferation (gliosis) and enhanced phagocytosis in order to contain contaminated tissue and scavenge toxic substances. This ability extends not only to foreign pathogens but also to endogenous signalling molecules. In this capacity, astrocytes are capable of limiting excitotoxicity during ischemia/reperfusion injury and epileptic seizures through activation of glutamate uptake sites and enhanced glutamate metabolism (156,182). However, prolonged activation as the result of chronic cerebral inflammation may impede this ability. For example, exposure to reactive oxygen species inhibits glutamate uptake *in vitro* in astrocytic cultures and potentiates excitotoxicity (182). In addition to their role as phagocytes, specialized subsets of astrocytes maintain contact with the ependymal cells surrounding the blood-brain and blood-CSF barrier endothelium thus monitoring the integrity of the protective endothelial cell shell and facilitating immediate activation in the event of injury (115). This contact also mediates more routine tasks such as shuttling nutrients through brain parenchyma and expelling waste into the circulation.

Microglia are the more specialized glial cell responding only to chronic injury (77). Microglia are analogous to pluripotent macrophages of the PNS in that they are the only other cell type capable of expressing both classes of MHC antigens (5,77,121). Very little is known about the nature of microglial subtypes except that two distinct morphologies - ramified and ameboid - have been identified and two different progenitor populations - stem cells resident in the ependymal lining of CNS vasculature and 'brain-derived macrophages' located in the perivascular space - have been characterized (5,77,224). These latter cells are distinct from other CNS cell types in that they are derived from antigenically specific monocytes that migrate into neural tissue during fetal development and remain in the perivascular space (53,144). Once formation of the

blood-brain barrier is complete, these PNS monocytes differentiate into 'brain-derived macrophages' and lie quiescent until activated by inflammatory mediators. During viral infections, activated 'brain-derived macrophages' differentiate yet again into reactive ramified microglia and, like their PNS counterparts, can fuse into giant multinucleated cells to provide structural support to badly compromised tissue (see Chapter II, Section 2 and refs. (53,224)). It is not known whether the different types of microglial precursors confer distinctive characteristics upon differentiated daughter cells although it is quite plausible that, like PNS macrophages and lymphocytes, particular subtypes of microglia are specified for different immunoregulatory functions (121). For example, some microglia act as the brain's antigen-presenting cells in analogous fashion to B-lymphocytes, proteolytically altering foreign material to ensure binding of the resulting peptide fragment to the MHC class II molecules (77). Whether these cells express the same repertoire of antigen-presenting molecules required for the processing and presentation of MHC antigen as their PNS counterparts is not yet known. Certainly, activated microglia express a wide variety of inflammatory cell markers such as LFA-1, leukocyte common antigen, macrophage colony stimulating factor receptor, Fc receptor, and type 3 complement receptor, indicating that, as a group, they assume many of the same functions as specialized PNS inflammatory cell types (2,5,121,224,228).

Chronic inflammatory processes and neurodegenerative lesions

The differences in CNS cell proliferative abilities underline the severe limitations placed on the brain's ability to compensate for anomalous increases (or decreases) in cell growth and cell death. In fact, the terminally differentiated state of adult neurons renders the CNS uniquely susceptible to disorders of cell ablation. While cell death is a necessary and natural process in the developing CNS (contributing to the formation and organization of the spinal cord, sympathetic ganglia, retina, and corpus callosum (207)), any sustained disruption in the homeostatic regulation of healthy neurons leading to their premature demise results in irreversible pathology. Accelerated neuronal death has been shown to be mediated, *in vitro*, by proinflammatory agents released by activated glia. These agents can have opposite effects in neurons and glia. For example, conditioned medium from activated microglia stimulates astrocytic proliferation while inducing

neuronal death. These effects are the result of enhanced interleukin-1 and glutamate synthesis respectively (81,179). Since microglia are activated only during the chronic phase of the inflammatory response *in vivo*, increases in the rate of astrocytic division presumably serves to limit the extent of neuronal death by scavenging the excess glutamate released by microglia. However, as indicated above, this activity can become impaired after prolonged exposure to oxyradicals (ie. during chronic inflammatory conditions). Increased levels of reactive oxygen species have been localized in the CNS to areas exhibiting the greatest numbers of neurodegenerative lesions (50,121). Furthermore, exposure to oxyradicals has been shown *in vitro* to recruit additional cell types into the production of plaque precursor molecules. For example, TPA has been shown to stimulate β-amyloid precursor protein (APP) expression in endothelial cell culture by activation of the TPA responsive element in the APP promoter (121). Oxyradicals can also permanently damage terminally differentiated neurons (50,123). Increased expression of NO synthase by both neurons and glia in response to LPS and cytokines has been associated with enhanced cytotoxicity (170).

Inflammation is common to most (if not all) progressive neurodegenerative disorders. Proinflammatory agents are produced predominantly by activated glia although neurons have been shown to be capable of limited synthesis following injury or upon specific stimulation (for a review see (121). As indicated above, inflammatory responses appear to be confined to neurodegenerative plaques in degenerating brain. For example, increases in the numbers of proliferating microglia in Alzheimer's Disease, Down Syndrome, Parkinson's Disease, and Huntington's Disease are limited to the immediate vicinity of β-amyloid containing lesions and extracellular neurofibrillary tangles and not throughout injured tissue (39,121,198). The degree of cellular activation depends upon the conformation of the deposit. Diffuse amyloid plaques, such as those found in the cerebellum of Alzheimer's patients and within the cerebrum of patients suffering from prion-related disorders, are infiltrated by fewer microglial processes than concerted β-amyloid deposits (141,195). Furthermore, the increased concentrations of such inflammatory mediators as interleukin-1, S-100 protein, and glial fibrillary acidic protein (GFAP) observed in the cerebrum of patients with Alzheimer's Disease can be attributed to upregulation of both mRNA

surrounding neurodegenerative lesions (14,86,121,151,229). While these observations provide evidence for the existence of numerous chronic inflammatory responses within diseased brain, it is difficult to determine whether a prolonged inflammatory reaction (1) contributes to the etiology of the initial lesion, (2) results from chronic irritation elicited by pathological CNS deposits, and/or (3) plays a dual role in both the pathogenesis and progression of neurodegenerative plaques and tangles.

Certainly, glial cell activation is elicited by plaque components. For example, astrocytes have been shown, both *in vitro* and *in vivo*, to synthesize TNFα, interleukin-1, and basic fibroblast growth factor (FGF) upon exposure to lipopolysaccharide (LPS) or β-amyloid (105,106,121). However, glia are also capable of producing APP and processing the precursor into aberrant β-amyloid (37,121,194,201). Again, these abilities are mediated by agents released within the inflammatory environment. For example, interleukin-1 and FGF have been reported to induce APP expression in glial cell culture (121,201). This effect is achieved through protein kinase C (PKC) activation resulting in AP-1 complex formation and interaction with the AP-1 binding site on the APP promoter (121). At high concentrations, APP has been shown to be proteolytically altered by activated microglia into β-amyloid (194). Microglia are also capable of synthesizing *in vitro* many of the glycoproteins found *in vivo* at the core of amyloid-containing plaques (198). It is not difficult to envisage how these feedback loops could exacerbate chronic neuropathology. As indicated above, FGF stimulates APP expression while proteolytically altered β-amyloid stimulates FGF production in astrocytes (121). In a more involved feedback loop, proinflammatory agents exert both positive and negative effects on neurodegenerative lesions. Interleukin-1 and TNFα have been shown to promote the production of interleukin-6 as well as to increase interleukin-6 receptor levels in both neurons and glia *in vitro* (121). This mechanism may explain the increased cytokine expression observed *in vivo* around senile plaques (10,121). Since interleukin-6 mediates hepatic synthesis of a repertoire of acute phase proteins including α2macroglobulin, it probably exerts similar effects in the cerebrum thus compounding the regional inflammatory response (198). In support of this hypothesis, increases in α2macroglobulin receptor have been demonstrated throughout neurodegenerative plaques *in vivo* (217). The

α2macroglobulin receptor also regognizes the complement regulatory protein, clusterin, as a ligand. Clusterin mediates immune differentiation of 'self' from 'non-self' by binding to autologous tissue and preventing complement mediated lysis (See Chapter II, Section 2 and ref. 30). Clusterin mRNA expression and protein are selectively up-regulated in both experimental lesions and neurodegenerative plaques and can be induced *in vitro* in astrocytic cultures by TGFβ, interleukin-1,and/or TNFα treatment (131b,118,148,153). In neurodegenerative plaques, it is not yet known whether clusterin acts to protect neighbouring healthy neurons or whether clusterin 'hides' the presence of chronic lesions from the cerebral immune system. Finally, as in the PNS inflammatory responses, activated phagocytic cells secrete a wide variety of proteolytic enzymes that facilitate access of inflammatory phagocytes to the lesion sites by destabilizing the surrounding extracellular matrix. For example, microglia can be induced to secrete plasminogen activator inhibitor (1). Loss of parenchyma integrity could, potentially, trigger production of normal and pathophysiological ECM components such as APP, β-amyloid, and the vast repertoire of PAS^+ glycoproteins associated with neurodegenerative plaques and tangles in a non-productive attempt to stabilize the surrounding matrix. These data implicate the inflammatory cascade in both the etiology and the progression of neurodegenerative lesions.

Immune-mediated inflammatory responses: activation of complement

The brain is the only organ other than the liver capable of generating complement factor mRNAs (117,231). Expression is chronically unregulated in progressive neurodegenerative disorders suggesting that sustained complement fixation may play a role in exacerbating neurodegenerative damage (65,110,117,121,122,231). This speculation gains credence when one examines the mechanisms underlying activation. The complement cascade in the human brain appears to be exclusively generated through the classical pathway given that CNS tissue cannot generate crucial alternative pathway components (151). As described earlier (Chapter II, Section 2), classical pathway complement activation requires an antigenic target to elicit binding and proteolytic activation of C1. However, unlike liver-derived molecules, C1q in the CNS does not require the formation of intermediate IgG or IgM immune complexes to recognize offending

epitopes (151,189). Instead, in the case of Alzheimer's Disease, Downs' Syndrome, Pick's Disease, and prion conditions, C1q is preferentially directed against highly aggregated β-amyloid polymers (65,110,121,122). In prion-related disorders, complement and other acute phase proteins are not associated with PrP^{sc}-containing plaques but are found within amyloid-containing lesions indicating specificity for the β-amyloid molecule (122,123). Diffuse amyloidosis, characteristic of lesions found within the cerebellum of patients suffering from Alzheimer's Disease or in cerebrum of patients afflicted with prion-associated disorders, is affiliated with fewer complement components than the concerted β-amyloid deposits localized to the cortex of Alzheimer's, Down's, or Pick's patients (65,139). As in the PNS, β-amyloid-induced complement cascade culminates in the assembly of MAC. In the CNS, MAC appears to be exclusively directed against neurons (151). Attempts have been made to determine how MAC is so specifically targeted. It is presumed that β-amyloid stimulates the release of downstream complement factors from neurons that signal to phagocytic glia the presence of cerebral contamination (189). Activated glial cells initiate an immune response and direct MAC assembly against irreversibly damaged cells (238). Certainly, β-amyloid has been shown to be cytotoxic to neuronal cultures *in vitro* (71,126). Furthermore, C1q and C3 mRNA have been shown to be expressed exclusively by microglia and astrocytes (91,121,151) while C4 mRNA is predominantly associated with neurons (117). Again, it is important to note that CNS complement is produced locally in response to injury since circulating components, mobilized in majority of PNS responses, are unable to cross the blood-brain barrier. This characteristic limits the extent of the immune response to those cells producing later-stage components of the MAC and permits specific cell death targeting rather than regional responses.

Overview

Two mechanisms are proposed by which inflammatory responses may result in sustained cell death. One possibility is referred to as the 'bystander lysis' mechanism (121). According to this hypothesis, a futile complement cascade is initiated in response to neuronal contact with β-amyloid. Given the insoluble nature of the protein, fixation of β-amyloid-containing cells fails to

completely lyse the offending protein and a chronic inflammatory condition develops. C3b, continually secreted by activated glia, promotes phagocytic interaction, chemotaxis to the site of damage, and prolonged gliosis. C3a and C5a induce synthesis and secretion of additional proinflammatory agents inducing vascular permeability in neighbouring capillaries. Extravasation of circulating material compounds the response by introducing activated peripheral inflammatory cells into the privileged environment of the CNS. Ultimately, MAC targeting of injured neurons is extended to include neighbouring healthy cells. In short, the inability of complement fixation to successfully remove the offending 'antigen' results in a breakdown in the ability of CNS cells to differentiate 'self' from 'non-self' and subsequent autologous tissue destruction. The veracity of the 'bystander lysis' mechanism remains highly speculative given that it assumes that the multiplicity of complement regulatory proteins such as clusterin, CD59, and C4 binding proteins are unable to protect against ambiguity in 'self/non-self' determination. Needless to say, this assumption is highly controversial (22b,121,183,225). Alternatively, inflammatory agents released during chronic inflammation may actually mediate the formation of neurodegenerative lesions and directly induce cell death by promoting the synthesis and activation of β-amyloid. As indicated above, astrocytes and microglia can be stimulated to produce APP and process this precursor into non-degradable β-amyloid in the presence proinflammatory agents. β-amyloid acts not only as an antigenic determinant or irritant, but also *directly* activates the complement cascade and induces neuronal death. Thus, glia process β-amyloid that, in turn, elicits neuronal cell death and maintains production and proteolytic activation of C3, increasing the rate of non-specific cell fixation and gliosis and promoting chronic inflammation thereby exacerbating the entire neurodegenerative process (91,236).

In summary, the identification of a unique CNS inflammatory response and its intimate relationship with neurodegenerative lesions suggests that the accelerated neuronal death observed in progressive neurodegenerative disorders may be influenced by repeated exposure to proinflammatory mediators.

5. Platelet Activating Factor

As evident in the previous reviews, proinflammatory agent is a general term denoting a number of diverse compounds. Specifically, these agents have been categorized into complement factors and inhibitors, acute phase proteins and associated factors, serpins and coagulation factors, cytokines and lymphokines, cell adhesion molecules, and inflammatory autacoids. PAF or 1-*O*-alkyl-2-acetyl-*sn*-glycero-3-phosphocholine is an inflammatory autacoid. The term platelet activating factor is, however, highly misleading since the ligand possesses a wide range of biological activities that have far-reaching effects over a variety of cells and tissues other than platelets. In fact, rat platelets are one of the few cell types definitively shown not to express PAF receptors (226).

PAF first appeared in the literature in 1972 when Benveniste et al. isolated an endogenous, soluble substance released from IgE-stimulated basophils that was capable of inducing platelet aggregation at remarkably low concentrations (22). This same factor was concurrently identified by Muirhead and associates as Antihypertensive Polar Renal Lipid (APRL), a hypotensive agent generated in the kidney (162). It was not until 1979 that the chemical structure of both PAF and APRL was identified as 1-*O*-alkyl-2-acetyl-*sn*-glycero-3-phosphocholine and the two compounds recognized as the same agent (23,28,56). Presently, PAF continues to be the generic term used to describe the growing family of endogenous bioactive 1-alkyl-2-acetyl-*sn*-glycero-3-phosphocholines and related plasmalogen analogues (152,173,216). The most potent of these agents are depicted in Figure 6.

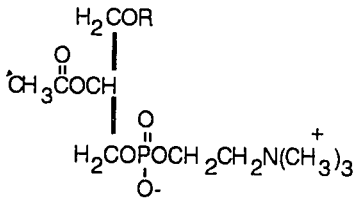

Figure 6. Chemical structure of PAF

The two predominant molecular species of the PAF family are indicated by the R group at the *sn*-1 position as $C_{16}H_{33}$ or $C_{18}H_{37}$. Unless otherwise stated, these two forms are referred to collectively as PAF in all of the experiments reviewed or described in this thesis.

PAF: General principles

PAF occupies an unique position in the extensive list of endogenous ligands. The

compound was the first naturally produced, biologically active, phospholipid ever isolated (22). Its receptor was the first lipid-activated binding protein to be cloned (102). Perhaps most importantly, PAF ranks as the most potent lipid mediator yet identified (209). Reliable biological responses can be elicited at concentrations as low as 1 fM within 1 min of exposure (25). *In vivo*, PAF concentrations have been shown to range between 1 pM - 1 μM, considerably less than its critical micelle concentration estimated to be approximately 3 μM (17). PAF elicits a wide variety of responses in different cell types including vasodilation (119), smooth muscle contraction (54), angiogenesis (7), inflammatory cell activation (12,19,41,59,61,100,130,150,155,177,206), respiratory burst (75,87,100,125,142), cytokine production (32), blastocyst implantation in the epithelial cell lining of the uterus (93,240), neuronal differentiation (127), and apoptosis (66). As indicated in Figure 7, PAF contributes to almost every facet of inflammatory cell activation. In platelets and polymorphonuclear leukocytes, PAF induces a powerful proinflammatory response stimulating cell aggregation (41,61,177,181,206,219), degranulation (19,61,89,137), adherence to endothelial cells (12,59,100,130,150,155), chemotaxis (157,176,233), and superoxide production (75,87,100,125,142). In non-inflammatory cells, PAF increases cytokine production (107,184,190), induces calcium transients (127), stimulates oxyradical generation (184), and may play a role in inducing cell proliferation (143,159) and cell differentiation (127). At higher concentrations or with extended exposure, PAF can have profound pathophysiological

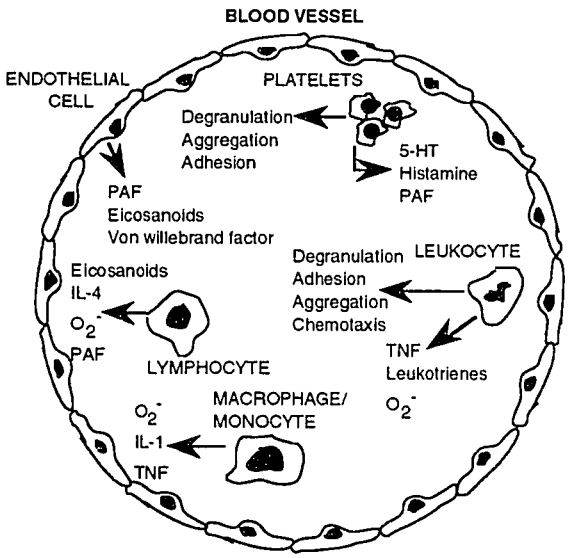

Figure 7. PAF-mediated responses in inflammatory cells

Schematic summarizes the functional consequences of PAF stimulation in inflammatory cells. As indicated, a variety of other proinflammatory agents are synthesized and released in response to PAF emphasizing its role in maintaining inflammatory feedback loops.

consequences implicating the ligand in the pathogenesis of such diverse conditions as ischemia (31,101,196), asthma (104,233,237), diabetes (98,181,203), endotoxic shock (85,92), cholera (90), liver cirrhosis (58,213), arthritic conditions (64,243), autoimmune disorders (147), and chronic inflammatory conditions (43,57). These disorders are often accompanied by disruption of tightly regulated PAF metabolic and catabolic pathways (64,101,147,196).

Metabolism: Synthesis and catabolism

PAF is produced by mammalian cells in response to such proinflammatory agents and immune molecules as thrombin, TNFα, interleukin-1, histamine, zymosan, fMet-Leu-Phe, immunoglobulins and complement (45,68,135,180,209,227). Two different biosynthetic pathways - *de novo* synthesis and 'remodelling' - have been identified. The *de novo* pathway is predominantly responsible for basal level regulation of the ligand, generating both the potent $C_{16}H_{33}$ or $C_{18}H_{37}$ molecular species and the plasmalogen analogues (Figure 8). Inducible PAF-mediated cell signalling, however, requires a more rapid synthesis of ligand than that afforded by *de novo* production. Inflammatory cell types have been shown to form large quantities of PAF via a two step 'remodelling' of a specific family of ether-linked phospholipids, alkylacylglycero-

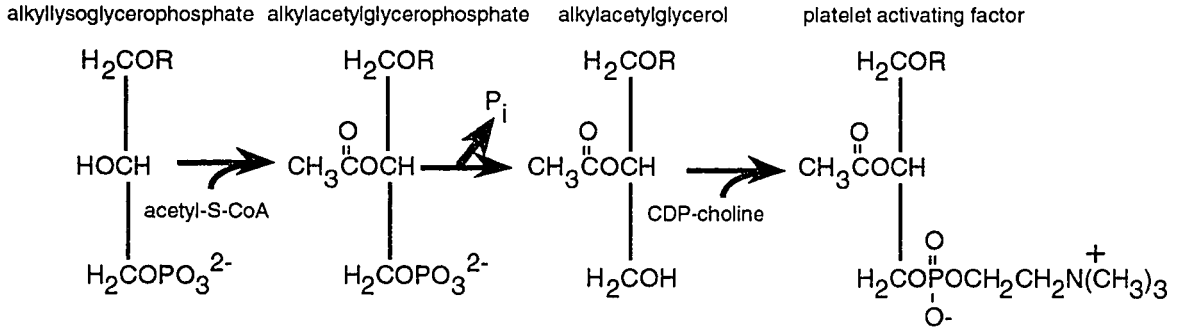

Step 1: an acetyl-CoA:alkyl-lysoglycerophosphate acetyl-transferase substitutes an acetate group for the hydroxyl group at the *sn*-2 position

Step 2: an alkylacetylglycero-phosphate phosphohydrolase removes the phosphate group at the *sn*-3 position

Step 3: a dithiothreitol-insensitive cholinephospho-transeferase completes the transfer of phosphocholine from CDP-choline to PAF

Figure 8. *De novo* synthesis of PAF

De novo production of PAF from an O-alkyl derivative of lysophosphatidic acid is analogous to the biosynthesis of phosphatidylcholine. Three main steps are involved: (1) acetylation, (2) phosphate hydrolysis, and (3) phosphocholine transfer from CDP-choline to a diradylglycerol. The enzymes involved in this pathway are calcium independent. R=$C_{16}H_{33}$ or $C_{18}H_{37}$.

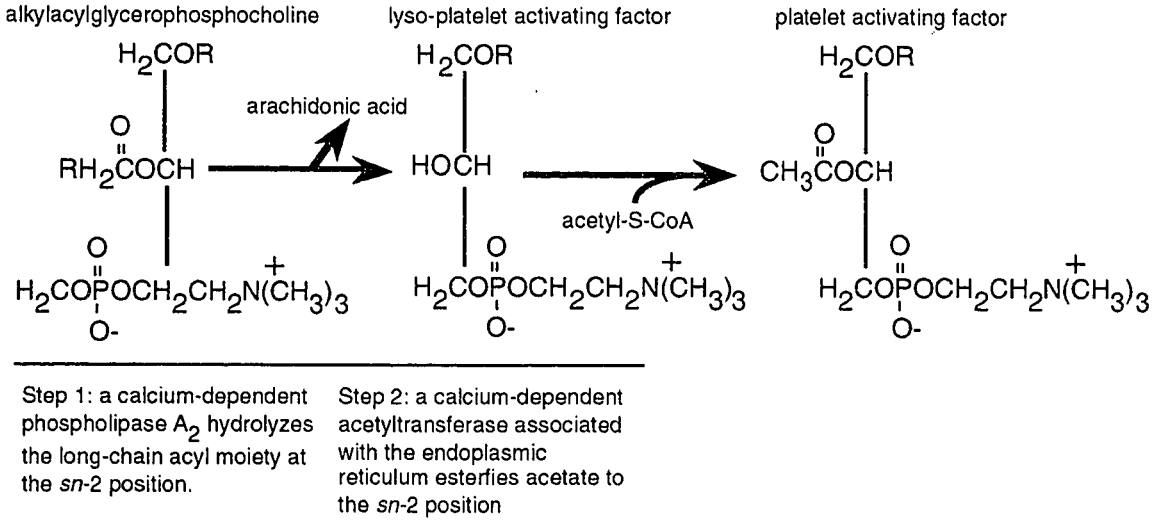

Figure 9. 'Remodelling' of PAF

The remodelling route of PAF biosynthesis involves only two steps: (1) fatty acid hydrolysis of a subclass of membrane structural components identified as alkylacylglycerophosphocholine and (2) acetate transfer at the *sn*-2 position. Each step is, however, calcium-dependent, and is stimulated by increases in intracellular calcium concentrations. R=$C_{16}H_{33}$ or $C_{18}H_{37}$.

phosphocholine (AAGPC), resident as structural components in cell membranes (Figure 9).

Metabolism through the 'remodelling' pathway is triggered, in part, by transient increases in intracellular calcium concentrations. Of additional consideration is the fact that the long-chain fatty acids released from the *sn*-2 position of the parent lipid during PAF metabolism are predominantly polyunsaturates, specifically AA. AA can then be converted into a variety of potent bioactive eicosanoid mediators (ie. prostaglandins and leukotrienes via cyclooxygenase metabolism and 5-HETE metabolites via lipooxygenase metabolism). As a result, PAF 'remodelling' is usually accompanied by a metabolic cascade of AA-derived second messengers.

The duration of PAF signalling is tightly controlled. This regulation ensures an *in vivo* half-life of PAF in plasma of 2-12 min depending upon local conditions and systemic illness (84,133). PAF catabolism is depicted in Figure 10. Inactivation of PAF is achieved through the actions of PAF-specific intracellular and extracellular acetylhydrolases, isolated from both plasma and a wide variety of tissues (8,96,113,133,165,178,210,241). These enzymes are part of the calcium-independent phospholipase A_2 family (96). Hydrolysis of the acetyl group at the *sn*-2

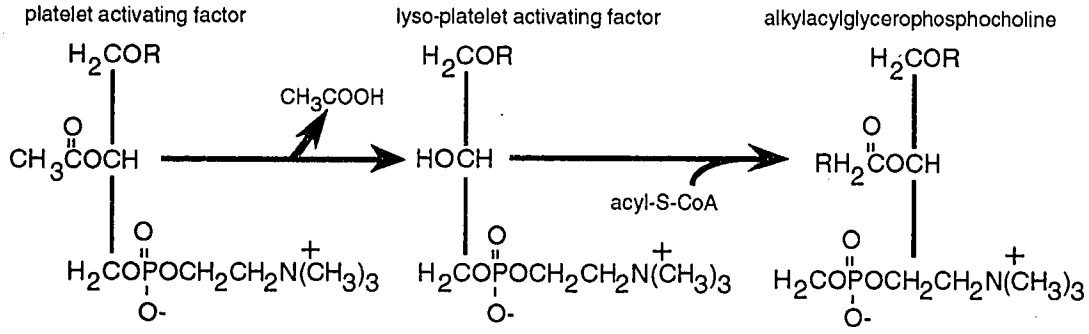

Step 1: a PAF specific acetylhydrolase removes the acetyl group from the *sn*-2 position. The enzyme is activated when phosphorylated. Activation is inhibited by intracellular calcium increases.

Step 2: Depending on cell type, a lyso-PAF specific arachidonate transcyclase, phospholipase D, or a lyso-PAF specific acyltransferase substitutes a long-chain acyl moiety at the *sn*-2 position. Each reaction is calcium-dependent.

Figure 10. Catabolism of PAF

PAF degradation involves two steps: (1) deactylation and (2) substitution of a long-chain acyl group for the hydroxyl group at the *sn*-2 position. The process is calcium dependent and is inhibited by increases in intracellular calcium concentrations.

position generates lyso-PAF, a related phospholipid that lacks specific biological activity but can be cytotoxic due to the detergent properties associated with the hydroxyl group at the *sn*-2 position. Lyso-PAF is rapidly converted to a structural lipid component of cell membranes by substitution of a long chain fatty acid at the *sn*-2 position. Since lyso-PAF is not only PAF's primary metabolite during catabolism but also its immediate precursor in the 'remodelling' pathway (Figure 9), it is tempting to envisage how metabolic feedback loops might be established during an inflammatory response ensuring prolonged PAF turnover and/or repeated transient exposure (84,90). A variety of mechanisms would be involved. For example, inflammatory stimuli such as TNFα, interleukin-1, and LPS, that stimulate PAF 'remodelling' have been shown to also inhibit acetylhydrolase secretion (166). In chronic inflammatory conditions, exposure to these ligands could raise local PAF concentrations and extend the compound's half-life. Conversely, thrombin and PAF augment the synthesis and release of both additional PAF and PAF-specific acetylhydrolases (128,169) Exposure to these ligands could result in sustained ligand turnover.

Signal transduction

PAF, like other related lipid mediators such as the prostaglandins and leukotrienes, exerts its effects by acting on unique cell-surface receptors. In 1991, Honda et al. successfully cloned the extracellular PAF receptor (PAFR) cDNA from guinea pig lung representing the first lipid-binding receptor ever sequenced (102). The cDNA for the same molecule has been subsequently identified in rat spleen (26), human heart (214), and human leukocytes (132,239). Sequence analysis (26,102,132,214,239) and pharmacological characterization (34,109,134) have demonstrated that the cell-surface PAFR is a seven-transmembrane spanning G protein-linked receptor homologous to the β-adrenergic and rhodopsin binding proteins (79). A schematic of the molecule is depicted in Figure 11.

PAFR mRNA is expressed at extremely low levels in human heart, spleen, lung, kidney, and brain and somewhat more intensely in peripheral white blood cells (26,163). Two different transcripts have been identified driven by two different promoters alternatively spliced onto the same open reading frame (26). Pharmacological studies have identified high and low affinity binding sites on smooth muscle cells, leukocytes, macrophages, eosinophils, and Kupffer cells (36,46,88,97,99,114,145,199,220,226). Specificity of binding has been shown to be absolutely dependent upon the acetyl moiety at the *sn*-2 position of the PAF ligand and, to a lesser extent,

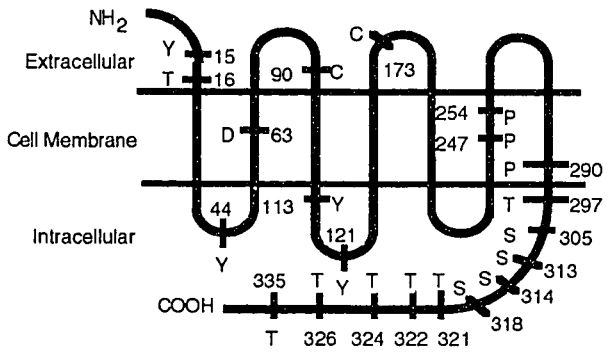

Figure 11. Extracellular PAF Receptor

Diagrammatic representation of the 342 amino acid sequence generated from the guinea pig lung PAF receptor (102). The molecular mass of the protein is 38.93 kD. Hydropathy analysis reveals seven hydrophobic putative transmembrane spanning segments characteristic of G protein-coupled receptors. Numbers indicate location of salient amino acids. When compared to both the β-adrenergic and rhodopsin receptors, several amino acids are highly conserved including an aspartic acid (D) in the second transmembrane loop, two cysteines (C) in the second and third extracellular loops respectively, and three prolines (P) in the sixth and seventh transmembrane sections. The cytoplasmic tail of the PAF receptor contains several serines (S) and threonines (T), potential phosphate acceptor sites. There are a total of 12 tyrosines (Y) throughout the receptor including three in the first and second cytoplasmic loops. Several asparagine residues are present at the external surface of the receptor indicating potential glycosylation sites.

modulated by the ether linkage at the *sn*-1 position and the polar head group containing choline at the *sn*-3 position (33). The kinetics of receptor binding are altered by exposure to the ligand or downstream effector molecules. Prolonged treatment with either PAF or prostaglandin E_2 selectively desensitizes cells to PAF (116). It is important to note that prostaglandin E_2 does not directly bind to PAF receptors (116). The mechanisms underlying this phenomenon remain ambiguous. Deactivation has been attributed to both diminished affinity and diminished receptor number (74,76,116,164,172,215). More recently, it has been suggested that the phosphorylation state of the PAFR alters ligand-binding potential. PAF-induced kinase activity resulting in phosphorylation of PAFR has recently been reported to down-regulate receptor sensitivity (215). How this down-regulation is accomplished remains unclear although it is possible that phosphorylation induces receptor internalization (80).

In inflammatory cells, activation of the PAF receptor has been shown to cause a number of early biochemical changes in cells commonly associated with signal transduction mechanisms. A schematic overview of these events is presented in Figure 12. PAF-induced changes include calcium transients (75,188), arachidonate (21,131,134,223) and phosphoinositide (46,164,242) turnover, protein kinase C (PKC) activation (171,232), increases in tyrosine phosphorylation (44,82), stimulation of interleukin-4, c-*fos*, and EGR-2 mRNA expression (18,149), and synthesis and release of interleukin-8 and TNFα (14). In addition, PAF stimulates phospholipase A_2 activity thus promoting not only its own synthesis in target cells but also generating prostaglandin and leukotriene second messengers (13). At low concentrations, the ligand works synergistically with other proinflammatory agents to perpetuate the inflammatory response (13,14). Although the effects of PAF on non-inflammatory cell types have not been as extensively studied, the ligand has been shown to induce calcium transients, activate MAP kinase (103), increase c-*fos*, c-*jun*, *zif*/268, and TPA-Inducible Sequence (TIS-1) mRNA expression (40,46,55,127,143,211,221,222,239), and activate secondary response genes containing AP-1 responsive elements in their promotors in both murine and human cells of fibroblast, epithelial, neuronal and astroglial origin (211).

PAF acts not only on specific cell surface receptors but also on intracellular receptors pharmacologically characterized (45,476,202,226). In this way, PAF has been shown to be not

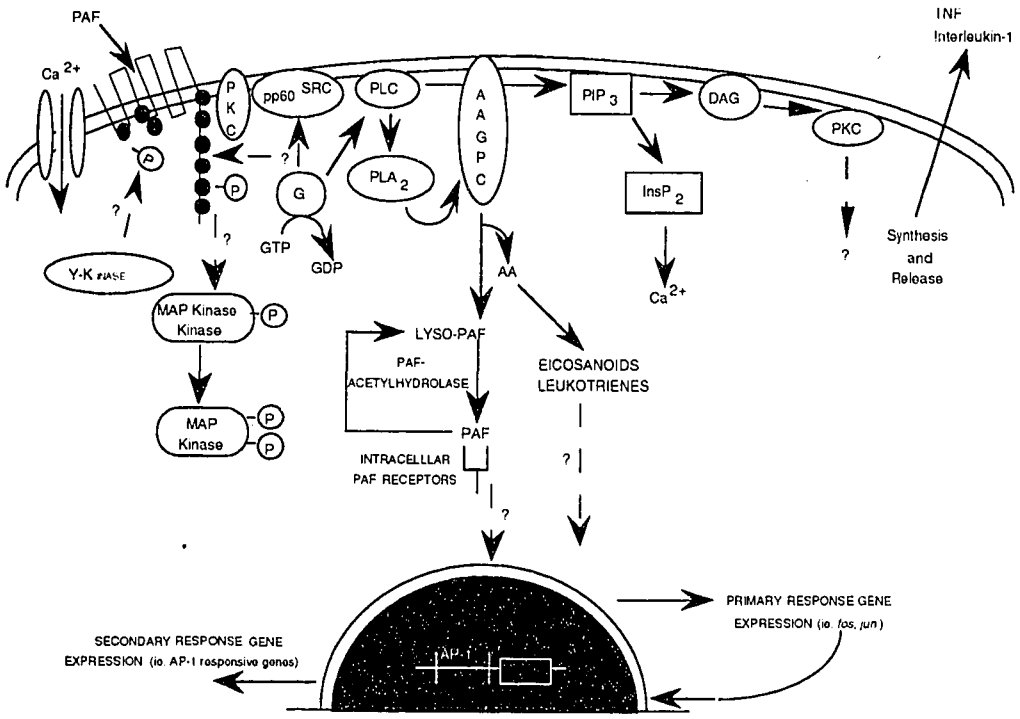

Figure 12. PAF-induced signal transduction

Schematic depicts cell membrane and nucleus. Signalling pathways known to be stimulated by PAF in a number of cell types are represented (see text). Dashed lines indicate unknown intermediates. Abbreviations are as defined in Chapter I.

only an extracellular ligand but also a second messenger, synthesized and retained in response to extracellular stimulation. In fact, it would appear that the vast majority of cells stimulated to produce PAF retain more of the ligand than they secrete (33,45,209). Both extracellular and intracellular increases in local PAF concentrations have been implicated in PAF-mediated pathophysiology. Accumulation of intracellular PAF may also act in receptor-independent fashion. For example, in rat Kupffer cells, there is a small residual PAF-specific calcium influx that cannot be attenuated by PAF antagonist administration (212). The biological relevance of this activity has yet to be determined.

PAF and cancer

Circulating PAF levels are reported to be elevated in Crohn's disease, a preneoplastic inflammatory disorder, (35,67,210) as well as in prostatic carcinoma (78), leukemia (78),

nasopharyngeal carcinoma (78), histiocytic lymphoma (78), and metastatic melanoma (78). Although increased ligand concentrations are predominantly associated with an increase in inflammation, substantial PAF levels have also been demonstrated in tissues devoid of inflammatory cell infiltration. For example, increased PAF concentrations have been found in colonic mucosa of Crohn's disease patients in the absence of an enhanced inflammatory cell response (210). The relative importance of these alterations to the underlying pathophysiologies is unknown. As mentioned above, Maggi et al. (143) have demonstrated that PAF is responsible for maintaining the continued proliferation of an endometrial carcinoma cell line *in vitro* by establishing a mitogenic autocrine feedback loop while Bazan et al. (20) have shown that PAF can induce collagenase expression in corneal epithelial cells. It is possible, then, that the increased concentrations of PAF observed *in vivo* in preneoplastic and metastatic disorders may play a role in mediating tumour cell growth and/or degradation of ECM related to tumour cell metastasis.

Paradoxically, synthetic PAF and lyso-PAF analogues have been used as chemotherapeutic agents. The antineoplastic potential of ether-linked lipids has been widely reported with respect to their cytotoxicity, ability to induce tumour cell differentiation, and immune modulating effects (9,24,160,186,204). Unlike many other antitumour agents, ether lipids do not appear to induce DNA damage (9,160,186,204). None of PAF's synthetic analogues, tested for chemotherapeutic value, stimulate PAFR. However, cell kinetic experiments demonstrate that these analogues are capable of inducing both a G_1 and a G_2 block in the cell cycle as well as attenuating the transition from late S to G_2. The point of arrest depends upon which stage of the cell cycle tumour cells are in when first exposed to the phospholipid (9,24,160,1876,204). How these effects are mediated remains unknown. It is hypothesized that PAF analogues disrupt lipid metabolism and consequently compromise cell membrane integrity (160). In sharp contrast to the synthetic analogues, endogenous ligands do not exert antineoplastic actions. The concentrations of PAF and lyso-PAF required to elicit comparable gross cytotoxicity are physiologically irrelevant and show no specificity for rapidly cycling tumour cells compared to normal cells (24,160,186,204). Furthermore, unlike their non-metabolizable counterparts, the limited cytotoxicity induced by physiologically relevant concentrations of PAF and lyso-PAF can be attenuated by administration (or endogenous exposure) to growth factors (9).

PAF and neurodegeneration

PAF metabolism is tightly regulated in brain. Transient exposure to low concentrations of the ligand induces neuronal differentiation (127), long-term potentiation (48,124), and immediate early gene expression in neurally derived cultures *in vitro* (146,211) while extended exposure to high concentrations of the ligand induces cytotoxicity (127). Endogenous overproduction and/or a failure to inactivate the phospholipid have been implicated in the pathophysiology of ischemia/ reperfusion injury (62,211,217), meningitis (38,218), epileptic brain damage (21,146), and CNS developmental disorders (95). With respect to this latter problem, a bovine brain PAF-specific acetylhydrolase has recently been purified and shown to be a heterotrimer consisting of a 45, 30, and 29 kD subunit. The 45 kD subunit has been cloned and identified as the bovine homolog of human LIS-1, the causative gene underlying Miller-Dieker lissencephaly, a human brain deformation syndrome manifested by a smooth cerebral surface and abnormal neuronal migration resulting in profound retardation (95). These data indicate a role for PAF in brain development and cerebral insult.

Overview/ Thesis questions

Do endogenous proinflammatory agents influence tumour progression and provoke progressive neurodegeneration? Certainly, sustained inflammatory responses are intimately involved in the pathophysiologies complicating these disorders. However, the relative importance of this involvement remains speculative. The literature suggests that a variety of proinflammatory mediators may contribute to cell regulatory disorders affecting cell number. PAF's powerful proinflammatory abilities coupled with preliminary evidence that the ligand can affect both the rate of cell growth and cell death *in vitro* in receptor-mediated fashion identifies the autacoid as an promising candidate molecule. To determine whether PAF has the potential to contribute to tumour progression and neurodegeneration, this thesis is divided into four sections designed to investigate the following questions:

(1) Can PAF selectively mediate cell growth and cell death in non-inflammatory cell types (Chapter III: Transformation Potential)?

(2) What signal transduction pathways are responsible for PAF's effects in fibroblasts and epithelial cells (Chapter IV: Signal Transduction)?

(3) Can PAF elicit additional phenotypic alterations in cells already transformed (Chapter V: Tumour Progression)?

(4) Is PAF implicated in the pathogenesis of chronic lesions in an *in vivo* model of progressive neurodegeneration (Chapter VI: Neurodegeneration)?

III

TRANSFORMATION POTENTIAL

1. Introduction

Does PAF play a role in mediating cell regulatory disorders related to human cancers? Tumour formation represents a breakdown in the balance between cell proliferation (cell division) and withdrawal from the cell cycle (terminal differentiation or cell death). To assess whether exposure to PAF contributes to either of these phenomena, primary cells were isolated and tested for prolonged *in vitro* alterations in growth kinetics (phenotypic transformation) following PAF treatment. In each of the following series of investigations, two experimental models were employed. PAF was administered to primary rat embryo cells (RECs) and selective changes in the rate of cell growth and/or the rate of cell death were determined. To demonstrate relevancy to human cancers, primary human fibroblasts (HFs) were treated with PAF and assayed for phenotypic transformation. Specific alterations in growth kinetics in both cell lines were then characterized and preliminary attempts made to identify underlying mechanisms mediating these PAF-induced effects.

2. Mitogenicity and Active Cell Death Induced by PAF

Abstract

The mitogenic and cytotoxic potential of PAF was determined by treating quiescent RECs and HFs with 0.001 nM - 1 μM PAF for up to 72 hr and assaying for changes in growth kinetics. RECs are a mixed population of rodent cells, explanted from day 14-16 Sprague Dawley embryos. Third passage RECs are composed predominantly of fibroblasts (>90%), with a sizable sub-population of epithelial cells (approximately 10%) and occasional neuronal and muscle cells (<0.1%). HFs are a primary explant of diploid neonatal human fibroblasts derived from neonate foreskin. In both cell lines, PAF was found to elicit an inverted U dose-response curve. Low doses of ligand (0.001 - 0.1 nM) increased incorporation of [^{3}H] thymidine into DNA and augmented cell number. *In situ* hybridization demonstrated that this increase in radiolabelling was the result of DNA synthesis indicative of cell proliferation and not of DNA repair suggestive of genetic damage. High doses of PAF (10 nM - 1 μM) decreased [^{3}H] thymidine incorporation into DNA and induced cell loss. Morphological changes accompanying cell death were characteristic of an active cell death process. This evaluation was confirmed by demonstration of nucleosome ladders in isolated DNA. These data indicate that PAF is capable of dose-dependently modulating both the rate of cell growth and the rate of cell death in RECs and HFs.

Introduction

The clonal expansion of a tumour cell requires either a prolonged *increase* in the rate of cell growth or, conversely, an unregulated *decrease* in the rate of cell death. Sustained increases and decreases in cell number are readily observed during inflammation in which both inflammatory and non-inflammatory cells in and around a site of injury produce autocrine and paracrine factors that maintain cell growth or, conversely, elicit cell death (Chapter II, Section 2). These responses facilitate the containment of toxic agents, removal of damaged tissue, and wound repair. Given the association between chronic inflammatory conditions and increased predisposition to cancer, it was hypothesized that PAF may be capable of regulating cell growth in non-inflammatory cells leading to a sustained increase in overall cell number. To determine whether the proinflammatory agent can mediate cell proliferation and/or cell death in fibroblasts and epithelial cells, quiescent RECs and HFs were chronically exposed to different doses of the ligand and assayed for changes in cell number, morphology, and DNA integrity.

Materials and Methods

Cells and Culture Conditions

Primary REC cultures were prepared from day 14-16 Sprague Dawley rat embryos (Charles Rivers, PQ). Freshly dissected embryos were homogenized, incubated in 0.5% trypsin (Gibco, Ont), 5.3 mM ethylenediamine tetraacetic acid (EDTA; Sigma, MO), and dissociated into single cells. RECs were suspended in Dulbecco's minimal essential medium (DMEM; Gibco, Ont) plus 10% fetal calf serum (FCS; Flow Laboratories, VA) (DMEM+10%FCS), seeded at a density of approximately $6x10^6$ cells per 15 cm dia. tissue culture dish, and allowed to grow for 2 days at 37°C in a 5% CO_2/95% air atmosphere. While still sub-confluent, cells were trypsinized and either passaged in fresh medium or stored at -100°C. Samples of third passage cells were determined to be mycoplasma-free as judged by staining with a fluorescent dye, Hoechst 33258, and by reverse transcriptase-polymerase chain reaction (RT-PCR) analysis as described in Chapter IV, Section 2 using probes from a commercial mycoplasma detection kit (Stratagene, NY).

Normal human diploid fibroblasts (HFs) were prepared from neonatal foreskins essentially as described (19) and grown in DMEM+10% FCS (Gibco, Ont). While still sub-confluent, cells were trypsinized and either passaged in fresh medium or stored at -100°C. Samples of third passage HFs were determined to be mycoplasma-free, as described above.

Cell characterization

The REC population was characterized immunohistochemically and by flow cytometry. For immunohistochemistry, third passage RECs were plated at a density of 1,000 cells on gelatin-coated 22 mm^2 glass coverslips, washed in phosphate buffered saline (PBS; 154 mM NaCl, 10 mM sodium phosphate, pH 7.2), fixed in cold 3.7% formaldehyde for 10 min, washed in PBS, exposed to 1% normal goat serum in PBS for 30 min at 25°C, and reacted at 37°C for 2 hr with monoclonal anti-vimentin (IgM: 1:100, Sigma). Antibodies were diluted in Ab buffer (154 mM NaCl, 100 mM sodium phosphate, pH 7.2, 3% bovine serum albumin (BSA), 0.3% Triton X-100). Samples were washed and immunopositive cells were visualized with a Texas Red-conjugated total Ig goat anti-mouse secondary antibody (1:100, Oncogene Science, NY). Sections

were then double-labelled with one of the following primary antibodies: monoclonal anti-rat endothelium (1:100, Serotec, Ont), monoclonal anti-cytokeratin 8.13 (1:100, Sigma, MO), rabbit anti-GFAP (1:100, Sigma, MO), rabbit anti-neurofilament 200 kD (1:100, Sigma, MO), or rabbit anti-desmin (1:50, Serotec, ONT). Samples were washed in PBS and immunopositive cells visualized with a fluoroscein-conjugated IgG-specific goat anti-mouse or goat anti-rabbit (1:100, Oncogene Science, NY) secondary antibody diluted in Ab buffer. For flow cytometry, subconfluent third passage RECs were removed from culture by addition of PBS + 2 mM EDTA and diluted to 100,000 cells/sample. Cell samples were fixed in cold 3.7% formaldehyde for 3 min with vigourous vortexing, reacted with primary antibodies as described above, washed with PBS, and labelled with a fluoroscein-conjugated total Ig or a IgG-specific goat anti-mouse or a goat anti-rabbit secondary antibody (1:100, Oncogene Science, NY) as appropriate. Cells were then washed with PBS and suspended in 1 ml PBS for flow cytometric analysis using an Epics flow cytometer (Coulter, Ont).

Treatment and assay conditions

Exponentially growing third passage RECs or fourth passage HFs were trypsinized and 100,000 cells per 6 cm tissue culture dish were allowed to attach overnight in complete medium (DMEM+10% FCS). Cultures were then made quiescent by incubation in low serum medium (DMEM+0.5% FCS). Time until quiescence was determined by monitoring [^{3}H]thymidine (Dupont, Ont) incorporation into DNA. Cells were pulsed with [*methyl*-^{3}H]thymidine (0.1 μCi/ml) for 6 hr per test point. Cultures were then washed with PBS, solubilized in 1 ml 0.5 N NaOH, and DNA was precipitated by acidification with 150 μl 5 N HCl at 0°C for 30 min. Samples were centrifuged in a microfuge and the precipitates were washed twice with 0.5 ml of ice-cold 0.5 N HCl. Pellets were solubilized in 200 μl 0.2 N NaOH. Aquasol scintillation fluid (1 ml, Dupont, Ont) was added and radioactivity determined in a liquid scintillation counter. To determine non-specific binding of radiolabel to samples, cultures were exposed to [^{3}H]thymidine immediately prior to harvesting and processed as described above.

Quiescent samples were treated with either (a) vehicle (0.1% dimethyl sulfoxide (DMSO; Fisher, Ont), (b) PAF (0.1 nM-1 μM, Avanti Biochemicals, PA), (c) lyso-PAF (0.1 nM-1 μM,

Sigma, MO), (d) PAF (100 nM- 1μM) + CV3988 (10 μM, Calbiochem, CA), or (e) DMEM+10% FCS. In each case, the treatment compound (DMSO, PAF, lyso-PAF, PAF+CV3988, or FCS) was added directly to existing low serum medium. Medium was not replaced. Cell proliferation/viability was determined by cell counts using a Coulter Counter, trypan blue exclusion, [^{3}H]thymidine incorporation into DNA as described above, and *in situ* [^{3}H]thymidine-labelling. In addition, some cultures were immunoreacted with anti-vimentin as described above or fixed with methanol and stained with ethidium bromide for morphological analysis of the cytoplasm and nucleus respectively. For *in situ* experiments, cells were plated at a density of 1,000 on gelatin-coated 22 mm^2 glass coverslips in 6 cm dishes, quiesced, and treated as described above. Cells were pulsed for 72 hr with [^{3}H]thymidine (0.1 μCi/ ml). Cultures were washed extensively in PBS and coverslips removed, dipped in nuclear track photographic emulsion, and exposed for 3 weeks at 4°C. Slides were developed for 5 min at 15°C in Kodak-D19 developer, 30 sec in 2% acetic acid, 5 min in Kodak Rapid Fix, and 30 min in running water. Photographic chemicals were from Kodak, Ont. Slides were examined under bright- and dark-field microscopy using a Zeiss Axioskop microscope. For DNA analysis, nucleic acids were isolated as described in (16) and electrophoretically separated on a 1.2% agarose gel.

Statistical analysis

Data were analyzed using one-way factorial ANOVA tests or unpaired Student's *t* tests, as applicable. Following detection of a statistically significant F value with respect to the effect of a given series of treatments, *post hoc* Dunnett's tests were used to identify which treatment condition differed statistically from control (vehicle-treated RECs). P values of <0.05 were considered statistically significant differences (shown as *); P values of <0.01 were considered highly statistically significant differences (shown as **).

Results and Discussion

Characterization of REC population

RECs are a primary explant of Sprague Dawley embryo cells. The cell types composing the REC population were determined by immunohistochemistry and flow cytometry (Figure 13).

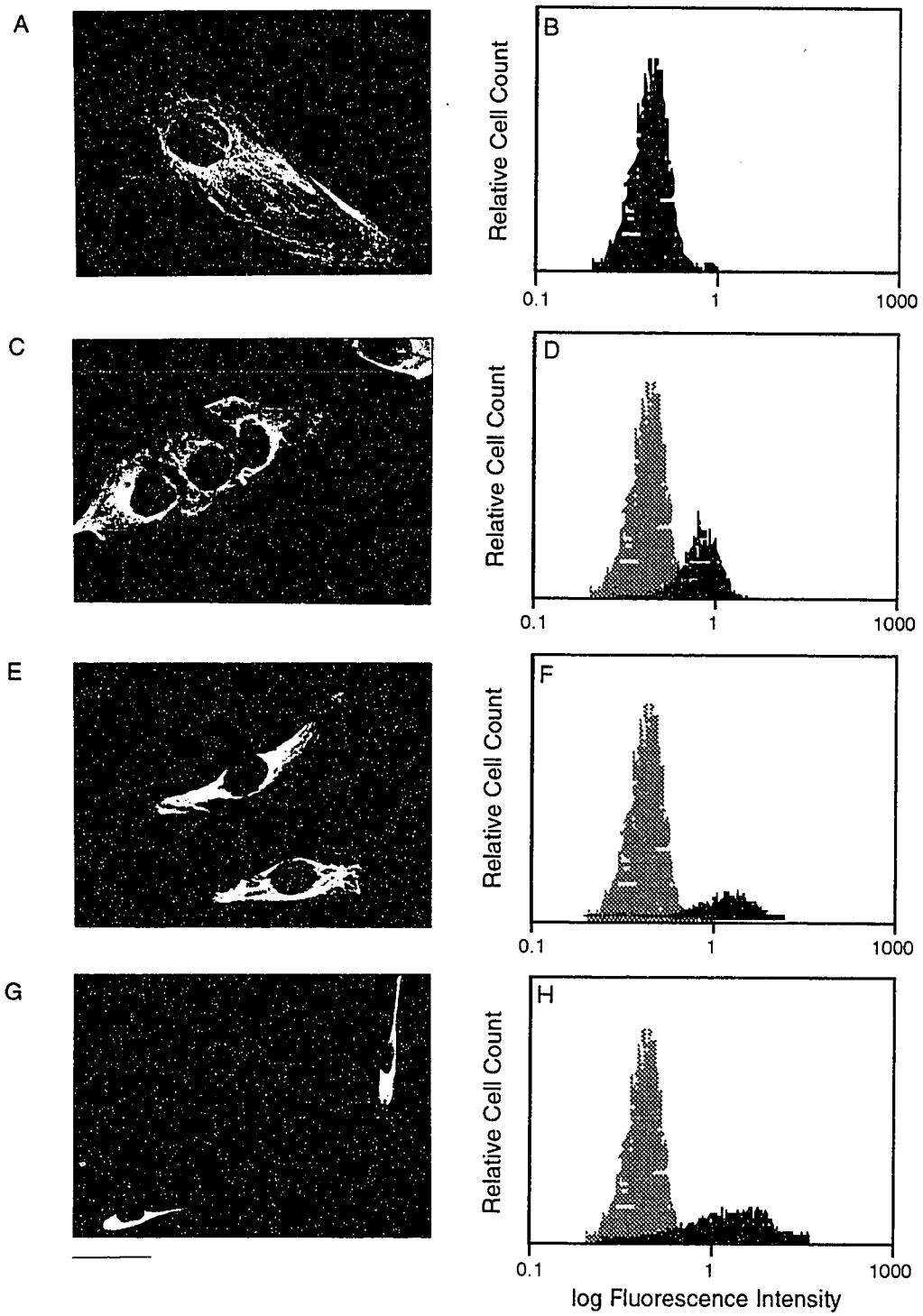

Figure 13. Characterization of RECs by immunohistochemistry and flow cytometry

RECs were processed for immunohistochemistry (A,C,E,G) and flow cytometry (B,D,F,H) as described in Materials and Methods. (A,B) , fibroblasts; (C,D), epithelial cells, (E,F) neuronal cells; (G,H) muscle cells. Representative photomicrographs are depicted. Scale bar=12 μm

Fibroblasts, endothelial cells, and epithelial cells were identified using monoclonal antibodies directed against vimentin, rat endothelium, and cytokeratin, respectively. Muscle cells, glia, and neurons were identified using polyclonal antibodies directed against desmin, GFAP, and neurofilament 200 kD, respectively. As depicted in Figure 13A, cells in the REC explants were immunoreactive to anti-vimentin, consistent with a predominance of fibroblasts in the population. Since cell types other than fibroblasts have also been shown to be vimentin-positive *in vitro,* cultures were double-labelled with additional antibodies. The majority (>90%) of cells were fibroblasts (ie. they reacted only with anti-vimentin). Approximately 10% of cells reacted with both anti-vimentin and anti-cytokeratin, indicating epithelial cells (Figure 13C), while <0.1% of neuronal and muscle cells were detected by double-labelling with anti-vimentin and anti-neurofilament (Figure 13E) or anti-vimentin and anti-desmin (Figure 13G), respectively. No other cell types were detected. The accuracy of this distribution was confirmed by flow cytometry (Figure 13B,D,F,H).

Effect of PAF on REC growth kinetics

RECs were rendered quiescent by 96 hr incubation in low serum medium. Quiescence was confirmed by the absence of [^{3}H]thymidine incorporation into DNA (data not shown). RECs were then treated for 72 hr with PAF, vehicle, or 10% serum. Following treatment, the medium was removed and cells were incubated for an additional 96 hr in low serum medium (DMEM+0.5% FCS). Treatment with PAF was found to dose-dependently alter incorporation of [^{3}H] thymidine into DNA inducing an inverted U dose-response cure (Figure 14A). Continual exposure to low doses of PAF (0.001-0.1 nM) proved to be mitogenic increasing radiolabel incorporation into DNA while high doses (10-1000 nM) were observed to decrease radiolabelling. Peak mitogenic effects were obtained with 0.1 nM PAF. These data were compared to the effect of PAF on cell kinetics. Cell number was assessed by Coulter counts. After 72 hr of treatment, PAF (0.1 nM) increased cell growth compared to vehicle-treated cells. Surprisingly, cell proliferation was maintained for at least 96 hr after ligand removal (Figure 14B). The validity of these observations was confirmed by autoradiography. [^{3}H]thymidine incorporation into DNA can indicate either an increase in *de novo* DNA synthesis or in DNA repair mechanisms following

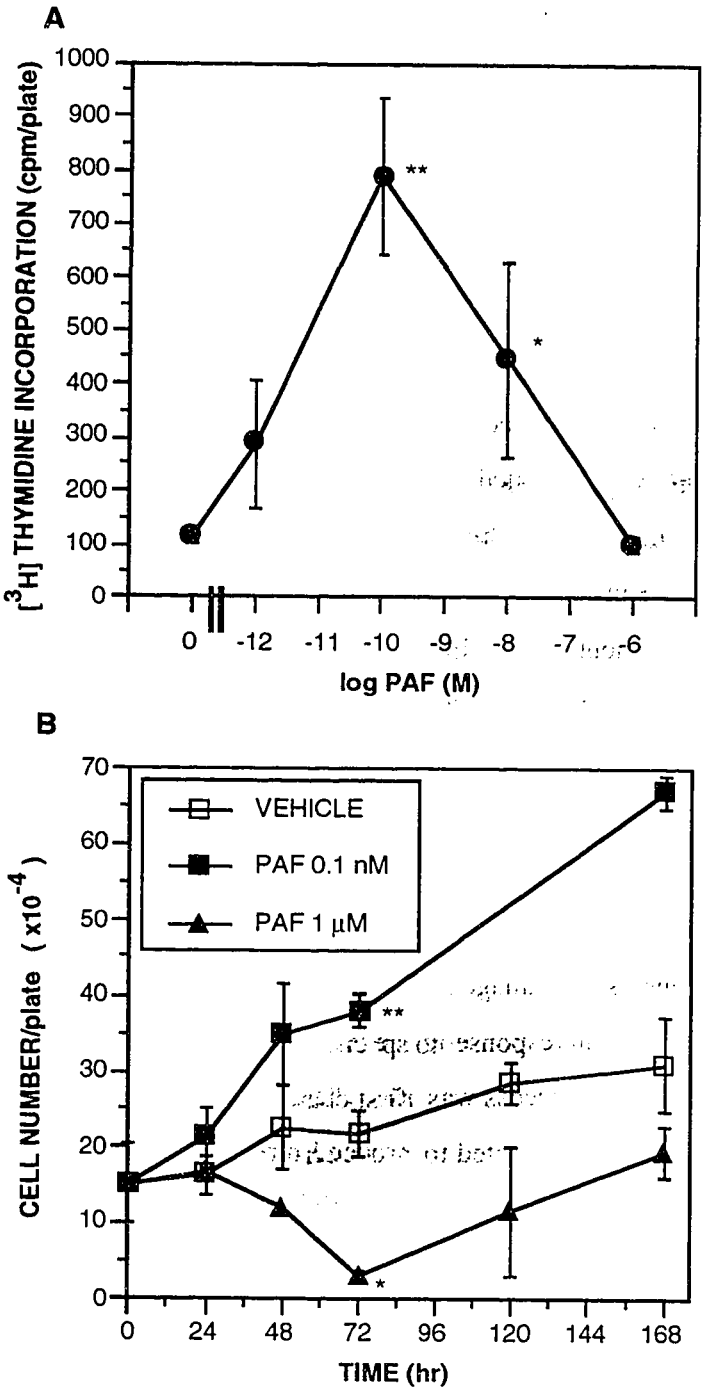

Figure 14. PAF dose-dependently influences cell proliferation and cell loss in RECs

RECs were made quiescent by serum starvation, treated with vehicle, PAF (1 pM - 1 µM), or complete medium, and assayed for changes in [^{3}H]thymidine radiolabelling or cell number. Details as described in Materials and Methods.

(A) PAF exposure results in an inverted U [^{3}H] thymidine incorporation dose-response relationship in RECs.

Data represent mean±SEM cpm/plate from a minimum of 5 plates/condition after 72 hr of continual ligand treatment. Statistically significant differences were as follows: ANOVA: $F=4.8$, $df=4,36$, $p<0.01$. Dunnett's *t*: PAF (0.1 nM) vs. Vehicle, $p<0.01$; PAF (10 nM) vs. Vehicle, $p<0.05$. 10% FCS (positive control) increased [^{3}H]thymidine incorporation to 2989.3 ± 1053.7 cpm/plate at the same time point.

(B) Low doses of PAF induce cell proliferation; high doses of ligand induce cell death.

Data represent mean±SEM cell number from a minimum of 5 plates/treatment/time point using a Coulter Counter. Only adherent RECs were counted. After 72 hr of treatment, medium was replaced with fresh DMEM+0.5% FCS and cells were incubated in the absence of ligand for an additional 96 hr. Statistics were performed after 72 hr of continual PAF treatment on all of the doses tested. Data depicted are derived from treatment with 0.1 nM and 1 µM PAF only. Statistically significant differences were as follows: ANOVA: $F=5.2$, $df=3,29$, $p<0.01$. Dunnett's *t*: PAF (0.1 nM) vs. Vehicle, $p<0.01$; PAF (1 µM) vs. Vehicle, $p<0.05$. 10% FCS (positive control) increased cell number to $8.5\times10^5 \pm 8.4\times10^4$ cells/plate 72 hr after treatment.

genetic damage. Although this possibility is unlikely in the present experiments given the close association between cell number and incorporated radiolabel (Figure 14), autoradiograms of PAF (0.1 nM)-treated RECs were examined to determine the specificity of [^{3}H] thymidine uptake Representative photomicrographs are depicted in Figure 15. The clustering of silver grains over the nucleus of cells exposed to PAF is characteristic of *de novo* DNA synthesis rather than DNA repair. These data support the conclusion that, at low doses, PAF is mitogenic.

By contrast, exposure to PAF (1 μM) decreased overall cell number compared to vehicle-treated cells (Figure 14B). This reduction corresponded with a decrease in cell viability. After 72 hr of treatment, RECs were trypsinized from monolayer culture and combined with unattached cells found in the supernatant. 95% of vehicle-treated cells were viable as determined by trypan blue exclusion while only 40% of PAF (1 μM)-treated cells were capable of dye exclusion. Unlike PAF's mitogenic effects, PAF-induced cell death was dependent upon continued ligand exposure. Removal of the PAF from the medium 'rescued' surviving cells as indicated by renewed cell growth 120 hr after initial treatment (Figure 14B). Furthermore, PAF-induced cell death did not occur if quiescent cells were treated with ligand (1 μM) for a limited period of time (1-6 hr) or if cells were exposed to PAF in DMEM+10% FCS (data not shown).

Cell death can generally be classified under one of two categories: *necrosis* - occurring as a passive result of tissue injury, and *apoptosis* - occurring as an active process of cellular self-destruction requiring specific gene transcription and protein synthesis. Necrosis refers to non-specific cell death in response to exogenous tissue damage and can involve a substantial immune response. Apoptosis refers to selective cell loss in response to specific signalling molecules in the absence of immune involvement. The apoptotic process was first characterized morphologically by Wyllie and colleagues (21,42) and was demonstrated to proceed through three phases: 1) cellular condensation - interactions between the dying cell and its neighbours are lost as the cell shrinks and its cytoplasmic and nuclear components condense; 2) cellular fragmentation - target cells fragment into numerous smaller 'apoptotic bodies' without leakage of any of the cellular components into the extracellular space; and, 3) cellular degradation - apoptotic fragments are phagocytosed by neighbouring cells and degraded either by the lysosomes of these recipient cells or by degradative enzymes within the apoptotic bodies themselves. This phase proceeds without

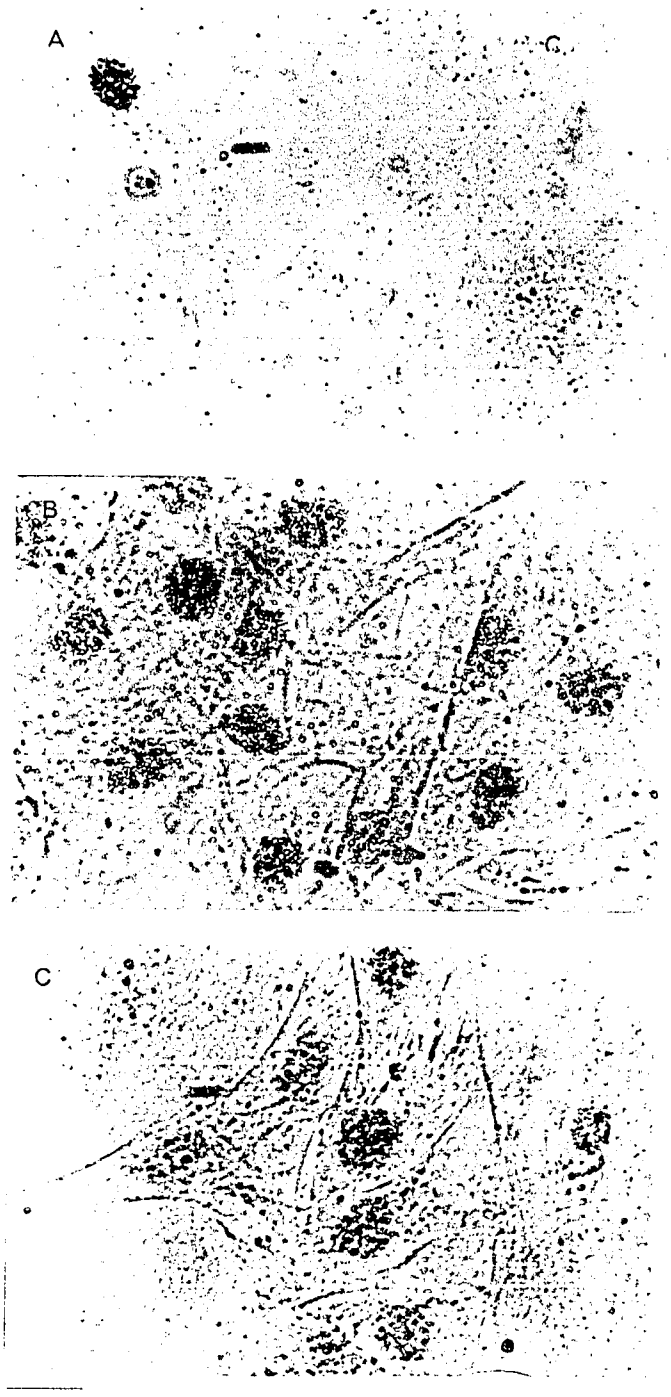

Figure 15. *In situ* incorporation of [^{3}H]-thymidine into REC nuclei following PAF treatment is characteristic of DNA synthesis rather than DNA repair

RECs were made quiescent by serum starvation and then treated with (A) vehicle, (B) complete medium, or (C) PAF (0.1 nM). Autoradiograms were performed after 72 hr of treatment as described in Materials and Methods. The large number of silver grains distributed uniformly over the majority of radiolabelled nuclei in cultures treated with either DMEM+10% FCS (B) or PAF (C) is indicative of increased DNA synthesis. Representative photomicrographs are depicted. Scale bar= 12 μm.

recourse to a complement-based immune response. More recently, a fourth phase - the pre-condensation phase - has been identified. Lasting anywhere from a few minutes to several hours or days, this phase precedes morphological indications of apoptosis and encompasses most of the biochemical events required to trigger gene expression (and/or gene silencing) necessary for the initiation and successful completion of the cell death process (37). These and related forms of targeted cell death are collectively referred to as Active Cell Death (ACD).

To assess whether ACD pathways should be considered in future analyses of PAF's cytotoxic properties, cultures exposed to either vehicle or PAF (1 μM) were immunoreacted with anti-vimentin at various times after treatment and cell morphology examined for physical evidence of ACD (Figure 16). Cytoplasmic changes were found to be consistent with an ACD-like process. By 72 hr after PAF treatment, cells were pyknotic, intercellular contact was lost, and cell fragmentation was evident. Morphologically altered cells were easily removed by aspiration, indicating a loss of adherent properties. However, over 80% of PAF-treated RECs were still capable of excluding trypan blue 48 hr after ligand exposure indicating that cell membranes were still intact; a characteristic feature of ACD. As previously indicated, this percentage dropped to 40% after 72 hr of treatment.

Finally, treatment with lyso-PAF, PAF's immediate metabolite, had no effect on the rate of REC growth or death (data not shown). Co-administration of PAF with CV3988 (10 μM) blocked both PAF-induced cell growth and PAF-elicited cell death (data not shown).

In interpreting these data, it is tempting to speculate that PAF is capable of transducing both a mitogenic and an apoptotic signal depending upon the dose and duration of ligand stimulation.

Effect of PAF on HF growth kinetics

To determine whether PAF mediates mitogenicity and/or ACD in human cells, HFs were rendered quiescent by serum starvation and treated with vehicle, PAF, or complete medium. As with RECs, low doses of PAF induced both a dose-dependent increase in [^{3}H]-thymidine incorporation into DNA and a concomitant increase in cell number while high doses elicited a decrease in radiolabel incorporation and a reduction in overall cell number (Figure 17). As with RECs, cell morphology and cytotoxicity kinetics following treatment with 1 μM PAF were

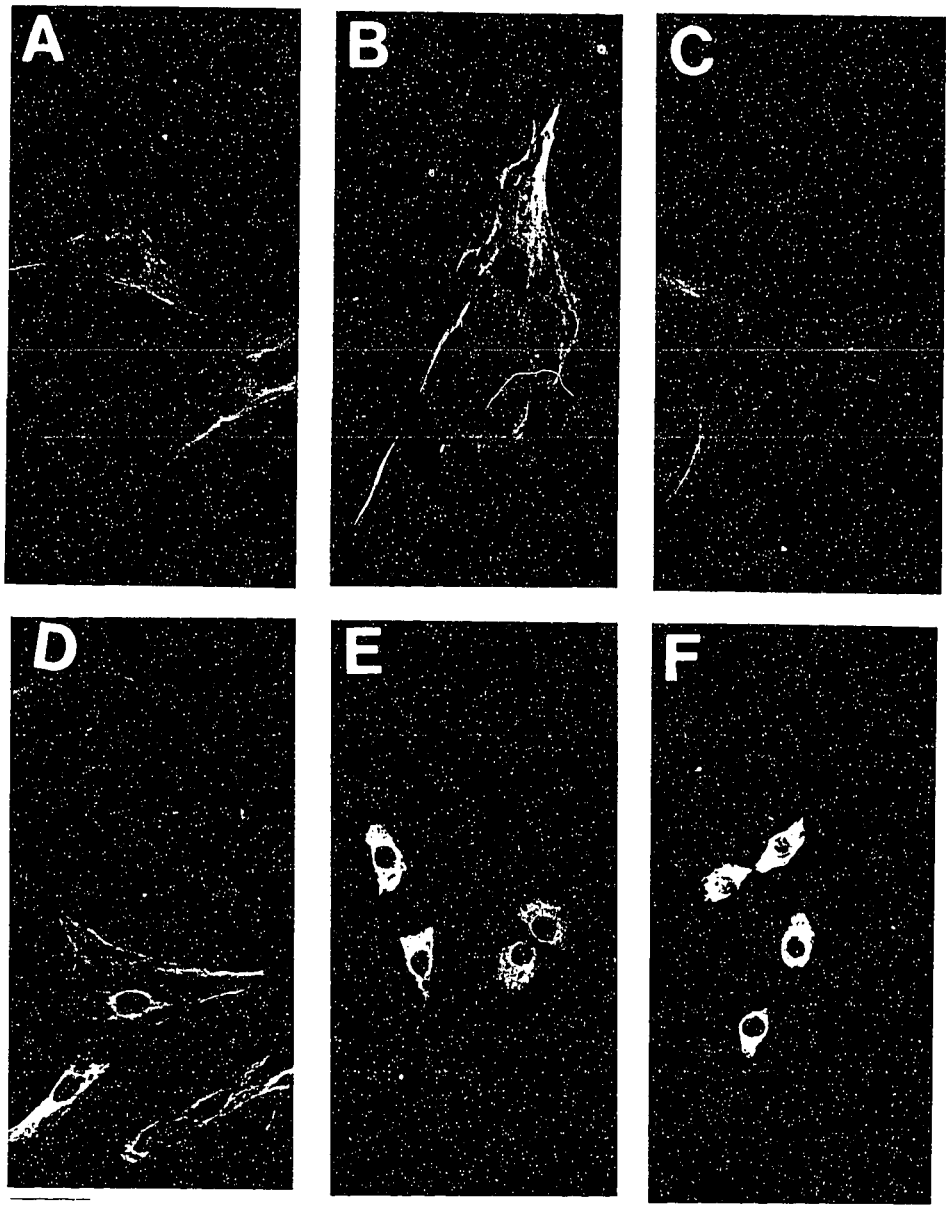

Figure 16. RECs exhibited cytoplasmic condensation characteristic of ACD following continual treatment PAF (1 μM)

RECs were made quiescent by serum starvation and then treated with vehicle or PAF (1 μM). After 24, 48, and 72 hr, RECs were immunoreacted with anti-vimentin and cytoplasmic changes evaluated as described in Materials and Methods. RECs were observed to become pyknotic and condense upon exposure to PAF. Apoptotic cellular bodies were not observed. (Nuclear changes were assessed in HFs (Figure 19)). Representative photomicrographs are depicted. (A) Vehicle, 24 hr. (B) Vehicle, 48 hr. (C) Vehicle, 72 hr. (D) 1 μM PAF, 24 hr. (E) 1 μM PAF, 48 hr. (F) 1 μM PAF, 72 hr. (A,B,C) Scale bar=12 μm. (D,E,F) Scale Bar=10 μm.

consistent with putative activation of ACD. HFs demonstrated morphological alterations characteristic of apoptosis (ie. nuclear condensation and fragmentation) (Figure 18) while retaining the ability to exclude trypan blue 72 hr after treatment (data not shown). Cell viability was not compromised until 96 hr after treatment. Like RECs, HFs required continued stimulation with PAF (1 μM) to induce cell death but continued to demonstrate enhanced cell growth after the removal of 0.1 nM PAF (Figure 17).

The role of ACD in PAF (1 μM)-induced cell loss was further investigated by electrophoretic analysis of isolated DNA. Double-strand cleavage of nuclear DNA leading to the production of oligonucleosomal fragments is a characteristic biochemical feature of ACD (20). PAF (1 μM) was found to induce DNA ladders in HFs 24-72 hr after treatment (Figure 19).

These data suggest that the endogenous, proinflammatory agent, PAF, is capable of mediating both cell growth and cell death in RECs and HFs. This finding warrants further investigation as to a putative role for PAF in cell regulative disorders affecting cell number.

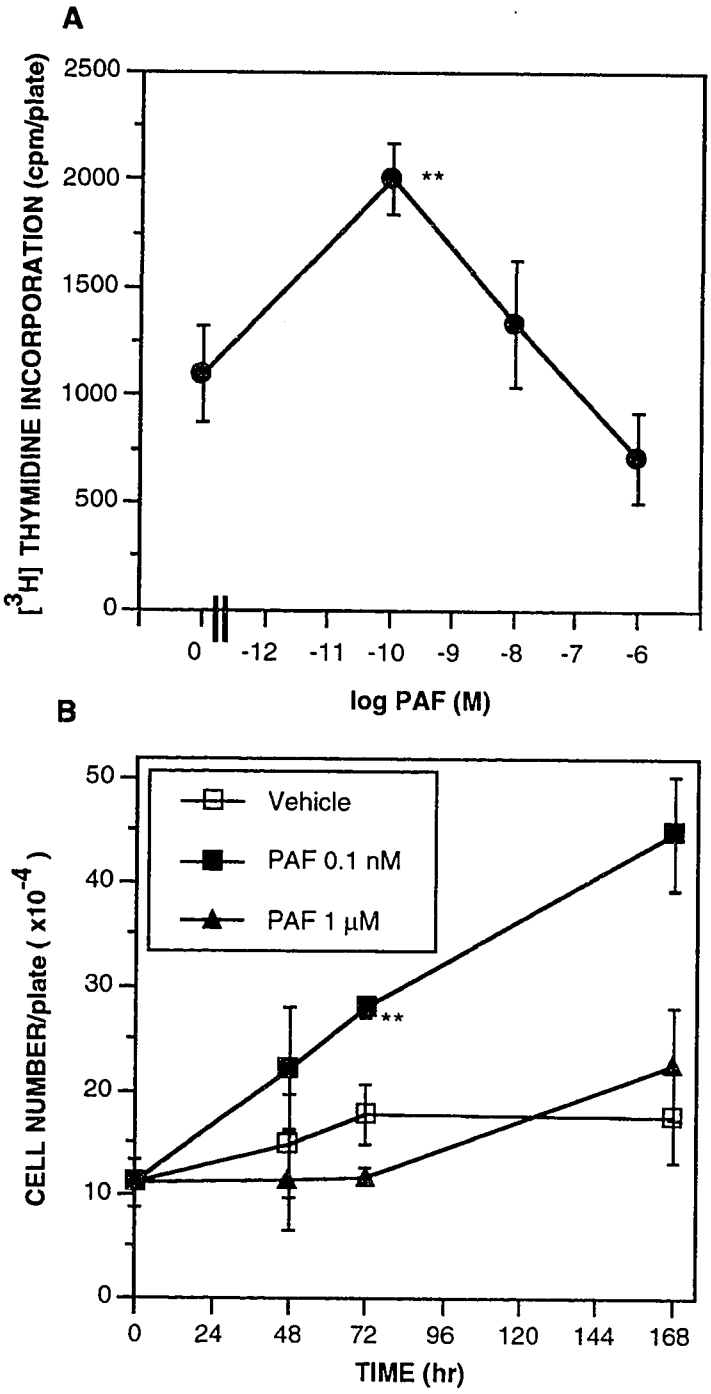

Figure 17. PAF dose-dependently alters cell proliferation and cell loss in HFs

HFs were made quiescent by serum starvation, treated with vehicle, PAF (0.1 nM-1 μM), or complete medium, and assayed for changes in [^{3}H]thymidine radiolabelling or cell number. Details as described in Materials and Methods.

(A) PAF exposure results in an inverted U [^{3}H]thymidine incorporation dose-response relationship in HFs.

Data represent mean±SEM cpm/plate from a minimum of 5 plates/condition after 72 hr of continual ligand treatment. Statistically significant differences were as follows: ANOVA: $F=5.1$, $df=3,29$, $p<0.01$. Dunnett's *t*: PAF (0.1 nM) vs. Vehicle, $p<0.01$. 10% FCS (positive control) increased [^{3}H]thymidine incorporation to 4445.6 ± 1026.9 cpm/plate at the same time point.

(B) Low doses of PAF induce cell proliferation; high doses of ligand induce cell death.

Data represent mean±SEM cell number from a minimum of 5 plates/treatment/time point using a Coulter Counter. Only adherent HFs were counted. PAF (1 μM)-treated HFs proved to be more capable of maintaining their attachment to tissue culture plates than RECs. After 72 hr of treatment, medium was replaced with fresh DMEM+0.5% FCS and cells were incubated in the absence of ligand for an additional 96 hr. Statistics were performed after 72 hr of continual PAF treatment on all of the doses tested. Data depicted are derived from treatment with 0.1 nM and 1 μM PAF only. Statistically significant differences were as follows: ANOVA: $F=4.4$, $df=3,29$, $p<0.01$. Dunnett's *t*: PAF (0.1 nM) vs. Vehicle, $p<0.01$. 10% FCS (positive control) increased cell number to 7.2×10^5 ± 3.6×10^4 cells/plate 72 hr after treatment.

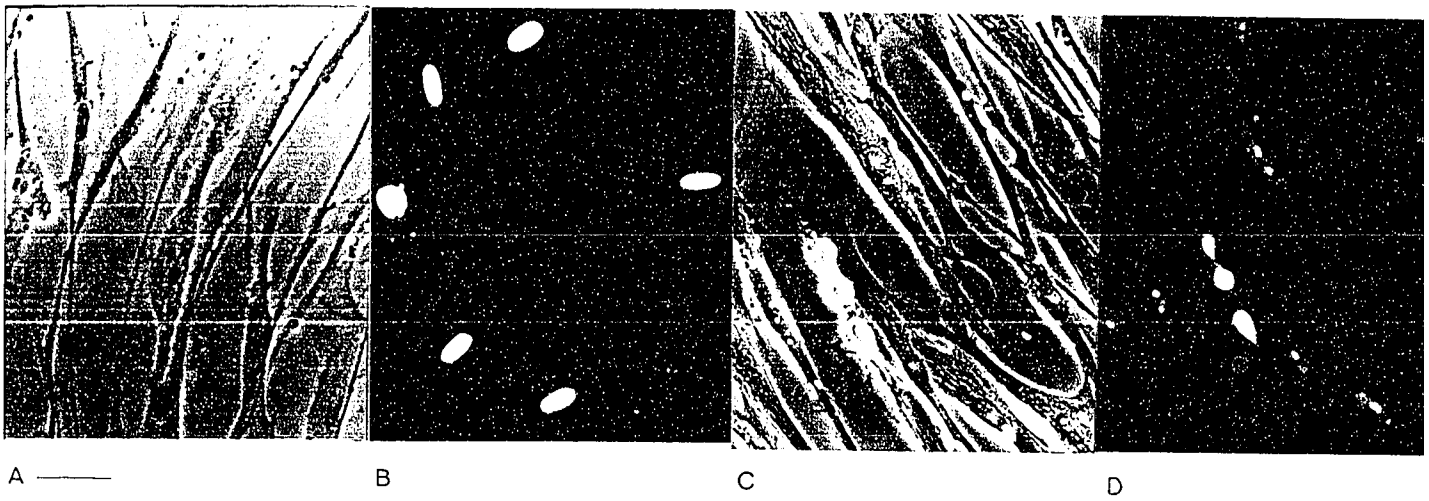

Figure 18. HFs exhibit nuclear condensation and fragmentation characteristic of ACD following treatment with PAF (1 μM)

HFs were made quiescent by serum starvation and then treated with vehicle or PAF (1 μM). After 48 hr, HFs were fixed with methanol and stained with ethidium bromide to assess nuclear changes as described in Materials and Methods. HFs were observed to become pyknotic and exhibit nuclear fragmentation and elaboration of apoptotic bodes upon exposure to PAF. Representative photomicrographs are depicted for the same sections after phase contrast and ethidium bromide visualization. (A) Vehicle, 48 hr, phase contrast. (B) Vehicle, 48 hr, ethidium bromide. (C) 1 μM PAF, 48 hr, phase contrast. (D) 1 μM PAF, 48 hr, ethidium bromide. Scale bar=10 μm.

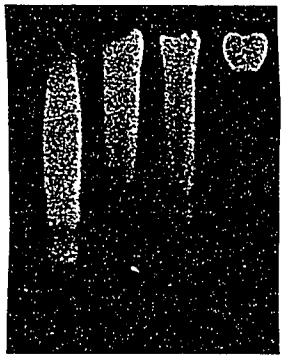

Figure 19. Demonstration of DNA ladders in PAF (1 μM)-treated cells

DNA was isolated from PAF (1 μM)-treated HFs at 0, 24, 48, and 72 hr (Lanes 1-4) after ligand administration as described in Materials and Methods. Nucleosome ladders were observed after 24-72 hr of treatment.

3. Long-term Phenotypic Transformation Induced by Brief Exposure to PAF

Abstract

Inflammation is a recognized risk factor for human cancer. To determine whether proinflammatory agents such as PAF can contribute to neoplastic transformation, RECs and HFs were exposed to physiologically relevant concentrations of the autacoid (1 pM - 1 μM) and assayed for long-term alterations in cell proliferation kinetics. A 1 hr exposure to PAF (10 nM - 1 μM) increased the ability of RECs to (i) form foci, (ii) reach a high saturation density in complete medium, (iii) grow in low serum-containing medium, and (iv) exhibit AI growth. Similar alterations in growth kinetics were achieved with C-PAF (0.1 - 10 nM), an active, non-metabolizable analogue of PAF, but not by lyso-PAF (0.1 - 1 μM), a biologically inactive metabolite of PAF. These results demonstrate that a brief exposure to PAF is capable of conferring enhanced growth potential in RECs. The relevancy of this observation to human cancers was determined by performing identical experiments on HFs. A 1 hr exposure to PAF increased the ability of HFs to (i) proliferate in low serum medium and (ii) grow in an AI environment. PAF did not affect HF growth kinetics in complete medium. Treatment with lyso-PAF, the immediate metabolite of PAF, did not impact on HF phenotype. These observations provide the first evidence that short-term treatment of normal rodent or human cells with PAF can induce long-term alterations in cell growth and demonstrate that this effect is specific for PAF and is not dependent upon downstream metabolites.

Introduction

Chronic inflammatory conditions have been associated with increased probability of developing cancer at sites such as lung, bladder, bowel, breast, and skin (1,2,5,8,17,27-31,34,36). Although the mechanisms underlying this correlation are uncertain, it is postulated that activated phagocytic cells at sites of inflammation release agents that promote the malignant conversion of non-inflammatory cells (30,31). One means of identifying candidate inflammatory 'carcinogens' is to assay for *in vitro* phenotypic transformation following exposure to the test compound. Tumour cells exhibit characteristic alterations in growth kinetics compared to normal cells when cultured *in vitro*. These phenotypes include altered morphology, growth factor independence, increased saturation density, focus formation, and anchorage AI growth (18). *In vitro* AI growth can be predictive of *in vivo* tumourgenicity (18). In Chapter III, Section 2, PAF was shown to dose-dependently mediate cell growth and cell death. These experiments were carried out in the constant presence of ligand. However, it is hypothesized that exposure to PAF during chronic inflammation takes the form of repeated transient stimulation (Chapter II, Section

5). *In vivo,* PAF is rapidly metabolized by specific intra and extracellular acetylhydrolases. Half-life has been found to range between 2 and 12 minutes systemically. Deficient PAF catabolism, resulting in extended half-life or sustained PAF turnover, exerts pathophysiological effects (Chapter II, Section 5). To determine whether extended but transient exposure to physiologically relevant concentrations of PAF is capable of conferring a transformed phenotype upon normal RECs and HFs, cells were treated for 1 hr with the autacoid and assayed for subsequent changes in morphology, viability, doubling time, focus formation, saturation density, growth in low serum-containing medium, and AI growth.

Materials and Methods

Treatment with PAF and related compounds

RECs and HFs (characterized in Chapter III, Section 2) were maintained in DMEM+10% FCS. RECs were between second and fifth passage and HFs were between third and seventh passage when treated. Exponentially growing cultures were trypsinized and 100,000 cells or 200 cells per 6 cm tissue culture dish were allowed to attach overnight. Cultures were washed twice with serum-free DMEM and subjected to one of the following treatments for 1 hr in DMEM containing 0.2% BSA (Sigma, MO): (a) vehicle (DMSO), (b) PAF (1 pM - 10 μM), (c) C-PAF (1 pM - 10 nM, Biomol Research, PA), or (d) lyso-PAF (0.1 nM - 1 μM). Cultures were then washed and incubated for 24 hr in DMEM+10% FCS before being tested for phenotypic transformation.

Assays of Cell Transformation

Following treatment, RECs were assayed for changes in (i) cell viability, (ii) doubling time, (iii) saturation density, (iv) focus formation, (v) growth in low serum medium, and (vi) AI growth. Cell viability was assessed by trypan blue exclusion and by clonogenic assay. In this latter procedure, cells were plated at a density of 200 cells/6 cm dish, treated for 1 hr as described above, and allowed to grow undisturbed in DMEM+10% FCS for 10 days with twice weekly feedings. Cultures were then fixed with methanol and stained with 1% methylene blue in 50% ethanol. The number of colonies comprising >50 cells were scored. Doubling time and saturation

density were determined over a 25 day period of exponential growth by cell counts using a Coulter Counter. Cell count data was confirmed by [^{3}H]thymidine incorporation into DNA as described in Chapter III, Section 2. Focus formation was determined by allowing cultures to grow undisturbed following treatment for 21 days, with gentle medium replacement every 5 days. Plates were then stained as described in Chapter III, Section 2. Foci of piled cells (>60 μm dia.) were scored using an Olympus inverted microscope. Growth in low serum medium was assessed by incubating cells in DMEM+0.5% FCS for 25 days and estimating growth kinetics by counting cells at intervals using a Coulter Counter. AI growth was determined by suspending cells at 37°C in 2 ml 0.3% molten agarose (BRL, MD) containing DMEM+10% FCS. This suspension was poured over a 3 mm layer of 0.6% agarose containing DMEM+10% FCS. The soft agarose layer was overlaid with 2 ml of liquid medium that was replaced every 5 days. AI colonies (>80 μm in dia.) were scored 10, 20, 30, 40, 50, and 60 days after plating using an inverted microscope. Several individual foci and AI colonies were isolated and cultured to determine cell viability and cloning efficiency. Some clones were analysed by immunohistochemistry as described in Chapter III, Section 2 to determine cell type. Statistical analyses were performed as described in Chapter III, Section 2.

Results and Discussion

Although a correlation between chronic inflammation and predisposition to cancer in humans has been recognized for many years, causal mechanisms have only begun to be determined. A wide variety of cytokines and proinflammatory agents are released by both activated phagocytes and non-inflammatory cells in and around sites of injury and irritation. It is hypothesized that these agents may play a role in tumour progression. To determine whether PAF is capable of mediating the sustained cell proliferation characteristic of transformed cells, RECs and HFs were isolated, treated with physiologically relevant concentrations of ligand (1 pM - 1 μM), and assayed for subsequent transformation.

Effect of PAF treatment on REC phenotype

The effects of PAF on doubling time, focus formation, saturation density, growth in low

serum, and AI growth are presented in Table 3. No indication of cytotoxicity was seen after any of the treatments (data not shown).

PAF had no effect on REC doubling time in complete medium although the compound did significantly increase saturation density with maximal effects observed following treatment with 1 μM PAF. This increase was accompanied by a dose-dependent augmentation in the number of foci observed. Foci were defined as tightly packed three-dimensional growths of piled cells (>60 μm in dia.) surrounded by a monolayer of contact-inhibited cells (Figure 20). The maximal quantifiable increase in focus formation (approximately 3-fold) occurred in RECs treated with 10 nM PAF. At higher concentrations (1 μM), scoring was not possible because discrete foci could not be accurately identified due to the substantial overgrowth of PAF-treated RECS (Figure 20C). This observation was substantiated by the 3-fold increase in saturation density exhibited in cultures treated with 1 μM PAF compared to vehicle-treatment (Table 3). Finally, PAF-induced foci were more irregular in shape, denser (i.e., cells stained more intensely), and exhibited a more disorderly pattern of growth than foci seen in vehicle-treated cultures (Figure 20).

A brief exposure to PAF was also capable of inducing cell proliferation under suboptimal growth conditions. For example, growth in low serum containing medium is one measure of autonomous cell growth (ie. the ability of cells to proliferate with limiting amounts of exogenous growth factors). As indicated in Table 3, PAF significantly reduced the doubling time of RECs grown in DMEM+0.5% FCS and increased the length of time that cells were able to sustain growth in low serum, as compared to vehicle-treated cultures. Furthermore, PAF also induced AI growth in RECs. AI growth represents the ability of cells to form colonies in a semi-solid medium. Colonies (>80 μm in dia.) were scored at 20, 40, and 60 days after treatment. Only data from day 40 are presented in Table 3. PAF (10 nM - 1 μM) induced a dose-dependent increase in AI ability. The growth rate of colonies was very slow. Small colonies (approximately 50 μm in dia.) could be seen at Day 20 after treatment. By Day 40, colonies had reached sizes of >80 μm in dia. By Day 60, colony size was not significantly larger than at day 40, suggesting that the growth of the AI cells had slowed or stopped. Growth cessation was not due to cell death since cloning efficiency of cells derived from day 40 and day 60 colonies did not differ (data not

Table 3. Transformation-associated properties in RECs exposed to PAF

Properties	Treatment[a]					
	Vehicle	PAF				
		1 pM	0.1 nM	10 nM	100 nM	1 μM
Doubling Time (h)[b]						
Cell count	33.5	37.2	31.6	32.4	ND	36.2
Thymidne incorp.	33.5	30.1	35.4	35.5	ND	36.3
Focus Formation[c] (colonies/plate)	50 ±18.1 n=5	63.4±19.3 n=5	78.3±25.9 n=6	135.9±32.4* n=7	OG	OG
Saturation Density[d] (cells/plate)	$1.1x10^6$ $\pm 3x10^5$	$8.8x10^6$ $\pm 5x10^4$	$1.1x10^6$ $\pm 9x10^4$	$2.1x10^6$ $\pm 1x10^{5*}$	ND	$3.8x10^6$ $\pm 5x10^{5**}$
Growth in low serum[e]						
Doubling time (h)	127±4.9	ND	90.6±1.3**	83.8±5.5**	ND	86.0±0.3**
Days of growth	6		21	21		21
AI colonies[f]	0	0	0	4.8±2.5	8.6±1.1*	22±5.3**

	C-PAF			Lyso-PAF		
	1 pM	0.1 nM	10 nM	0.1 nM	10 nM	1 μM
Doubling Time (h)[b]						
Cell count	ND	29.8	ND	ND	30.7	ND
Thymidne incorp.	ND	49.1	ND	ND	34.0	ND
Focus Formation[c] (colonies/plate)	66.4±10.9 n=3	95.5±7.3 n=3	OG	43±4.0 n=3	31±2.0 n=3	23.8±6.5 n=5
Saturation Density[d] (cells/plate)	ND	$9.3x10^5$ $\pm 2x10^4$	ND	ND	8.4 ± 10^5 $\pm 3x10^4$	ND
Growth in low serum[e]						
Doubling time (h)	ND	85±0.3**	ND	ND	135.6±5.2	ND
Days of growth		21			6	
AI colonies[f]	0.8±0.4	22.1±4.1**	ND	0	0	0

[a]Data represent the mean ± SEM of n=5 plates unless otherwise indicated. Asterisks indicate statistically significant differences as described in Materials and Methods (* $p<0.05$; ** $p<0.01$). ND, not determined.

[b]Doubling time in complete medium (DMEM+10%FCS) was determined using cell counts (n=3 plates) and [^{3}H]thymidine incorporation (n=2 plates) as described in Materials and Methods. Mean values are indicated.

[c]Foci (>60 μm in diameter) were counted 21 days after treatment as described in Materials and Methods. n, number of plates counted. OG, overgrowth of cells to a degree that individual foci could not be scored. PAF ANOVA: $F=2.7$, $df=3,43$, $p<0.05$; Dunnett's *t*: PAF 10 nM vs.Vehicle, $p<0.05$; C-PAF ANOVA: $F=3.0$, $df=2,15$, $p<0.05$; Dunnett's *t*: C-PAF 0.1 nM vs.Vehicle, $p<0.05$.

[d]The number of cells/6 cm diameter tissue culture dish was counted 10 days after saturation had been reached in vehicle-treated cultures as described in Materials and Methods. PAF ANOVA: $F=8.7$, $df=4,19$, $p<0.01$; Dunnett's *t*: PAF 10 n M vs.Vehicle, $p<0.05$; PAF 1 μM vs.Vehicle, $p<0.01$.

[e]Following treatment, cells were grown in DMEM+0.5% FCS. Doubling time was estimated during the first 10 days of culture. The length of time cells were able to sustain culture is indicated. Observations were carried out for 25 days. PAF ANOVA: $F=30.8$, $df=3,16$, $p<0.01$; Dunnett's *t*: PAF 0.1 nM vs.Vehicle, $p<0.01$; PAF 10 nM vs.Vehicle, $p<0.01$; PAF 1 μM vs.Vehicle, $p<0.01$; C-PAF: Student's $t=8.7$, $df=8$, $p<0.01$.

[f]The number of AI colonies (>80 μm in diameter)/ 6 cm dish ($1x10^5$ cell plated; 15% plating efficiency ; $1.5x10^4$ viable cells) were counted 40 days following treatment (n=5). PAF ANOVA: $F=12.4$, $df=5,24$, $p<0.01$; Dunnett's *t*: PAF 100 nM vs.Vehicle, $p<0.05$; PAF 1 μM vs.Vehicle, $p<0.01$; C-PAF ANOVA: $F=28.3$, $df=2,12$, $p<0.01$; Dunnett's *t*: C-PAF 1 pM vs.Vehicle, $p<0.01$; PAF 0.1 nM vs.Vehicle, $p<0.01$.

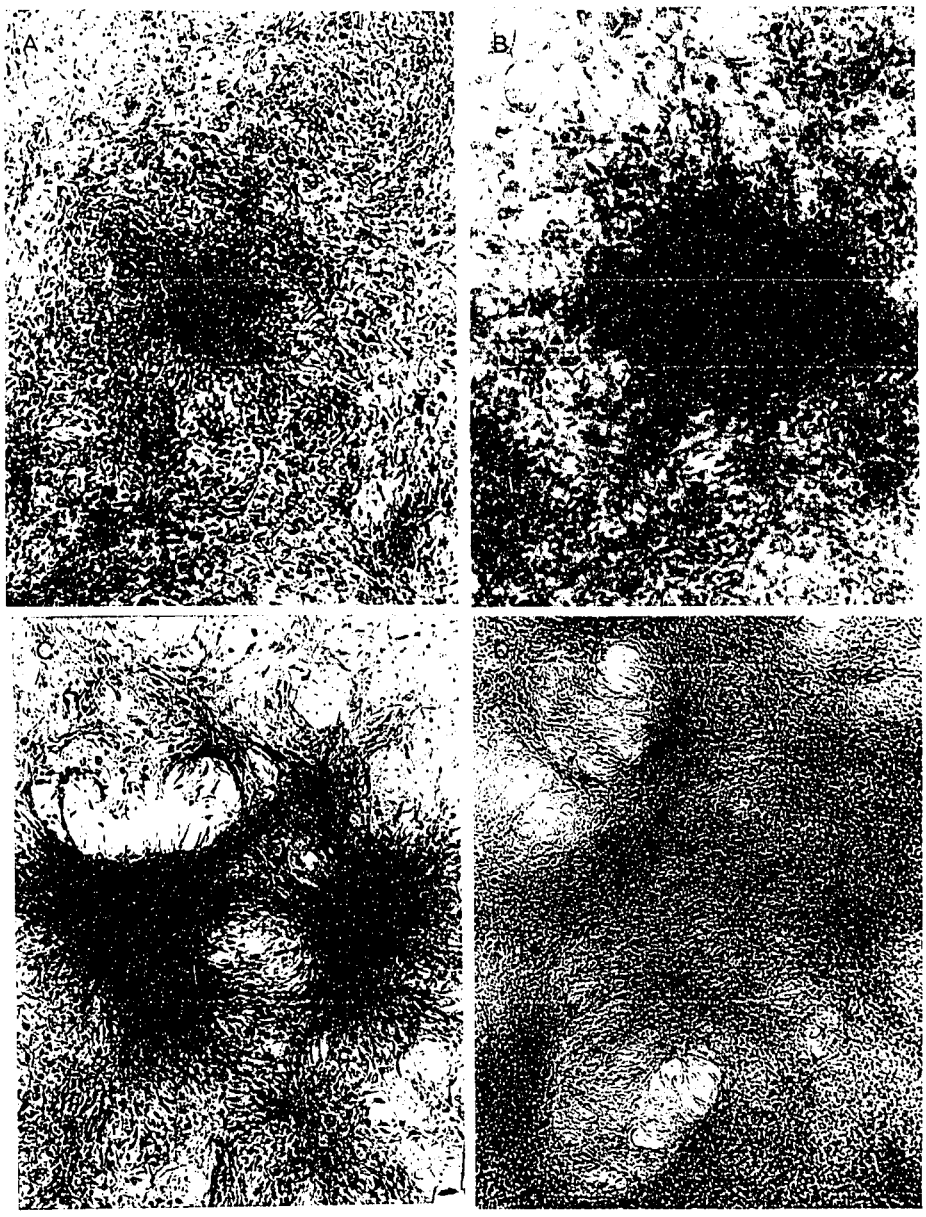

Figure 20. Focus formation in RECs following exposure to PAF

RECs were treated with PAF (1 pM - 1 μM) or vehicle (0.1% DMSO) as described in Materials and Methods and allowed to grow for 21 days undisturbed with twice weekly feedings. Cultures were stained with methylene blue and focus formation was quantified. Representative photomicrographs are depicted for the following treatments. (A) Vehicle. (B) 0.1 nM PAF. (C) 10 nM PAF. (D) 1 μM PAF. Scale bar = 20 μm.

shown).

The cell types involved in this response were identified immunohistochemically, Clones were isolated from 4 foci, 5 AI colonies, and 2 C-PAF-induced AI colonies. Two foci-derived clones were of epithelial cell origin; the rest were composed of fibroblasts. These data indicate that both fibroblasts *and* epithelial cells are capable of responding to PAF. This latter finding is of some importance given that epithelial cell-derived tumours (carcinomas) are the most common form of human malignancy.

The ability of PAF to induce phenotypic transformation appears to be PAF-specific since its effects follow the known potency of closely related compounds. C-PAF increased 3 of the 4 phenotypic properties tested at doses 2 orders of magnitude below that seen with PAF (Table 3). This 'shift to the left' in the dose-response curve is consistent with the fact that C-PAF is a non-metabolizable analogue of the endogenous ligand and hence capable of stimulating cells indefinitely. Lower doses are, as such, more effective at eliciting physiological responses. However, the compound also has a lower affinity for PAFR than PAF itself and, consequently does not produce the same intensity of response as the natural ligand (26). This property may explain the reduced magnitude of phenotypic transformation observed in the present experiments compared to PAF. Conversely, no phenotypic changes were observed after treatment with lyso-PAF, PAF's immediate (and inactive) metabolite.

In summary, these data indicate that the endogenous inflammatory agent, PAF, can induce long-term alterations in cell growth in RECs similar to those observed in tumour cells cultured *in vitro*.

Effect of PAF treatment on HF phenotype

Given that PAF, at physiologically relevant concentrations, can induce phenotypic changes associated with malignancy in murine cells, experiments were designed to determine relevancy to human cells. Figure 21 illustrates the dose-dependent effects of a 1 hr treatment with PAF (0.1 nM-10 μM) on growth of HFs in complete medium (Figure 21A), low serum medium (Figure 21B), and AI medium (Figure 21C). PAF had no observable effect on cell proliferation or morphology when cells were grown in complete medium. However, when cultured under serum-

deprived conditions, cells that had been treated with PAF (100 nM - 10 μM) sustained growth for a longer period of time than vehicle-treated cells. This effect was evident by Day 10 after ligand exposure and was statistically different by Day 25. When tested for growth in soft agarose (AI phenotype), colonies were seen in cultures treated with PAF at concentrations of 100 nM and higher. The growth rate of AI cells was very slow, requiring 40 days for colonies to reach >80 μm in dia. By day 60, colony size was not significantly larger than at day 40, suggesting that the growth of the AI cells had slowed or stopped. However, this apparent growth cessation was not due to cell death since the cloning efficiency of cells derived from day 40 and day 60 colonies did not differ (data not shown). These results demonstrate that PAF is capable of inducing phenotypic characteristics in normal human cells commonly associated with tumour cells cultured *in vitro*, viz., the ability to proliferate with limiting amounts of exogenous growth factors (autonomous cell growth in low serum medium) and the ability to clonally expand in a non-permissive environment (AI growth). As with RECs, lyso-PAF was inactive in mediating the phenotypic transformation of HFs in all three assays (Figure 22). This lack of effect was not the result of cytotoxicity since 1 hr treatments with either PAF or lyso-PAF did not alter cell viability at any of the concentrations tested (data not shown).

In summary, PAF is capable of inducing a transformed phenotype in HFs similar to that observed in RECs with one exception. PAF was capable of increasing cell proliferation in rodent cells under conditions of normal and suboptimal growth (ie. PAF treatment caused an increase in REC saturation density, focus formation, growth in low serum medium, and AI growth.) In HFs, an effect of PAF was seen only under suboptimal growth conditions (ie. enhanced growth in low serum medium and AI growth). If PAF is indeed a factor contributing to the enhancement of malignancy associated with inflammation, its efficacy and underlying signal transduction pathways in human and rat may differ.

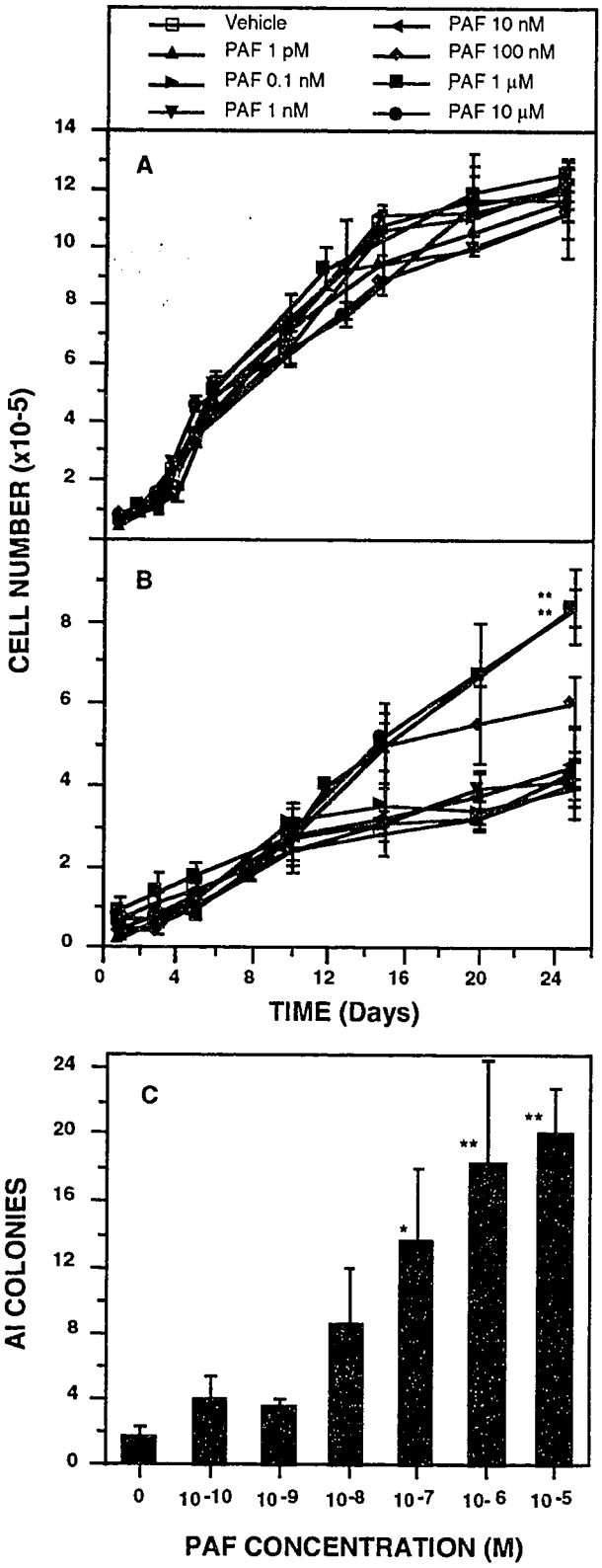

Figure 21. Phenotypic transformation of HFs by PAF

Cells were treated with PAF and assayed for changes in
(A) saturation density
(B) growth in low serum medium
(C) AI growth.

In (A) and (B), data represent cell counts from a minimum of 5 plates per treatment per time period. In (C), data represent the number of AI colonies (>80 µm dia.) per 100,000 cells plated, as scored at Day 40 after treatment (n= 5 plates/condition). Statistical tests (ANOVA, *post hoc* Dunnett's *t* test) were performed on day 25 (A and B) and day 40 (C). Statistically significant results are as follows: Growth in low serum (B): ANOVA, F=7.1, df=7,40, $p<0.01$; Dunnett's *t* test, PAF (1 µM) versus vehicle, $p<0.01$; PAF (10 µM) versus vehicle, $p<0.01$. AI growth (C): ANOVA, F=4.1, df=6,28, $p<0.05$; Dunnett's *t* test, PAF (100 nM) versus vehicle, $p<0.05$; PAF (1 µM) versus vehicle, $p<0.01$; PAF (10 µM) versus vehicle, $p<0.01$. Cloning efficiency in soft agarose was calculated by dividing the number of AI colonies observed per plate by the number of cells capable of forming monolayer colonies when plated in liquid medium (plating efficiency) x 100. Untreated or vehicle-treated HFs exhibited a cloning efficiency in soft agarose of 0.01%. PAF (1 µM) treatment increased cloning efficiency 15 fold (0.15%). Other details as in Material and Methods.

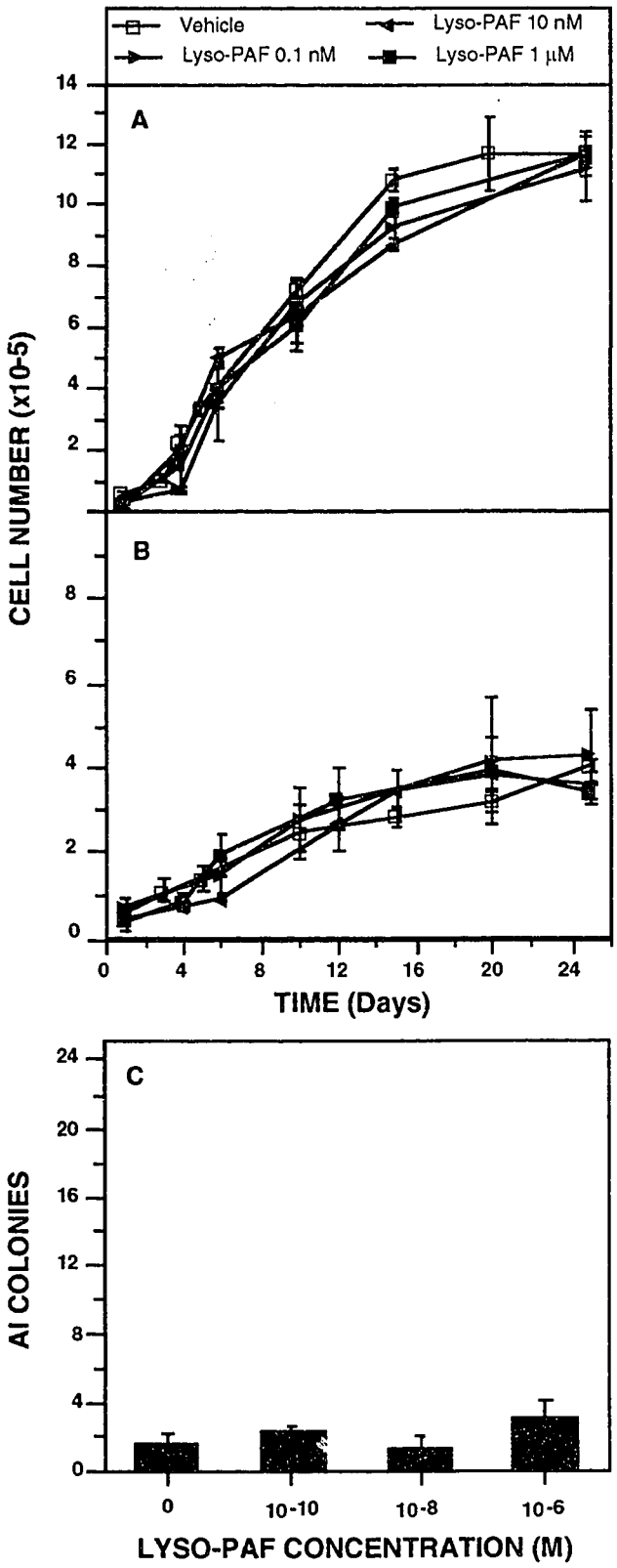

Figure 22. Absence of phenotypic transformation of HFs by lyso-PAF

Cells were treated with lyso-PAF and assayed for changes as in Figure 21. Data represent cell counts from a minimum of 5 plates per treatment per time period in (A) and (B). In (C), data represent the number of AI colonies (>80 μm dia.) per 100,000 cells plated as scored on Day 40 after treatment (n= 5 plates/condition). No statistically significant effect was observed in any of the assays. Other details as in Figure 21.

4. Signal Transduction Events Underlying PAF-Mediated Transformation

Abstract

A brief exposure to PAF was found to induce sustained cell growth in RECs and HFs within a variety of phenotypic assays. To identify putative signal transduction molecules mediating these effects, cells were treated with PAF in the presence of either a PAF antagonist (CV3988, 1 μM or 10 μM), a tyrosine kinase inhibitor (genestein, 1 μg/ml), a PKC inhibitor (staurosporine, 50 nM), or a cyclooxygenase inhibitor (indomethacin, 200 nM - 20 μM). Cells were assayed for changes in (i) cell viability, (ii) doubling time, (iii) focus formation, (iv) saturation density, (v) growth in low serum medium, and (vi) AI growth. PAF increased REC focus formation and saturation density and induced growth in low serum and AI growth in both RECs and HFs. These growth enhancements could be inhibited by treatment with either CV3988 or genestein, suggesting involvement of PAFRs and tyrosine kinase activity in PAF-mediated signal transduction in both cell types. In RECs, indomethacin attenuated PAF-induced increases in focus formation and saturation density without affecting PAF-induced alterations in growth in low serum or AI phenotype. RECs were insensitive to effects of staurosporine on PAF-induced transformation. In HFs, indomethacin had no effect while staurosporine blocked PAF-induced growth enhancement. These data indicate that PAF-mediated alterations in REC and HF phenotype are likely receptor-mediated and dependent upon protein tyrosine kinase activity. These data also suggest either that prostaglandins may mediate PAF-induced growth potentiation under optimal but not sub-optimal growth conditions or, alternatively, that species differences in PAF signal transduction pathways differentiate the two cell types.

Introduction

In other experimental systems, PAF has been shown to work through specific cell surface and intracellular receptors to induce calcium transients, arachidonic acid metabolism, phosphoinositide turnover, protein kinase activity, and proto-oncogene expression (Chapter II, Section 5). Since previous investigations demonstrate that PAF is capable of altering the cell growth and cell death kinetics in RECs and HFs (Chapter III, Sections 2 and 3) and recent reports reveal that systemic PAF levels are elevated in Crohn's disease, a preneoplastic inflammatory disorder (9,10,35), prostatic carcinoma (14), leukemia (14), nasopharyngeal carcinoma (14), histiocytic lymphoma (14), and metastatic melanoma (14), attempts were made to identify candidate signal transduction molecules underlying PAF's potential contribution to these malignant disorders.

Materials and Methods

Treatment and transformation assays

RECs and HFs (characterized in Chapter III, Section 2) were treated as described in Chapter III, Section 3 with the exception that cultures were also exposed to either vehicle or PAF (100 nM or 1 μM) in combination with CV3988 (1 - 10 μM, Calbiochem, CA), indomethacin (200 nM - 2 μM, Sigma, MO), staurosporine (50 nM, LC Services, MA), or genestein (1 μg/ml, UBI, MA). When treated with two compounds, the antagonist or inhibitor was added 15 min prior to coincubation and treatment continued for 1 hr following PAF or vehicle administration. Cultures were then washed and incubated for 24 hr in DMEM+10% FCS before being assayed for phenotypic transformation as described above (Chapter III, Section 3). Statistical analyses were performed as described in Chapter III, Section 2.

Results and Discussion

In other cell types, interaction of PAF with its receptor has been shown to lead to increases in PKC activity (4,25,38), tyrosine phosphorylation (6,15,33,38), and metabolism of arachidonic acid through the cyclooxygenase pathway (13). To ascertain whether these biochemical steps mediate PAF-induced phenotypic transformation of RECs and HFs, cells were coincubated with PAF and either CV3988 (a PAFR antagonist), staurosporine (a putative PKC inhibitor), genestein (a putative tyrosine kinase inhibitor), or indomethacin (an inhibitor of cyclooxygenase metabolism of arachidonic acid).

Effect of inhibitor treatment on PAF-induced REC phenotype

None of the treatments altered cell viability with the exception of staurosporine (50 nM) or staurosporine+PAF (1 μM). Cell viability was reduced by 30% under these conditions (data not shown). These results are in accordance with other data demonstrating toxic effects of staurosporine across a variety of concentrations (3). The effects of pharmacological manipulation on PAF-induced focus formation, saturation density, growth in low serum, and AI growth are depicted in Figures 23 and 24. Administration of CV3988 (1 μM) attenuated PAF-induced increases in each of the four growth parameters, indicating that PAF most likely works through a

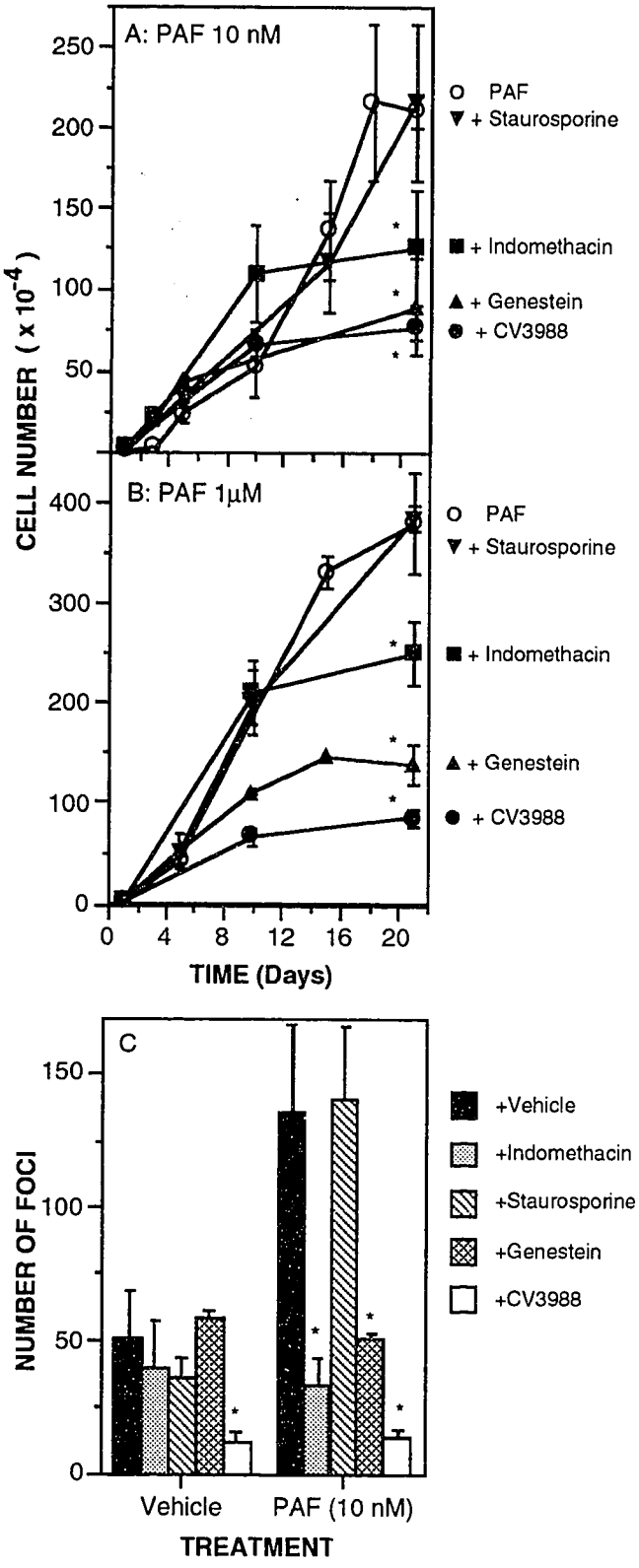

Figure 23. PAF-induced phenotypic transformation of RECs grown in complete medium is dependent upon PAFR, tyrosine kinase activity, and cyclooxygenase metabolites of AA but not on PKC activity.

RECs were treated with either vehicle or PAF (10 nM or 1 μM) and CV3988 (1 μM), indomethacin (200 nM), staurosporine (50 nM), or genestein (1 μg/ml) for 1 hr as described in Materials and Methods. Cells were subsequently assayed for changes in
(A,B) saturation density
(C) focus formation

Data represent cell or foci counts from a minimum of 5 plates per treatment per time period. Co-treatment had no effect on the saturation density phenotype of vehicle-treated cells (data not shown) but did alter focus formation. Statistical tests (ANOVA, post hoc Dunnett's *t* test) were performed on day 21. Statistically significant results are as follows: Saturation density: PAF (1 μM) ANOVA, $F=21.4$, $df=4,25$, $p<0.01$. Dunnett's *t* test: PAF vs. PAF+CV3988, $p<0.01$, PAF versus PAF+Genestein, $p<0.01$. PAF (10 nM) ANOVA, $F=7.1$, $df=4,25$, $p<0.05$. Dunnett's *t* test: PAF vs. PAF+CV3988, $p<0.05$, PAF vs. PAF+Genestein, $p<0.05$. Focus Formation: Vehicle ANOVA, $F=4.6$, $df=4,29$, $p<0.05$. Dunnett's *t* test: Vehicle vs. Vehicle+CV3988, $p<0.05$. PAF (10 nM) ANOVA, $F=5.2$, $df=4,29$; $p<0.05$. Dunnett's *t* test: PAF vs. PAF+CV3988, $p<0.05$, PAF vs. PAF+Genestein, $p<0.05$, PAF vs. PAF+Indomethacin, $p<0.05$.

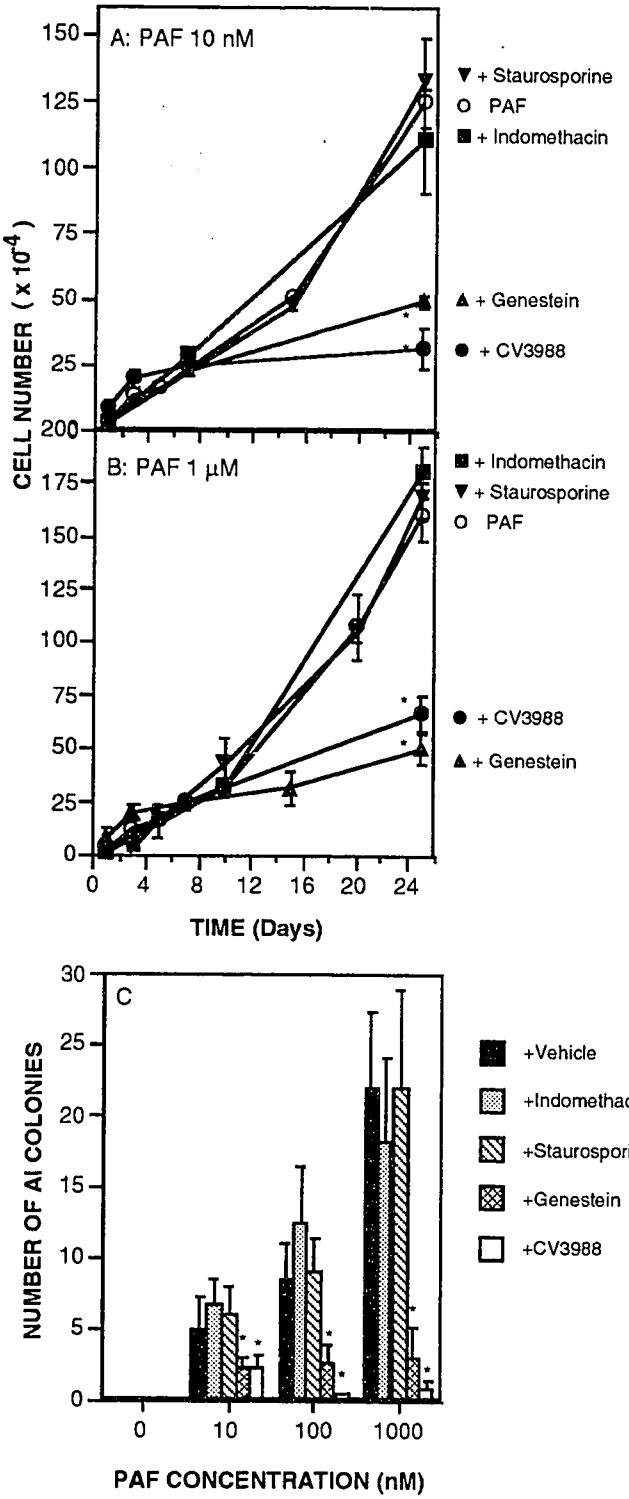

Figure 24. PAF-induced phenotypic transformation of RECs grown under suboptimal growth conditions is dependent upon PAFR and tyrosine kinase activity but not on cyclooxygenase metabolites of AA or PKC activity.

RECs were treated with either vehicle or PAF (10 nM or 1 μM) and CV3988 (1 μM), indomethacin (200 nM), staurosporine (50 nM), or genestein (1 μg/ml) for 1 hr as described in Materials and Methods. Cells were subsequently assayed for changes in (A,B) growth in low serum medium (C) AI growth

Data represent cell or AI colony counts from a minimum of 5 plates per treatment per time period. Co-treatment had no effect on the phenotype of vehicle-treated cells (data not shown). Statistical tests (ANOVA, post hoc Dunnett's *t* test) were performed on day 25 (A,B) or day 40 (C). Statistically significant results are as follows: Growth in low serum: PAF (1 μM) ANOVA, $F=31.5$, $df=4,25$, $p<0.01$. Dunnett's *t* test: PAF vs. PAF+CV3988, $p<0.01$, PAF vs. PAF+Genestein, $p<0.01$. PAF (10 nM) ANOVA, $F=23,6$, $df=4,25$, $p<0.01$. Dunnett's *t* test: PAF vs. PAF+CV3988, $p<0.01$, PAF vs. PAF+Genestein, $p<0.05$. AI growth: PAF (1 μM) ANOVA, $F=10$, $df=4,20$, $p<0.01$. Dunnett's *t* test: PAF vs. PAF+Genestein, $p<0.01$; PAF vs. PAF+CV3988, $p<0.01$.

specific receptor in RECs. Genestein (1 μg/ml) pretreatment also prevented all of the PAF-induced changes. This observation suggests that stimulation of PAF receptors with ligand leads to a protein tyrosine phosphorylation event(s) that is important in PAF-mediated transformation of RECs. Despite its cytotoxic effects, staurosporine failed to alter the kinetics of any of the four growth parameters even when corrected for the reduction in cell viability, suggesting that PKC may not play a role in PAF-induced proliferation in RECs. Indomethacin (200 nM) blocked PAF-induced changes in focus formation and saturation density but failed to alter PAF-induced growth in low serum or AI growth. These data suggest that PAF acts through multiple pathways and that the phenotypic transformation observed when cells are grown under optimal conditions (ie. anchorage-dependent environment, complete medium) may depend upon PAF-induced synthesis of cyclooxygenase metabolites (eg. prostaglandins). Indomethacin's inability to alter other transformation parameters suggests that cyclooxygenase metabolites may not mediate alterations in cell growth under suboptimal conditions (ie. AI environment, low serum medium).

Effect of PAF treatment on HF phenotype

PAF was found to induce growth in low serum medium and AI growth in HFs. The effect of coincubation with indomethacin (200 nM - 20 μM), staurosporine (50 nM), genestein (1 μg/ml), or CV3988 (10 μM) on these growth parameters is depicted in Figure 25 and 26 respectively. Treatment with CV3988 in conjunction with PAF was found to inhibit all growth potentiation associated with PAF treatment, indicating that the observed phenotypic alterations are likely receptor-mediated. Similar attenuation was observed when cells were coincubated with PAF and either staurosporine (50 nM) or genestein (1 μg/ml). These data implicate protein kinases in PAF-mediated HF transformation. Indomethacin (200 nM - 20 μM) had no effect on PAF-induced growth in low serum medium or AI phenotype, suggesting that cyclooxygenase metabolites may not influence PAF's ability to transform HFs.

As with RECs, PAF-mediated transformation of HFs was receptor-mediated, PAF-specific, and tyrosine kinase-dependent. However, unlike RECs, HFs behaved differently with respect to cyclooxygenase and protein kinase C inhibitors. PAF-induced transformation of rodent cells was partially inhibited by indomethacin and insensitive to staurosporine while PAF-mediated

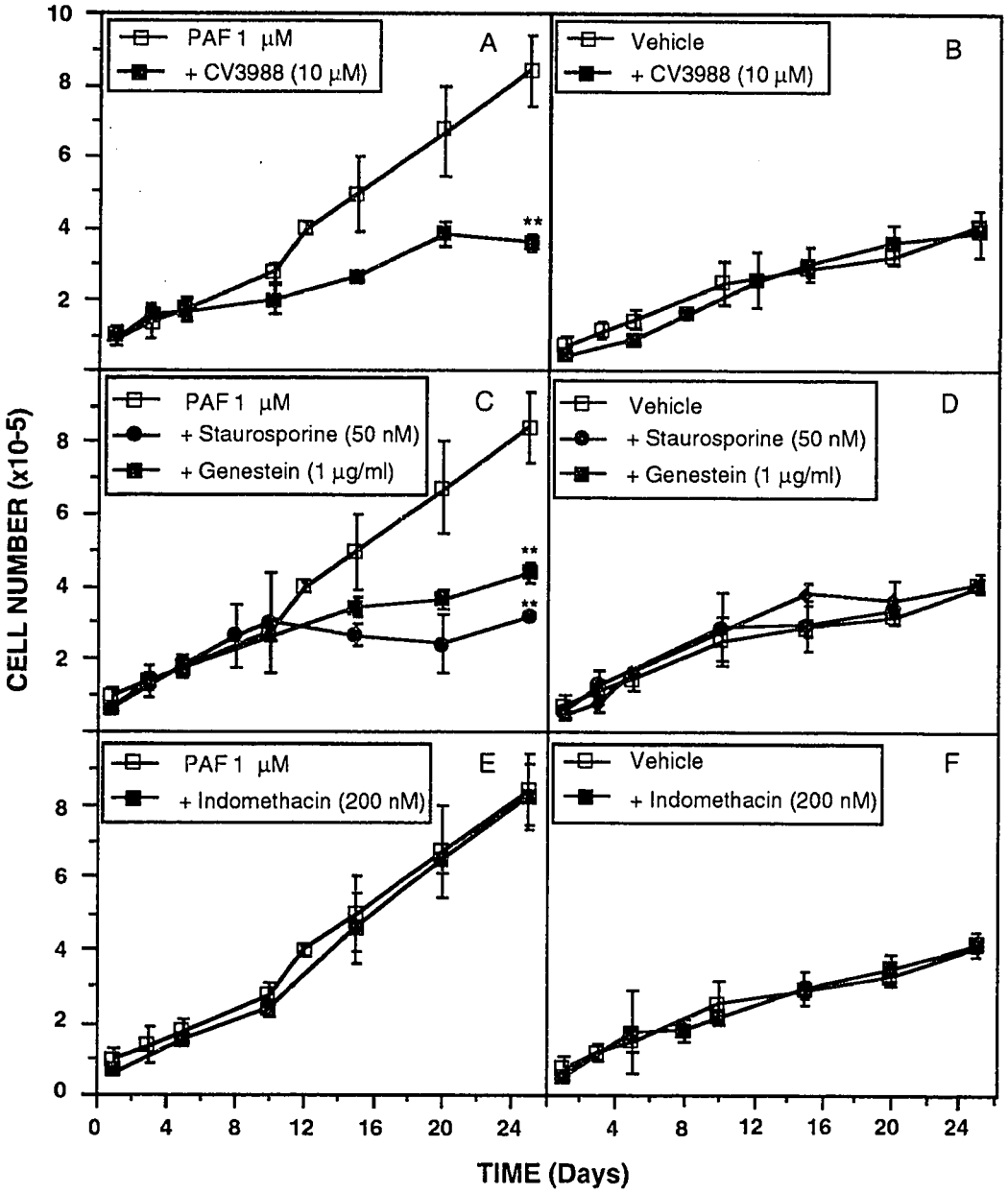

Figure 25. PAF-induced phenotypic transformation of HFs under suboptimal growth conditions is dependent upon PAFR and tyrosine kinase activity but not on cyclooxygenase metabolites of AA or PKC activity

HFs were treated with either vehicle (B,D,F) or PAF (1 μM) (A,C,E) and CV3988 (1 μM) (A,B), indomethacin (200 nM-20 μM) (E,F), staurosporine (50 nM) (C,D), or genestein (1 μg/ml) (C,D) for 1 hr as described in Materials and Methods. Cells were subsequently assayed for changes in growth in low serum medium. In E and F, data are presented only for 200 nM indomethacin. Increasing the concentration of inhibitor had no effect on PAF-induced growth in low serum (data not shown). Data represent cell counts from a minimum of 5 plates per treatment per time period. Statistical tests (Students *t* test or ANOVA, *post hoc* Dunnett's *t* test) were performed on day 25. Statistically significant results are as follows: PAF vs. PAF + CV3988: Student's $t = 4.8$, df=9, $p<0.01$; PAF vs. PAF + Kinase Inhibitors: ANOVA, F=18.7, df=2,23, $p<0.01$; Dunnett's *t* test: PAF vs. PAF + Staurosporine, $p<0.01$, PAF vs. PAF + Genestein, $p<0.01$.

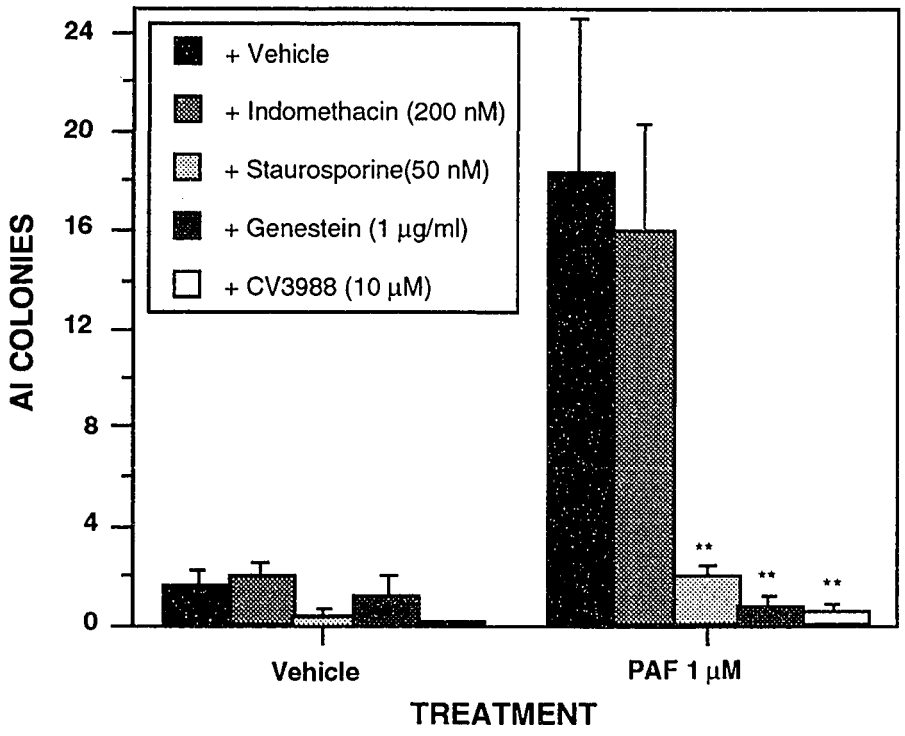

Figure 26. PAF-induced AI growth in HFs is dependent upon PAFR and tyrosine kinase activity but not on cyclooxygenase metabolites of AA or PKC activity

HF's were coincubated with PAF (1 µM) or vehicle and either CV3988 (10 µM), staurosporine (50 nM), genestein (1 µg/ml), or indomethacin (200 nM) for 1 hr as described in Materials and Methods. Data represent the number of AI colonies >80 µm per 100,000 cells plated as scored on day 40 after treatment (n= 5 plates/ condition). Statistical tests (ANOVA, *post hoc* Dunnett's *t* test) were performed on Day 25. Statistically significant results are as follows: PAF treatment: ANOVA, $F=4.8$, $df=4,22$, $p<0.01$; Dunnett's *t* test: PAF versus PAF+ CV3988, $p<0.01$, PAF vs. PAF+Staurosporine, $p<0.01$, PAF vs. PAF+Genestein, $p<0.01$.

HF transformation was insensitive to indomethacin and inhibited by staurosporine. However, it is important to note that indomethacin was only effective in inhibiting PAF-induced alterations in REC phenotype when cells were tested under optimal growth conditions. This fact indicates that indomethacin may only influence PAF signal transduction when stimulation occurs in the presence of excess endogenous growth factors. These data are summarized in Table 4. If PAF is indeed a factor contributing to the enhancement of malignancy associated with inflammation, its efficacy and underlying signal transduction pathways in human and mouse may differ depending upon environmental conditions.

Table 4. Summary of antagonist/inhibitor data

Treatment[a]	Transformation assays[b]							
	REC				HF			
	Optimal[c]		Suboptimal		Optimal		Suboptimal	
	1	2	3	4	1	2	3	4
PAF	+	+	+	+	NE	NE	+	+
+ Indomethacin	+/-	+/-	+	+	NE	NE	+	+
+ Staurosporine	+	+	+	+	NE	NE	-	-
+ Genestein	-	-	-	-	NE	NE	-	-
+ CV3988	-	-	-	-	NE	NE	-	-

[a]Concentrations as indicated in text

[b]1=saturation density; 2=focus formation; 3-growth in low serum medium; 4=Al growth. +, indicates enhanced growth; +/-, indicated partial attenuation of PAF-induced phenotype; -, indicates inhibition of PAF-induced phenotype; NE, indicates no effect.

[c]Assays are categorized into optimal and suboptimal culture conditions based on parameters described in the text.

5. Oxyradical Contribution to PAF-Mediated Transformation

Abstract

Exposure to oxyradicals has been shown to induce heritable morphological alterations, decreases in cell doubling time, autonomous cell proliferation, and AI growth in normal epithelial cells and fibroblasts (28,40,44). To determine whether PAF depends upon oxyradical production to induce long-term growth enhancement in RECs and HFs, phenotypic transformation following 1 hr treatment with oxyradicals or oxyradical-generating systems was compared to that elicited by PAF administration. RECs and HFs were exposed to vehicle, H_2O_2 (12.5 - 50 μM), TPA (0.1 - 100 nM), xanthine (100 μM)-xanthine oxidase (0.1 - 4 μg/ml), PAF (0.1 nM - 1 μM), or isolated human neutrophils activated with either TPA or PAF in the presence or absence of superoxide dismutase (SOD: 25 μg/ml) and/or catalase (6.25 - 100 U/ml). Target RECs and HFs were assayed for changes in (i) cell viability, (ii) doubling time, (iii) focus formation, (iv) saturation density, and (v) AI growth. Oxyradicals and oxyradical-generating systems were dose-dependently cytotoxic to RECs and HFs. No cytotoxicity was observed following PAF treatment. Relative cytotoxicity correlated with either the concentration of reactive oxygen species added to the medium or to the efficacy of the system in generating a respiratory burst. PAF was the least effective agent tested in eliciting oxyradical production and the least cytotoxic. However, only PAF, TPA, PAF-treated neutrophils, and TPA-treated neutrophils were found to increase phenotypic transformation. Equimolar concentrations of PAF were more effective at transforming RECs and HFs (3-fold increases in saturation density and AI cloning efficiency) than TPA (no increases in saturation density and a 2-fold increase in AI cloning efficiency). TPA-induced AI transformants were, however, more genetically stable than PAF-transformed clones demonstrating faster growth rates in soft agarose and enhanced cloning efficiency upon retesting compared to PAF-treated colonies. Both TPA- and PAF-induced phenotypic transformation following direct exposure could be attenuated by treatment with SOD and/or catalase, implicating $O_2^{\cdot}$ and H_2O_2 in the mediation of long-term growth enhancements. When RECs were co-cultured with TPA- or PAF-activated neutrophils, PAF treatment was more effective than TPA in eliciting target cell transformation despite the fact that TPA (10 nM) induced a 10-fold stronger respiratory burst in human neutrophils than PAF (10 nM). Data demonstrate that TPA- and PAF-treated neutrophils release agent(s) that elicit cell proliferation in RECs and HFs. Two possibilities are discussed. (1) DNA damage elicited by H_2O_2 mediates target cell transformation. (2) Stimulation with proinflammatory agents elicits an autocrine feedback loop through an H_2O_2 intermediary that sustains cell proliferation. It is suggested that TPA works through the former mechanism to elicit phenotypic transformation while PAF works through the latter mechanism to sustain cell growth.

Introduction

As reviewed in Chapter II, Section 3, oxyradicals may be involved in the pathogenesis of cell proliferative disorders. Oxidative damage of DNA is believed to mediate malignant transformation by promoting successive genetic alterations in exposed cells leading to growth deregulation (27,39,43). Because PAF has been shown, in inflammatory cells, to elicit a weak respiratory burst (Chapter II, Section 5), the possibility that oxyradicals may play a role in PAF-induced phenotypic transformation of RECs and HFs was assessed. Cells were exposed to

oxyradical-generating agents (TPA, xanthine-xanthine oxidase), oxyradicals (H_2O_2), or human neutrophils activated with either TPA or PAF in the presence or absence of oxyradical scavengers (superoxide dismutase (SOD), catalase) and alterations in growth kinetics were determined as described in the previous experiments (Chapter III, Sections 3-4).

Materials and Methods

Cells and cell culture

RECs and HFs were as described in Chapter III, Sections 2-4. Polymorphonuclear neutrophils were isolated from normal human donors essentially as described in (39) with the exception that sterile solutions and procedures were employed. Neutrophils were judged to be 99% polymorphonuclear leukocytes by microscopic examination of Wright's stained samples.

Treatment and transformation assays

RECs and HFs (characterized in Chapter III, Section 2) were treated as described in Chapter III, Section 3 with the exception that cultures were exposed to either vehicle, PAF (1 μM), PAF + SOD (25 μg/ml; Sigma, MO) and/or catalase (100 U/ml; BDH, Ont), H_2O_2 (12 - 50 μM; Sigma, MO), TPA (0.1 nM - 1 μM), or xanthine (100 μM; Sigma, MO) - xanthine oxidase (0.1-4 μg/ml; Sigma, MO). RECs were also coincubated with vehicle-treated human neutrophils, TPA (10 - 100 nM)-treated neutrophils, or PAF (1 pM - 10 nM)-treated neutrophils. Where treatment with oxyradical scavengers is indicated, inhibitors were added 15 min prior to co-incubation and treatment continued for 1 hr following PAF or vehicle administration. The ability of these compounds to induce oxyradical production in human neutrophils was confirmed spectrophotometrically by reduction of cytochrome C as described in (24). Where treatment with neutrophils is indicated, $5x10^5$ white blood cells were exposed to ligand or vehicle in DMEM+0.2% BSA for 5 min at 37°C, washed free of activator in PBS, and co-incubated with target cells for 1 hr in DMEM+0.2% BSA. REC and HF cultures were then assayed for phenotypic transformation as described above (Chapter III, Section 3). Some AI colonies were cloned and grown to a suitable density to permit further immunohistochemical analysis as

described in Chapter III, Section 3. These cells were also retested for long-term phenotypic transformation in the absence of further treatment as described in Chapter III, Section 7. Statistical analyses were performed as described in Chapter III, Section 2.

Results and Discussion

Comparison of treatment with oxyradical-generating agents and PAF on REC transformation

Activated phagocytes at sites of chronic inflammation release agents that may mediate malignant transformation of neighbouring cells. As indicated in Chapter II, Section 3, experimental evidence implicates oxyradicals in this process. TPA acts directly on PKC to induce a powerful respiratory burst in inflammatory cells and may stimulate oxyradical production in non-inflammatory cells. Xanthine-xanthine oxidase treatment chemically generates exogenous O_2^- that spontaneously converts into H_2O_2. PAF has been shown to elicit a wide variety of responses associated with phagocytic activation including respiratory burst, adherence to endothelial cells, and enhanced phagocytosis (Chapter II, Section 5). Coincubation of primary murine cell explants with activated phagocytes or oxyradical-generating systems has been shown to induce heritable *in vitro* phenotypic alterations in target cells and increased tumourgenicity when transformed clones are implanted in syngeneic or athymic hosts (5,11,12,32,39,43). In the present series of experiments, a similar rate of *in vitro* transformation was observed upon direct exposure of RECs to oxyradical-generating agents (Table 5). TPA (100 nM) was found to induce AI growth. While cloning efficiency did not reach statistical significance, the reliability of the data was confirmed by four observations. First, TPA-induced AI colonies were the fastest growing colonies observed across treatments with colony size reaching over 300 μm in 30 days. Second, induction of AI growth appeared to be blocked by co-administration of 100 U/ml catalase during TPA treatment indicating specificity of the response for oxyradical (H_2O_2) production (data not shown). Third, cells derived from TPA-induced AI colonies were morphologically transformed (Figure 27). Fourth, TPA-induced clones (Aga1-5) demonstrated enhanced AI growth (Cloning efficiency: Aga1, 0.28%; Aga2, 0.28%; Aga3, 0.46%; Aga4, 0.37%; Aga5, 0.67%) compared to untreated RECs cultured for an equivalent period time (Cloning efficiency: <0.01%).

In every case, PAF was more effective at eliciting alterations in REC focus formation,

Table 5. Transformation-associated properties in RECs exposed to oxyradicals

Properties	Treatment[a]						
	Vehicle	PAF		TPA			
		10 nM	1 μM	0.1 nM	1 nM	10 nM	100 nM
Cytotoxicity[b] (% viability)	100±6.3 (n=6)	103.2±11.7 (n=6)	112.7±9.3 (n=6)	107 ±2.7	117.8 ±17.1	82.7 ±10.5	45.2 ±3.9**
Focus Formation[c] (colonies/plate)	50 ± 18.1 (n=5)	135.9±32.4* (n=7)	OG	41.1 ±6.9	60.7 ±18.6	38.4 ±8.5	26.7 ±11.6
Saturation Density[d] (cells/plate)	$1.1x10^6$ $\pm 3x10^5$	$2.1x10^6$ $\pm 1x10^{5*}$	$3.8x10^6$ $\pm 5x10^{5**}$	ND	$1.6x10^6$ $\pm 2x10^5$	ND	ND
AI colonies[e]	0	4.8±2.5	22±5.3**	ND	0.4±0.2	0.6±0.6	1.2±0.4
Cloning efficiency [f] (%)	<0.01	0.03	0.15	ND	<0.01	<0.01	0.02

	Xanthine (100 μM)/Xanthine Oxidase					
	0 μg/ml	0.1 μg/ml	0.5 μg/ml	1 μg/ml	2 μg/ml	4 μg/ml
Cytotoxicity[b] (% viability)	100±3.4	ND	ND	86.7±1.4	ND	ND
Focus Formation[c] (colonies/plate)	62.8 ±0.7	72.7 ±11	69.1 ±11.3	64.5 ±12.8	55.9 ±9.8	48.7 ±1.5
AI colonies[e]	0.6±0.4	0.8±0.3	0.6±0.3	0.5±0.2	0.6±0.3	1.0±0.5
Cloning efficiency [f] (%)	<0.01	<0.01	<0.01	<0.01	<0.01	<0.01

[a] Data represent the mean ±SEM of n=5 plates unless otherwise indicated. Asterisks indicate statistically significant differences as described in Materials and Methods (* $p<0.05$; ** $p<0.01$). ND, not determined.

[b] Cytotoxicity was assessed by plating 200 cells/6 cm dia. dish, treating for 1 hr with the indicated compounds as described in Materials and Methods and allowing cells to grow in complete medium for 10 days. Colonies (>50 cells) were scored. n, number of plates counted. TPA ANOVA: $F=8.9$, $df=5,27$, $p<0.01$; Dunnett's *t*:TPA 100 nM vs. Vehicle $p<0.01$.

[c] Foci (>60 μm in diameter) were counted 21 days after treatment as described in Materials and Methods. n, number of plates counted. OG, overgrowth of cells to a degree that individual foci could not be scored. Number of foci /TPA treatment reported in Table was not corrected for cytotoxicity. Correction did not affect statistical significance (data not shown). PAF ANOVA, Dunnett's *t*: See Table 3

[d] The number of cells/6 cm diameter tissue culture dish was counted 10 days after saturation had been reached in vehicle-treated cultures as described in Materials and Methods. PAF ANOVA, Dunnett's *t*: See Table 3.

[e] The number of AI colonies (>80 μm in diameter)/ 6 cm dish were counted 40 days following treatment (n=5). PAF ANOVA, Dunnett's *t*:See Table 3.

[f] AI cloning efficiency in soft agarose was estimated by correcting for both the plating efficiency of cells in monolayer culture ($1x10^5$ cell plated; 15% plating efficiency ; $1.5x10^4$ viable cells) and cytotoxicity associated with treatment. Cloning efficiency was expressed as the percentage of viable cells plated in soft agarose.

saturation density, and AI growth than all of the other agents tested despite the fact that PAF was less effective at promoting a respiratory burst in isolated white blood cells (data not shown). However, unlike TPA-transformed RECs, PAF-transformed clones were not genetically stable. This phenomenon is examined in detail in Chapter III, Section 7. Briefly, enhanced growth kinetics were observed for up to 60 days after treatment followed by phenotypic reversion.

The present series of experiments also replicate previous experiments (5,11,39) indicating that TPA-activated phagocytes can mediate *in vitro* alterations in REC phenotype (Table 6). In addition, new evidence is provided demonstrating that PAF-activated cells can elicit long-term changes in REC growth kinetics (Table 6). These data permit comparisons of direct and indirect PAF exposure. Co-culture of RECs with PAF (10 nM)-treated neutrophils elicited comparable (or greater) focus formation, saturation density, and AI growth (Table 6) as direct administration of 1 μM PAF to REC cultures (Chapter II, Section 2, Table 3). Thus, the ability of PAF-treated neutrophils to induce REC transformation was dose-dependent and saturable at a lower concentration than that observed following direct treatment of target cells. These data, and the fact that PAF-activated phagocytes were washed free of ligand prior to REC exposure, suggest that it is unlikely that REC growth enhancement was elicited by residual PAF present in neutrophil suspensions. Rather it would appear that PAF-activated neutrophils release factor(s) that trigger long-term changes in REC proliferative capabilities. These data permit speculation into the mechanisms underlying PAF-induced phenotypic transformation following either direct or indirect exposure to ligand. Transient stimulation with PAF could trigger the release of 'transforming factors.'

How might this process influence long-term transformation? Two possibilities are suggested: (1) the 'transforming agent(s)' putatively produced in both RECs and neutrophils in response to PAF are mutagenic inducing malignant transformation by damaging DNA and/or (2) an autocrine feedback loop is elicited in RECs following brief exposure to PAF or to the downstream 'transforming agent(s)' that promotes sustained cell growth in the absence of permanent genetic alterations.

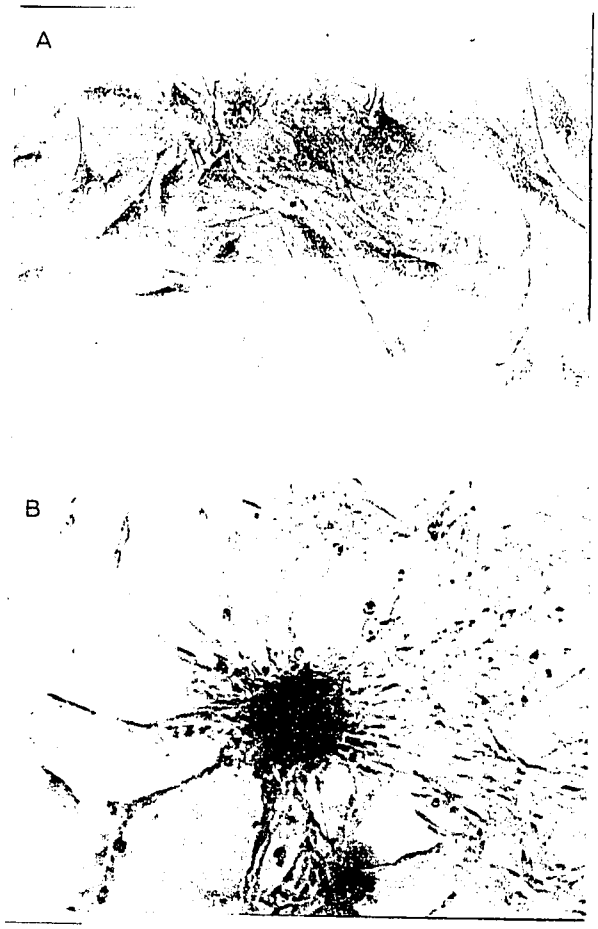

Figure 27. Morphological transformation of TPA (10 nM)-induced AI clones

RECs were exposed to 10 nM TPA for 1 hr and then assayed for phenotypic transformation as described in Materials and Methods. Five AI colonies were cloned and grown to a suitable density to permit evaluation. Transformed cells were demonstrated to be fibroblast in origin by immunohistochemistry (data not shown). Representative photomicrographs depict phase contrast microscopy of methylene blue stained cultures illustrating morphological transformation of TPA-treated clones. (A) untreated RECs. (B) Representative TPA-induced AI clone (Aga3). Control cells were grown for the same amount of time as TPA-treated clones. PAF-treated clones did not exhibit morphological transformation. (A) Scale bar=10 μm. (A) Scale bar=20 μm.

Table 6. Transformation-associated properties in RECs exposed to activated neutrophils

Properties	Treatment[a]						
	Untreated	Activated Neutrophils					
			PAF			TPA	
		Vehicle	1 pM	0.1 nM	10 nM	10 nM	100 nM
Focus Formation[b] (colonies/plate)	50 ±18.1	46.4±6.3 n=12	97.5±31.8 n=17	180.3±59* n=6	160.4±48.6* n=12	66.2 ±12.5	49.5±4.1 n=7
Saturation Density[c] (cells/plate)	$1.2x10^6$ $\pm 3x10^5$	$1.3x10^6$ $\pm 2x10^5$	ND	ND	$2.2x10^6$ $\pm 8x10^{4**}$	$1.8x10^6$ $\pm 8x10^5$	ND
AI colonies[d]	0.7±0.3	0.7±0.2	ND	ND	6.3±2.1* n=6	2.8±0.6**	ND
Cloning efficiency[e] (%)	<0.01	<0.01	ND	ND	0.04	0.02	ND

[a] RECs were either left untreated or coincubated with $5x10^5$ neutrophils previously activated with the indicated compounds. The effect of direct ligand administration to target cells is summarized in Chapter II, Section 2, Table 3 and Table 5 above. Neutrophils were washed free of activating agents prior to REC exposure. Details are as in Materials and Methods. Data represent the mean ±SEM of n=5 plates unless otherwise indicated. Asterisks indicate statistically significant differences as described in Materials and Methods (* $p<0.05$; ** $p<0.01$). ND, not determined

[b] Foci (>60 µm in diameter) were counted 21 days after treatment as described in Materials and Methods. n, number of plates counted. PAF-treated neutrophils ANOVA: F=2.4, df=4,48, $p<0.05$; Dunnett's *t*: PAF 0.1 nM vs. Vehicle, $p<0.05$; PAF 10 nM vs. Vehicle:, $p<0.05$.

[c] The number of cells/6 cm diameter tissue culture dish was counted 10 days after saturation had been reached in untreated cultures as described in Materials and Methods. PAF 10 nM vs. Vehicle Student's $t=3.8$, df=8, $p<0.01$.

[d] The number of AI colonies (>80 µm in diameter)/ 6 cm dish ($1x10^5$ cell plated; 15% plating efficiency ; $1.5x10^4$ viable cells) were counted 40 days following treatment (n=5). Neutrophils vs. PAF+ Neut. Student's *t*: -2.4, df=9, $p<0.05$; Neutrophils vs. TPA+ Neut. Student's *t*: -3.9, df=8, $p<0.01$.

[e] AI cloning efficiency in soft agarose was estimated by correcting for both the plating efficiency of cells in monolayer culture ($1x10^5$ cell plated; 15% plating efficienc ; $1.5x10^4$ viable cells) and cytotoxicity associated with treatment. Cloning efficiency was expressed as the percentage of viable cells plated in soft agarose.

Role of oxyradicals in PAF-mediated HF transformation

To determine whether PAF-mediated transformation of HFs in the absence of neutrophils depends upon oxyradical production, HFs were treated with either vehicle or PAF (1 µM) in association with SOD (25 µg/ml) and/or catalase (20-100 U/ml) and assayed for growth in low serum medium. Data are presented in Figure 28. Exposure to oxyradical scavengers attenuated PAF's ability to induce autonomous cell growth in HFs. Catalase was equally effective in inhibiting PAF-induced growth in low serum as the combination of SOD and catalase, implicating H_2O_2 in PAF-induced transformation (Figure 28, inset). Since H_2O_2 has been shown to be both mutagenic or mitogenic depending on cell type, PAF may work through the reactive oxygen species to elicit phenotypic transformation in target cells by either damaging DNA or stimulating cell growth. If H_2O_2 is the primary effecter of PAF's actions, then it follows that exposure to the

reactive oxygen species under the same experimental conditions should elicit similar rates of transformation in HFs as PAF itself. To test this hypothesis, HFs were exposed to H_2O_2 (0-50 μM) for 1 hr in serum-free DMEM and assayed for growth in low serum. Data are presented in Table 7. H_2O_2 was dose-dependently cytotoxic and, consequently, *decreased* cell number on Day 25 after treatment compared to vehicle-treated cells. When cell number was corrected for cytotoxicity, bolus exposure to H_2O_2 had no effect on HF growth in low serum medium even at subtoxic concentrations (12 μM). However, these data do not rule out the possibility that exposure to a low, constant flux of H_2O_2 over the 1 hr treatment period could influence the ability of HFs to exhibit autonomous cell growth

These data provide preliminary evidence that brief exposure to PAF elicits synthesis and release of 'transforming' factor(s) that enhance cell growth in normal cells. In addition, these data extend the previous inhibitor studies (Chapter II, Section 4), indicating that PAF works through not only PAFR, tyrosine kinases, and, in some cases, cyclooxygenase metabolites of AA and/or PKC but also requires H_2O_2 intermediaries to transduce a sustained mitogenic signal.

Table 7. Cytotoxicity and growth in low serum in HFs following exposure to H_2O_2

Properties	H_2O_2 Treatment[a]			
	Vehicle	12 μM	25 μM	50 μM
Cytotoxicity[b] (% viability)	100 ±3.8	78.7 ±16	55.4 ±13.4*	48.3 ±9.9**
Growth in low serum[c] (cells/plate)	$4.0x10^5$ $\pm1.6x10^4$	$3.2x10^5$ $\pm8.3x10^4$	$2.2x10^5$ $\pm7.0x10^4$	$1.9x10^5$ $\pm5.1x10^4$

[a]Data represent the mean ±SEM of n=5 plates unless otherwise indicated. Asterisks indicate statistically significant differences as described in Materials and Methods (* $p<0.05$; ** $p<0.01$). ND, not determined.

[b]Cytotoxicity was assessed by plating 200 cells/6 cm dia. dish, treating for 1 hr with the indicated compounds as described in Materials and Methods and allowing cells to grow in complete medium for 10 days. Colonies (>50 cells) were scored are reported. n, number of plates counted. ANOVA: $F=4.0$, $df=3,16$, $p<0.05$; Dunnett's *t*: Vehicle vs. H_2O_2, $p<0.05$; Vehicle vs. H_2O_2, $p<0.01$.

[c]Following treatment, cells were grown in DMEM+0.5% FCS. Observations were carried out for 25 days. Data represent total cell number/ plate (n=5 plates/condition) without correction for increases in the rate of cell death observed immediately after H_2O_2 treatment. No statistically significant difference was observed when final cell number was corrected for cytotoxicity observed during the 1 hr treatment.

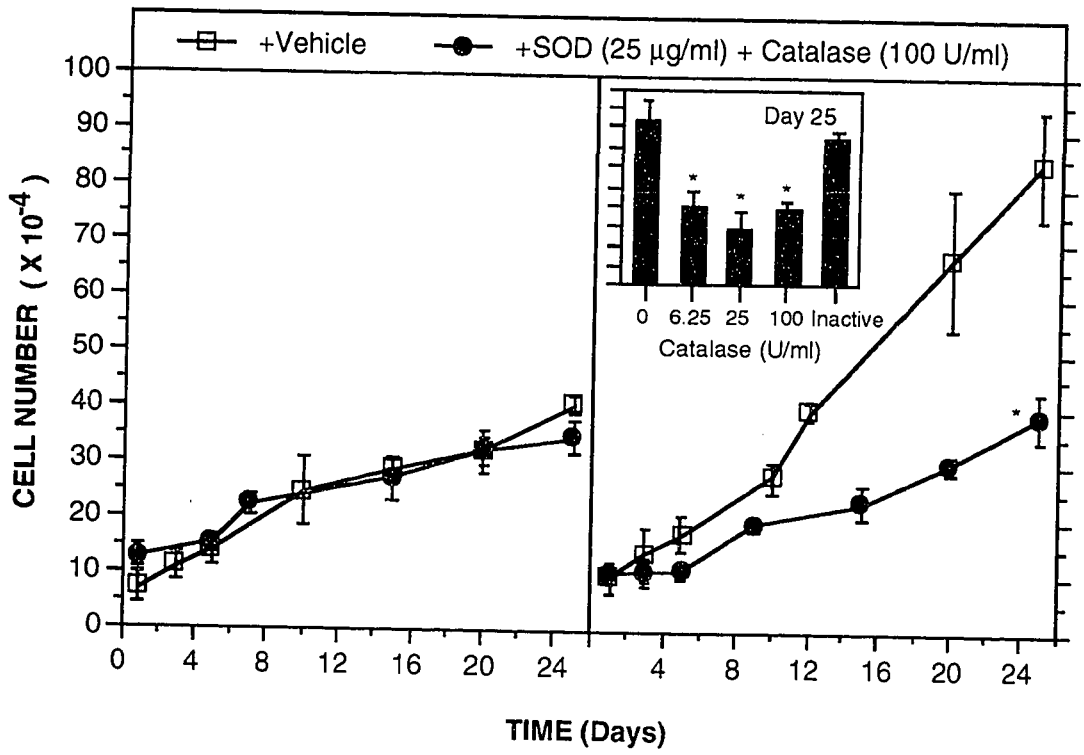

Figure 28. Oxyradical scavengers inhibit PAF-induced HF growth in low serum medium

HFs were treated for 1 hr with either vehicle (A) or PAF (1 µM) (B) in conjunction with SOD (25 µg/ml) and catalase (100 U/ml) and subsequently assayed for growth in low serum medium. Data represent cell counts from a minimum of 5 plates per time period. Statistical comparisons were made on Day 25 after treatment. Inset in (B) depicts the effect of treatment with catalase (0-100 U/ml) in the absence of SOD on PAF (1 µM)-induced growth in low serum medium on Day 25. Inactive refers to 100 U/ml heat-inactivated catalase. Details as described in Materials and Methods. Statistically significant results are as follows: PAF (1 µM) vs. PAF+SOD+catalase: Student's *t*=2.4, df=11, p<0.05; PAF+Catalase ANOVA: F=10.7, df 4,27=, p<0.01; Dunnett's *t*: PAF vs. PAF+catalase (12 µM), p<0.01; PAF+catalase (25 µM), p<0.01; PAF+catalase (50 µM), p<0.01; PAF+catalase (100 µM), p<0.01.

6. Mutagenic Potential of PAF

Abstract

The possibility that PAF induces heritable genetic alterations in non-inflammatory cells was assessed in RECs and MC cells by evaluating changes in hypoxanthine/guanine phosphoribosyltransferase (*hprt*) gene function following ligand treatment. MC cells are derived from a hypotetraploid male fibrosarcoma murine tumour cell line that has been mutated and selected to be sensitive to mutagenic and clastogenic damage (41). RECs or three phenotypically distinct MC clones were treated with PAF for various periods of time. MC clones were chosen on the basis of their inherent genetic stability with respect to *hprt* gene function. MN3 exhibits a low spontaneous mutation rate; MC20 exhibits an intermediate spontaneous mutation rate; MC25 exhibits a high spontaneous mutation rate (41). None of these cell lines exhibited increased induction of *hprt*$^-$ mutants in response to PAF treatment. In keeping with the lack of genotoxicity reported for PAF in the literature, these results suggest that PAF is not a strong mutagen and hence probably does not induce long-term cell proliferation through heritable genetic alterations.

Introduction

Malignant transformation is generally accepted to be a multi-step process of successive genetic alterations within a single cell and its progeny. These heritable changes usually represent genetic mutations, translocations, clastogenic loss, or other DNA damage within crucial sequences of specific genes (proto-oncogenes or tumour suppressor genes). Genetic damage can abrogate subsequent protein function and induce growth deregulation and/or other metastasis-related phenotypes. There is evidence to suggest that the inflammatory environment may contribute to this process (Chapter II, Section 3). A number of proinflammatory agents, most notably oxyradicals, have been shown to be mutagenic *in vitro*. Since PAF depends upon oxyradical intermediates (specifically H_2O_2) to alter REC and HF phenotype (Chapter III, Section 5), then it is possible that PAF may be mutagenic. To evaluate this hypothesis, alterations in the hypoxanthine/guanine phosphoribosyltransferase (*hprt*) gene function following exposure to the ligand were monitored in RECs and MC cells.

In terms of mutagenic experimentation, the *hprt* gene provides an ideal, endogenous target to monitor the rate of random mutagenic and clastogenic events induced by environmental agents. This system has been discussed extensively in (41). Briefly, the presence or absence of functional protein can be detected phenotypically by drug selection. HPRT$^+$ cells are sensitive to the drug 6-thioguanine (6-TG) and resistant to the combination of hypoxanthine, aminopterin, and thymidine

(HAT). Conversely, HPRT$^-$ cells are resistant to 6-TG and sensitive to HAT. *In vitro* experimental design profits from exploitation of this phenotype. Target cells are exposed to HAT to ensure homogeneity of *hprt* gene expression (HPRT$^-$ cells are killed), treated with potential mutagens, and selected in 6-TG-containing medium. The number of HPRT$^-$ mutants (6-TG-resistant cells) generated by the treatment is quantified permitting assessment of relative mutagenic potential. In the present studies, the mutagenic ability of PAF was evaluated. RECs and MC tumour cells were assayed for alterations in HPRT phenotype following ligand treatment. MC cells are a mouse fibrosarcoma line designed by D. Wilkinson and H.C. Birnboim to exhibit enhanced sensitivity to clastogenic and mutagenic agents compared to other cell lines (41).

Materials and Methods

Cell lines

RECs were isolated as described in Chapter III, Section 2. MC cell lines were derived from a hypotetraploid male fibrosarcoma murine tumour with three X chromosomes and numerous autosomal-X translocations. These cell lines were engineered by D. Wilkinson and H.C. Birnboim to be more sensitive to a variety of mutagenic and clastogenic agents than many other cell lines. This process is described in detail in (41). Briefly, all *hprt* loci were inactivated by treatment with methylnitrosourea and a single revertant was selected and cloned. Clones were then characterized for spontaneous loss of *hprt* gene function (HPRT$^-$ phenotype) and endogenous *hprt* reactivation (reversion to HPRT$^+$phenotype). Different MC lines were shown to exhibit different degrees of genetic instability, presumably related to which *hprt* gene was re-activated during cloning selection. Stability was assessed by quantifying the rate of spontaneous *hprt* gene function loss. Three clones were employed in the present study: (1) MN3 exhibiting low spontaneous induction of HPRT$^-$ phenotype, (2) MC20 exhibiting intermediate spontaneous gene deactivation, and (3) MC25 exhibiting a high frequency of spontaneous HPRT$^-$ mutants. MN3 also contains a neomycin resistance gene construct rendering it sensitive to G418 drug selection (7).

Treatment and Mutagenic assay

Cells were cultured in DMEM+10% FCS+HAT (0.1 mM hypoxanthine/0.4 μM aminopterin/15 μM thymidine) for 5 days to rid cultures of contaminating 6TG-resistant cells. Media was replaced with DMEM+10% FCS+HT (no aminopterin) and cells maintained for an additional 2-3 days. 100,000 cells were then seeded per 10 cm dia. tissue culture dish in DMEM+10% FCS (non-selection medium) and allowed to plate overnight. The following day, cultures were treated with PAF (10 nM - 1 μM) or vehicle in serum-free DMEM + 0.2% BSA for 1, 24, 48, or 72 hr. Following treatment, cells were incubated for 48 hr in non-selection medium. $HPRT^-$ mutants were selected in DMEM+ 10% FCS containing 50 μM 6-TG (selection medium) for 14 days with twice weekly feedings. Plates were fixed in methanol and stained with 1% methylene blue in 50% ethanol. Colonies >50 cells were scored. Cells were also plated in soft agarose and fed with selection medium ensuring a final concentration of 40 μM 6-TG throughout the agarose layer. Colonies >80 μm in dia. were counted 26 days after plating. All drugs were obtained from Sigma, MO.

Results and Discussion

Table 8 indicates the number of $HPRT^-$ mutants generated in MN3, MC20, and MC25 cells following exposure to PAF. In each case, PAF failed to increase mutation frequencies.

Table 8. PAF has no effect on HPRT phenotype

Treatment[a]	Spontaneous Mutation Rate ($HPRT^-$ phenotype)											
	Low : MN3				Intermediate: MC20				High: MC25			
	1 hr	24 hr	48 hr	72 hr	1hr	24 hr	48 hr	72 hr	1 hr	24 hr	48 hr	72 hr
Vehicle	0.8 ±0.5 n=9	ND	ND	ND	0.9 ±0.3 n=10	5.6 ±1.6 n=7	1.9 ±0.6 n=9	0.6 ±0.3 n=10	38.7 ±4.3 n=10	60.6 ±7.0 n=5	24.4 ±3.6 n=5	33 n=1
PAF 10 nM	2.0 ±0.6 n=3	ND	ND	ND	1.3 ±0.3 n=11	2.3 ±1.1 n=10	0.7 ±0.4 n=10	0.2 ±0.2 n=10	60.6 ±8.8 n=5	98 ±10.6 n=5	58.2 ±8.0 n=5	ND
PAF 1 μM	1.4 ±0.4 n=5	ND	ND	ND	0.6 ±0.3 n=10	2.9 ±1.2 n=9	2.5 ±0.6 n=10	0.1 ±0.1 n=10	54.6 ±3.5 n=5	27 n=1	47.2 ±2.0 n=5	11.3 ±2.3 n=3

[a]Data represent the number of $HPRT^-$ colonies/10^5 cells treated as described in Materials and Methods (mean ± SEM). n, number of replicates.

Because MC cells are already transformed, it is possible that PAF may not elicit the same effects in these cells as in RECs. (It is also possible that MC cells lack PAF receptors and, hence, are unable to respond to the ligand. This possibility is addressed in Chapter III, Section 2.) Alterations in HPRT locus were also assessed in RECs. RECs failed to demonstrate any spontaneous $HPRT^-$ mutants under any of the treatment conditions. Given the difficulty in establishing low level mutation frequencies, these data cannot definitively rule out the possibility that PAF can induce some form of genetic damage. However, these experiments do establish that the compound is not highly mutagenic. This conclusion is supported by the literature. As discussed in Chapter II, Section 5, synthetic PAF analogues have been used as chemotherapeutic agents. These analogues have been engineered for enhanced cytotoxicity and reduced catabolic deactivation. Despite extensive investigation, none of these compounds have been shown to elicit DNA damage or increase mutagenesis. It would appear then that PAF probably does not induce alterations in cell number through heritable genetic mutation.

7. Stability of PAF-Induced Phenotypic Transformation

Abstract

PAF-induced phenotypic transformation of RECs and HFs was not genetically stable and was not heritable. PAF induced focus formation, increased saturation density, autonomous cell growth, and AI growth was shown to be limited to a 50 day period (RECs) or a 40 day period (HFs) observable 10 days after treatment. Cells then reverted to a normal phenotype. PAF-transformed focus and AI clones exhibited slightly enhanced rates of cell growth when re-assayed in the absence of PAF with cell proliferation lasting up to 80 days after treatment. However, these properties were not stable (ie. < 100 days) and were not substantially enriched compared to the parent population. The atypical temporal kinetics of this effect were surprising. Although exposure to PAF failed to immortalize RECs or HFs, results indicate that approaching senescence was not the reason for phenotypic reversion. These data demonstrate that PAF can induce long-term phenotypic transformation in the absence of further PAF stimulation but suggest that this effect is not permanent and, therefore, is probably not the result of heritable DNA alterations.

Introduction

In preceding experiments, brief exposure to PAF was found to induce long-term phenotypic changes in REC and HF growth kinetics without inducing any measurable increase in mutagenesis. Although this finding does not rule out the possibility that PAF is a weak mutagen, it does demonstrate that mutational events in rare cells probably does not account for the large-scale growth enhancement observed throughout the treated population. These data indicate that PAF-induced alterations in primary cell proliferation may not be the result of heritable changes in the genome of affected cells and, hence, do not represent a permanent phenotype. To determine the longevity of PAF-induced transformation of RECs and HFs, PAF-treated cells were assayed for focus formation, increases in saturation density, growth in low serum, and AI growth over a 100 day period in the absence of further treatment.

Materials and Methods

Treatment, transformation assays, and cloning

RECs and HFs were treated with 1 μM PAF or vehicle and assayed for (i) cell viability, (ii) doubling time, (iii) saturation density, (iv) focus formation, (v) growth in low serum medium, and (vi) AI growth as described in Chapter III, Section 3. Following treatment, cells in group (iii) and (v) were trypsinized and 100,000 cells were allowed to attach overnight in complete medium in 6

cm dia. dishes. Cells were retested for changes in cell viability, doubling time, saturation density, and growth in low serum medium over four or five successive 20 day periods (a total of 80-100 days of growth) in the absence of further PAF exposure. In addition, individual foci and AI colonies were isolated following the initial assay and grown in DMEM+10% FCS until a suitable cell number was obtained for immunohistochemical characterization as described in Chapter III, Section 2. These clones were also reassayed for phenotypic transformation in the absence of further PAF exposure.

Results and Discussion

Stability of REC transformation

Transformed clones were isolated from PAF (10 nM)-treated foci (n=4), PAF (1 μM)-treated AI colonies (n=5), and C-PAF (0.1 nM) (PAF's unmetabolizable analogue)-treated AI colonies (n=2). Clones were picked 25-30 days after treatment and grown to a suitable density to permit further investigation (a range of 25-40 days depending upon the clone). Untreated cells were cultured for the maximal period of time to permit comparison. Data are summarized in Table 9. As indicated, cell types were identified by immunohistochemistry; two clones were epithelial in origin while all others were composed of fibroblasts. The observation that PAF can act on both fibroblasts and epithelial cells is a finding of some relevancy to human cancers given the predominance of epithelial cell carcinomas over fibrosarcomas. However, PAF-induced growth enhancement in RECs was not genetically stable. Cloning of foci and AI colonies did not substantially enrich phenotypic transformation. PAF-transformed foci did not demonstrate increased focus-forming ability or saturation densities, exhibited modest increases in growth in low serum, and displayed only occasional AI growth compared to untreated cells. PAF- and C-PAF-transformed AI colonies retained their altered phenotype to a slightly greater extent than focus clones, exhibiting enhanced focus formation and the ability to sustain growth in low serum. However, they failed to maintain autonomous cell growth indefinitely (ie. > 60 days) or to exhibit substantial increases in AI growth compared to untreated controls. These data suggest that brief exposure to PAF induces transient, albeit long-lasting, changes in REC growth kinetics that do not depend upon heritable genetic alterations.

Table 9. Transformation-associated properties of PAF- and C-PAF-induced focus and AI clones

Properties[a]	Untreated Recs	Clones				
		PAF (1 μM)-induced AI clones				
		PA61	PA62	PA63	PA64	PA65
Doubling Time (h)						
Cell count	31.4	33.1	41.7	35.4	37.7	37.1
Thymidne incorp.	31.4	30.1	28.1	37.9	38.6	38.1
Focus Formation[b] (colonies/plate)	50.6 ±8.3	>500	>500	88.5±1.0	515.5±30.9**	465.2±48.2**
Saturation Density[c] (cells/plate)	$1.2x10^6$ ±$3x10^5$	$3.9x10^6$ ±$5x10^5$**	$2.2x10^6$ ±$6x10^5$*	$1.0x10^6$ ±$1x10^4$	$1.3x10^6$ ±$2x10^4$	$1.0x10^6$ ±$2x10^4$
Growth in low serum[d]						
Doubling time (h)	142±10.8	115.6±0.3	66.1±0.9**	147.4±5.8	92.6±2.8**	48.5±2.8**
Days of growth	6	20	30	6	30	20
AI colonies[e]	0	3.3±0.8**	1.5±0.2	2±0*	2.1±0.6*	2±0.6*
Cell type[f]	F/E	F	F	F	F	F

	C-PAF (0.1 nM)-induced AI clones		PAF (10 nM)-induced focus clones			
	CP101	CP102	PF81	PF82	PF83	PF84
Doubling Time (h)						
Cell count	44.7	29.2	33.1	52.8	58.3	40.5
Thymidne incorp.	46.5	25.1	32.7	50.2	60.1	41.2
Focus Formation[b] (colonies/plate)	ND	ND	58±9.8	108±6.3**	53.7±2.6	69.4±11.4
Saturation Density[c] (cells/plate)	$1.6x10^6$ ±$9x10^4$	$1.4x10^6$ ±$7x10^4$	$8.8x10^5$ ±$5x10^4$	$8.0x10^5$ ±$2x10^5$	$7.2±10^5$ ±$3x10^4$	$6.7x10^5$ ±$4x10^4$
Growth in low serum[d]						
Doubling time (h)	83.9±2.5**	71.6±1.7**	71.2±0.5**	120.8±4.1*	69.4±2.6**	158.4±0.6
Days of growth	30	30	8	8	30	30
AI colonies[e]	2.5±0.5**	1.4±0.1*	0	0	1.6±0.3**	0
Cell Type[f]	F	F	F	E	E	F

[a]Details described in Materials and Methods.. Data represent mean ± SEM of n=5 replicates (100,000 cells plated in each trial/15,000 viable cells). ND, not determined

[b]Statistically significant comparisons PAF AI clones ANOVA: F=71.3, df=3,16, p<0.01; Dunnett's *t*: PA64 vs. Untreated, p<0.01; PA65 vs. Untreated, p<0.05; PAF focus clones ANOVA: F=8.1, df=4,20, p<0.01; Dunnett's *t*: PA64 vs. Untreated, p<0.01; PA65 vs. Untreated, p<0.01.

[c]Statistically significant comparisos: PAF AI clones ANOVA: F=10.0, df=5,24, p<0.01; Dunnett's *t*: PA61 vs. Untreated, p<0.01; PA62 vs. Untreated, p<0.05.

[d]Growth was determined over a maximal 30 day period. Statistically significant comparisons: PAF focus clones ANOVA: F=58.5, df=4,20, p<0.01; Dunnett's *t*: PF81 vs. Untreated, p<0.01; PF82 vs. Untreated, p<0.05; PF83 vs. Control, p<0.01; PF84 vs. Untreated, p<0.05; PAF AI clones ANOVA: F=77.2, df=5,24, p<0.01; Dunnett's *t*: PA61 vs. Untreated, p<0.01; PA62 vs. Untreated, p<0.01; PA64 vs. Untreated, p<0.01; PA65 vs. Untreated, p<0.01; C-PAF AI clones ANOVA: F=33.7, df=2,12, p<0.01; Dunnett's *t*: CP101 vs. Untreated, p<0.01; CP102 vs. Untreated, p<0.01.

[e]Statistically significant comparisons: PAF AI clones ANOVA: F=5.0, df=5,24, p<0.01; Dunnett's *t*: PA61 vs. Untreated, p<0.01, PA63 vs. Untreated, p<0.05; PA64 vs. Untreated, p<0.05; PA65 vs. Untreated, p<0.05; PAF focus clones ANOVA: F=51.2, df=4,19, p<0.01; Dunnett's *t*: PF83 vs. Untreated, p<0.01; C-PAF AI clones ANOVA: F=16.9, df=2,12, p<0.01; Dunnett's *t*: CP101 vs. Untreated, p<0.01; CP102 vs. Untreated, p<0.05.

[f]Untreated RECs , cultured identically to clones, are composed almost entirely of fibroblasts <0.1% epithelial cells. F, fibroblast; E, epithelial cells.

RECs are not immortal. This characteristic could account for the apparent lack of genetic stability observed following PAF treatment. Putative genetic alterations and consequent phenotypic enrichment might not be detected if clones were reaching senescence at the time they were retested. There is some indication that this may be the case. Although the majority of clones and passage-matched controls exhibited comparable doubling times to early passage RECs (approximately 33 hr), four clones (PF82, PF83, PF84, and CP101) demonstrated a substantially delayed rate of cell replication (Table 9). Two clones (PF82 and PF83) were composed of epithelial cells and this homogeneity probably accounts for the difference in doubling time compared to the mixed parent population. However, PF84 and CP101 were fibroblast in origin. It is possible that these clones were derived from a phenotypically different anatomical or embryonic site within the primary explant and this difference explains their altered doubling time compared to the majority of cells comprising the REC population. Alternatively, the extended doubling time could also be the result of approaching senescence. To test this hypothesis, RECs were treated for 1 hr with either PAF (1 μM) or vehicle, assayed for growth in complete medium or growth in low serum over a 20 day period, passaged in the absence of further PAF exposure, and retested for enhanced growth in either medium. This time frame precludes observation of PAF-induced increases in REC saturation density. The protocol was repeated four more times (100 days of growth). Data are presented in Figure 29. As described in Chapter III, Section 3, PAF had no effect on cell doubling time in complete medium (Figure 29A). Both PAF- and vehicle-treated cells showed signs of approaching senescence at approximately the same time (90 days after treatment) after approximately 75-80 doublings. (This estimate takes into consideration the number of doublings third passage RECs had sustained prior to treatment.) When cultured in low serum medium, PAF increased the ability of RECs to sustain autonomous cell growth over a 50 day period between Day 10 and Day 60 (Figure 29B). Prior and subsequent to these time points, cell doubling times (ie. slope) were equivalent. In each 20 day test period, vehicle-treated cells demonstrated approximately 1.1 doublings over the first 10 days of testing and 0.25 doublings over the second 10 day period. PAF-treated cells exhibited 1.4 doublings over the entire 50 day 'proliferative window.' Cells grown in low serum containing medium sustained approximately 7-10 doublings (depending on treatment). These cultures did not show any

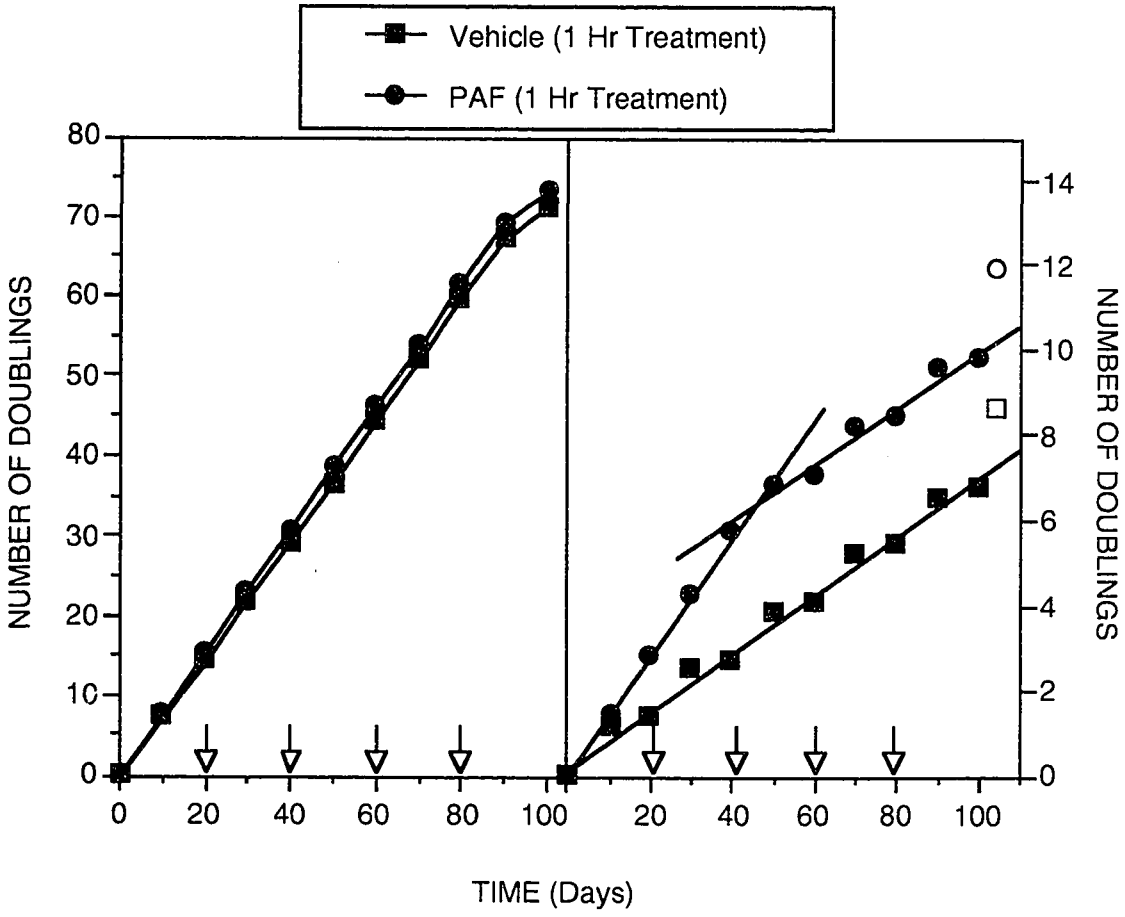

Figure 29. Stability of PAF-induced REC growth enhancement

RECs were treated for 1 hr with either vehicle or PAF as described in Materials and Methods. 100,000 cells were then cultured in complete medium (A) or low serum medium (B) and the number of doublings calculated using Coulter Counter cell counts over successive 20 day periods. Cells were fed twice weekly and were passaged at the end of each 20 day test period (arrows) Data represent the mean of 5-12 replicates per time period. In (B), open symbols indicate replacement of low serum medium for complete medium (3 day exposure) 100 days after treatment. Multiple regression analysis was performed on the slope of lines generated in (B). The growth of PAF-treated cells was found to statistically significantly differ from the slope of vehicle-treated cells between Day 1 and Day 50. MGLH ANOVA, df=2,15, F=22.1, $p<0.05$.

indication of reaching early senescence as the result of growth factor starvation. When cells were exposed to complete medium after 100 days of testing, both vehicle- and PAF-treated cultures demonstrated analogous increases in cell number (Figure 29B) as those described for quiescent third passage RECs (Figure 14; Chapter III, Section 2). These data indicate that brief exposure to PAF induces transient (albeit long-term) growth enhancement and not stable phenotypic transformation. This conclusion is strengthened by the observation that phenotypic reversion occurs well before any indication of primary cell senescence. As a result, the enhanced growth characteristics observed in transformed clones are more likely due to enrichment for those cells in the population that are in the process of proliferating in response to transient PAF stimulation rather than to the identification of a single, genetically altered cell and its progeny.

Stability of HF Transformation

The stability of PAF (1 μM)-induced autonomous cell growth in HFs was assessed over a 80 day period as described above for RECs. Data are presented in Figure 30. As discussed in Chapter III, Section 3, PAF had no effect on HF growth rates in complete medium (Figure 30A). Both vehicle- and PAF-treated cells demonstrated 80 days of exponential growth or approximately 60-65 doublings (taking into consideration the number of doublings fourth passage HFs had sustained prior to treatment). HFs showed no signs of approaching senescence during the experimental time frame (Figure 30A). As demonstrated earlier (Chapter III, Section 3), PAF-treated cells exhibited enhanced growth in low serum medium. As with RECs, this enhancement was transient in that it was limited to the 40 days between Day 10 and Day 50 following treatment. Growth rates were comparable in PAF- and vehicle-treated cells both before and after this proliferative 'window.' In each 20 day test period, vehicle-treated cells demonstrated approximately 1.4 doublings over the first 10 days of testing and 0.6 doublings over the second 10 days. PAF-treated cells sustained 1.7 doublings throughout the entire 40 day proliferative period. Both vehicle- and PAF-treated HFs exposed to serum starvation conditions for 80 days remained viable and were as capable of responding to complete medium (Figure 30B) as quiescent fourth passage HFs (Figure 17; Chapter III, Section 2). Finally, these data are also in accordance with the kinetics of PAF-induced AI colonies (Chapter III, Section 3). Growth in soft agarose

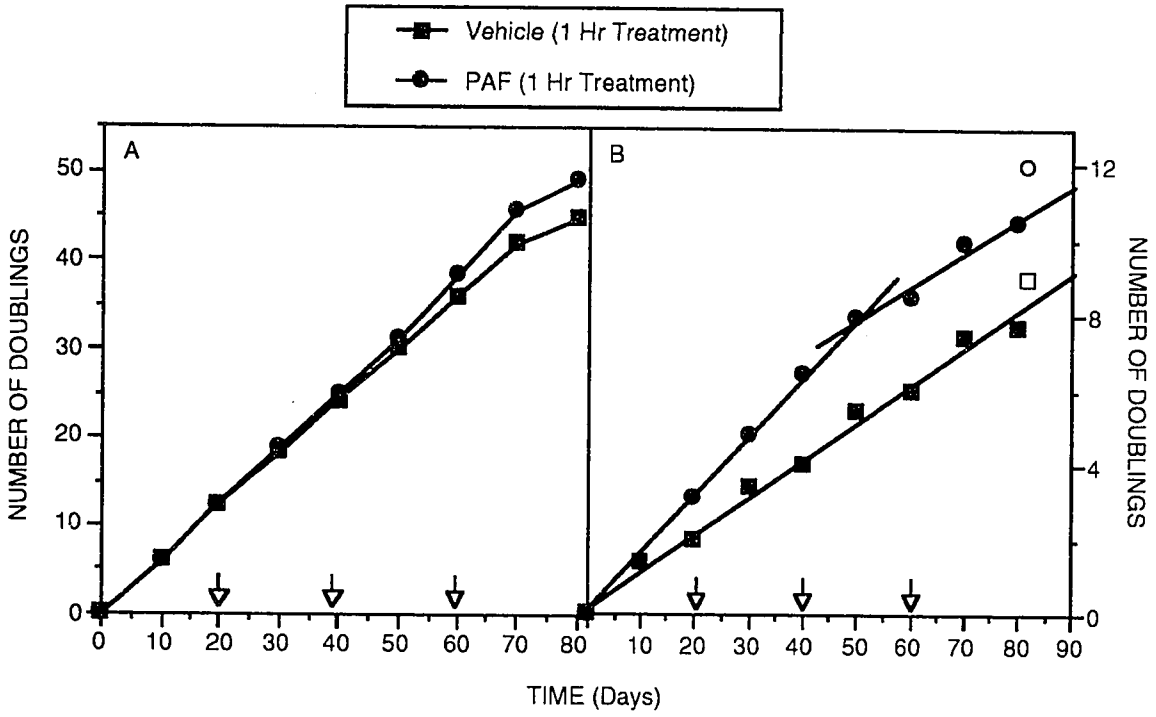

Figure 30. Stability of PAF-induced HF growth enhancement

HFs were treated for 1 hr with either vehicle or PAF as described in Materials and Methods. 100,000 cells were then cultured in complete medium (A) or low serum medium (B) and the number of doublings calculated using Coulter Counter cell counts over successive 20-25 day periods. Cells were fed twice weekly and were passaged at the end of each test period (arrows) Data represent the mean of 5-12 replicates per time period. In (B), open symbols indicate replacement of low serum medium for complete medium (3 day exposure) 75 days after treatment. Multiple regression analysis was performed on the slope of lines generated in (B). The growth of PAF-treated cells was found to statistically significantly differ from the slope of vehicle-treated cells between Day 1 and Day 50. MGLH ANOVA, df=2,15, $F=18.9$, $p<0.05$.

increased until Day 40. Cells remained viable after this time point but colony size ceased to expand.

These data strengthen the conclusion that PAF does not contribute to the process of multiple genetic alterations characteristic of tumour progression but does promote long-term cell proliferation. It was previously hypothesized (Chapter III, Section 5) that transient PAF stimulation elicits release of 'transforming agents' that influence long-term growth potentiation through mutagenesis or through induction of an growth-promoting autocrine feedback loop. The former explanation now appears unlikely. However, evidence has been provided to support the latter hypothesis. PAF stimulation appears to promote the release of growth-promoting factor(s) whose effects can last as long as 50 days after treatment. These rather atypical kinetics remains puzzling. How does PAF alter cell growth kinetics 10-40 days *after* treatment in the absence of additional stimulation?

8. Autocrine Stimulation Underlying PAF-Induced Cell Proliferation

Abstract

Exogenous PAF stimulation appears to induce intracellular PAF accumulation leading to synthesis and release of fluid-phase growth factors capable of mediating cell growth. RECs and HFs were treated with either PAF (1 μM) or vehicle for 1 hr. Conditioned medium was harvested from these cultures and tested for the ability to induce phenotypic transformation. Medium derived from PAF-treated cells between Day 1 and Day 30 elicited AI and autonomous cell growth in target cells. Medium harvested from PAF-treated cells between Day 45 and Day 75 had no effect on target cells. Conditioned medium harvested from vehicle-treated cells had no growth enhancing abilities. Cells exposed to growth enhancing conditioned medium did not continue to proliferate when cultured in DMEM+0.5% FCS. These data indicated that brief PAF stimulation induces long-term synthesis and release of autocrine growth factors. However, direct exposure to these putative growth factors is not sufficient in and of itself to trigger production of additional mitogenic agents. Continual treatment with PAF antagonists *after* treatment with exogenous PAF completely inhibits both PAF-induced AI phenotype and growth in low serum. However, inclusion of antagonists in conditioned medium harvested from PAF-treated cultures had no effect on subsequent phenotypic transformation. A hypothetical model is presented to interpret this data. Brief PAF stimulation induces prolonged synthesis of intracellular PAF. Once sufficient elevations in intracellular PAF concentration are achieved (approximately 10 days after initial treatment), cells produce and release fluid-phase growth factors capable of mediating cell proliferation. This feedback circuit can be maintained only in cells originally stimulated with exogenous PAF and lasts for approximately 40 days in the absence of further PAF treatment.

Introduction

Tumourigenesis is a multistep process requiring that the balanced systems of cell growth, differentiation, and death become uncoupled resulting in a progressive increase in cell number. One means of achieving clonal expansion of transformed cells is through permanent genetic alteration. However, PAF was not found to be quantifiably mutagenic (Chapter III, Section 6). Furthermore, the kinetics of PAF-induced growth enhancement suggest that a large proportion of PAF-treated cells proliferate in response to ligand rather than the rare, genetically mutated cell (Chapter III). These data provided in the preceding chapters suggest that PAF elicits transient (albeit long-lasting) cell replication. *In vivo*, cell growth is often initiated through sustained autocrine, paracrine, or juxtacrine stimulation whereby a cell is continually stimulated by a mitogenic factor that is either synthesized by the cell itself (autocrine stimulation), is produced and released locally by neighbouring cells (paracrine stimulation), or is produced and remains associated with the plasma membrane of neighbouring cells promoting intercellular contact with

the target cell (juxtacrine stimulation). These phenomena are readily observed in both inflammatory and non-inflammatory cells during an inflammatory response.

Autocrine production of PAF has been shown to mediate sustained cell growth in HEC-1A endometrial adenocarcinoma cells (22) and rat mesangial cells (23). Paracrine production of PAF has been demonstrated to play a role in mediating embryonic cell proliferation (40). To determine whether similar mechanisms are responsible for PAF-induced growth enhancement in RECs and HFs, conditioned medium harvested from PAF- or vehicle-treated cells was tested for its ability to promote either growth in low serum or AI growth. In addition, PAF-treated cells were incubated with PAF antagonists *following* the 1 hr ligand exposure to determine whether PAF itself is the putative 'transforming factor' identified in Chapter III, Section 4.

Materials and Methods

Conditioned Medium Experiments

RECs and HFs were treated with either vehicle or 1 μM PAF as described in Chapter III, Section 3 and incubated in low serum containing medium. Cultures were fed twice weekly. Target RECs or HFs were plated in 6 cm dia. dishes (100,000 cells/plate) in DMEM+10% FCS or suspended in soft agarose as described in Chapter III, Section 3. Medium was replaced twice weekly with conditioned medium harvested from PAF- or vehicle-treated cultures. RECs were divided into two experimental groups - those receiving conditioned medium harvested between Day 1-30 after treatment and those receiving medium harvested between Day 45-75. Cells were assayed for autonomous cell growth or AI phenotype as described in Chapter III, Section 3. Statistical analysis was as described in Chapter III, Section 2.

PAF Antagonists

RECs or HFs were treated with PAF (1 μM) or vehicle for 1 hr as described in Chapter III, Section 3. Cultures were assayed for changes in cell viability, growth in low serum, or AI growth as described in Chapter III, Section 3, in the presence of one of the following PAF antagonists: CV3988 (1 μM), gliotoxin (1 μM, Calbiochem, CA), trans-dioxolane (1 μM, Calbiochem, CA), its inactive stereo-isomer cis-dioxolane (1 μM, Calbiochem, CA), or T-PAF (1 μM, Calbiochem,

CA), an inactive analogue of PAF. Cultures were fed with appropriate medium + antagonists twice weekly. Statistical analysis was as described in Chapter III, Section 2.

Results and Discussion

Effect of conditioned medium on REC phenotype

Conditioned medium, harvested from PAF (1 μM)-treated cultures between Day 1-30 after treatment, was found to induce both AI growth (Figure 31) and sustained cell proliferation in low serum (Figure 32). Maximal effects were approximately 50% of that observed in cultures directly treated with ligand. Medium harvested between Day 45-75 after treatment or from vehicle-treated cultures had no discernible growth enhancing effects in either assay. These data provide strong evidence for the hypothesis that brief exposure to PAF induces subsequent sustained production of unidentified growth factor(s) capable of stimulating cell proliferation. These data also conform to the kinetics of the PAF-induced response (Chapter III, Section 7) in that production of this growth factor(s) appears to be limited to the first 50 days following treatment.

Effect of conditioned medium on HF phenotype

Conditioned medium derived from PAF (1 μM)- or vehicle-treated cultures 1-25 days after treatment was tested for its ability to induce autonomous cell growth in HFs. Data are presented in Figure 32. As with RECs, conditioned medium harvested from PAF-treated cells induced autonomous cell growth with maximal cell number reaching approximately 50% that of cells directly exposed to the ligand. Growth enhancement was not evident until Day 6-10 after exposure. Given these kinetics, it is tempting to speculate that a feedback loop is induced by transient PAF stimulation, priming cells to synthesize increasing amounts of a mitogen(s) and resulting in cell proliferation when these factors are produced in sufficient quantity. In keeping with PAF's role as a pro-inflammatory agent, this response would be self-perpetuating over an extended (albeit limited) period of time.

It was of note that the growth enhancement elicited by conditioned medium itself did not elicit an analogous feedback loop. When cells proliferating in conditioned medium were replated and retested in the absence of further exposure, these HFs did not sustain autonomous cell growth

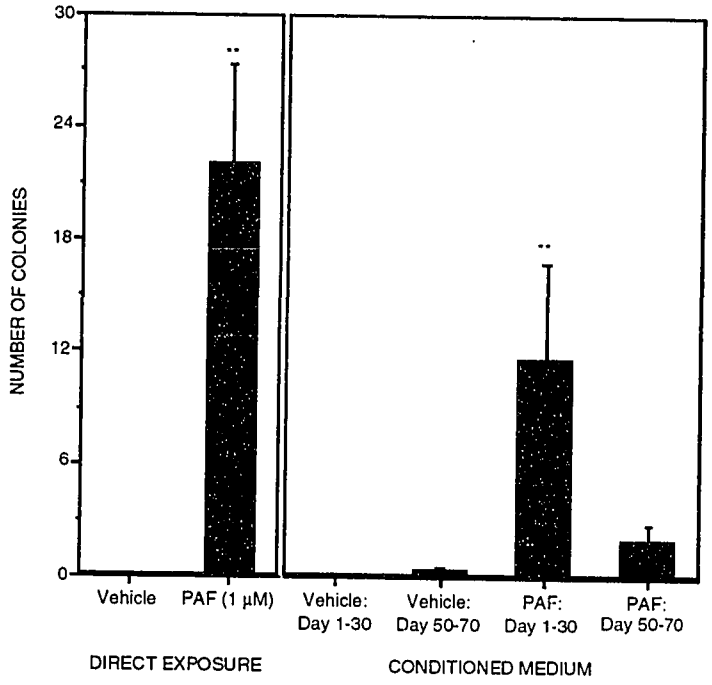

Figure 31. Conditioned medium harvested from PAF-treated cultures induces AI growth in RECs

RECs were treated for 1 hr with either vehicle or PAF as described in Materials and Methods. Conditioned medium harvested from cultures between Day 1-30 and Day 45-75 was tested for an ability to induce AI growth in target RECs. Data represent the mean number of colonies ± SEM per 100,000 cells plated (15,000 viable cells) from a minimum of 5 replicates. Statistically significant comparisons are as follows: PAF vs. Vehicle Treatment: See Table 3; Conditioned Medium ANOVA: $F=4.7$, $df=3,17$, $p<0.01$; Dunnett's *t*: PAF (Day 1-30) vs. Vehicle (Day 1-30), $P<0.01$.

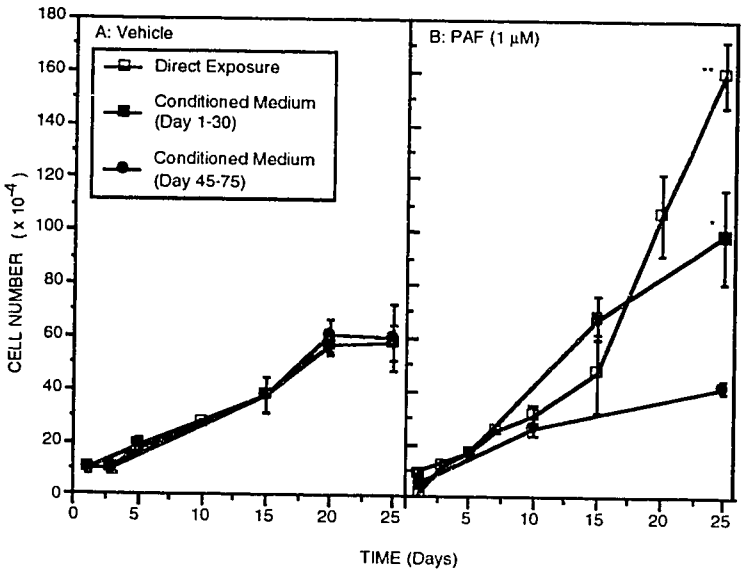

Figure 32. Conditioned medium harvested from PAF-treated cultures induces autonomous cell growth in RECs

RECs were treated for 1 hr with either vehicle or PAF as described in Materials and Methods. Conditioned medium harvested from cultures between Day 1-30 and Day 45-75 was tested for an ability to induce growth in low serum in target RECs. Data represent the mean cell number ± SEM from a minimum of 5 replicates per time point. Statistical analysis was performed on Day 25. Statistically significant comparisons are as follows: PAF vs. Vehicle treatment: See Figure 23; Vehicle vs. PAF Conditioned Medium Student's *t* test: $t=5.8$, $df=8$, $p<0.01$.

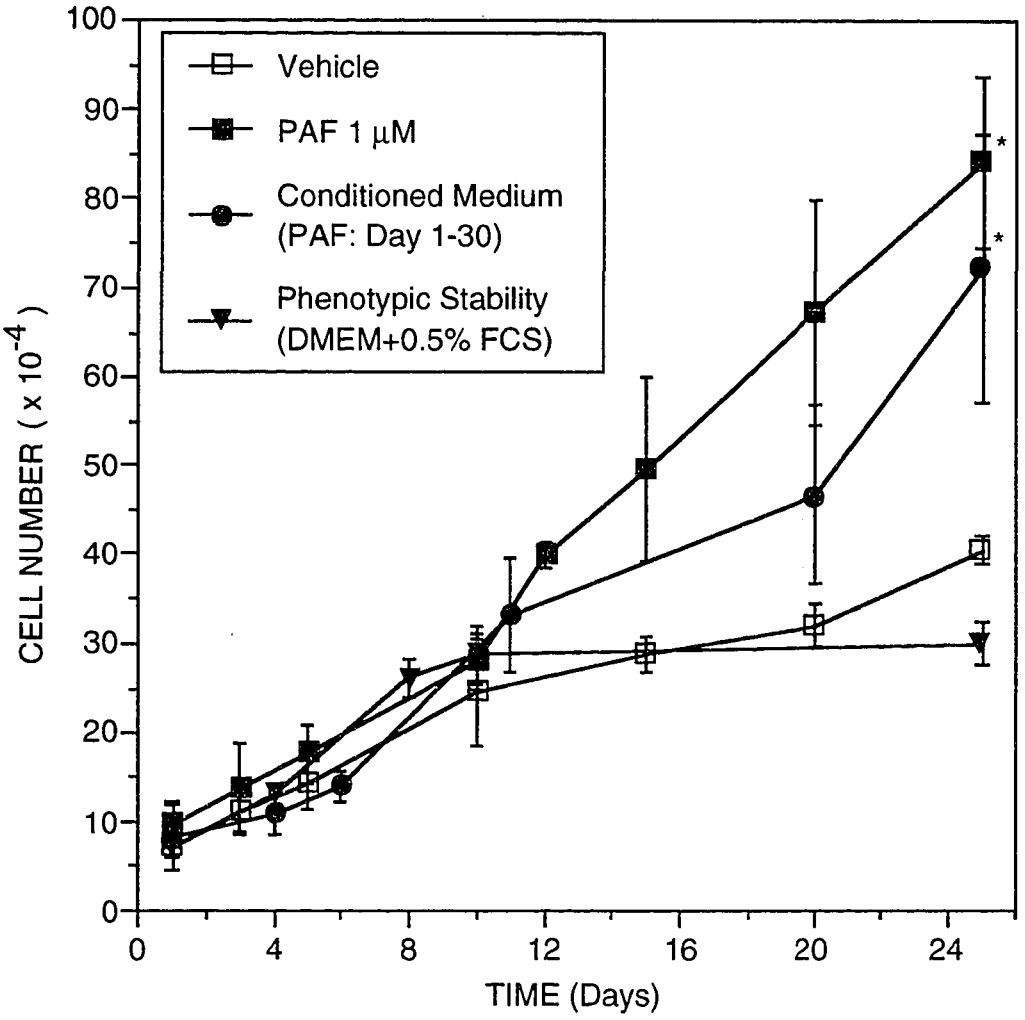

Figure 33. Conditioned medium harvested from PAF-treated cultures induces autonomous cell growth in HFs

HFs were treated for 1 hr with either vehicle or PAF as described in Materials and Methods. Conditioned medium harvested from cultures between Day 1-30 was tested for an ability to induce growth in low serum in target HFs. Following 25 days of growth, cell treated with conditioned medium were trypsinized and 100,000 cells replated. Cultures were tested for phenotypic stability (ie. the ability to maintain growth in low serum medium in the absence of additional conditioned medium). Cultures previously exposed to conditioned medium harvested from either vehicle- or PAF-treated cells did not exhibit enhanced growth when grown in standard DMEM+0.5% FCS. Data represent the mean cell number $\pm$ SEM from a minimum of 5 replicates per time point. Statistical analysis was performed on Day 25. Statistically significant comparisons are as follows: PAF vs. Vehicle treatment: See Figure 21; Vehicle vs. PAF Conditioned Medium Student's *t* test: t=6.2, df=8, $p<0.01$.

unlike cells that had been briefly exposed to exogenous PAF. These data suggest that induction of the putative feedback loop depends upon the initial PAF signal. Downstream signalling agents mediate immediate mitogen production and cell proliferation but these factors do not elicit continued cell growth when removed.

Effect of PAF antagonists on sustained cell growth

The postulates offered above represent an attempt to reconcile the following observations: (1) brief exposure to PAF elicits long-term cell proliferation, (2) growth enhancement is not observed until 10 days after treatment, and (3) exposure to conditioned medium is sufficient to induce immediate cell proliferation but is not capable of inducing sustained cell growth. Three distinct events are hypothesized. First, exposure to PAF elicits sustained production of a 'priming' factor(s). Second, this factor induces synthesis and release of other 'mitogenic' factor(s). Third, these mitogenic factors act directly on target cells to stimulate cell division. Presumably, the 'priming' factor is either an intracellular messenger or, conversely, an inherently unstable, rapidly metabolized extracellularly secreted ligand. This assumption is based on the fact that 'priming' is not elicited by conditioned medium. Cells treated with conditioned medium do not demonstrate sustained cell growth when subsequently grown in standard low serum medium. These results indicate the 'priming' factor is either absent from conditioned medium or is too unstable to be detected in the present assay. Conversely, the 'mitogenic' factor is a stable, extracellularly active mediator in that it retains much of its biological activity when harvested in conditioned medium.

If these assumptions are to direct subsequent experimentation, the existence of the putative 'priming' factor must be established. One possibility, discussed in Chapter III, Section 5, is that H_2O_2 acts as the 'priming' factor. Certainly, the data indicate that PAF signal transduction seems to require H_2O_2 for subsequent cell signalling given that catalase blocks PAF-induced phenotypic transformation. However, it is unlikely that long-term production of the oxyradical stimulates mitogen production given that direct administration of a bolus dose of H_2O_2 did not induce cell proliferation (Chapter III, Section 5). (The effects of a continual flux of H_2O_2 on HF and REC proliferative capabilities have yet to be determined). However, another possibility is that PAF

itself mediates subsequent mitogen production. In other cell systems, activation of the extracellular PAF receptor induces intracellular accumulation of the ligand (Chapter II, Section 5). Subsequent signal transduction depends upon this increase. In most non-inflammatory cells, the vast majority of PAF produced in response to stimulation is retained intracellularly (Chapter II, Section 5). In fact, only inflammatory cells have been shown to be capable of releasing physiologically relevant quantities of the ligand (Chapter II, Section 5). It is possible that stimulation of RECs and HFs with exogenous PAF elicits intracellular PAF production. This speculation is supported by recent claims that endothelin-induced proliferation of rat mesangial cells is mediated by intracellular PAF (23) and that HEC-1A adenocarcinoma cells maintain autonomous cell growth by induction of a PAF-dependent autocrine growth circuit (22).

To assess this hypothesis, HFs and RECs were treated for 1 hr with either PAF (1 μM) or vehicle and subsequently assayed for growth in low serum medium and AI phenotype in the presence or absence of 5 different PAF antagonists. Figure 34 depicts the effect of PAF antagonists on PAF-induced REC AI phenotype. All of the PAF antagonists inhibited phenotypic transformation except the cis isomer of dioxolane, a compound without effect at the PAF receptor because of its stereospecificity. Significantly, the antagonists did not inhibit conditioned medium-induced AI phenotype (Figure 34). Figure 35 depicts the effect of PAF antagonists on PAF-induced HF autonomous cell growth. Exposure of PAF-treated HFs to either T-PAF (1 μM) or CV3988 (1 μM) over a 25 day period attenuated PAF-induced growth in low serum medium and, surprisingly, reduced growth rates to below that of vehicle-treated cells. Continual treatment with PAF antagonists also abolished the residual ability of HFs to grow in low serum (data not shown). Antagonist treatment had no effect on cell viability as assessed by trypan blue exclusion (data not shown) or by determining growth rates upon re-exposure to complete medium in the absence of PAF antagonists. These data indicate that exogenous PAF administration induces intracellular PAF accumulation of ligand that, in turn, mediates synthesis and release of growth factors capable of stimulating cell proliferation. In addition, preliminary evidence is presented to suggest that basal levels of intracellular PAF turnover may even be responsible for the minimal amount of autonomous cell growth observed in control cultures. These findings suggest that PAF is a crucial mediator of cell proliferation in normal fibroblasts under non-permissive growth conditions.

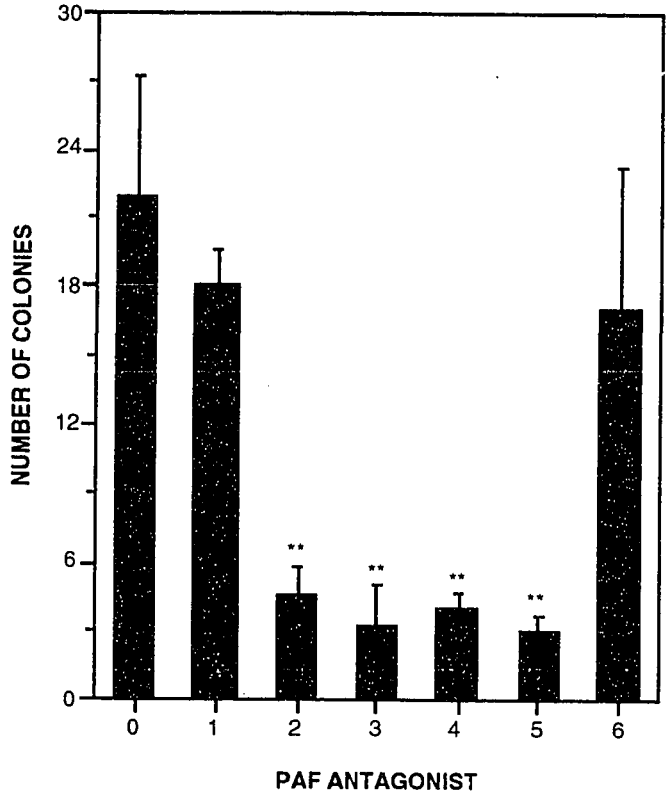

Figure 34. Continual exposure to PAF antagonists *after* PAF treatment blocks AI growth in RECs

RECs were treated for 1 hr with PAF (1 μM) and assayed for AI phenotype in the presence of PAF antagonists as described in Materials and Methods. 0, + Vehicle; 1, + cis-dioxolane; 2, + trans-dioxolane; 3, + gliotoxin; 4, + T-PAF; 5, + CV3988. 6, CV3988 was included in conditioned medium harvested from PAF-treated cultures between Day 1-30. Antagonist concentration was 1 μM. Data represent the mean number of colonies ± SEM per 100,000 cells plated (15,000 viable cells) from a minimum of 5 replicates. Statistically significant comparisons are as follows: PAF vs. PAF+Antagonists Treatment ANOVA: $F=4.7$, $df=3,17$, $p<0.01$; Dunnett's *t*: 0 vs. 2, $p<0.01$; 0 vs. 3, $p<0.01$; 0 vs. 4, $p<0.01$; 0 vs. 5, $p<0.01$.

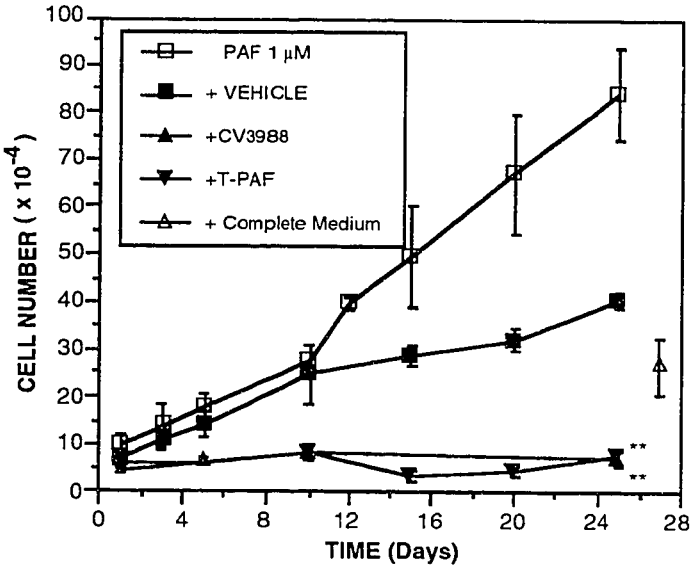

Figure 35. Continual exposure to PAF antagonists *after* PAF treatment abolishes HF autonomous cell growth

HFs were treated for 1 hr with PAF (1 μM) and assayed for growth in low serum in the presence of T-PAF (1 μM) or CV3988 (1 μM) as described in Materials and Methods. Data represent the mean cell number ± SEM from a minimum of 5 replicates per time point. Statistical analysis was performed on Day 25. Following testing, antagonist-treated cultures were incubated in complete medium (Δ) to ensure viablity. Statistically significant comparisons are as follows: PAF vs. PAF+ Antagonists ANOVA: $F=6.1$, $df=3,17$, $p<0.01$. Dunnett's *t*: PAF vs. PAF+T-PAF, $p<0.01$; PAF vs. PAF+CV3988, $p<0.01$; Vehicle vs. Vehicle + Antagonists ANOVA: $F=4.7$, $df=3,17$, $p<0.01$. Dunnett's *t*: Veh. vs. Veh.+T-PAF, $p<0.01$; Veh. vs. Veh.+CV3988, $p<0.01$.

9. Overview

The data presented in 'Transformation Potential' indicate that PAF mediates both cell growth and cell death in primary rodent and human non-inflammatory cells. Brief exposure to the ligand induces long-term growth enhancement in cells without permanent genetic alterations. Prolonged exposure elicits cell death. Immediate signal transduction leading to cell growth depends upon PAF receptor activation, protein kinase activity (PKC and/or tyrosine kinases depending on cell species), and oxyradical production but not upon cyclooxygenase metabolism of arachidonic acid. Because phenotypic transformation is transient, PAF does not appear to elicit heritable genetic alterations in the DNA of transformed cells. With respect to tumour progression, it is suggested that brief stimulation of the PAF receptor leads to increased synthesis of intracellular PAF, subsequent production and release of autocrine growth factors, and consequent cell proliferation. The ability to maintain cell growth is characteristic both of the inflammatory response and of the metastatic process indicating that transient exposure to PAF within the inflamed environment may contribute to tumourigenesis by inducing sustained cell proliferation of non-inflammatory cells within a potentially mutagenic environment.

IV
SIGNAL TRANSDUCTION

1. Introduction

The previous chapter demonstrates that PAF can mediate both cell proliferation and cell death in primary rodent and human fibroblasts and epithelial cells. The mechanisms underlying these actions remain ambiguous. PAF signal transduction has only begun to be elucidated in non-inflammatory cells (Chapter II, Section 5). Using antagonists and inhibitors, indirect evidence was presented indicating that PAF modulates PKC, tyrosine kinase, and oxyradical activity in receptor-mediated fashion in RECs and HFs (Chapter III, Sections 4 and 5). To substantiate this data, PAF's ability to activate specific second messengers was evaluated.

2. Identification of Specific PAF Receptors on Rodent and Human Fibroblasts

Abstract

The existence of specific PAF receptors on HFs, RECs, and MC cells (MN11) was confirmed by RT-PCR and Northern analyses. Positive controls included U937 cells. Negative controls included undifferentiated HL60 cells. Results indicate that PAFR is expressed in HFs, RECs, and MN 11 cells in low copy number. By Northern analysis, PAFR mRNA could only be detected upon evaluation of 3 μg poly A^+ RNA. Expression was not evident upon evaluation of 20 μg total RNA indicating low endogenous mRNA levels. RT-PCR products and mRNA were identical in size in both inflammatory and non-inflammatory cell types.

Introduction

The PAFR cDNA was first cloned from guinea pig lung by Honda et al. in 1991 (17). Since then, identical PAF receptor cDNAs have been isolated from human leukocytes (41), human heart (33), U937 cells (20), and differentiated HL60 cells (41). In 1994, rodent PAFR was sequenced from rat spleen (5) and demonstrated to be 83% homologous to human cDNA. Genomic analysis indicates that the human PAF receptor gene exists as a single copy on chromosome 1. The gene spans over 20 kB in length and is composed of three exons (27). Exons 1 and 2 are 5'-noncoding exons, each with distinct transcriptional initiation sites. Exon 3 contains the total open reading frame for the complete PAFR sequence. Exon 1 or 2 is alternatively spliced onto a common splice acceptor site within the third exon generating two different species of functional mRNA (Figure 36).

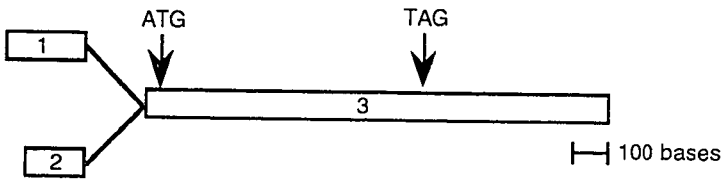

Figure 36. Map of human PAFR gene

Diagram depicts a schematic representation of the human PAF mRNA adapted from (27). Exon 1 and 2 are alternatively spliced onto exon 3. Exon 3 contains the entire PAFR open reading frame. Two functional mRNA species of the same molecular size driven by different promoters are generated.

The 5' untranslated region of transcript 1 contains consensus sequences for the transcription factors NF-κB and Sp-1 as well as the initiator (*Inr*) sequence homologous to the

murine terminal deoxynucleotidyltransferase gene (27) instead of the usual TATA or CCAAT boxes associated with promoter sequences. The gene product is ubiquitously expressed in human heart, lung, spleen, kidney, brain, peripheral leukocytes, and a number of promyelocytic cell lines. Transcript 2 contains consensus sequences for the AP-1, AP-2, and Sp-1 transcription factors. Although two initiation sites were identified in close proximity, the 5' region upstream of these START sites lacks TATA box, CCAAT box, or *Inr* sequences characteristic of most promoter regions. The expression pattern of transcript 2 completely overlaps that of transcript 1 with the notable exception that transcript 2 cannot be detected in leukocytes, promyelocytic cell lines, or brain (27). In the absence of multiple open reading frames, these differential expression patterns indicate that PAFR transcription is regulated by two different promoters alternatively spliced onto exon 3 (27). With respect to cell types, PAFR expression has been demonstrated in U937 cells, HL60 cells, and human monocytes. Non-inflammatory cells have yet to be investigated. However, pharmacological characterization has indicated the presence of PAF binding sites on guinea-pig tracheal epithelial cells (16) and A431 human epidermoid carcinoma cells (34) while functional studies suggest that PAFR may be present on immortal murine L cells (41) and HEC-1A and -1B epithelial cells derived from a human endometrial carcinoma cell line (1,23).

To determine whether HFs, RECs, and MC cells have specific PAF receptors, reverse transcriptase-polymerase chain reaction (RT-PCR) and Northern analyses were performed on total and poly A^+ RNA.

Materials and Methods

Cells and Culture Conditions

Primary fifth passage REC and HF cultures, MC cells (MN11), U937 cells, and HL60 cells were grown in DMEM+10% FCS. MN11 cells are a sister clone of the MN3 line described in Chapter III, Section 6. U937 and HL60 cells are two different human promyelocytic leukemia cell lines obtained from ATCC. PAFR transcripts are known to be constitutively expressed in U937 cells (20) and differentiated HL60 cells but not in undifferentiated cultures (41).

Reverse transcriptase polymerase chain reaction (RT-PCR)

Total cellular RNA was prepared from 2 x 10^6 cells essentially as described in (2,3). 10 pmol oligo (dT) 20mer reverse primers (kindly provided by Dr. M. Tenniswood, Alton Jones Cell Science Centre, Lake Placid) were added to 500 ng of total RNA in 12 µl H_2O and denatured for 5 min at 70°C. The mixture was cooled on ice and dNTP mix (0.5 mM each, Pharmacia, Ont), Tris-HCl (50 mM, pH 8.3), KCl (40 mM), $MgCl_2$ (6 mM), BSA (0.1 mg/ml), and DTT (10 mM) were added (final concentrations are listed). Following equilibration for 1 min at 37°C, RNA was reverse transcribed by the addition of 200 U Superscript reverse transcriptase (Gibco, Ont) in a total volume of 20 µl. Reactions were incubated at 42°C for 1 hr, then 50°C for 30 min. 5 µl of reverse transcriptase mix (approximately 200 ng cDNA) was used for PCR amplification. PAF receptor (PAFR) primer sequences were 5'GCATCCTACTTCCTCATCCT3' (forward) and 5'ACTTCAGTGACCGTATCCGT3' (reverse) defining a 537 bp fragment of the human mRNA (20). PCR amplifications were carried out in a volume of 50 µl, containing 0.8 mM each of the four dNTPs, 50 mM KCl, 10 mM Tris-HCl (pH 8.3), 50 µg/ml BSA, 2 mM $MgCl_2$, 3 U Taq DNA polymerase, and 20 pmol of each primer. The program of the reaction was denaturation at 94°C for 30 sec, annealing at 57°C for 1 min, and extension at 72°C for 1 min for 30 cycles using a M.J Research thermal reactor. The absence of genomic DNA contamination was demonstrated by carrying out identical reactions as described above in the absence of reverse transcriptase. PCR products and 100 bp markers (Pharmacia, Ont) were size-fractionated by electrophoresis on a 0.8% (w/v) agarose gel and visualized by ethidium bromide staining.

Northern Analysis

Total cell RNA was extracted essentially as described in (5). Poly A^+ mRNA was isolated from cell lysates by binding to oligo(dT) columns using a Quick-Prep Kit (Pharmacia, Ont). Northern analysis was carried out essentially as described in (3). Briefly, total RNA (10 µg) was isolated, formaldehyde denatured, electrophoretically separated on a 1.2% agarose gel containing 0.2 M formaldehyde, transferred to a Hybond-N nylon filters (Amersham, Ont.) using a vacuum system, and hybridized to ^{32}P-labelled DNA probes. Pre-hybridization and hybridization were

carried out as described in (11). The DNA probes used were a 1 Kb enzyme fragment from the pCDM8 plasmid containing the human leukocyte PAFR gene (PAFR probe) (kindly provided by Drs N. and C. Gerard, Harvard Medical School, Boston) and a 1.2 kb PstI fragment from the pGAPDH plasmid containing the glyceraldehyde-3-phosphate dehydrogenase (GAPDH) gene (GAPDH probe) (31). Probes were labelled with [^{32}P]dCTP using a random primer labelling kit (Pharmacia, Ont). At the end of the hybridization procedure, membranes were air-dried and exposed to X-ray film (Kodak, Ont) for 3-48 h at -100°C. When membranes were re-probed, the first probe was removed by exposing the membranes to 0.25% SDS, 10 mM sodium citrate, pH 6.8, at 95°C for 5 min.

Results and Discussion

The existence of specific PAFR transcripts in HF, RECs, and MC cells was demonstrated by RT-PCR analysis (Figure 37). In keeping with the low copy number of PAFR mRNA expressed in inflammatory cells under resting conditions, PAFR mRNA could not be detected by Northern analysis of 20 µg total RNA (data not shown). These data are not surprising given that, in inflammatory cells, 2-10 µg poly A^+ RNA is routinely required to visualize PAFR message (5,17,20,27,33,41). Northern analysis of purified mRNA (3 µg) confirmed RT-PCR results demonstrating the presence of a 4 kb PAFR band in HFs and RECs (Figure 37). (MC cells were not tested). Positive controls included U937 cells. Negative controls included undifferentiated HL60 cells.

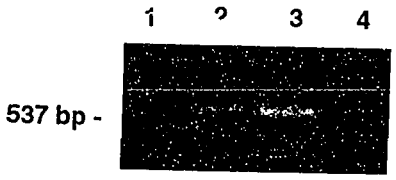

Figure 37. RT-PCR analysis of PAFR expression in undifferentiated HL60 cells, U937 cells, RECs, and HFs

Cells were cultured, total RNA isolated, and RT-PCR analysis conducted as described in Materials and Methods. Lane 1, HL60; Lane 2, U937 cells; Lane 3, RECs; Lane 4, HFs. Control reactions were carried out in the absence of 1 U reverse transcriptase to ensure that observed product was not the result of DNA contamination (data not shown). MN11 cells were also demonstrated to express PAFR transcript (data not shown).

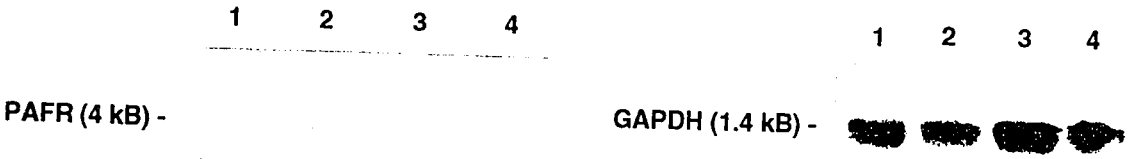

Figure 38. Northern analysis of 3 μg poly A^+ RNA isolated from HL60 cells, U937 cells, HFs, and RECs

Cells were cultured, mRNA isolated, and Northern analysis conducted as described in Materials and Methods. Lane 1, HL60 cells; Lane 2,U937 cells; Lanes 3, HFs; Lanes 4, RECs. (A), PAFR; (B), GAPDH.

3. PAF Activates Protein Kinase C and Induces Tyrosine Phosphorylation

Abstract

The temporal relationship of PKC activation and tyrosine phosphorylation of proteins following PAF (1 pM - 1 μM) treatment was characterized in RECs, HFs, and human neutrophils. Plasma membrane-associated PKC activity was assayed by quantifying the incorporation of ^{32}P from [γ-^{32}P] ATP into a PKC-selective substrate characterized by Chakravarthy et al. (8). Tyrosine phosphorylation was characterized by Western blotting using a monoclonal anti-phosphotyrosine antibody. In RECs, PAF was found to dose-dependently increase the length of time PKC remained activated following stimulation. Lower doses (1 pM - 0.1 nM) were more effective than higher doses (10 nM - 1 μM) at maintaining PKC activity. Increasing PAF dose did not increase the magnitude of the PKC response (3-fold augmentation in activity compared to vehicle-treated cells) but did alter the kinetics of the activation. Higher doses of PAF induced activation of membrane-bound PKC earlier than lower doses of ligand. This response was compared to PKC activation following TPA treatment, a powerful inducer of PKC. TPA (10 nM) induced a 4-fold increase in PKC activation evident 2 min after stimulation that did not diminish across the 1 hr test period. By contrast, in HFs, altering PAF concentrations had no effect on the duration or initiation of the PKC activation in HFs and human neutrophils but did increase the magnitude of response. These data confirm the species to species differences in PAF-induced PKC cell signalling suggested by Chapter III, Section 4. Both RECs and HFs exhibited similar patterns of tyrosine phosphorylation following PAF stimulation. Two peak periods of putative kinase activity were observed after treatment. PAF stimulated tyrosine phosphorylation of higher molecular weight substrates (60-110 kD) within 2-5 min of exposure and of lower molecular weight proteins (20-50 kD) within 60 min of exposure.

Introduction

In Chapter III, Section 2-4, PAF was shown to mediate growth enhancement of HFs and RECs. This transformation was differentially modulated by pretreatment with either tyrosine kinase or PKC inhibitors depending upon cell species. In RECs, PAF-induced cell proliferation was inhibited by exposure to tyrosine kinase inhibitors but not by PKC inhibitors. In HFs, PAF-induced cell growth was blocked by either treatments. These data suggest that the PAF's ability to transiently transform human and rodent fibroblasts is mediated by some form of protein kinase activation although PAF's ability to induce serine, threonine, or tyrosine phosphorylation in fibroblasts has yet to be demonstrated.

The present experiments were designed to identify potential signal transduction molecules downstream of the PAF receptor in rodent and human fibroblasts that might be relevant to the observed biological effects. Specifically, the ability of PAF to act through PKC or induce tyrosine phosphorylation in receptor-mediated fashion in RECs and HFs was investigated. The kinetics of the PKC response to PAF were compared to that of TPA, a known PKC activator.

Materials and Methods

Cells and Culture Conditions

Fifth passage RECs and HFs were plated in 10 cm dia. tissue culture plates and grown to confluence ($3x10^6$ cells/dish) in DMEM+10% FCS with twice weekly medium replacement. Once confluence was attained, cells were maintained without medium replacement for four days prior to treatment. Cell types in this later passage REC population were determined by immunohistochemistry as described in Chapter III, Section 2. Human neutrophils were isolated as described in Chapter III, Section 5.

Measurement of PKC activity

Cultures were washed twice with serum-free DMEM and approximately 6 $x10^6$ cells (two 10 cm dia. tissue culture dishes) were treated with one of the following compounds in DMEM containing 0.2% bovine serum albumin: (a) vehicle (0.1% dimethyl sulfoxide (DMSO), Fisher, Ont.); (b) PAF (1 pM - 1 μM, Avanti Biochemicals, PA); (c) TPA (10 nM, Biomol Research, PA). In some cases, cells were pretreated with either a PKC inhibitor, staurosporine (50 nM, LC Corp, NY) or a PAF antagonist, CV3988 (1 μM, Calbiochem, CA). When pretreatment is indicated, staurosporine or CV3988 were added 15 min prior to addition of TPA or PAF and maintained in the medium for the treatment duration. Following stimulation for 0-60 min, cells were assayed for PKC activity essentially as described (8). Briefly, cells were washed with ice-cold phosphate buffered saline (PBS: 2.7 mM KCl, 1.5 mM potassium phosphate, 0.14 M NaCl, 8 mM sodium phosphate) and suspended by scraping the plate with a rubber policeman in 1 ml hypotonic lysis buffer (0.1 M NaCl, 0.02 M Tris-HCl (pH 7.5), 5 mM $MgCl_2$, 100 μM sodium vanadate, 100 μM sodium pyrophosphate, 1 mM sodium fluoride, 100 μM phenylmethylsulfonylfluoride). Suspensions were sonicated for 5 sec on ice using a 1/8" probe of a Microson Ultrasonic Cell Disrupter set to lowest power. Large cell fragments were removed by low speed centrifugation at 500g, for 5 min, at 4°C, and the membranes present in the supernatant were isolated by centrifugation at 16,000g, for 20 min at 4°C. The membrane pellet was suspended in 100 μl Assay Buffer (50 mM Tris-HCl (pH 7.5), 5 mM $MgCl_2$, 1μM $CaCl_2$, 100 μM sodium vanadate, 100 μM sodium pyrophosphate, 1 mM sodium fluoride, 100 μM

phenylmethylsulfonylfluoride) and protein content measured according to Bradford (6). Membrane-associated PKC activity was assayed by quantifying the incorporation of ^{32}P from [γ-^{32}P] ATP into a PKC-selective substrate described by Chakravarthy et al. (8). This peptide substrate, FKKSFKL-NH_2, corresponds to the amino acid sequence targeted by PKC in the MARCKS protein . The PKC assay reaction mixture consisted of 30 µl of membrane suspension (10 µg protein), 10 µl of 750 µM peptide substrate, and 10 µl of 500 µM [γ-^{32}P] ATP (220 cpm/pmol, 0.5 µCi/tube) in Assay Buffer. Following incubation at 25°C for 10 min, samples were immediately spotted on 1 cm^2 pieces of P81 Whatman paper (kindly provided by Dr. H. Yamazaki, Carleton Univ., Ottawa, Ont) and immersed in 5% acetic acid. Samples were washed twice in acetic acid for 10 min with shaking. The amount of radioactive substrate bound to filters was measured using a liquid scintillation counter. Control reactions were carried out either (1) in the presence of membrane extract alone (no peptide substrate) or (2) in the presence of 10 µg BSA alone (no peptide substrate or membrane extract). These controls were used to quantify radioactive background attributable to (1) phosphorylation of endogenous PKC substrates present in the membrane preparation bound to P81 paper and (2) non-specific binding of radiolabel itself.

Western analysis

Cultures (95% confluent/ 10 cm dia. tissue culture dish) were incubated with PAF (10 nM) for various time periods as described in Chapter III, Section 2. At each time point, cell plates were placed on ice, culture medium was removed, and monolayer cells were rapidly suspended in 1 ml cold PBS by scraping using a rubber policeman. Cells were pelleted by brief centrifugation at 4°C and lysed in 50 µl extraction buffer (140 mM NaCl, 25 mM Na acetate pH5.0, 2% mercaptoethanol, 20 mM phenylmethylsulfonyl fluoride, 0.5 mM sodium orthovanadate, 10 mg/ml *p*-nitrophenyl phosphate, 0.5% SDS, and 1 mM CDTA). Protein content was determined according to Bradford (6). Samples were diluted in half by the addition of 50 µl 2x SDS sample loading buffer (0.125 M Tris-HCl, pH 6.8, 4% SDS, 20% glycerol, 10% mercaptoethanol). This mixture was boiled for 5 min prior to electrophoresis. 10 µg protein was loaded into each well of a Biorad Minigel apparatus. Proteins were size-fractionated by 10% SDS-polyacrylamide gel

electrophoresis as described in (22). Resolved proteins were transferred electrophoretically to a Millipore Immobilon-P membrane as described in (35). Membranes were blocked for 1 hr at 50°C with 1% BSA and immunoblotted overnight at 4°C with biotinylated anti-phosphotyrosine (Amersham, Ont, 1:80) diluted in TBST (10 nM Tris-HCl (pH 8.0), 150 mM NaCl, 0.05% Tween 20). Membranes were washed extensively in TBST and incubated with strepavidin alkaline phosphatase (1:300, Amersham, Ont) for 90 min at room temperature. Immunoreactive bands were visualized by exposure to bromocholorindoyl phosphate (BCIP: 0.66%; Boeringer-Mannheim, Ont) and nitroblue tetrazolium (NBT: 0.66%; Boeringer-Mannheim, Ont) dissolved in 50% and 70% dimethylformamide (DMF; Calbiochem, CA) respectively.

Statistical analysis

PKC kinetics data were analyzed using multiple analyses of variance (MANOVAs). Data obtained after PAF or TPA treatment were contrasted across time with data obtained after vehicle treatment to identify statistically significant time points. PKC inhibitor data were analysed as described in Chapter III, Section 2.

Results and Discussion

PKC activation in RECs

Although the ability of PAF to induce signal transduction through PKC has been convincingly demonstrated in inflammatory cells (30,38) and cerebral microvessels (7), activation of the kinase in response to PAF in a normal, non-inflammatory cell type has not previously been documented. Early passage RECs are a mixed population composed of fibroblasts, epithelial cells, neurons, and muscle cells (Chapter III, Section 2). However, at the time of testing, fifth passage RECs were demonstrated by immunohistochemistry to be a homogeneous population composed entirely of fibroblasts (data not shown). Using a highly specific PKC activity assay developed by Chakravarthy et al (8), exposure of RECs to PAF (10 nM) was found to induce a rapid, transient increase in membrane-bound active PKC (Figure 39A) with maximal induction occurring 2 min after initiation of treatment. Activity returned to basal levels within 5 min of stimulation. The PKC response of vehicle-treated cells did not differ from non-specific

background, defined as the amount of radiolabel bound to P81 paper when cell extracts were incubated with [^{32}P]-γ-ATP in the absence of peptide substrate. This background appears to measure true non-specific binding of [^{32}P]-γ-ATP to P81 paper and is not attributable to phosphorylation and binding of an endogenous protein substrate in the membrane extract since identical values were obtained following incubation of radiolabel with either 10 μg BSA or in the absence of protein substrate (data not shown).

The kinetics of the PAF-induced response were compared to that of a known PKC activator, TPA (Figure 39B). TPA (10 nM) treatment rapidly increased PKC activity in RECs reaching maximal response within 2 min of stimulation. The phorbol ester was more effective in activating PKC than equimolar concentrations of PAF, eliciting a four-fold increase in kinase activity over vehicle-treated cells compared with PAF's ability to elicit a three-fold increase. However, in sharp contrast to the transient PKC response induced by PAF, TPA was capable of sustaining the increase in kinase activity for at least 1 h.

The specificity of the PAF-induced increase in substrate phosphorylation for PKC was determined by pretreating cultures with a PKC inhibitor, staurosporine (50 nM), both prior to and during stimulation with PAF (10 nM) or TPA (10 nM). Staurosporine completely inhibited the increase in membrane-bound kinase activity in both PAF- and TPA-treated RECs (Figure 40) indicating that phosphorylation of the synthetic peptide substrate FKKSKL-NH_2, is very likely a specific PKC event.

The specificity of the PAF-induced response for PAF receptor activation was confirmed by treating RECs with a PAF receptor antagonist, CV3988 (1 μM), both prior to and during exposure to PAF (10 nM) or TPA (10 nM). As expected, blocking the PAF receptor abolished the increase in PAF-induced kinase activity without altering TPA-stimulated PKC activity (Figure 40) indicating that PAF acts through PAFR to stimulate PKC.

An unexpected observation was made when the effect of different doses of PAF was tested. Varying the concentration of PAF was found to alter the kinetics of membrane-bound PKC activation without affecting the magnitude of the response (Figure 41). PKC activation in response to PAF (1 pM - 1 μM) was analyzed over the first 10 minutes of treatment. The highest level of PKC activity observed was similar at all doses tested. However, low doses (1 pM - 0.1

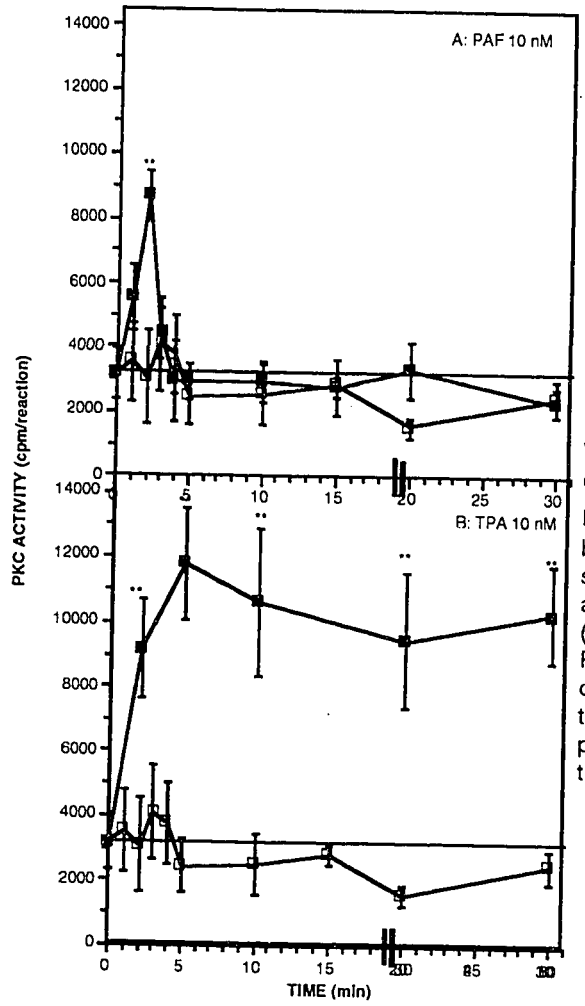

Figure 39. PAF- and TPA-induced PKC activity in RECs

RECs were treated with PAF (10 nM) (A) or TPA (10 nM) (B). Membrane-associated PKC activity was quantified as the amount of ^{32}P incorporated into the synthetic PKC peptide substrate FKKSFKL-NH_2 during a 10 min incubation at 25°C as described in Materials and Methods. Data are expressed as the average cpm ± SEM from a minimum five and a maximum of seven independent experiments conducted in duplicate. Variation between duplicate measurements in each experiment was less than 10%. □, vehicle treatment; ■, PAF (A) or TPA (B) treatment; ——, non-specific binding of ^{32}P to P81 paper in the absence of peptide substrate. Statistically significant differences in PKC activity across time and treatments are as follows: PAF (10 nM) vs. vehicle MANOVA: df=1,54; 2 min treatment, F=18.2, p<0.01. TPA (10 nM) vs. vehicle MANOVA: df=1,54; 2 min treatment, F=8.7, p<0.01; 5 min treatment, F=22.3, p<0.01; 10 min treatment, F=13.0, p<0.01; 30 min treatment, F=14.7, p<0.01; 60 min treatment, F=14.2, p<0.01.

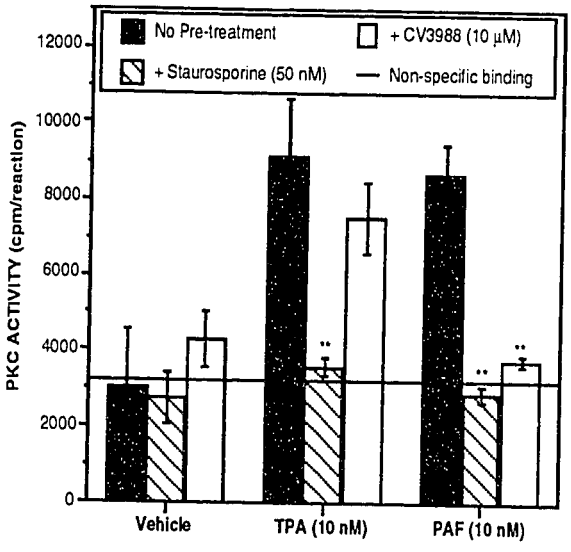

Figure 40. The effect of kinase inhibitor and PAF antagonist pretreatment on vehicle, TPA, or PAF-induced PKC activity in RECs

Cells were pretreated with either staurosporine (50 nM) or CV3988 (1 μM) prior to 2 min exposure to vehicle, TPA (10 nM) (A), or PAF (10 nM) (B). Data are expressed as the average cpm ± SEM from three independent experiments conducted in triplicate. Variation between triplicate measurements in each experiment was less than 10%. The specific activity of [^{32}P] ATP used was 220 cpm/pmol. Statistically significant differences in PKC activity are as follows: TPA ANOVA: df=2,13, F=9.2, p<0.01; Dunnett's *t* test, TPA versus TPA+Staurosporine, p<0.01. PAF ANOVA: df=2,13, F=46.3, p<0.01; Dunnett's *t* test, PAF vs. PAF+Staurosporine, p<0.01; PAF vs. PAF+CV3988, p<0.01. For statistically significant differences between vehicle and PAF or TPA treatment see Figure 39.

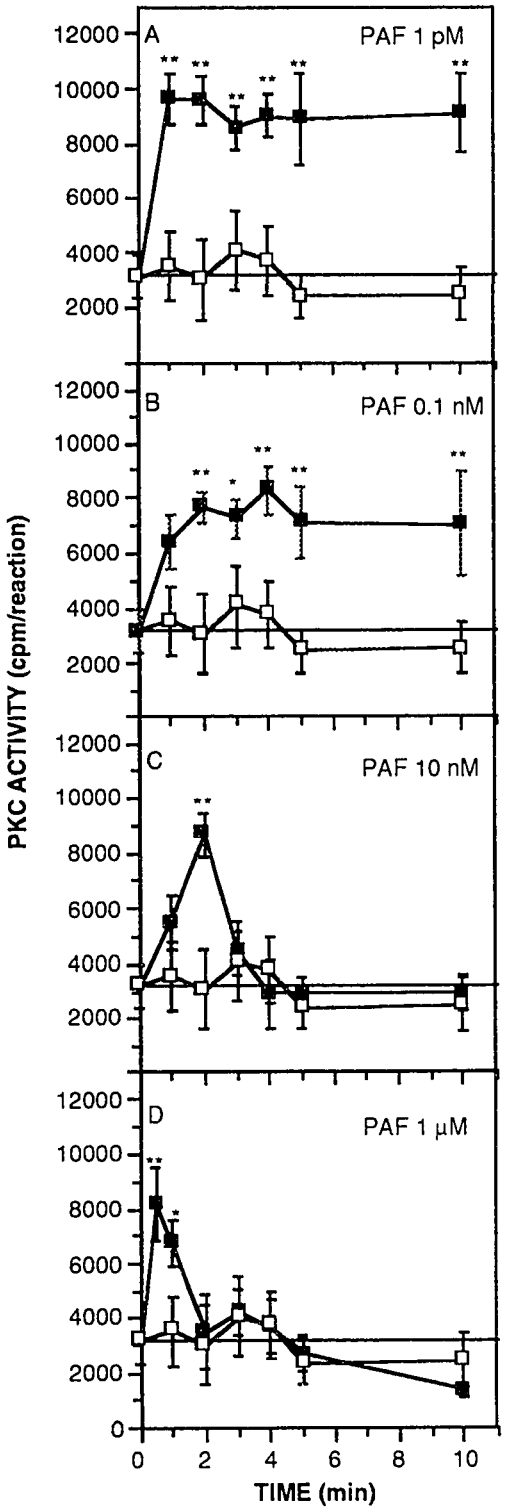

Figure 41. The effect of PAF concentration on membrane-associated PKC activity in RECs

Cells were treated with PAF and kinase assays were performed as described in Materials and Methods. □, vehicle (0.1% DMSO) treatment; ■,PAF (1 pM) (A), PAF (0.1 nM) (B), PAF (10 nM) (C), or PAF (1 µM) (D); ——, non-specific binding of ^{32}P to P81 paper in the absence of peptide substrate. Statistically significant differences in PKC activity across time and treatments are as follows: PAF (1 pM) versus vehicle: MANOVA, df=1,60; 1 min treatment, F=14.7, $p<0.01$; 2 min treatment, F=17.0, $p<0.01$; 3 min treatment, F=8.0, $p<0.01$; 4 min treatment, F=11,0, $p<0.01$; 5 min treatment, F=16.1, $p<0.01$; 10 min treatment, F=17.2, $p<0.01$. PAF (0.1 nM) versus vehicle: MANOVA, df=1,60; 2 min treatment, F=8.4, $p<0.01$; 3 min treatment, F=3.9, $p<0.05$; 4 min treatment, F=8.0, $p<0.01$; 5 min treatment, F=8.7, $p<0.01$; 10 min treatment, F=7.9, $p<0.01$. PAF (10 nM) versus vehicle as in Figure 40. PAF (1 µM) versus vehicle: MANOVA, df=1,70; 0.5 min treatment, F=13.1, $p<0.01$; 1 min treatment, F=4.6, $p<0.05$.

nM) of PAF elicited sustained PKC activation while high doses (10 nM - 1μM) elicited a transient increase in membrane-bound PKC activity. With increasing PAF doses, the kinetics of the PKC response was shifted to the left with 1 μM PAF eliciting maximal PKC activation within 30 sec of stimulation while 10 nM PAF eliciting peak activity within 2 min of stimulation. These data indicate that higher doses of PAF are capable of activating PKC faster than lower doses while lower doses sustain PKC activation to a greater extent than higher doses.

PKC Activation in HFs and human neutrophils

Activation of membrane-bound PKC in HFs and human neutrophils following PAF stimulation was demonstrated to be both quantitatively and temporally different from that exhibited by RECs. PAF elicited a dose-dependent increase in PKC activity with maximal activation occurring within 2 min of stimulation in both HFs (Figure 42) and human neutrophils (Figure 43). Human neutrophils were slightly more responsive to PAF than HFs. PAF (1 μM) induced a three-fold increase in PKC activation in human neutrophils compared to vehicle-treated cells (an increase comparable to REC enhancement) and a two-fold increase in kinase activity in HFs. However, unlike RECs, different concentrations of PAF failed to alter the kinetics of PKC activation in either HFs or human neutrophils. Dose-dependent alterations were confined to the magnitude of response and not the duration of activity. Specificity of the PAF-induced response was confirmed by pre-treating cells with the PAF receptor antagonist, CV3988 (10 μM). Blocking PAF receptors effectively inhibited the increase in PKC activity observed 2 min after PAF administration (data not shown). These data demonstrate not only that PAF is capable of activating PKC-dependent signalling pathways but also confirm the observation that there exists some species to species differences in one of the signalling pathways triggered by PAF stimulation (see Chapter III, Section 4).

Tyrosine Phosphorylation in RECs and HFs

PAF has been shown to increase tyrosine phosphorylation in rat Kupffer cells (9,10), rabbit platelet (28), and human A431 epidermoid carcinoma cells (34,36). Following PAF exposure, increases in tyrosine phosphorylated proteins were demonstrated by Western analysis in

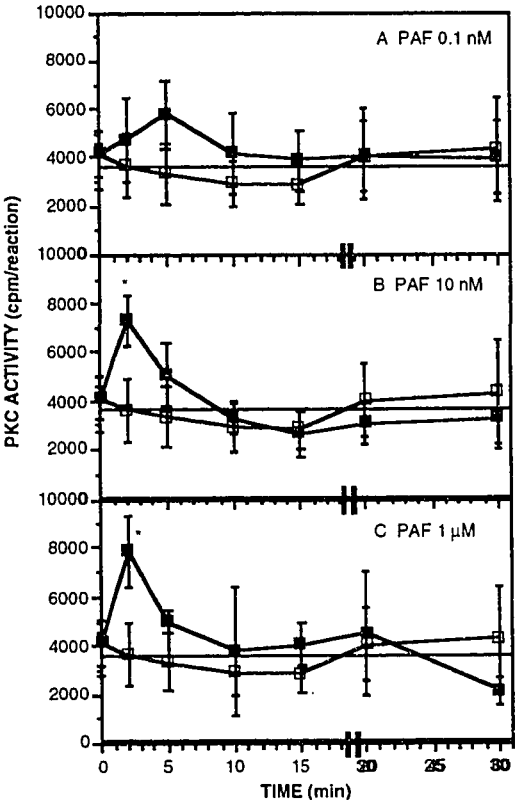

Figure 42. PAF dose-dependently increases membrane-associated PKC activity in HFs

Cells were treated with PAF and kinase assays were performed as described in Materials and Methods. □, vehicle (0.1% DMSO) treatment; ■, PAF (0.1 nM) (A), PAF (10 nM) (B), or PAF (1 μM) (C); ——, non-specific binding of ^{32}P to P81 paper in the absence of peptide substrate. Statistically significant differences in PKC activity across time and treatments are as follows: PAF (10 nM) versus vehicle MANOVA: df=1,60; 2 min treatment, F=8.4, p<0.05. PAF (1 μM) vs. vehicle MANOVA: df=1,60; 2 min treatment, F=8.4, p<0.05.

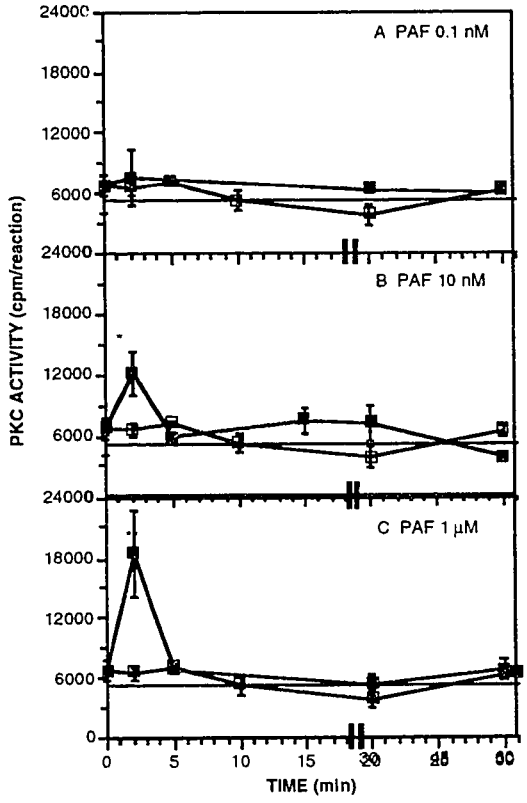

Figure 43. PAF dose-dependently increases membrane-associated PKC activity in human neutrophils

Cells were treated with PAF and kinase assays were performed as described in Materials and Methods. □, vehicle (0.1% DMSO) treatment; ■, PAF (0.1 nM) (A), PAF (10 nM) (B), or PAF (1 μM) (C); ——, non-specific binding of ^{32}P to P81 paper in the absence of peptide substrate. Statistically significant differences in PKC activity across time and treatments are as follows: PAF (10 nM) versus vehicle MANOVA: df=1,60; 2 min treatment, F=8.4, p<0.05. PAF (1 μM) vs. vehicle MANOVA: df=1,60; 2 min treatment, F=8.4, p<0.01.

RECs and HFs. Data are presented for RECs (Figure 44). The pattern of immunoreactivity was similar for both rodent and human fibroblasts although immunoprecipitation of radiolabelled phosphotyrosine containing proteins is required for greater resolution and more precise analysis. PAF increased tyrosine phosphorylation of proteins with approximate molecular weights of 112, 89, 34, and 23 kD. Maximal effects were observed after 5 min of stimulation. Phosphorylation could be inhibited by the PAF antagonist CV3988 (Figure 44). These data are in accordance with the relative size and kinetics of tyrosine phosphorylated proteins induced by PAF stimulation in other cell types (34,36).

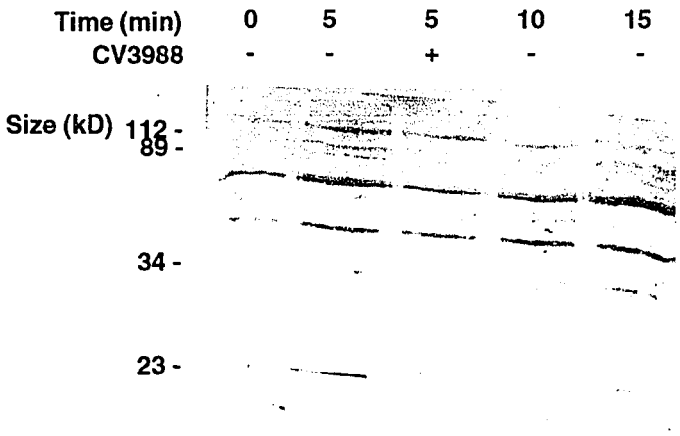

Figure 44. PAF (10 nM) time-dependently alters tyrosine phosphorylation in RECs

Cells were treated with PAF and SDS-PAGE and Western analysis were performed as described in Materials and Methods. A representative immunoblot of PAF (10 nM)-treated RECs is depicted. Co-exposure with CV3988 (1 μM) + PAF (10 nM) inhibited tyrosine phosphorylation of proteins with molecular weights of 112, 89, 34, and 23 kD.

4. PAF Induces Gene Expression Associated with Cell Growth and Cell Death

Abstract

PAF stimulation (1 pM - 1 μM) was found to increase c-*fos* and clusterin mRNA but not urokinase plasminogen activator (UPA) mRNA expression in RECs and HFs. These data provide the first evidence that PAF can influence gene expression in primary rodent and human fibroblasts. PAF was found to transiently increase *fos* expression in RECs 5 min after stimulation. In keeping with the kinetics of PKC activation observed in Chapter IV, Section 3, lower doses (1 pM) elicited longer lasting increases in mRNA levels (up to 30 min) than higher doses (1 μM) (up to 15 min). The magnitude of *fos* expression following superinduction with cycloheximide (10 μg/ml) was greater in TPA (10 nM)-treated RECs than PAF (10 nM)-treated cells, consistent with degree of PKC activation observed in Chapter IV, Section 3. Induction was mediated by PAFR stimulation given that CV3988 (1 μM) blocked PAF-induced increases in *fos* expression but not TPA-induced increases. In HFs, unlike RECs, PAF (1 μM) was found to elicit sustained c-*fos* expression 10 min after ligand exposure lasting 1 hr after initial stimulation. PAF was also capable of eliciting clusterin expression (a gene product involved in regulation of complement fixation during an inflammatory response) in HFs.

Introduction

PAF has been demonstrated to increase transcription of c-*fos*, zif/268, and early growth response gene-2 (EGR2) in inflammatory cells (12,21,24,28). In many of these systems, attenuation of PAF-induced changes in gene expression have been achieved by treatment with either tyrosine kinase or PKC inhibitors, permitting the elucidation of a hierarchy of signal transduction events occurring immediately after receptor stimulation (21). In non-inflammatory cell lines, PAF-induced expression of c-*fos*, c-*jun*, and TIS-1 has been demonstrated in A431 (human epidermoid carcinoma) cells, HEC-1A (endometrial carcinoma) cells, and NG108 (glioma/neuroblastoma hybrid) cells (1,19,24,32,36). Subsequent formation of AP-1 transcription complexes have been shown to alter AP-1-responsive gene expression (32).

Since PAF signalling has been implicated in both enhanced cell proliferation and increased cell death in RECs and HFs (Chapter III, Section 2), the possibility that PAF elicits gene expression was investigated. Three candidate genes were chosen for evaluation, c-*fos*, clusterin, and urokinase plasminogen activator (UPA), based on their association with cell growth, cell ablation, and the inflammatory response in cancer and progressive neurodegenerative disorders (Chapter II, Sections 2-4). C-*fos* is a proto-oncogene known to play a role in immediate cell

signalling responsible for induction of cell growth, cell death, and transcriptional modulation depending upon the circumstances and duration of activation (for a review see ref. (19)). The clusterin gene product appears to function as a complement inhibitor whose expression is up-regulated during apoptosis and probably facilitates in ensuring that both healthy and apoptotic cells avoid immune surveillance and complement fixation (15). Clusterin may preferentially ensure cell survival in the face of apoptotic signals given the *in situ* localization of mRNAs to surviving rather than apoptotic cells after morphological evaluation. UPA is a protease capable of activating the metalloprotease plasminogen thus facilitating breakdown of various protein components of the ECM. Increased expression of UPA is associated with inflammatory cell migration, active cell death, and the metastatic process (15,19,39).

To determine whether PAF can specifically modulate c-*fos*, clusterin, or UPA expression in receptor-mediated fashion, Northern analyses were performed on total RNA isolated from RECs and HFs stimulated with ligand in the presence or absence of a PAF receptor antagonist, CV3988.

Materials and Methods

Cells and Culture Conditions

Fifth and sixth passage RECs and HFs were grown as described in Chapter IV, Section 2. Cultures were allowed to reach confluence prior to treatment.

Measurement of Gene Expression

Cells were treated with PAF (1 pM - 1 μM) for 1 hr in the presence or absence of 1 μM CV3988 (PAF receptor antagonist) as described in Chapter III, Section 3. Where indicated, CV3988 was added 15 min prior to PAF exposure and co-incubated with PAF for 1 hr following ligand stimulation. In some experiments, cells were pretreated with 10 μg/ml cycloheximide added 10 min prior to ligand administration to increase the lifetime of PKC-responsive genes (4). Following stimulation with PAF for various time intervals, total cell RNA was extracted and Northern analysis carried out as described in Chapter IV, Section 2. The DNA probes used were a 1 Kb *Pst* 1 fragment of p-*fos*-1 (c-*fos* probe) (4), a 1.7 Kb *EcoRI* fragment of p17H (clusterin

probe) (40), a 1.5 Kb *PSTI* fragment of pHUK8 (UPA probe) (14), and a 1.2 kb *Pst*I fragment from the pGAPDH (GAPDH probe) (31). Probes were labelled with [^{32}P]dCTP using a random primer labelling kit (Pharmacia, Ont). Pre-hybridization and hybridization were carried out as described in Chapter IV, Section 2. At the end of the procedure, membranes were air-dried and exposed to X-ray film for 3-48 h at -100°C. When membranes were re-probed, the first probe was removed by exposing the membranes to 0.25% SDS, 10 mM sodium citrate (pH 6.8), at 95°C for 5 min. Densitometric analysis were performed on autoradiograms determined to be within linear range using an optical wedge by a GelScan XL densitometer.

Results and Discussion

Induction of gene expression in RECs

PAF (10 nM) had no effect on UPA expression (data not shown). An increase in *fos* mRNA levels was observed in total cellular RNA isolated from RECs as early as 2 min following PAF treatment in the presence of cycloheximide (Figure 45A). This induction was blocked by pretreatment with CV3988 (1 μM) indicating involvement of PAF receptors (Figure 45C). As expected, TPA (10 nM) induced *fos* mRNA expression (Figure 45B) and there was no effect of CV3988 (1 μM) (Figure 45C). Densitometric analysis revealed that the degree of induction was 2 fold greater in TPA (10 nM)-treated RECs than in PAF (10 nM)-treated RECs following superinduction of mRNA by cycloheximide. The kinetics of PAF-induced *fos* mRNA induction were consistent with the pattern of PKC activation observed in Chapter IV, Section 3. In the absences of cycloheximide, lower doses of PAF induced longer-lived *fos* expression (Figure 46A) than higher doses (Figure 46B).

Induction of gene expression in HFs

PAF did not affect UPA expression in HFs (data not shown). However, similar increases in c-*fos* expression were observed in HFs treated with PAF (1 μM) as observed in RECs with the exception that the kinetics of c-*fos* activation were slightly delayed and longer lasting in HFs compared to RECs (Figure 47). PAF-induced an 5 fold increase in c-*fos* mRNA within 10 min of stimulation lasting up to 1 hr after ligand exposure. REC expression, at the same PAF dose,

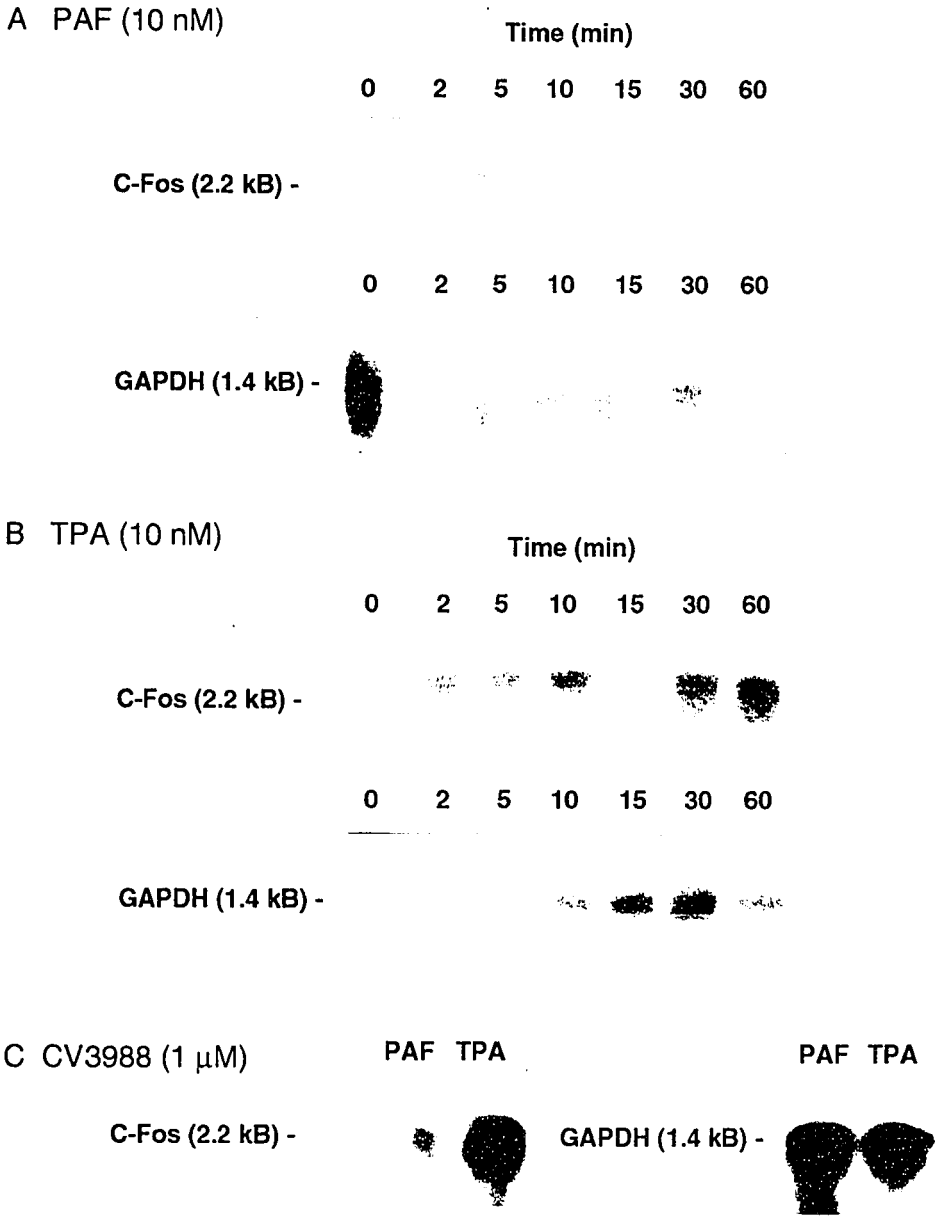

Figure 45. PAF induces expression of the proto-oncogene c-*fos* and the ACD-related gene clusterin in RECs

Cells were treated with (A) PAF (10 nM) or (B) TPA (10 nM) in the presence or absence of a (C) PAF receptor antagonist, CV3988 (1 μm). Superinduction was achieved by pretreating cells with of a protein synthesis inhibitor, cycloheximide (10 μg/ml), prior to RNA extraction. Following stimulation for various time periods, total RNA was isolated and Northern analysis was performed as described in Materials and Methods. Representative autoradiograms are depicted.

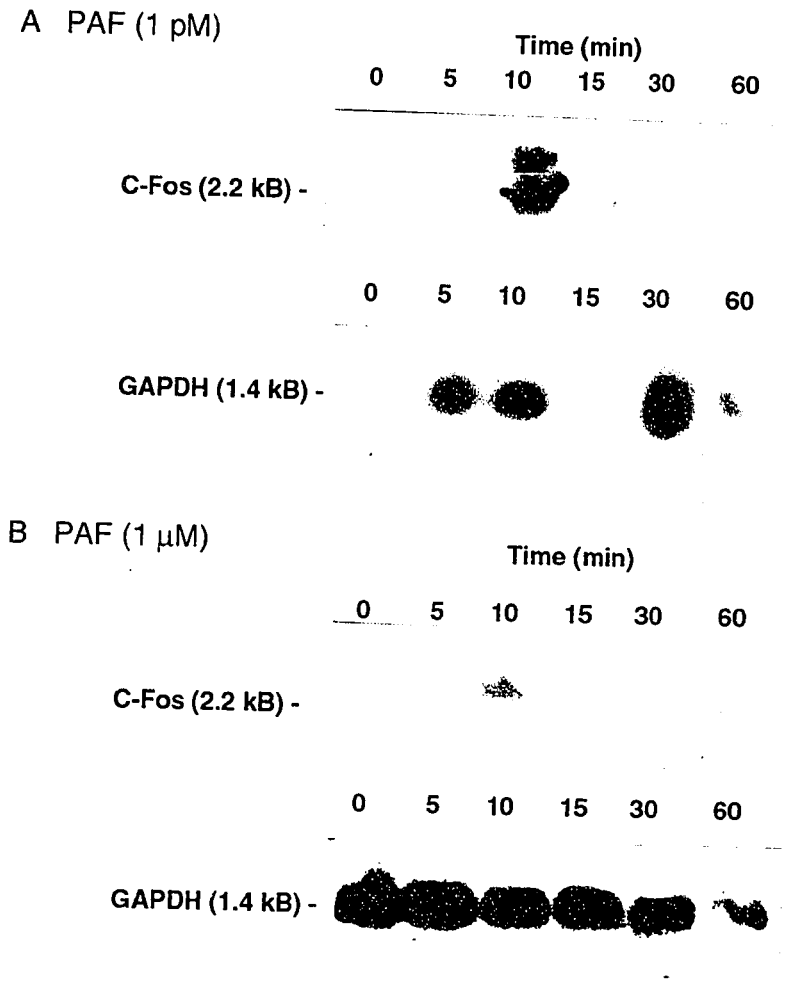

Figure 46. Dose-dependent modulation of c-*fos* expression during PAF stimulation of RECs

Cells were treated with (A) PAF (1 pM) or (B) PAF (1 μM) for various time periods. Cells were not pretreated with cycloheximide prior to RNA extraction. Following stimulation, total RNA was isolated and Northern analysis was performed as described in Materials and Methods. Representative autoradiograms are depicted.

PAF stimulation was also capable of increasing clusterin mRNA expression suggesting that PAF treatment primes fibroblasts to survive activation of complement within the inflammatory environment. PAF (10 nM) induced an 2-fold increase over basal clusterin expression within 2 min of stimulation (Figure 47B). Clusterin is a complement-regulatory protein that is believed to protect cells from complement fixation and immune-mediated lysis by preventing binding of C3b (Chapter II, Section 2). Clusterin may also attenuate PAF production by attenuating complement activation. Stimulation of decidual macrophages with activated complement inhibits secretion of PAF-acetylhydrolase, thus prolonging exogenous PAF half-life in neighbouring tissue (29). Activation of inflammatory cells with C3b induces PAF synthesis and release (13,37). Because clusterin attenuates the binding of complement to healthy cells, it presumably plays some role in mediating paracrine induction of PAF synthesis in cells exposed to circulating complement factors. In fact, activation of clusterin may represent a self-regulatory response designed to limit expansion of the inflammatory response by modulating the complement/PAF feedback loop, and/or a protective response designed to prime healthy cells within injured tissue to survive the inflammatory environment.

These data provide the first evidence that PAF modulates gene expression in rodent and human fibroblasts.

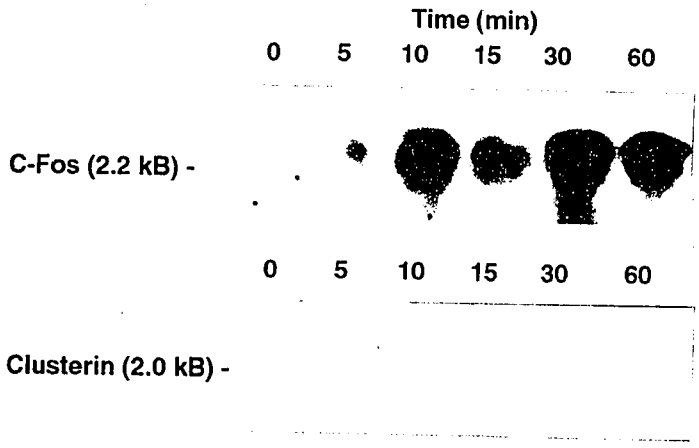

Figure 47. PAF induces c-*fos* and clusterin expression in HFs

Cells were treated with PAF (1 μM) for various time periods. Cells were not pretreated with cycloheximide prior to RNA extraction. Following stimulation, total RNA was isolated and Northern analysis was performed as described in Materials and Methods. Representative autoradiograms from two different membranes are depicted. Equivalent amounts of RNA were loaded in each lane as assessed by ethidium bromide staining (data not shown).

5. PAF-Induced Growth Enhancement is Accompanied by Gene Expression

Abstract

A 1 hr exposure to PAF (1 μM) induces long-term cell proliferation in HFs grown under suboptimal conditions (Chapter III). This growth enhancement is accompanied by increases in clusterin and UPA mRNA levels over a 30 day period in the absence of further PAF stimulation. C-*fos* gene expression was not affected following ligand removal. The enhanced expression in clusterin and UPA could be inhibited by exposure to PAF in the presence of a specific PAF receptor antagonist, CV3988 (10 μM). Induction of mRNA was first observed 5 days after treatment, corresponding with increased cell proliferation, and lasted for at least 30 days after treatment. Vehicle-treated cells, cultured under identical conditions, did not exhibit any changes in *fos*, clusterin, or UPA gene expression. These data indicate that brief stimulation of HFs with PAF is sufficient to modulate chronic gene expression in parallel with increases in autonomous cell growth.

Introduction

Chapter III describes a series of experiments demonstrating that a 1 hr treatment with PAF is sufficient to induce long-term growth enhancement of HFs grown under sup-optimal conditions and in the absence of further exogenous ligand exposure. Given this phenotypic observation, it was hypothesized that alterations in gene transcription accompany this effect. To test this hypothesis, expression of the three candidate genes described in Chapter IV, Section 4 was monitored over a 30 day period in HFs following brief exposure to PAF (1 μM).

Material and Methods

Cells and Culture Conditions

Sixth passage HFs were grown as described in Chapter IV, Section 2.

Measurement of Gene Expression

Cells were treated for 1 hr with PAF (1 μM) or vehicle as described in Chapter III, Section 3. Following stimulation, HFs were washed free of ligand and were incubated in low serum medium for up to 30 days . Medium was replaced twice weekly. Total cell RNA was extracted at various time points after treatment and Northern analysis carried out as described in Chapter IV, Section 2. The DNA probes used were the c-*fos*, clusterin, UPA, and GAPDH probes described

in Chapter IV, Section 4. Probes were labelled with [^{32}P]dCTP using a random primer labelling kit (Pharmacia, Ont). Pre-hybridization and hybridization was carried out as described in Chapter IV, Section 2. Membranes were then air-dried and exposed to X-ray film (Kodak) for 3-48 h at -100°C. When membranes were re-probed, the first probe was removed by exposing the membranes to 0.25% SDS, 10 mM sodium citrate, pH 6.8, at 95°C for 5 min.

Results and Discussion

Brief PAF stimulation (1 hr) was found to induce UPA and clusterin but not *fos* expression over a 30 day period (Figure 48). These increases were not observed in vehicle-treated cultures or cells exposed to PAF in the presence of CV3988 (10 μM) (data not shown). UPA mRNA induction was first evident 3 days after PAF treatment and lasted for 25 days after stimulation. Transient enhancement of clusterin mRNA levels was first apparent during PAF treatment (Chapter IV, Section 4) and then reappeared 5 days after ligand removal lasting for 25 days after stimulation. It was of interest to note that these kinetics correspond to the induction of cell proliferation observed in PAF-treated HFs cultured under the same sub-optimal conditions. These data demonstrate that PAF induces sustained expression of genes capable of regulating ECM-degrading proteases (UPA) and of facilitating escape from immune surveillance (clusterin). These findings encourages speculation that PAF has the potential to transiently influence tumour cell invasion and metastasis.

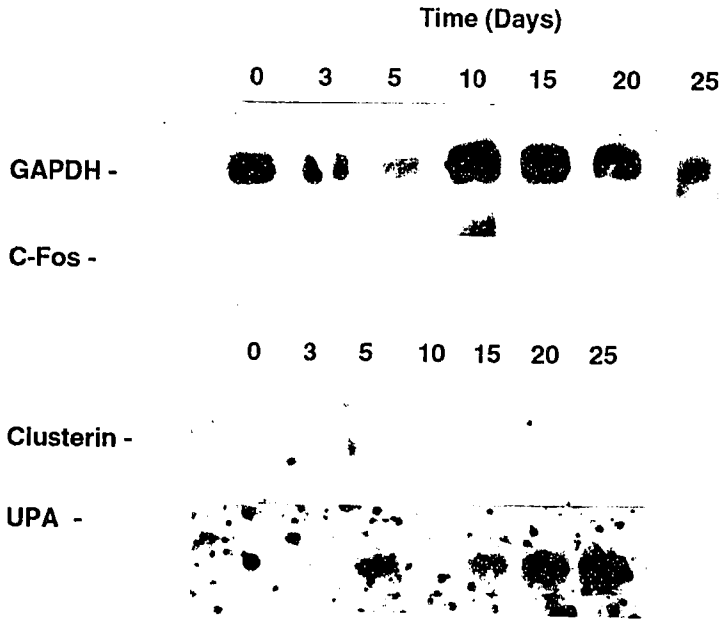

Figure 48. Transient PAF stimulation induces urokinase plasminogen activator (UPA) and clusterin expression but not c-*fos* expression in HFs

Cells were treated with PAF (1 μM) for 1 hr and incubated in low serum medium for 30 days with twice weekly feeding. Total RNA was isolated at various time points and Northern analysis was performed as described in Materials and Methods. Representative autoradiograms are depicted.

6. Overview

The data presented in 'Signal Transduction' provide direct evidence for the hypothesis that PAF-induced cell signalling in RECs and HFs is mediated by specific PAF receptors, PKC activation, and phosphorylation of, as yet, uncharacterized proteins on tyrosine residues. Immediate signal transduction events observed in the presence of PAF could be distinguished from the subsequent cell signalling observed in the absence of ligand. PAF stimulated transient, immediate expression of the c-*fos* proto-oncogene and the complement-regulatory gene, clusterin, but did not alter transcription of UPA. Subsequent expression of clusterin and *de novo* increases in UPA mRNA were observed 5 days after PAF treatment with enhanced expression lasting up to 30 days after the initial stimulation. Increases in c-*fos* mRNA were not observed upon removal of the ligand indicating that, although this immediate-early gene product may assist in eliciting long-term growth enhancement by linking extracellular receptor stimulation to immediate intracellular alterations in transcription, it is not required for subsequent gene expression or cell proliferation in the absence of PAF. These data provide the first insight into PAF-mediated signal transduction in rodent and human fibroblasts and document the unexpected result that brief exposure to PAF is sufficient to alter gene expression for up to 30 days after ligand removal.

V

TUMOUR PROGRESSION

1. Introduction

In the preceding chapters, PAF has been shown to induce either cell growth or cell death in primary RECs and HFs depending upon the dose and the duration of ligand exposure. Evidence is presented to suggest that these effects are mediated by a variety of signal transduction molecules including PAFR, intracellular PAF, PKC, tyrosine kinase, and H_2O_2 and are accompanied by transient expression of the proto-oncogene c-*fos* and prolonged expression of both the protease-encoding gene UPA and the ACD-associated gene clusterin.

The observation that proto-oncogenes and metastasis-related genes accompany PAF-induced growth enhancement underlines another similarity between the 'inflammatory phenotype' and malignant conversion. Transient growth enhancement, ECM remodelling, and the ability of healthy cells to avoid complement fixation are necessary components of wound healing. However, when constitutively expressed, these characteristics also define the tumour cell phenotype. Malignant transformation requires mutagenic conversion of a proto-oncogene to an oncogene, loss of tumour suppressor function, and/or permanent activation of metastasis-related genes. The data presented in the previous chapters indicate that it is unlikely that PAF is directly mutagenic. In fact, in extrapolating the *in vitro* evidence presented in Chapters II-IV to the *in vivo* situation, it is tempting to speculate that PAF elicits ACD in non-inflammatory cells *continually* exposed to high concentrations of inflammatory agents (ie. cells located at the centre of inflamed tissue) while promoting proliferation in cells *transiently* exposed to lower concentrations of ligand (ie. cells located at the periphery of injured tissue). During a normal inflammatory response, this response could serve to protect against the survival of cells exposed to high levels of potentially damaging proinflammatory agents (for a list see Chapter II, Section 3) while still facilitating wound healing in neighbouring tissue. However, during chronic inflammatory conditions, PAF-induced protracted cell proliferation could also serve to increase the likelihood that rare cells are exposed to DNA-damaging agents while in the process of replicating. As indicated in Chapter II, Section 3, many genetic alterations observed in human cancers *in vivo* and elicited by proinflammatory agents *in vitro* require cell division (ie. chromosome loss, duplication, and

translocation). Given the strong correlation between chronic inflammatory conditions and increased predisposition to many cancers (Chapter II, Section 3), this model suggests that repeated exposure to PAF, as a consequence of chronic inflammation, may influence tumourigenesis by increasing the probability that a non-inflammatory cell survives and proliferates within a non-permissive and potentially damaging inflammatory environment.

Given the hypothesis that PAF contributes to tumourigenesis by increasing the rate of cell growth, what role (if any) could PAF play in tumour progression? By definition, tumour cells are already capable of autonomous cell growth. Presumably, these cells are also routinely exposed to proinflammatory agents as their tumour expansion has been shown to elicit inflammatory and immune responses in surrounding tissue and perpetuate chronic inflammatory conditions (32,43). What effect, then, does PAF have on cells already transformed? Since the ligand has been implicated in proto-oncogene activation, ECM remodelling, and escape from immune surveillance, it seems possible that these effects could influence metastatic potential in cells already genetically altered. Once again attention is drawn to the similarities between the 'inflammatory phenotype' and the 'metastatic phenotype'. PAF plays an integral role in inducing inflammatory cell migration, extravasation of activated phagocytes into and out of the circulatory system, and immune system modulation (Chapter II, Section 5). Could tumour progression be influenced by long-term (albeit transient) phenotypic alterations in the presence of existing genetic mutations. To address this question, primary RECs were transformed with an activated human *ras* oncogene and phenotypic/genotypic changes in response to PAF treatment were evaluated.

2. Recovery of a Rare Clone from a Population of Unstable Retroviral Vector-Expressing RECs

Abstract

Although a useful and important method of gene transfer, retroviral vectors can be genetically unstable. In the course of routine experiments using DOEJS, a retroviral vector able to confer expression of a c-Ha-*ras* oncogene and a neomycin resistance gene (*neo*) on mammalian cells (9), it was demonstrated that the vast majority of infected RECs, recovered on the basis of *neo* activity (ie., G418 resistance), did not express *ras* mRNA. It was subsequently found that most cells in the ψ2 cell line used to propagate the DOEJS retrovirus failed to produce virion capable of expressing both *ras* and *neo* in RECs. A simplified RNA extraction and slot-blot technique was developed to screen mRNA from several hundred fibroblast clones and, in doing so, successfully infected REC/*ras* cells (producing both *neo* and *ras* mRNA) were identified at low frequency (0.8%). The DOEJS/ψ2 packaging line was subcloned and individual cell lines screened for their ability to confer appropriate gene expression on target RECs. DOEJS/ψ2-D6 was eventually isolated after screening 24 DOEJS subclones and 240 infected REC colonies. DOEJS/ψ2-D6 was shown to reliably induce G418 resistance indicative of both *ras* and *neo* mRNA expression in RECs. Thus, the RNA extraction and screening procedure was useful for (1) recovering an infrequent subclone producing a retrovirus with the original properties and (2) establishing a *ras*-transformed REC line (REC/*ras* cells).

Introduction

Cloning vectors employing replication deficient retroviruses are important tools for efficiently introducing genetic sequences into the DNA of mammalian cells. This technology has been used to insert foreign genes into embryos (9) and is increasingly being explored for human gene therapy (14,28). However, retroviral vectors can be genetically unstable (26,40) highlighting one of the many obstacles thwarting successful therapeutic usefulness. This chapter describes work with the DOEJS retroviral vector designed by Compere et al (9) and obtained for the purpose of introducing an activated *ras* oncogene and a selectable drug resistance marker into third passage RECs. DOEJS, containing a human c-Ha-*ras*-1 oncogene driven by a Moloney murine leukemia virus long terminal repeat (Mo-MuLV LTR) and a Tn*10* neomycin resistance gene (*neo*) driven by a simian virus 40 (SV40) early-region promoter, was maintained in an appropriate ψ2 packaging cell line permitting virion propagation into culture medium. This construct has been shown to successfully transduce *ras* and *neo in vivo* in murine embryos (9) and *in vitro* in rodent epithelial cells (43). However, under the present conditions, when virion were harvested from DOEJS/ψ2 culture supernatant and used to infect RECs, only 0.8% of the G418-

resistant infectants exhibited morphological transformation characteristic of oncogenic *ras* activation. A rapid RNA extraction and slot-blot procedure was designed to recover rare clones in the infected REC population expressing both *neo* and *ras* and to permit identification of a functional DOEJS/ψ2 clone from a population composed primarily of viral variants.

Materials and Methods

Cells, retrovirus, and culture conditions

Third passage RECs were as described in Chapter III, Section 2. DOEJS/ψ2 cells, kindly provided by Dr. R. Jaenisch, are a ψ2 cell packaging line that produces a replication-deficient retrovirus containing the DOEJS construct (9). The construct is composed of the EJ bladder carcinoma human Ha-*ras*-1 oncogene, driven by a Mo-MuLV LTR, and a Tn*10* neomycin resistance gene, driven by a SV40 early-region promoter conferring resistance to the drug G418 sulfate. NIH 3T3 cells (ATCC) are an established murine fibroblast line used to titre virus potency. RECs, DOEJS/ψ2 cells, and NIH 3T3 cells were cultured in DMEM+10% FCS as described in Chapter III, Section 2.

Retrovirus-mediated gene transfer

Virion were harvested from the supernatant of 90% confluent DOEJS/ψ2 cells, 24 hr after medium change. The supernatant was filtered through a 0.45 μm filter to remove cell debris. RECs or NIH 3T3 cells, seeded at $5x10^5$ cells per 10 cm dia. tissue culture dish 24 hr prior to infection, were exposed for 18 hr to retrovirus in 5 ml of DOEJS/ψ2 supernatant containing 8 μg/ml polybrene (Sigma, MO). The medium was diluted with fresh DMEM+10% FCS reducing the polybrene concentration to 1.6 μg/ml and incubation was continued for 48 hr. Cells were detached by trypsinization and replated at $1x10^5$ per 10 cm dia. tissue culture dish. Infected target cells were grown for 10 days in selection medium containing 400 μg/ml G418 sulfate (Gibco/BRL, Ont) with twice weekly feedings. For Northern analysis, DOEJS-infected population and isolated clones were grown in selection medium until a suitable cell density was obtained. For slot-blot analysis, DOEJS-infected cells were plated in 24-well tissue culture dishes

under selection pressure until nucleic acids extraction.

Extraction of DNA and total cellular RNA

DNA was extracted as described in (5). For Northern blot analysis (*standard* protocol), RNA was extracted from $5x10^6$ cells as described in Chapter IV, Section 2. For slot-blot analysis (*slot-blot* protocol), a simplified extraction procedure eliminated precipitation and DNA removal steps. Cultures containing $4x10^3$ to $5x10^5$ RECs per well in a 24-well culture plate were washed with a balanced salt solution before addition of 250 µl RNA extraction solution (RES) containing 25-75 µg/ml proteinase K (depending on the cell number). RES is 0.5 M LiCl, 1 M urea, 0.25% sodium doedcyl sulfate (SDS), 20 mM sodium citrate, 5 mM CDTA, pH 6.8, modified slightly from (5). Plates were maintained at 50°C with shaking until the digested material was clear and could be easily pipetted ($\leq$ 2 h). Extracts were transferred to 2 ml microcentrifuge tubes and individually sonicated with a 1/8" microprobe at low power. Samples were sequentially extracted with 50 µl phenol/chloroform and 100 µl chloroform, leaving behind the organic (bottom) phase and interface material. The final volume of the aqueous samples was approximately 200 µl. Contaminating DNA was not removed for reasons described below. Samples were analyzed in duplicate (100 µl), except where very small amounts of material were available. Traces of chloroform were removed by evaporation to avoid damaging the plastic slot-blot apparatus.

Southern, northern, and slot-blot analyses

Southern analysis was performed as described in (10). Samples were digested with *Sst*I prior to electrophoretic separation on a 0.8% agarose gel. Electrophoretic and transfer conditions were as in (8). Northern analysis (of RNA prepared by the *standard* protocol) was carried out essentially as described in Chapter IV, Section 2. Briefly, purified total RNA (approximately 10 µg) in CCS (1 mM sodium citrate, 1 mM CDTA, 0.1% SDS, pH 6.8) was denatured with formaldehyde, electrophoretically separated on a 1.2% agarose gel containing 0.2 M formaldehyde, and transferred to a Hybond-N nylon membrane filter using a vacuum system. For slot-blot analysis (of RNA prepared by the *slot-blot* protocol), 100 µl samples, prepared as

described above, were mixed with 10 µl 37% formaldehyde and heated for 30 min at 65°C. Contaminating double-stranded DNA is not expected to be denatured under these conditions and, therefore, is not expected to bind in significant amount to membrane filters. Hybond-N membranes were hydrated for 15 min in 0.5 M to 2.5 M of either NaCl, LiCl, CsCl, or KCl, or in 0.5 to 10xSSC (10xSSC: 1.5 M NaCl, 0.15 M sodium citrate) and mounted in a BioRad slot-blot manifold. 100 µl of the corresponding high salt solution was added to the denatured RNA samples prior to transfer. A 150 W heat lamp was used to maintain an elevated temperature in the manifold throughout the transfer to avoid precipitation of detergent. Samples were applied under 40 cm water vacuum and wells were washed once with 200 µl 10xSSC. Membranes were removed from the slot-blot apparatus, air-dried, heated for 20 min at 80°C, and irradiated with ultraviolet light for 3 min. Pre-hybridization and hybridization were carried out as described in Chapter IV, Section 4.

The DNA probes used were a 2.4 kb *Bam*HI/*Hind*III fragment of the pSV2 plasmid containing the neomycin resistance gene (*neo* probe) (34), a 2.9 kb Sac1 fragment from the pEJ6.6 plasmid containing the human c-H-*ras* gene (*ras* probe) (32) and a 1.2 kb PstI fragment from the pGAPDH plasmid containing the GAPDH gene (GAPDH probe) (29). Probes were labelled with [^{32}P]dCTP using a random primer labelling kit (Pharmacia, Ont). Following hybridization, membranes were air-dried and exposed to X-ray film for 3-48 h at -100°C. When membranes were re-probed, the first probe was removed by heating the membranes in 0.25% SDS, 10 mM sodium citrate, pH 6.8, at 95°C for 5 min.

Results and Discussion

Retroviral infection of RECs

Genetic instability of an established retroviral construct was encountered during routine gene transduction experiments. Five REC cultures were infected using supernatant from the DOEJS/ψ2 virion producer line and selected for G418 drug resistance. No morphological transformation characteristic of oncogenic *ras* expression was detected in any of the drug-resistant populations. By Northern analysis, all G418-selected populations could be shown to express *neo*

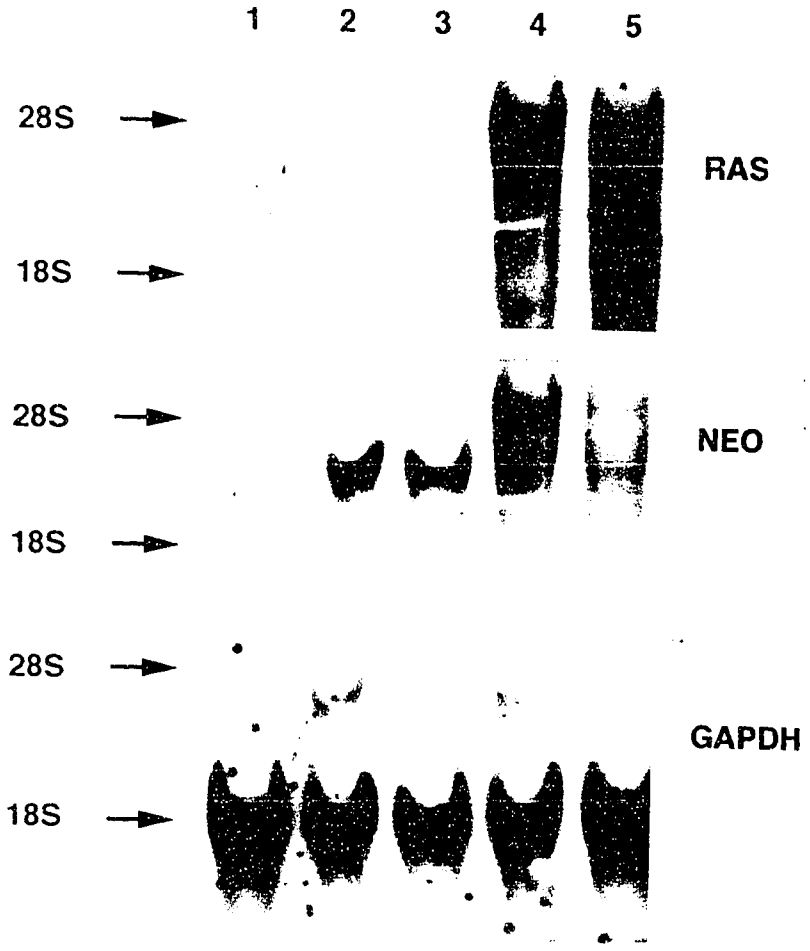

Figure 49. Northern blot of RNA isolated from control and DOEJS-infected REC populations.

RNA was extracted from the indicated cells using the *standard* procedure and probed with a *ras* probe, a *neo* probe, or a GAPDH probe as described in Materials and Methods. Lane 1, RECs; lane 2, DOEJS/ψ2-infected REC population #1; lane 3, DOEJS/ψ2-infected REC population #2; lane 4, DOEJS/ψ2-infected REC clone (REC/D #74); lane 5, DOEJS/ψ2 cells (producer line).

mRNA in the absence of detectable levels of *ras* mRNA (Figure 49). Thus, it appeared that the *ras* gene was either inactivated or lost.

Within the DOEJS vector, *ras* is driven by a Mo-MuLV LTR promoter while *neo* is driven by an SV40 promoter (Figure 50). This latter promoter is resilient to endogenous inactivation. However, primary rodent explants have been shown to express a variety of gene products that bind to and silence the Mo-MuLV LTR (26). Endogenous inactivation could account for the lack of morphological transformation observed in RECs following infection. The fact that G418-

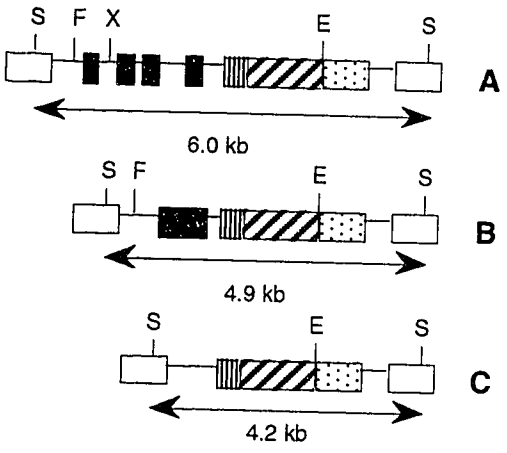

Figure 50. Structure of DOEJ-related recombinant retroviruses

Modified from Compere et al (9).

Key: Mo-MuLV LTR
Human Ha-*ras* exons
SV40 promotor
neo
pBR322 origin of replication

(A) DOEJ retrovirus, a replication-defective Mo-MuLV carrying the human c-Ha-*ras*-1 oncogene from EJ bladder carcinoma. (B) DOEJS virus, a spliced version of DOEJ lacking *ras* intron sequences. (C) Another DOEJ splicing variant lacking the entire *ras* sequence. Designated restriction endonuclease sites: X, *Xba*I; S, *Sst*I; E, *Eco*RI; F, *Bgl*II-*Bam*HI fusion sequence generated on insertion of EJ genomic sequences.

resistant NIH 3T3 cells, infected with DOEJS/ψ2 supernatant, did not demonstrate *ras*-induced transformation indicated that the problem was not specific to primary cells (data not shown). Another possibility is that the *ras* gene was lost during viral packaging or during integration of retroviral RNA into the target genome. High rates of genetic rearrangement during replication have been demonstrated in Mo-MuLV-based vectors (40). In fact, this inherent instability was evident during the original DOEJS construction. In Figure 50B, the DOEJS virus employed in the present study lacks endogenous *ras* introns. This construct represents a splice variant of the original DOEJ construct (Figure 50A) transfected by Compere et al (9) into ψ2 producer cells. Viron derived from DOEJ/ψ2 cells carried a variety of aberrantly spliced vector sequences with different degrees of functionality, including the construct depicted in Figure 50C in which the

entire *ras* sequence is missing. The DOEJS virus (Figure 50B), devoid of discernible *ras* intron sequences, was rescued from infected target cells and re-introduced into ψ2 packaging cells. Viron derived from this DOEJS/ψ2 line were shown to reliably infect target murine cells (9,43). In the present experiments, subsequent loss of DOEJS virus integrity during virion propagation may account for the inability to introduce both functional *ras* and *neo* gene into target cells. Southern analysis confirmed this hypothesis (Figure 51). When genomic DNA was isolated from DOEJS/ψ2 cells and G418-resistant RECs, digested with restriction endonucleases, and probed for *neo* sequence, a full-length DOEJS fragment (4.9 kb) as well as a faint larger band (6.0 kb) could be identified. This larger band is the same size as the original DOEJ construct. However, in the infected REC population, the predominant band was 4.2 kb with a faint signal at 4.9 kb indicating either that the DOEJS vector was truncated prior to integration or that some form of rearrangement occurred during assimilation of the construct into the REC genome. The faint band at 4.9 kb also suggested that rare *ras*-expressing RECs could be isolated from the mutant population. To accomplish this task, G418-resistant REC clones were screened for *ras* mRNA using the *slot-blot* protocol.

Development of the slot-blot protocol

Slot-blot analysis of gene expression is not a new screening procedure. Protocols have been developed to extract RNA from a small number of cells and permit direct application to membranes (6,7,24,36,37,40). Each technique has limitations such as variability in the efficiency of trapping of mRNA and a requirement for isolation of cytoplasm. The procedure developed in this chapter facilitates RNA extraction from multiple samples containing a relatively few number of cells by minimizing the number of steps involved in RNA purification. Ethanol precipitation is avoided and no attempts are made to remove DNA since double-stranded nucleic acids are not expected to bind to the nylon membrane under the conditions employed. These improvements permitted rapid screening of over 300 clones.

Effective binding of RNA to membranes requires high salt and improves with denaturation of the samples. The concentration of LiCl salt present in RES was not high enough to permit

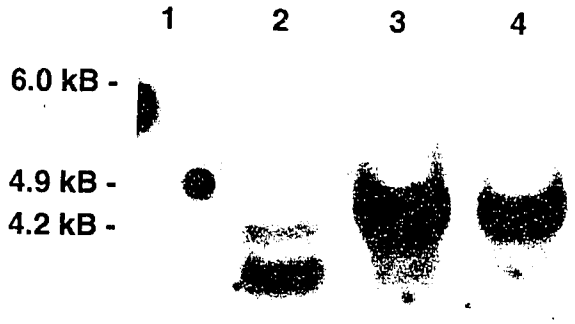

Figure 51. Southern analysis of DNA isolated from control and DOEJS-infected REC populations

DNA was extracted from the indicated cells and digested with *Sst*I. Southern analysis for *neo* was performed as described in Materials and Methods. Lane 1, RECs; lane 2, DOEJS/ψ2-infected REC population #1; lane 3, DOEJS/ψ2-infected REC clone (REC/D #74); lane 4, DOEJS/ψ2 cells (producer line).

optimal binding of RNA; however, raising the salt concentration above 0.5 M caused precipitation of SDS. Substitution of sarkosyl, a more soluble detergent, was not as effective in extracting RNA (data not shown). Consequently, several monovalent cations were tested for their ability to promote binding of RNA to nylon membrane, including 0.5 - 10xSSC and/or 0.5 - 2.5 M (final concentration) NaCl, LiCl, CsCl, and KCl. Only KCl (at 1.5 - 2.5 M final concentration) proved effective. Despite the fact that the potassium salt of dodecyl sulfate is insoluble at low temperature (4), precipitation could be avoided if samples were maintained at 55 - 65°C in a water bath both prior and subsequent to the addition of KCl (final concentration, 2.5 M) and the slot-blot apparatus was heated with a 150 W lamp. Thus, optimal conditions for binding of RNA to nylon membranes (*slot-blot* protocol) occurred when (1) preheated, formaldehyde-denatured samples in RES were mixed with an equal volume of preheated 5 M KCl and maintained at 65°C, (2) membranes were hydrated in 10xSSC, (3) diluted samples were quickly transferred to the heated slot-blot apparatus, and (4) wells were washed with 200 µl 10xSSC.

The sensitivity of this procedure was determined by comparing GAPDH mRNA in total RNA extracted from whole cells using either the *standard* or *slot-blot* protocol (Figure 52). Purified RNA, prepared by the *standard* protocol, was dissolved either in CCS or in RES plus indicated salts. RNA, prepared using the *slot-blot* protocol, was isolated from different numbers of RECs ($4x10^3$- $5x10^5$). These samples were applied to Hybond-N membrane using a slot-blot apparatus. A [^{32}P]-labelled GAPDH probe was used to monitor mRNA binding and efficacy was quantified by densitometric analysis of autoradiograms. Densitometry revealed a linear dose response relationship between the amount of RNA loaded and the intensity of the GAPDH signal (Figure 52D). The lower limit for detection of GAPDH mRNA was 200 ng of total RNA per slot. The upper limit of linearity was 3 µg of RNA per slot. RES was as effective as CCS in promoting binding during the transfer procedure (Figure 52A,B). The signal from 200 ng to 3 µg RNA corresponded to the signal obtained from approximately $8x10^3$ - $1.2x10^5$ cells extracted using the *slot-blot* protocol (Figure 52C). The maximum capacity of the membrane for RNA was also assessed by using a double thickness of membrane and staining the bottom membrane with 0.1% methylene blue in 50% ethanol. Overloading of the first membrane (i.e. recovery of RNA to

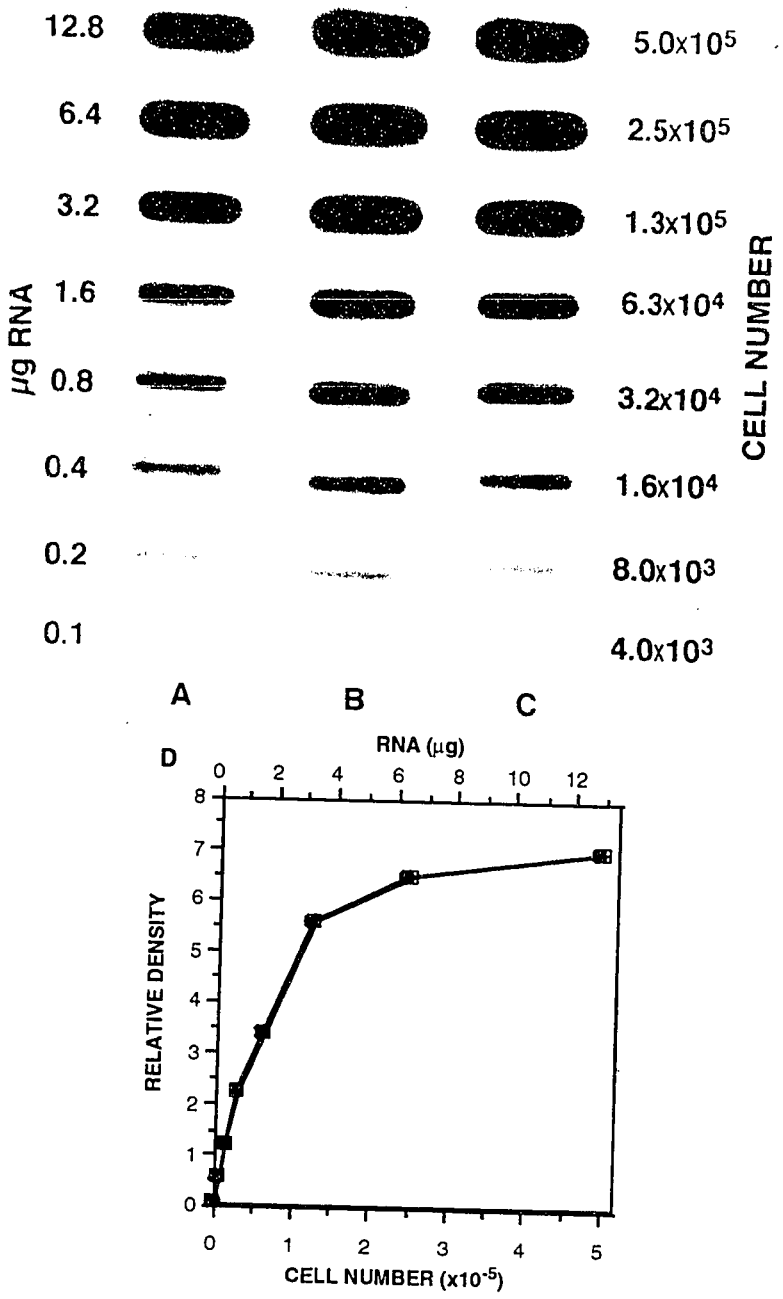

Figure 52. Comparison of total cellular RNA extracted using the *standard* or the *slot-blot* protocols

(A), *Standard* extraction dissolved in CCS; (B), *Standard* extraction dissolved in RES; (C), *Slot-blot* extraction dissolved in RES. The RNA samples were applied to a nylon membrane and probed with a GAPDH probe as described in Materials and Methods. (D), densitometric analysis of Panels A-C. ■, *Standard* extraction dissolved in CCS; □, *Standard* extraction dissolved in RES; ×, *Slot-blot* extraction dissolved in CCS. Note the complete overlap of symbols indicating equivalent binding of RNA to membrane and equal signal intensities achieved using either solvent and/or extraction procedure.

the second membrane) was observed at quantities greater than 3 μg per slot (9 mm^2 surface area of membrane).

Screening of DOEJS-infected REC clones

130 G418-resistant clones were isolated from the 5 different REC populations infected with supernatant harvested from the DOEJS/ψ2 producer line and analyzed using the *slot-blot* protocol. One clone (REC/D#74) or 0.8% of the G418-resistant population was found to express both the *neo* gene and an activated *ras* oncogene (Figure 53). This result was confirmed by Northern analysis (Figure 49).

To re-establish a stable DOEJS/ψ2 cell line capable of reliably infecting RECs, 24 DOEJS/ψ2 clones were isolated and grown to a suitable density for further study. The culture supernatant from each clone was harvested and used to infect RECs. Ten G418-resistant REC clones were isolated from each infection (a total of 240 clones). Of the 24 DOEJS/ψ2 clones examined, only DOEJS/ψ2-D6 reliably introduced both a functional *neo* and a human *ras* oncogene into cells (Figure 53). All 10 clones, isolated following infection of RECs with DOEJS/ψ2-D6 supernatant, expressed *ras* mRNA .

These experiments demonstrate that DOEJS/ψ2-D6 reliably produces virion capable of infecting primary rodent cells with the DOEJS construct and describe how this retrovirus was used to generate 11 G418-resistant REC clones transducing an activated human *ras* oncogene.

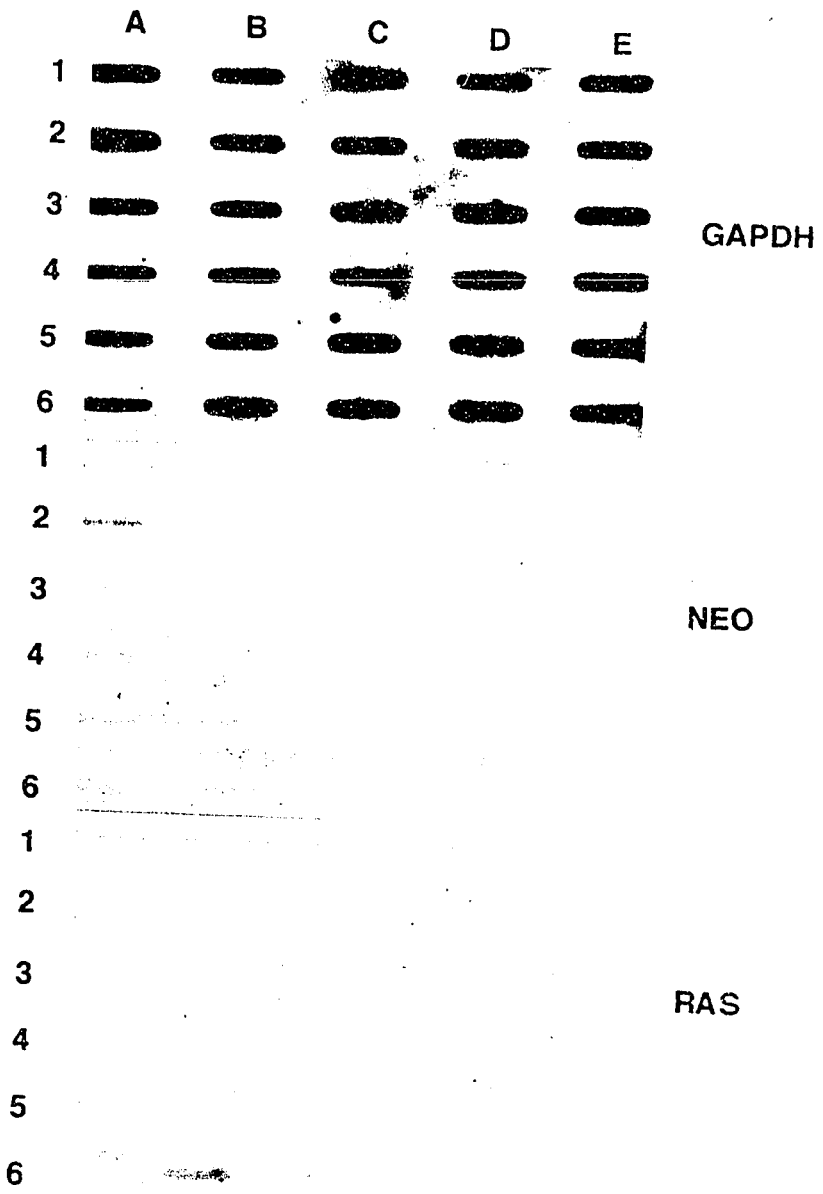

Figure 53. Slot-blot analysis of RNA extracted from G418-resistant REC clones.

Using the *slot-blot* protocol, RNA was extracted from RECs infected with virus from DOEJS/ψ2 clones D1-D24 (wells A1-6, B1-6, C1-6, D1-6) or from the parental DOEJS/ψ2 line (wells E1-6). The same membrane was hybridized with a *ras* probe, a *neo* probe, and a GAPDH probe as described in Materials and Methods. Only G418-resistant RECs derived from DOEJS/ψ2-D6 (well B6) and REC/D#74 (well E2) expressed detectable levels of *neo* and *ras*.

3. Characterization of REC/*ras* and REC/*neo* Clones

Abstract

RECs, REC/*neo* cells, and REC/*ras* cells were phenotypically characterized. Two clones (REC/*ras*-D62 and REC/*neo*-D14) were chosen for further experimentation. The *ras*-transformed clone was isolated on the basis of morphological transformation, oncogenic human c-Ha-*ras* mRNA production, and enhanced $p21^{ras}$ immunoreactivity. This clone exhibited a substantially reduced doubling time, a loss of contact inhibition, an ability to sustain indefinite growth in low serum, and a strong AI phenotype compared to both REC/*neo* cells and the parental REC population.

Introduction

Mutagenic damage to specific codons of genes known as proto-oncogenes typically results in phenotypic transformation. The dominant effects of oncogenic activation are mediated by permanent alterations in either gene expression or gene product that alter protein function. The *ras* genes were the first and perhaps best example of dominant oncogenes. *Ras* genes encode for a family of 21 kD proteins ($p21^{ras}$) that play an intrinsic role in mediating cell cycle by acting as G protein signal transduction molecules for cell surface growth factors receptors (20). Heterotrimeric G proteins and their monomeric *ras* counterparts are activated by specific G-protein linked receptors (ie. PAFR) that catalyze the exchange of GDP for GTP. The GTP-bound G protein is capable of transmitting a signal to an effector protein. Hydrolysis of GTP to GDP (GTPase activity) limits the duration of this signal. Point mutations in the Ha-*ras* gene, most commonly at codons 12,13, and 61, render the $p21^{ras}$ gene product constitutively active by rendering the protein unable to bind GTPase activating protein (GAP) and stimulate *ras* GTPase activity (ie. preventing the hydrolysis of GTP to GDP) (10,22). Oncogenic $p21^{ras}$ has been detected in both naturally- and chemically-induced tumours but is, in and of itself, usually insufficient to cause overt malignancy under experimental conditions (20). *In vitro*, the c-Ha-*ras* oncogene is capable of phenotypically transforming a variety of cell lines, inducing morphological alterations, decreases in cell doubling time, autonomous cell growth, and AI capabilities (1,21,25,32,38). In many cases, these cells acquire a metastatic phenotype when transfected with another co-operating oncogene (20).

In the present experiments, G418-resistant RECs, retrovirally infected with supernatant

derived from either DOEJS/ψ2-D6 (functional *ras/neo* vector) or DOEJS/ψ2-D3 (functional *neo* vector) as described in Chapter V, Section 2, were cloned and named REC/*ras* or REC/*neo* cells respectively. REC/*ras* clones were screened immunohistochemically for overexpression of *ras* mRNA and the $p21^{ras}$ protein. Clones were also examined for morphological transformation. One REC/*ras* clone (exhibiting the strongest immunoreactivity and greatest morphological alteration) and one REC/*neo* clone were chosen for further phenotypic characterization.

Materials and Methods

Cells, culture conditions, and characterization

REC/*ras* and REC/*neo* clones were prepared as described in Chapter V, Section 2. Cells were selected for 10 days in DMEM+10% FCS + 400 μg/ml G418 sulfate and maintained for the duration of the experiment in complete medium + 200 μg/ml G418 sulfate. Characterization of the REC/*ras* clones was accomplished using the panel of antibodies described in Chapter III, Section 2. Immunohistochemistry for $p21^{ras}$ protein was performed as described in Chapter III, Section 2 using a primary monoclonal antibody (1:100; Oncogene Science, NY) capable of detecting both endogenous and oncogenic $p21^{ras}$.

RT-PCR analysis of PAFR

Total cellular RNA was prepared from $2x10^6$ cells essentially as described in (4,5). PAFR RT-PCR was performed as described in Chapter IV, Section 2.

Phenotypic Transformation

Plating efficiency, doubling time, saturation density, growth in low serum medium, and AI growth of equal passage RECs, REC/*neo* cells, and REC/*ras* cells were determined as described in Chapter III, Section 3.

Results and Discussion

Characterization of REC/ras and REC/neo cells

REC/D#74 (see Chapter V, Section 2) and REC/*ras* clones infected with DOEJS/ψ2-D6 supernatant were morphologically transformed, expressed oncogenic *ras* mRNA, and exhibited enhanced *ras* immunoreactivity (data not shown). One clone, REC/*ras*-D62, exhibiting the strongest immmunoreactive signal, and one REC/*neo* clone, REC/*neo*-D14, were chosen for further investigation (Figure 54). Both clones expressed PAFR as determined by RT-PCR and were composed entirely of fibroblasts as determined by immunohistochemistry (data not shown).

REC/ras and REC/neo phenotype

Phenotypic characteristics are indicated in Table 10. Introduction of an active *neo* gene had no effect on REC phenotype. REC/*neo*-D14 behaved like equivalent passage RECs. By contrast, *ras*-transformed cells exhibited shorter doubling times, autonomous cell growth and AI phenotype. REC/*ras* cells were not contact inhibited and did not demonstrate saturation density *per se*. Once grown past confluence ($2x10^6$ cells/6 cm dia. dish), they were no longer able to adhere to tissue culture plates. (Cells remained viable if cultured immediately upon lifting.) These data indicate that REC/*ras*-D62 cells exhibit an enhanced growth potential, characteristic of oncogenic *ras*.

Table 10. Comparison of REC, REC/*neo* and REC/*ras* phenotype

Properties[a]	Cell Lines		
	REC	REC/*neo*-D14	REC/*ras*-D62
Plating Efficiency (%)	15%	10%	7.4%
Doubling Time (h)	33.5	32	20
Saturation Density (cells/6 cm. plate)	$1.2x10^6$	$1.4x10^6$	$2.0x10^6$
Growth in low serum Doubling time (h) Days of growth	 127.6 6	 128 6	 130 >60
AI cloning efficiency (%)	<0.01%	<0.01%	30.6%
Cell type	F	F	F

[a]Details as in Table 1

Figure 54. Morphology of RECs, REC/*neo*-D14, and REC/*ras*-D62

Details as in Materials and Methods. Representative photomicrographs are depicted. (A), untreated RECs. (B), REC/*neo*-D14 cells. (C), REC/*ras*-D62 cells. Scale bar= 20 μm.

5. Brief Exposure to PAF Induces ACD Followed by Long-term Growth Enhancement in REC/*ras* Cells

Abstract

Most solid tumours exhibit activated inflammatory cell infiltration. This observation suggests that repeated exposure to proinflammatory agents released by these cells may play a role in the malignant conversion of tumour cells already expressing one or more activated oncogenes. To test this hypothesis *in vitro*, RECs were retrovirally infected with the c-Ha-*ras* oncogene and/or a selectable *neo* marker, exposed to physiologically relevant concentrations of PAF (1 pM - 1 μM) for 1 hr, and assayed for long-term alterations in cell proliferation. As with parental RECs, a brief exposure to PAF (10 nM - 1 μM) increased the ability of REC/*neo* cells to (i) form foci, (ii) reach a high saturation density in complete medium, (iii) grow in low serum-containing medium, and (iv) exhibit AI growth. By contrast, PAF's ability to mediate REC/*ras* proliferation was dependent upon culture conditions. When grown in complete medium, PAF treatment dose-dependently enhanced growth of REC/*ras* cells. When cultured in low serum-containing medium, PAF elicited cell death 3-8 days after ligand exposure. Cell death was indicated by loss of adherence to tissue culture plates, morphological changes suggestive of ACD, and induction of DNA fragmentation. Effects were first observed 3 days after ligand administration, became maximal 5 days after exposure, and lasted up to 8 days after treatment. The ability of PAF to elicit cell loss was dose-dependent with peak effects observed following treatment with 1 μM PAF. By Day 10, ACD was no longer evident and remaining REC/*ras* cells were again capable of proliferating under sub-optimal growth conditions. When these cells were retested for autonomous cell growth 25 days after treatment in the absence of further ligand exposure, PAF-treated REC/*ras* cells demonstrated enhanced growth in low serum medium lasting up to 50 days after initial ligand exposure. Cell proliferative rates in PAF- and vehicle-treated cultures were equivalent after Day 50. Finally, when cells were grown in an AI environment, PAF was shown to dose-dependently attenuate REC/*ras* cells AI phenotype. This inhibition was evident 10-20 days after PAF exposure. Subsequent to this time period, PAF-treated REC/*ras* cells demonstrated transient enhancements in AI growth compared to vehicle-treated cells. These data are interpreted in light of the hypothesis presented in Chapter III in which brief exposure to PAF was shown to elicit putative intracellular PAF accumulation triggering synthesis and release of mitogenic factors into the extracellular milieu.

Introduction

In vivo tumour development often incites a inflammatory response in and around the site of aberrant cell proliferation resulting in elevated local levels of proinflammatory agents and significant inflammatory cell infiltration of the tumour mass (30,41). As indicated in Chapter III, Section 3, these activated phagocytes synthesize and release a number of inflammatory factors capable of mediating cell growth, cell death, and genetic mutations, including active oxygen species, AA and its metabolites, NO, interleukins, TNFα, and PAF. Oxyradicals and AA metabolites may contribute to tumour progression in cells already transformed by an activated oncogene by eliciting further genetic damage (18,41,44). In other cases, inflammatory cytokines

have been implicated in the process of tumour regression (1,27,42). To investigate the role of PAF in the development of malignant tumours, REC/*ras* and REC/*neo* cells were exposed to the ligand and alterations in cell doubling time, morphology, cell viability, saturation density, growth in low serum-containing medium, and AI growth were determined. Unexpectedly, PAF initially reduced REC/*ras* transformation apparently by inducing ACD in the treated population when cells were grown under sub-optimal growth conditions and/or by reducing cell division when cultures were exposed to an AI environment. These effects were followed by a transient potentiation of the *ras*-induced phenotype in the surviving cell population. These data indicate that PAF exerts paradoxical effects in REC/*ras* cells; effects associated with tumour progression as well as tumour regression.

Materials and Methods

Treatment with PAF and related compounds

REC/*ras* and REC/*neo* cells (characterized in Chapter V, Section 3) were maintained in DMEM+10% FCS+ 200 µg/ml G418 sulfate. Exponentially growing cultures were trypsinized and plated at the cell densities described in Chapter III, Section 3 on 6 cm tissue culture dishes (REC/*neo* cells) or on 10 cm tissue culture dishes (REC/*ras* cells). Cultures were treated with PAF (1 pM - 1µM) or vehicle for 1 hr as described in Chapter III, Section 3.

Assays of Cell Transformation and ACD

Following treatment, REC/*ras* cells and REC/*neo* cells were assayed for changes in (i) viability, (ii) morphology, (iii) doubling time, (iv) saturation density, (v) focus formation, (vi) growth in low serum medium, and (vii) AI growth as described in Chapter III, Section 3. Following 25 days of testing, cells were trypsinized and allowed to replate at a density of 100,000 per plate. Cells were then re-assayed for (i) saturation density, (ii) growth in low serum, and (iii) AI growth in the absence of further PAF exposure as described in Chapter III, Section 6. Induction of DNA ladders, indicative of an apoptotic process, was assessed as described in Chapter III, Section 2. Statistical analysis were as performed in Chapter III, Section 2.

Results and Discussion

Elevated levels of PAF in plasma have been documented in patients suffering from prostatic carcinoma, leukemia, nasopharyngeal carcinoma, histiocytic lymphoma, and metastatic melanoma (15). Maggi et al. (23) have demonstrated that autocrine production of PAF is responsible for the increased cell growth observed in an endometrial adenocarcinoma cell line, HEC-1A. Bazan et al (3) indicate that PAF is capable of inducing collagenase expression in normal epithelial cells. These experiments suggest that PAF has the potential to play a role in tumour progression in cells already genetically altered. Given that the tumour mass often elicits a substantial inflammatory response in neighbouring tissue, it is possible that tumour cells are chronically exposed to various concentrations of PAF. As discussed in Chapter II, Section 5, the kinetics of PAF metabolism and catabolism within the inflammatory environment suggest that this exposure represents repeated (cyclic) stimulation. To assess the effects of transient PAF treatment on RECs transformed with an activated human *ras* oncogene, REC/*ras* cells and REC/*neo* cells were treated for 1 hr with PAF and alterations in cell viability, morphology, doubling time, focus formation, saturation density, growth in low serum, and AI growth were evaluated.

No indication of cytotoxicity following 1 hr treatment with PAF (1 pM- 1 μM) was seen when REC/*ras* and REC/*neo* cells were maintained in complete medium (data not shown). As with RECs, PAF did not alter cell doubling times or morphology in either cell line over the first 5-10 days of growth in complete medium. PAF (10 nM- 1μM) did increase REC/*neo* saturation density (Figure 55A) and overall REC/*ras* cell number (Figure 55B). As with RECs and REC/*neo* cells, this enhancement in REC/*ras* phenotype could be maintained for at least 30 days after treatment when cells were replated and retested in the absence of additional ligand (data not shown). This enhancement in cell number was accompanied by increased focus formation. REC/*neo* cultures treated with PAF (10 nM) exhibited the same augmentation in focus formation (108±6.3 foci/6 cm dish) compared to vehicle-treated cultures (50.6±8.3 foci/6 cm dish) as RECs. Higher concentrations of PAF resulted in extensive overgrowth preventing accurate quantification of discrete colonies (data not shown). Similarly, due to the considerable overgrowth in REC/*ras* cultures and limited adherence of *ras*-transformed cells, focus formation could not be accurately determined.

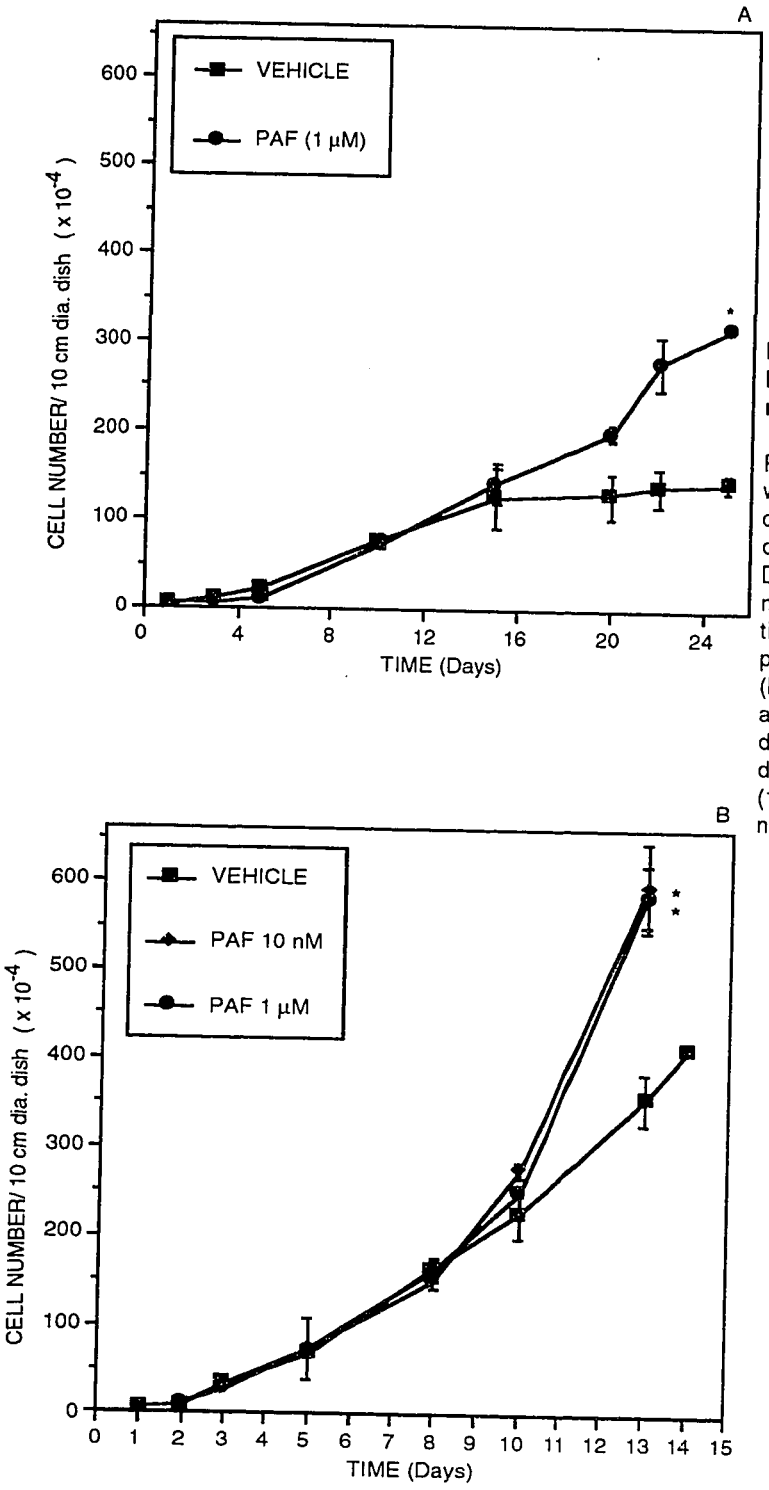

Figure 55. PAF increases REC/*neo* and REC/*ras* cell number in complete medium

REC/*neo* (A) and REC/*ras* cells (B) were treated with PAF and assayed for changes in saturation density as described in Materials and Methods. Data represent cell counts from a minimum of 5 plates per treatment per time period. Statistical tests were performed on Day 25 (A) and Day 15 (B). Statistically significant results are as follows: (A) Student's *t* test, t=8.2, df=8, $p<0.01$. (B) ANOVA, F= 5.4, df=3,15, $p<0.01$; Dunnett's t test, PAF (1 μM) vs. vehicle, $p<0.01$; PAF (10 nM) vs. vehicle, $p<0.01$.

Unexpectedly, PAF was observed to induce cell death in REC/*ras* cells (Figure 56). Cells became less adherent, exhibited morphological alterations indicative of ACD (Figure 57), and demonstrated DNA ladders characteristic of an apoptotic process (data not shown). Monolayer cell loss was first observed 3 days after treatment (Figure 56). However, cells floating in supernatant continued to exclude trypan blue until Day 6 after treatment. This time course corresponded to the induction of DNA ladders between Days 5-7 after treatment in cells retrieved from the supernatant. It must be emphasised that not all cells in the PAF-treated cultures were induced to die. By Day 10, REC/*ras* cells exhibited (1) a normal morphology, (2) no evidence of additional cell loss, DNA ladders or trypan blue permeability, and (3) a resurgence cell proliferation in low serum medium (Figure 56). In fact, when these cells were retested for growth in low serum medium 25 days after initial PAF exposure (and in the absence of further ligand administration), PAF-treated REC/*ras* cells demonstrated an enhanced ability to proliferate under sub-optimal conditions when compared to vehicle-treated cells (Figure 58). As with REC/*neo* cells, this effect was transient, abating approximately 50 days after ligand exposure. By the third cycle of growth in low serum assay, autonomous cell growth did not differ in PAF- and vehicle-treated cells (data not shown). In contrast to the effects of oncogenic *ras*, infection of RECs with an active *neo* construct had no additional impact on PAF-mediated phenotype beyond that observed in RECs. PAF transiently enhanced autonomous cell growth in REC/*neo* cells with the same kinetics as those observed in RECs (Figure 59).

With respect to AI phenotype, PAF dose-dependently *reduced* the ability of REC/*ras* cells to grow in soft agarose (Figure 60) while enhancing phenotypic transformation in REC/*neo* cells to the same extent as in RECs (data not shown). PAF-induced growth inhibition of REC/*ras* cells was not apparent immediately after treatment. No differences were observed in the number or size of PAF- and vehicle-treated colonies by Day 10 (Figure 60 and 61). However, by Day 15, colonies derived from PAF-treated cultures were substantially smaller than those derived from vehicle-treated cells. Maximal effects were observed with PAF (1 μM). This reduction reached statistical significance on Day 20. On examination of PAF-treated cultures, AI colony size appeared unaltered from Day 10 (Figure 59). Cells were either quiescent or dead. The latter explanation is unlikely since no differences in cloning efficiency were detected when PAF- or

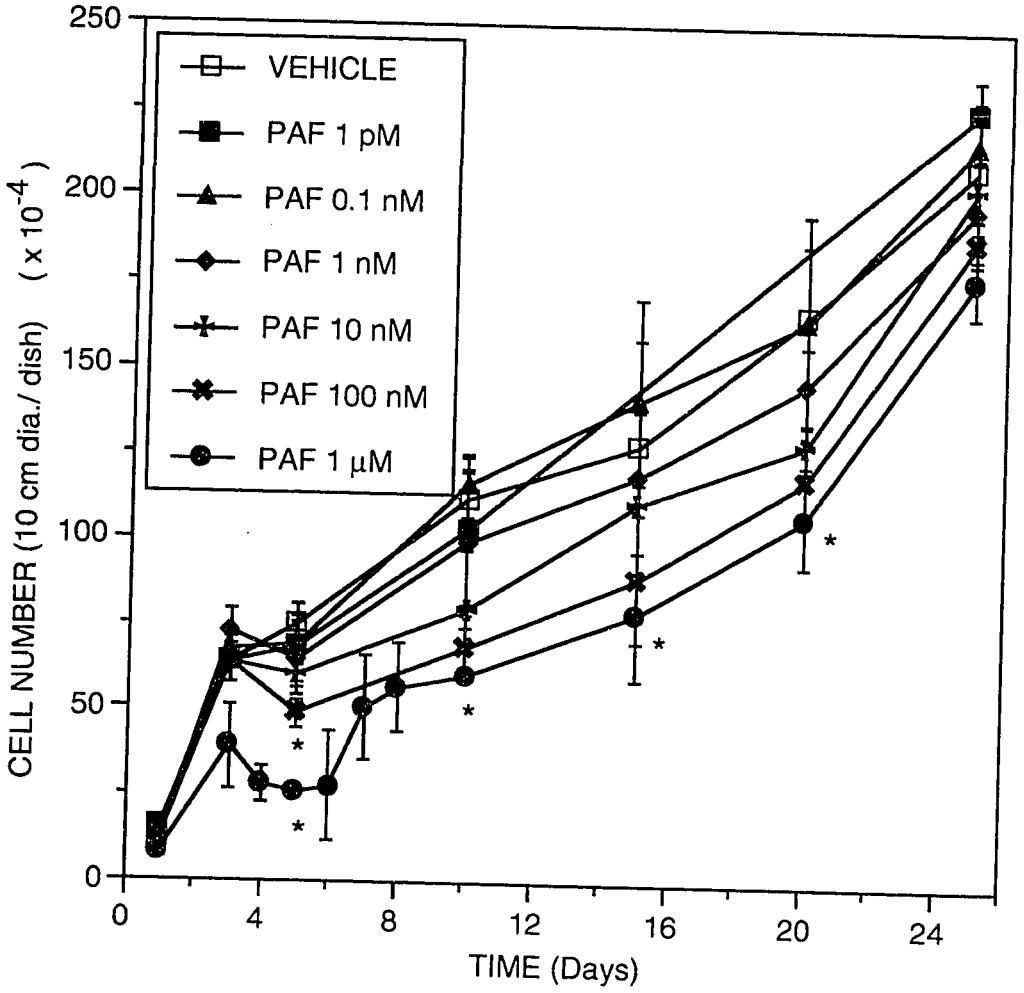

Figure 56. PAF induces cell death followed by growth enhancement in REC/*ras* cells grown in low serum medium

REC/*ras* cells were treated with PAF and assayed for changes in growth in low serum as described in Materials and Methods. Data represent cell counts from a minimum of 5 plates per treatment per time period. Statistical tests were performed on Day 3, 5, 10, 15, 20, and 25. Statistically significant results are as follows: Day 5 ANOVA, $F=9.7$, $df=7,33$, $p<0.01$; Dunnett's *t* test, PAF (1 μM) vs. vehicle, $p<0.01$; PAF (10 nM) vs. vehicle, $p<0.05$. Day 10 ANOVA, $F=3.1$, $df=7,33$, $p<0.05$; Dunnett's t test, PAF (1 μM) vs. vehicle, $p<0.05$. Day 15 ANOVA, $F= 2.7$, $df=7,33$, $p<0.01$; Dunnett's t test, PAF (1 μM) vs. vehicle, $p<0.05$.

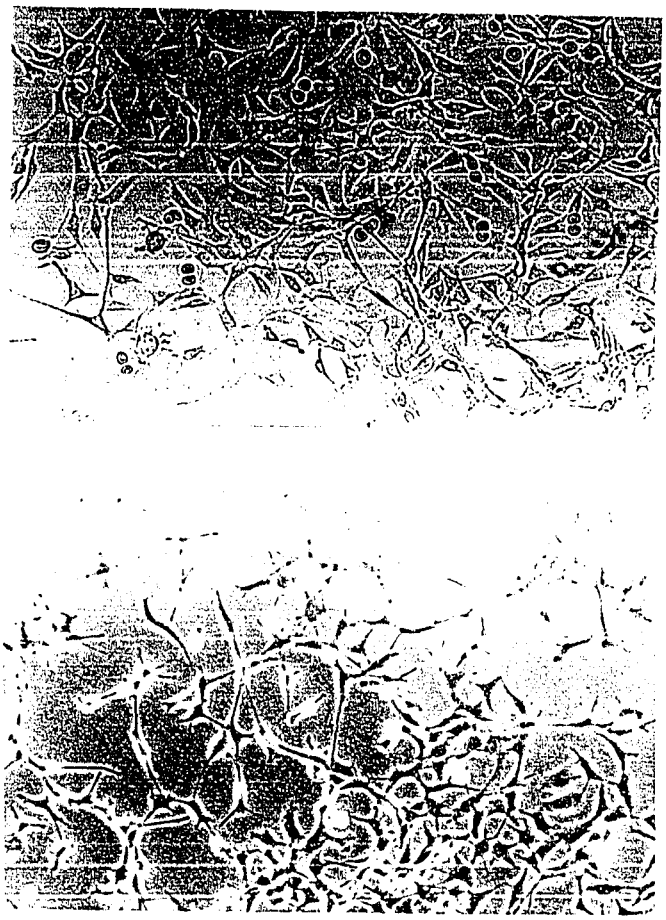

Figure 57. PAF (1 μM) induces morphological transformation and cell loss in REC/*ras* cells

REC/*ras* cells were treated with PAF or vehicle and grown in low serum medium as described in Materials and Methods. Representative photomicrographs are depicted. (A) Vehicle-treated, Day 3. (B) PAF (1 μM) - treated cells, Day 3. Scale bar= 30 μm.

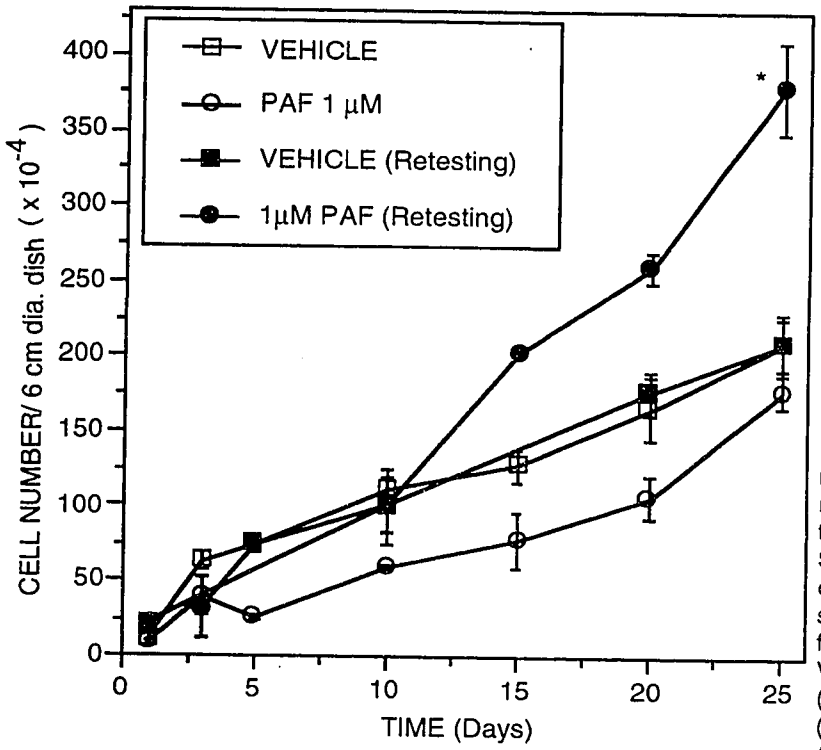

Figure 58. PAF enhances long-term cell growth enhancement in REC/*ras* cells grown in low serum medium

REC/*ras* cells were treated with PAF and assayed for changes in growth in low serum as described in Materials and Methods. Every 25 days cells were trypsinized and replated at a density of 100,000 cells per 10 cm dia. dish. Cultures were retested for autonomous cell growth in the absence of further ligand exposure as described in Materials and Methods. Data represent cell counts from a minimum of 5 plates per treatment per time period. Statistical tests were performed on Day 25. Statistically significant results are as follows: PAF treatment vs. Vehicle, See Figure 56. PAF (retesting) vs. Vehicle (retesting) Student's *t* test, t=5.9, df=8, $p<0.01$.

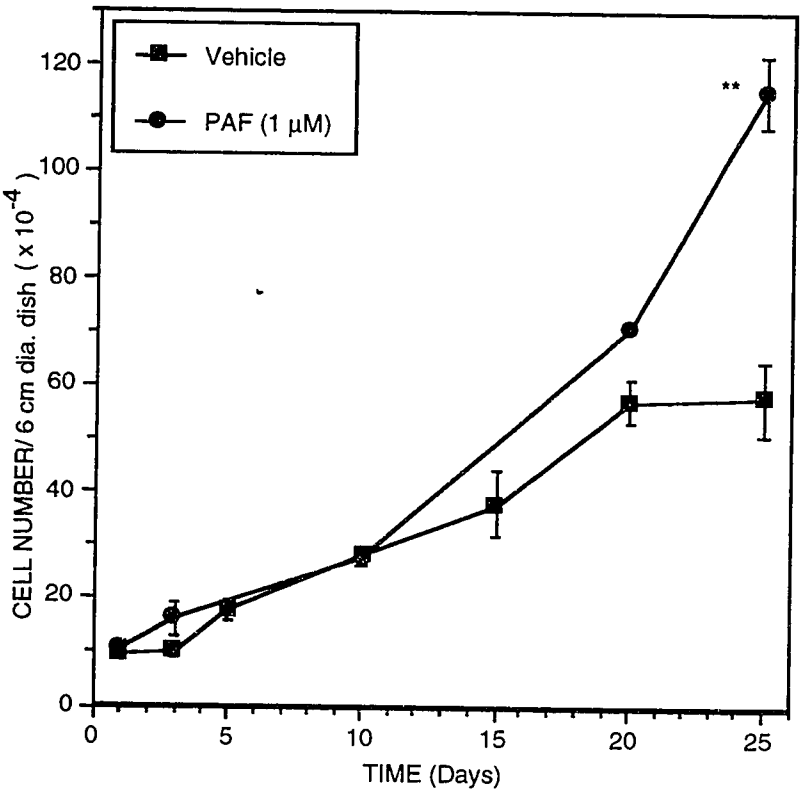

Figure 59. PAF elicits the same growth enhancement in REC/*neo* cells as in RECs.

REC/*neo* cells were treated with PAF or vehicle and assayed for growth in low serum as described in Materials and Methods. PAF-induced long-term growth cell proliferation 10 days after ligand removal. Data represent cell counts from a minimum of 5 plates per treatment per time period. Statistical tests were performed on Day 25. Statistically significant results are as follows: PAF treatment vs. Vehicle, Student's *t* test, t=6.2, df=8, $p<0.01$.

vehicle-treated AI colonies were picked and cloned on Day 10, 15, 20, and 30 after treatment (data not shown). It is also important to note that AI assays are performed in the presence of complete medium. PAF-treated monolayer cultures grown in complete medium show no evidence of cytotoxicity and, in fact, demonstrate sustained growth enhancement (see above). Furthermore, the reduction in AI growth rates observed following PAF exposure was transient. By Day 30, PAF-treated cultures exhibited the same number of AI colonies (> 80 μm) as vehicle-treated cells (Figure 60). Little distinction could be made between colony size in either treatment group suggesting that PAF-treated cells may have expanded at a faster rate that vehicle-treated colonies between Day 20 and Day 30 (Figure 61).

These results can be interpreted within the context of the model presented in Chapter III. Like RECs, in the presence of exogenous growth factors, PAF elicits growth enhancement in REC/*ras* cells. Presumably, this phenotype is mediated by intracellular PAF production and subsequent synthesis and release of mitogenic factors as described in Chapter III, Section 8. However, in the absence of exogenous growth factors, PAF elicits ACD. In RECs, this effect is dependent upon dose and duration of ligand exposure. In *ras*-transformed cells, PAF-induced ACD shows the same dose-response relationship as RECs but requires only transient PAF stimulation. This difference in cell signalling could be related to changes in PAFR. While REC/*ras* cells have been shown by RT-PCR to express PAFR (Chapter V, Section 2), relative levels of mRNA expression compared to normal cells and/or functional characterization of the receptor have not yet been determined. It should be noted that expression of oncogenic *ras* has been shown to upregulate expression of other extracellular receptors (2,17). Cells expressing higher levels of PAFR would likely be more sensitive to the ligand. In addition, *ras* has been shown to increase spontaneous mutation rates in murine cells (11). Cells expressing mutated forms of the PAFR (in which the cytoplasmic domain of the protein is absent) do not undergo receptor desensitization thus resulting in sustained cell signalling (35). Either phenotype could explain the increased sensitivity of REC/*ras* cells to PAF-elicited ACD. These hypothesis are, however, only speculative. Given that PAFR is a G protein linked receptor, it is equally plausible that $p21^{ras}$ plays some role in the intracellular transduction of the PAF-induced ACD signal (Chapter III, Section 2). PAF has been shown to share a variety of second messengers

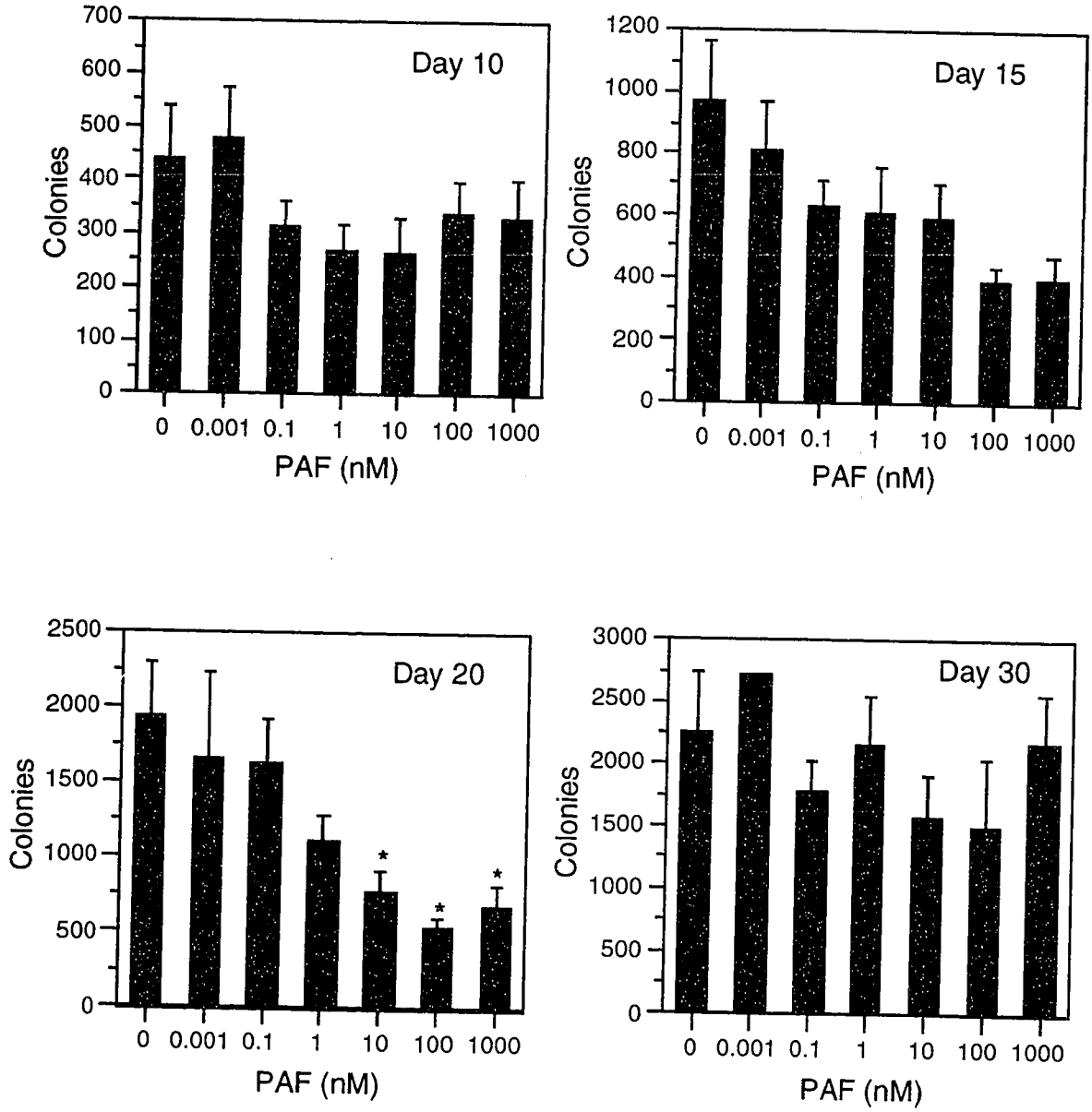

Figure 60. PAF transiently slows REC/*ras* AI growth

REC/*ras* cells were treated with PAF for 1 hr and assayed for changes in AI growth as described in Materials and Methods. Data represent the number of AI colonies (> 80 μm) per 100, 000 cells plated at Day 10, 15, 20, and 30 after treatment. Statistically significant comparisons are as follows: Day 20 ANOVA , F= 4.8, df=7,33, $p<0.05$; PAF (10 nM) vs. vehicle Dunnett's *t*, $p<0.05$; PAF (100 nM) vs. vehicle Dunnett's *t*, $p<0.05$; PAF (1 μM) vs. vehicle Dunnett's *t*, $p<0.05$.

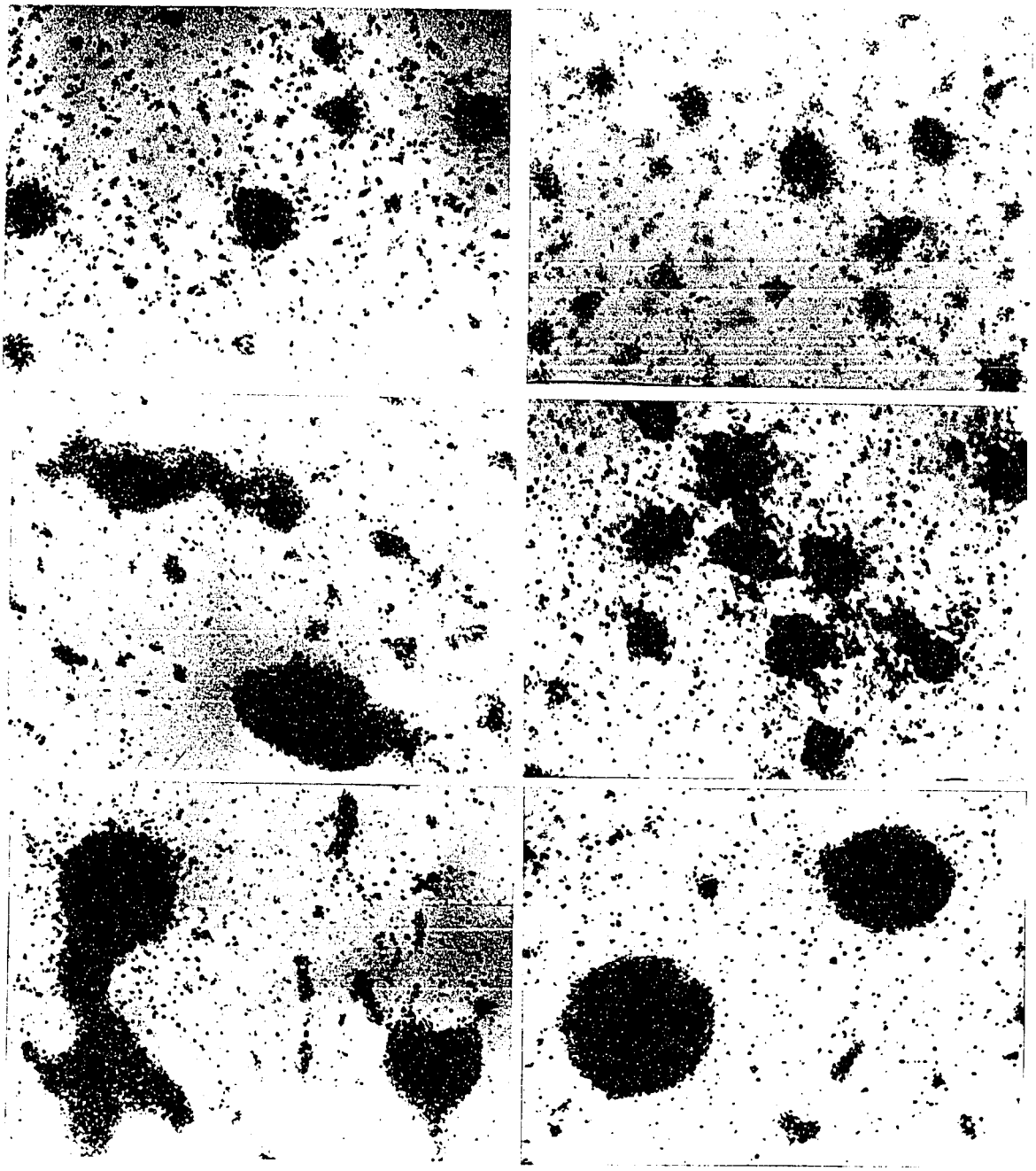

Figure 61. PAF inhibits REC/*ras* AI growth

REC/*ras* cells were treated with PAF (1 μM) or vehicle and assayed for changes in AI growth as described in Materials and Methods. (A), Vehicle-treated cells, Day 10. (B), PAF-treated cells, Day 10. (C), Vehicle-treated cells, Day 20. (D), PAF--treated cells, Day 20. (E), Vehicle-treated cells, Day 30. (F), PAF-treated cells, Day 30. Representative photomicrographs are depicted. Scale bar=50 μm.

downstream of the *ras* signal transduction pathway such as MAP kinase kinase and MAP kinase (13,19,31,39) suggesting some convergence in cell signalling mechanisms. Constitutive activation of a common pathway by oncogenic *ras* could conceivably sensitize transformed cells to undergo PAF-induced ACD upon transient exposure. This supposition has precedents. For example, *ras*-transformed cells are more sensitive to TNFα-mediated cell killing than normal cells (16).

However, *ras* may only play a role in PAF-induced ACD. Both RECs and REC/*ras* cells exhibit growth enhancement first observed approximately 10-15 days after ligand stimulation. These data suggest that REC/*ras* cells are capable of elaborating the putative mitogenic factors described in Chapter III, Section 6. These results also begin to hint at separate signal transduction pathways mediating cell growth and cell death in response to PAF.

6. Signal Transduction Events Underlying PAF-Mediated Alterations in REC/*ras* AI Phenotype

Abstract

Brief exposure to PAF was found to transiently decrease and subsequently increase AI growth of REC/*ras* cells. Enhancement of AI phenotype has been shown in normal RECs to depend upon PAFR and phosphorylation of proteins on tyrosine residues but not on PKC activity or cyclooxygenase metabolites of AA. To determine whether these same signalling intermediaries modulate PAF's effects on *ras*-transformed cells, REC/*ras* cells were treated with the ligand in the presence of either a PAF receptor antagonist (CV3988, 10 μM), a tyrosine kinase inhibitor (genestein, 1 μg/ml), a PKC inhibitor (staurosporine, 50 nM), or a cyclooxygenase inhibitor (indomethacin, 200 nM). Cells were assayed for changes in AI phenotype. Both the PAF-induced growth reduction phase and subsequent growth enhancement phase could be inhibited by CV3988 and genestein indicating dependence on PAFR and tyrosine kinase activity. No effect was observed following treatment with staurosporine or indomethacin suggesting that PAF does not work through PKC or cyclooxygenase metabolites of AA to alter REC/*ras* phenotype.

Introduction

In other experimental systems, PAF has been shown to work through specific cell surface and intracellular receptors to induce calcium transients, arachidonic acid metabolism, phosphoinositide turnover, protein kinase activity, and proto-oncogene expression (Chapter II, Section 5). Given the data presented in Chapters III and V demonstrating that PAF is capable of altering cell growth and cell death kinetics in RECs, HFs, and REC/*ras* cells and recent reports that systemic PAF levels are elevated in a preneoplastic inflammatory disorder, Crohn's disease (12,33), as well as in in prostatic carcinoma, leukemia, nasopharyngeal carcinoma, histiocytic lymphoma, and metastatic melanoma (15), an attempt was made to identify candidate signal transduction intermediates underlying PAF's potential contribution to these malignant disorders.

Materials and Methods

Treatment conditions and transformation assays

REC/*ras* and REC/*neo* cells were treated as described above (Chapter V, Section 3) with the exception that cultures were also exposed to either vehicle or PAF (1 μM) in combination with CV3988 (10 μM), indomethacin (200 nM), staurosporine (50 nM), or genestein (1 μg/ml). Where treatment with two compounds is indicated, the antagonist or inhibitor was added 15 min

prior to co-incubation and treatment continued for 1 hr following PAF or vehicle administration as described Chapter III, Section 4. Cultures were then washed and incubated for 24 hr in DMEM+10% FCS before being assayed for AI growth as described in Chapter III, Section 3. Statistical analyses were performed as described in Chapter III, Section 2.

Results and Discussion

In Chapter III, Section 3 and 4, PAF was shown to induce phosphorylation of proteins on tyrosine residues and to activate PKC. The former signalling mechanism was demonstrated by the use of specific inhibitors to mediate PAF-induced AI phenotype in RECs while PKC or cyclooxygenase metabolites of AA had no effect on AI growth (Chapter III, Section 4). In Chapter III, Section 8, indirect evidence was presented suggesting that stimulation of extracellular PAFR induces increases in intracellular PAF levels and subsequently triggers the synthesis and release of putative mitogenic factors. It is hypothesized that, in the presence of excess intracellular PAF, autocrine stimulation of RECs with these growth factors apparently sets up a feedback mechanism whereby the release of mitogenic factors is sustained. In Chapter III, Section 2, prolonged exposure to PAF elicited ACD. Finally, in the preceding section, constitutive activation of $p21^{ras}$ was shown to render cells more sensitive to the negative growth regulatory effects of PAF.

Effect of PAF and inhibitor treatment on REC/ras phenotype

REC/*ras* cells exhibit transient AI growth attenuation when treated with PAF followed by sustained enhancement of the *ras*-transformed AI phenotype. To determine whether PAFR, tyrosine kinase activity, PKC, and/or cyclooxygenase metabolites influence PAF-induced alterations in REC/*ras* phenotype, REC/*ras* and REC/*neo* cells were coincubated with PAF and either CV3988, staurosporine, genestein, or indomethacin, and assayed for AI growth.

As indicated in Figure 62, CV3988 (10 μM) and genestein (1 μg/ml) inhibited PAF-induced attenuation of AI phenotype. These agents also blocked subsequent PAF-induced growth enhancement (data not shown). Staurosporine (50 nM) and indomethacin (200 nM) had no effect

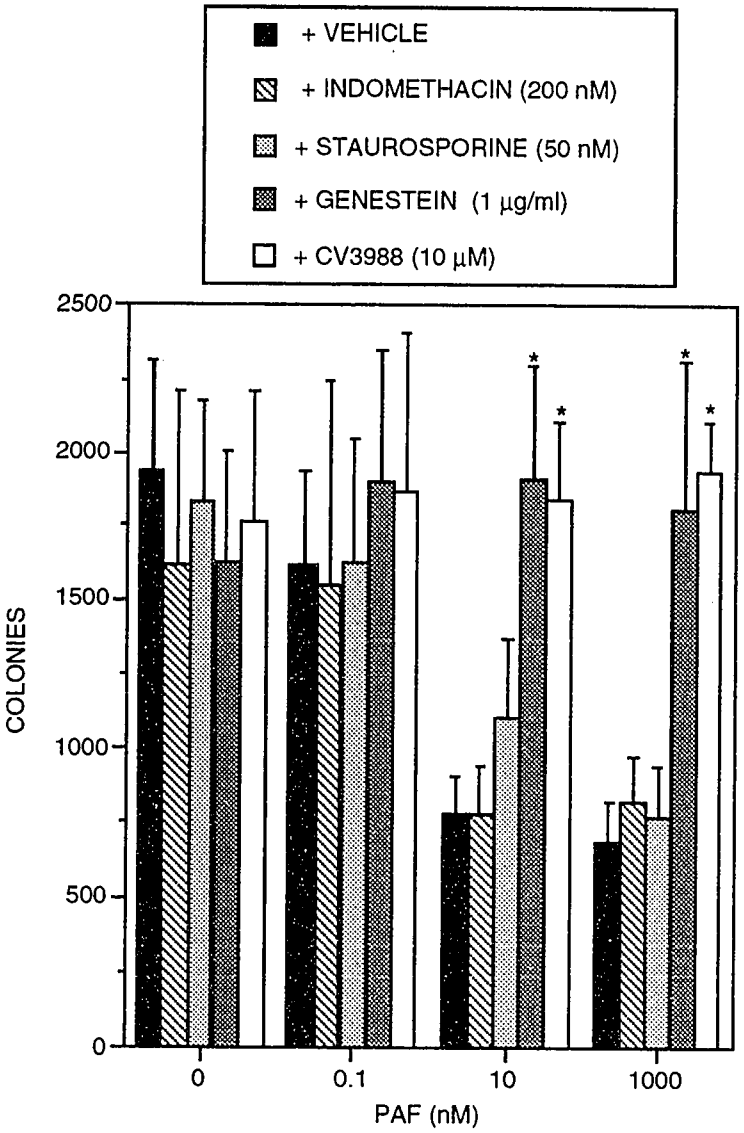

Figure 62. PAF-induced reduction of REC/*ras* Al growth on Day 20 is inhibited by a PAFR antagonist and a tyrosine kinase inhibitor but not a PKC inhibitor or a cyclooxygenase inhibitor

REC/*ras* cells were treated with either vehicle or PAF (1 μM) and one of the following compounds as described in Materials and Methods: CV3988 (10 μM), indomethacin (200 nM), staurosporine (50 nM), or genestein (1 μg/ml). Cells were assayed for changes in Al growth. Data represent the number of Al colonies (> 80 μm) at Day 20 per 100,000 cells plated. Statistically significant comparisons are as follows: PAF 10 nM ANOVA, $F=4.5$, $df=5,23$, $p<0.05$; PAF vs. PAF+CV3988 Dunnett's *t*, $p<0.05$; PAF vs. PAF+ Genestein Dunnett's *t*, $p<0.05$. PAF 1 μM ANOVA, $F=4.7$, $df=5,23$, $p<0.05$; PAF vs. PAF+CV3988 Dunnett's *t*, $p<0.05$; PAF vs. PAF+ Genestein Dunnett's *t*, $p<0.05$.

on PAF-induced AI growth attenuation or subsequent growth enhancement. The response of PAF-treated REC/*neo* cells to the various antagonists and inhibitors was identical to that described for RECs (data not shown). These results indicate that PAFR activation and phosphorylation of proteins on tyrosine residues are early events in PAF-mediated signal transduction pathways required for subsequent activation of both cell proliferative signalling and negative growth regulation.

7. Overview

The results presented in this chapter provide *in vitro* evidence in support of the hypothesis that tumour cell phenotype is affected by PAF. In fact, PAF appears to play a dual role in tumourigenesis, first eliciting ACD immediately after ligand exposure then stimulating transient growth enhancement in surviving cells in the presence of oncogenic c-Ha-*ras*. It is unknown how these effects may be influenced by the cyclic exposure to ligand presumed to be characteristic of an inflammatory response. Whether successive PAF treatments preferentially influence the rate of cell death or rate of cell growth in *ras*-transformed cells could have important clinical implications in the management of inflammation associated with solid tumours. These data also provide insight into the underlying mechanisms mediating PAF signal transduction in non-inflammatory cells. (1) PAF receptor activation and induction of tyrosine activity apparently represent early events in PAF-mediated cell signalling. (2) Growth enhancement appears to depend upon an increase in intracellular PAF that promote the synthesis and release of mitogenic factors. (3) PAF-induced cell death is modulated by $p21^{ras}$ and/or some downstream signalling event common to both PAF and *ras* signal transduction. (4) Finally, activation of the cell death pathway can be modulated by the availability of exogenous growth factors. These observations suggest that different signalling mechanisms can be elicited by the same ligand depending upon endogenous environmental conditions.

VI

NEURODEGENERATION

1. Introduction

Traditionally, the CNS has been considered to be immunologically privileged in that it is isolated from interaction with circulating inflammatory cells and immune molecules by the blood-brain barrier. Recent ground-breaking research has revised this dogma (for a review see Chapter II, Section 4 and ref. (28)). The brain is now recognized to be immunologically privileged in a positive sense in that it can mount its own immune and inflammatory response to injury without recourse to PNS involvement. Characterization of the inflammatory response in diseased brain suggests that chronic inflammation may play a role in the pathogenesis of Alzheimer's Disease and other related progressive neurodegenerative disorders (Chapter II, Section 4 and ref. (28,40,60)). As with the metastatic process, attention must be drawn to the correspondence between the progressive neurodegeneration and the 'inflammatory phenotype' (ie. sustained proliferation of activated phagocytes, irregularities in inflammatory cell and non-inflammatory cell morphology, increased synthesis of immunological and proinflammatory agents, and accelerated neuronal cell death).

What role do agents released in and around a site of cerebral inflammation play in exacerbating chronic brain lesions? PAF has already been shown to exacerbate meningeal inflammation (66) and enhance excitatory synaptic transmission in the mammalian hippocampal formation leading to neuronal cell loss in experimental models of epileptic seizure, ischemia/reperfusion injury, and retinopathy (10,18,53). Furthermore, overexpression of one of three genes encoding for the heterotrimer PAF-acetylhydrolase results in Müller-Dieker lissencephaly - a developmental disorder resulting in structural brain abnormalities and aberrant neuronal migration (26). *In vitro* experiments indicate that PAF is capable of inducing neuronal signal transduction through PAFR activation, calcium transients, phosphoinositide turnover, and immediate-early gene expression in NG108-15 neuro-glioma hybrid cells, PC12 cells, and rat brain slices suggesting an *in vivo* role for PAF in the brain and spinal cord (6,8,31,36,59,68).

To determine whether PAF could be involved in chronic neuropathology, alterations in PAFR with respect to ACD-related gene expression were investigated in an *in vivo* model of

neuropathology. The kainic acid model of myoclonic epilepsy was chosen because acute induction of severe epileptiform seizures induces many long-term pathologies (ie. neuronal loss, reactive gliosis, and deposition of non-degradable glycoproteins) common to a wide variety of neurodegenerative disorders.

These studies were carried out under the supervision of Dr. D.C.S. Roberts, Department of Life Sciences, Carleton University.

2. Relevance of the Kainic Acid Model of Myoclonic Epilepsy to the Study of Chronic Neurodegeneration

Abstract

The presence of PAS+ deposits in the CNS have been used clinically to stage the degree of neuropathology associated with a wide variety of neurodegenerative disorders including Alzheimer's Disease, Presenile Dementia, Parkinson's Disease, Diabetes Mellitus, Myoclonic Epilepsy, ALS, and Cerebral Palsy. The etiology of these plaques and their relationship to inflammatory mechanisms is under investigation. In the present study, the kainic acid model of limbic status epilepticus provides an useful system for the study of endogenous CNS responses to both acute and progressive injury. The relationship between PAS+ deposition, induction of *fos*-like immunoreactivity (FLI), neuronal loss, reactive gliosis, and blood-brain barrier breakdown following the kainic acid induction of status epilepticus was investigated. Epileptiform activity was elicited in rats by intraperitoneal (IP) administration of 10 mg/kg kainic acid and brain sections were examined 3, 5, 12, 24, 72, and 168 hr after drug injection. Four distinct types of PAS+ staining in rat brain were observed: **Type 1**-extracellular matrix (ECM) or blood vessel associated-material, **Type 2**-granular deposits, **Type 3**-glial labelling, and **Type 4**-neuronal labelling. Results demonstrated that the four types of PAS+ elements were differentially associated with specific markers of neuropathology: (1) **Type 1**-ECM staining and **Type 3**-glia were preferentially localized to edematous tissue; (2) Haemorrhaging vasculature were identified by **Type 1** staining; (3) the majority of **Type 3**-glia were identified as reactive astrocytes while a minority of were morphologically characteristic of proliferating microglia; (4) early deposition of **Type 2**-granules was predictive of subsequent cell loss; (5) chronic **Type 2**-granular deposits and **Type 4**-neuronal labelling not associated with cell death could be predicted by early changes in FLI; and (6) chronic deposition of all four forms of PAS+ material was correlated with earlier, transient blood-brain barrier compromise. The results provide new insight into the etiology of PAS+ glycoproteins found at the centre of many neurodegenerative plaques in diseased human brain and demonstrate that the kainic acid model of myoclonic epilepsy is a system appropriate for the study of proinflammatory agents and neurodegenerative disorders.

Introduction

The periodic acid-Schiff (PAS) reaction is used clinically to assist in identification of lesions characteristic to Alzheimer's Disease (21,30,37,42), Presenile Dementia (30,37,61), Parkinson's Disease (7,21), Diabetes Mellitus (52), Myoclonic Epilepsy (7), and Cerebral Palsy (17). However, the chemical identity, etiology, and relative importance of these deposits to pathological mechanisms are unknown. The PAS reaction stains a variety of carbohydrate-containing components of both cells and ECM, including glycogen, glycoproteins, glycolipids, sphingolipids, and some proteoglycans (12). Dimedone (5,5-dimethyl-1,3-cyclo-hexanedione) is used to improve the selectivity of the PAS reaction by blocking sugars that undergo minimal oxidation during periodate treatment. This selection effectively reduces the amount of PAS+

material in oxidized tissue accentuating the reactivity of highly polymerized carbohydrates. PAS-dimedone (PAS-D)-positive material includes glycogen, sialated glycoproteins, and sialated glycolipids. Under such selective conditions, pathological PAS-D^+ material is noted in the CNS of senescence-accelerated mice (1), aged cats (63) and dogs (62), and in rodent brain following irradiation (67) or stab-wounding (25).

The kainic acid model of status epilepticus can be used to induce progressive neurodegeneration in limbic and other closely related brain regions. Cell death occurs as a consequence of sustained neuronal excitation, edema, inflammation, reactive gliosis, and blood-brain barrier breakdown (4,5,16,34,35,43,46,58,64). These pathologies are also seen in clinical disorders. Focal sites of inflammation, activation of reactive astrocytes, and disruption of the blood-brain barrier are common features of a variety of neurodegenerative disorders (Table 2, Chapter II, Section 4). In the present experiments, the relationship between specific types of PAS-D staining and induction of *fos*-like immunoreactivity (FLI), neuronal loss, reactive gliosis, and blood-brain barrier breakdown was investigated in an attempt to describe an animal model of neuropathology suitable for the study of proinflammatory agents in chronic neurodegenerative conditions.

Materials and Methods

Induction of epileptiform seizures

Epileptiform seizures were induced in 41 male Wistar rats (Charles River, Que), weighing 250-300 g. Subjects received intraperitoneal injections of either 10 mg/kg kainic acid (Sigma, MO) (n=35) or physiological saline vehicle 1 ml/kg (n=6). Rats were monitored for ten hr following drug injection and their behaviour was rated according to previously published criteria (41): 0 = normal activity, 1 = increased frequency of 'freezing' and 'wet-dog shakes', 2 = weak clonic convulsions with rearing, 3 = increasingly severe convulsions with loss of postural control, 4 = generalized limbic seizures, and 5 = severe limbic seizures with respiratory difficulty. Three animals were implanted with electrodes and induction of epileptiform activity confirmed electrographically. Manipulations were carried out according to the strict ethical guidelines for animal experimentation established by the Canadian Council on Animal Care. Subjects reaching

stage 4 were anesthetized with sodium pentobarbital at 3, 5, 12, 24, 72, or 168 hr after treatment (n=5/time point) and were perfused with 60 ml of sodium phosphate buffered saline (PBS: 10 mM, pH 7.2), followed by 120 ml of a modified Zamboni fixative (4% paraformaldehyde, 0.2% picric acid in 0.16 M phosphate buffer, pH 6.9). Brains were removed and postfixed for 4 hr in the same fixative at 4°C and transferred to 10% sucrose in 10 mM PBS for 24 hr. Coronal sections, 15 μm in thickness, were cut on a cryostat and thaw-mounted on gelatin-coated microscope slides.

Morphological Studies

Sections were routinely stained using either cresyl violet or hematoxylin eosin to assess morphological degeneration associated with seizure activity. Edematous tissue was identified as areas exhibiting macroscopic swelling of perineuronal and perivascular astroglia accompanied by neuropil vacuolization and herniation (34). Swollen processes were confirmed as astroglial by Nissl staining sections immunoreacted with anti-GFAP as described below.

PAS-D staining

Sections were briefly hydrated and reacted at room temperature for 20 min in 0.5% periodic acid in distilled H_2O, dehydrated through progressively higher concentrations of ethanol, incubated for 1 hr at 60°C in 5% dimedone in 100% ethanol, rehydrated through a descending series of ethanols, reacted for 20 min at room temperature in Schiff's reagent (14 mM parasanoline, 42.4 mM sodium bisulfite in 1 N HCl), and developed for 10 min in distilled H_2O. Chemicals were purchased from Sigma (MO). Densitometry using a Zeiss scanning microscope attached to a Macintosh LC475 was performed on representative sections to determine the intensity of the reaction.

FLI and GFAP immunoreactivity

Sections were incubated with either a rabbit anti-*fos* antibody (1:500; Medac, USA) or a monoclonal mouse anti-GFAP antibody (1:40; Boehringer Manheim, Que) overnight at 4°C. Primary and secondary antibodies were diluted in 10 mM PBS (pH 7.2) containing 0.3% Triton

X-100. FLI was visualized by immunoperoxidase staining. Sections were washed repeatedly in PBS, incubated with biotinylated goat anti-rabbit antibodies (1:100; Amersham, Ont), washed repeatedly in PBS, and incubated with streptavidin-horseradish peroxidase (1:100; Amersham, Ont) in PBS. Secondary and tertiary reactions were carried out at room temperature for 1 hr. Immunoreactivity was developed by incubation in a 0.02% solution of 3,3'-diaminobenzidine tetrahydrochloride (Sigma, MO) in 50 mM Tris buffer (pH 7.4) followed by addition of H_2O_2 to a final concentration of 0.005%. GFAP immunoreactivity was assessed by immunofluorescence. Following incubation with anti-GFAP, sections were washed with PBS as above and reacted for 30 min at 37°C with FITC-labelled rabbit anti-mouse antibodies (1:20; Amersham, Ont) in PBS/Triton. Sections were mounted under glass coverslips in glycerol containing 0.1% *p*-phenylenediamine. To assess specificity, adjacent sections were processed as described above but in the absence of primary antibody. Some sections were double-labelled with both anti-GFAP and PAS-D or anti-GFAP and either hematoxylin eosin or cresyl violet. These sections were incubated for 1 hr with anti-GFAP antisera followed by fluorescent labelled secondary antibodies as described above. Because PAS-D staining is fluorescent under both FITC and rhodamine filters, anti-GFAP-labelled sections were examined and photographed prior to PAS-D processing. The short immunohistochemical incubation periods were required to preserve PAS-D reactivity and were sufficient to identify individual reactive astrocytes.

Blood-brain barrier breakdown

Blood-brain barrier breakdown was assessed by examining the extent of rat Ig extravasation into brain following kainic acid treatment essentially as described in (56). Sections were incubated overnight at 4°C with a goat anti-rat Ig (1:100; Amersham, Ont) in PBS/Triton and processed for immunoperoxidase staining as described above.

Results and Discussion

Kainic acid-induced seizures

Intraperitoneal injection of 10 mg/kg kainic acid induced stage 4 epileptiform activity within 2-3 hr of treatment. The time-course of seizure induction has been well-characterized elsewhere

(4,5,16,34,35,43,46,58,64). Briefly, animals exhibited stage 1 'wet-dog shakes' 15-30 min after treatment. Stage 2 rearing and weak clonic convulsions were observed 60 min after injection. Rats demonstrated loss of postural control and increasingly severe stage 3 convulsions within 90 min of treatment, progressing rapidly to generalized stage 4 limbic seizures 120-180 min after excitotoxin administration except for two animals that progressed to stage 5 within 130 min of treatment and were immediately sacrificed. No further investigation was conducted on these subjects. Behavioural indices of epileptiform activity continued for approximately 7 hr in the remaining animals subsiding 12 hr after kainate injection. Epileptiform activity was confirmed electrographically in 3 animals implanted with electrodes (data not shown). By 24 hr after treatment, animals were exhausted, severely dehydrated, and showed signs of motoric impairment. Subjects exhibited normal food and water intake within 48-72 hr of kainic acid injection and demonstrated normal locomotion 96 hr after treatment. Rats receiving intraperitoneal injections of saline showed no adverse effects.

Accumulation of PAS-D$^+$ material

The kainic acid model of epileptiform activity consistently results in a time-dependent accumulation of pathological PAS-D$^+$ material in rat brain while animals receiving intraperitoneal injections of saline did not exhibit any staining at any time point. (Figure 63). This accumulation was mapped and densitometry was performed on representative sections to determine the relative intensity of the PAS-D reaction over time. Increases are expressed as percent of background reactivity observed in saline-treated animals and are visually displayed in the graded shading of Figure 64. Moderate reactivity was first detected 12 hr after kainic acid treatment and was distributed diffusely throughout the brain. By 24 hr after kainic acid administration, intense PAS-D staining was distributed predominantly within limbic brain areas, most notably the piriform and entorhinal cortices, amygdaloid complex, hippocampal formation, specific thalamic nuclei, layers I and II of the neocortex, and throughout all layers of the perirhinal cortex. At 72 hr after treatment, PAS-D$^+$ material was distributed in a penumbra of approximately 50-150 µm in width around areas exhibiting neurodegeneration (see below). At 168 hr after kainic acid injection lightly

staining PAS-D$^+$ deposits were noted in the entorhinal cortex, layers I and II of the neocortex, around the third ventricle, and within the hippocampal formation. Four distinct types of deposits could be resolved: **Type 1**-ECM- and blood vessel-associated material, **Type 2**-granular deposits, **Type 3**-glial labelling, and **Type 4**-neuronal labelling (Figure 65). These deposits are similar in morphology to those detected in the human CNS of patients suffering from a variety of neurodegenerative disorders (Table 2, Chapter II, Section 4). The time course of these deposits and their relationship to other markers of neuropathology are described below.

Neurodegeneration and PAS-D$^+$ deposits

Two stages of nerve cell damage were observed: (1) an acute phase (3-24 hr after treatment) characterized by the appearance of edema and the presence of hyperchromatic, pyknotic, and fragmenting neurons and (2) a chronic phase (72-168 hr after treatment) characterized both by a marked improvement in acute parameters of neurodegeneration and substantial cell loss in discrete brain regions. Identification of these stages is consistent with previous studies of excitotoxin neurodegeneration (4,5,16,28,34,35,43,46,47,49,51,58,64). Data are presented in Table 11 for select midbrain structures. The first phase, 3 to 24 hr after treatment, was characterized by the appearance of hyperchromatic, pyknotic neurons in and around edematous tissue. Swollen astroglial processes in areas of neuropil vacuolization were anti-GFAP immunoreactive (described below). The degree of vacuolization within affected tissue increased with time as did the number of focal capillary haemorrhages preferentially localized to limbic structures. Blood vessel disruptions were assessed by extravasation of rat Ig into brain parenchyma around Nissl- and **Type 1**-PAS-D delineated blood vessels (described below). By 12 hr after treatment, large cystic cavities could be seen in the piriform and entorhinal cortices and entire cell fields within these areas were profoundly disrupted. Morphological alterations peaked with the cessation of epileptiform activity. By 24 hr post-treatment, many neurons within affected areas had fragmented and hyperchromatic debris was observed throughout the hippocampal formation, thalamic nuclei, entorhinal and piriform cortices, and throughout the neocortex in the vicinity of the rhinal fissure. The degree of neuropil vacuolization and astroglial swelling was

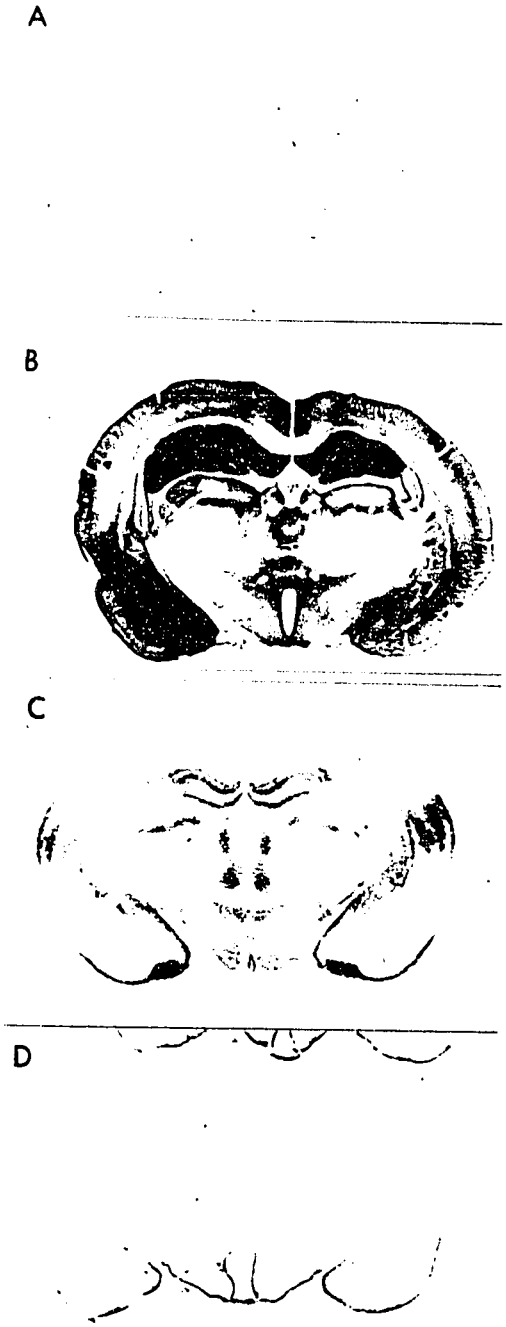

Figure 63. The pattern of PAS-D staining in kainic acid-treated animals

Representative photomicrographs of coronal sections are depicted. (A), Control subject 24 hr after saline injection. (B,C,D), Kainic acid (10 mg/kg)-treated subject 24, 72, and 168 hr after excitotoxin administration.

Figure 64. The pattern of PAS-D staining 12, 24, 72 and 168 hr after seizures induced by intraperitoneal injection of kainic acid (10 mg/kg)

Drawings represent coronal sections localizing PAS-D stained material from 5 rats. Staining was not detected at earlier time points. Shading intensity represents denistometric analysis of the intensity of staining compared to saline-treated animals. Shading Key: ▒ Very Light (25 fold increase over background); ▒ Light (50 fold increase over background); ▒ Moderate (100 fold increase over background); ■ Intense (200 fold increase over background). No attempt has been made to differentiate between types of PAS-D staining during densitometric analysis.

Abbreviations:

AC, anterior commissure
ACo, anterior cortical amygdaloid nucleus
AOP, anterior olfactory posterior nucleus
B, Bed nucleus
CA1-3, fields CA1-3 of Ammon's horn
CeA, central amygdaloid nucleus
Cli, caudal linear nucleus raphe
CPu, caudate/putamen
DLG, dorsal lateral geniculate
DR, dorsal raphe nucleus
EB, entopeduncular nucleus
f, fornix
HDB, nucleus of horizontal limb diaganol band
LA, lateral amygdaloid nucleus
LhB, lateral habenular nucleus
LS, lateral septal nucleus
MD, mediodorsal thalamic nucleus
MeA, medial amygdaloid nucleus
ml, medial leminiscus
MS, medial septal nucleus
PC, paracentral thalamic nucleus
Pir, piriform cortex
PO, preoptic nucleus
PRS, presubiculum
RE, reuniens thalamic nucleus
Ri, rostral interstitial nucleus mlf
SFi, septal fimbrial nucleus
SNR, substantia nigra
SuM, supramammillary nucleus
VMH, ventromedial hypothalamic nucleus
VPL, ventroposterolateral thalamic nucleus

Acb, nucleus accumbens
AHi, amygdaloid hippocampal area
APir, amygdaloid/piriform transition area
BLA, basolateral amygdaloid nucleus
cc, corpus callosum
CL, centrolateral thalamic nucleus
CM centromedial thalamic nucleus
DG, dentate gyrus
DMD, dorsal medial hypothalamic nucleus
DSC, lamina dissecans entorhinal area
Eth, ethnoid thalamic nucleus
GP, globus pallidum
ic, internal capsule
LD, lateral dorsal thalamic nucleus
LP, lateral posterior thalamic nucleus
MCPO, magnocellular preoptic nucleus
ME, median eminence
MG, medial geniculate nucleus
MM, mediamammillary nucleus
PaS, parasubiculum
PF, parafascicular nucleus
Pn, pontine nucleus;
PON, posterior thalamic nucleus
PV, paraventricular thalamic nucleus
RF, rhinal fissure
SC, superior colliculus
Shi, septohippocampal nucleus
st, stria terminalis
SY, striohypothalamic nucleus
VP, ventral pallidum
VPM, ventroposteromedial thalamic nucleus

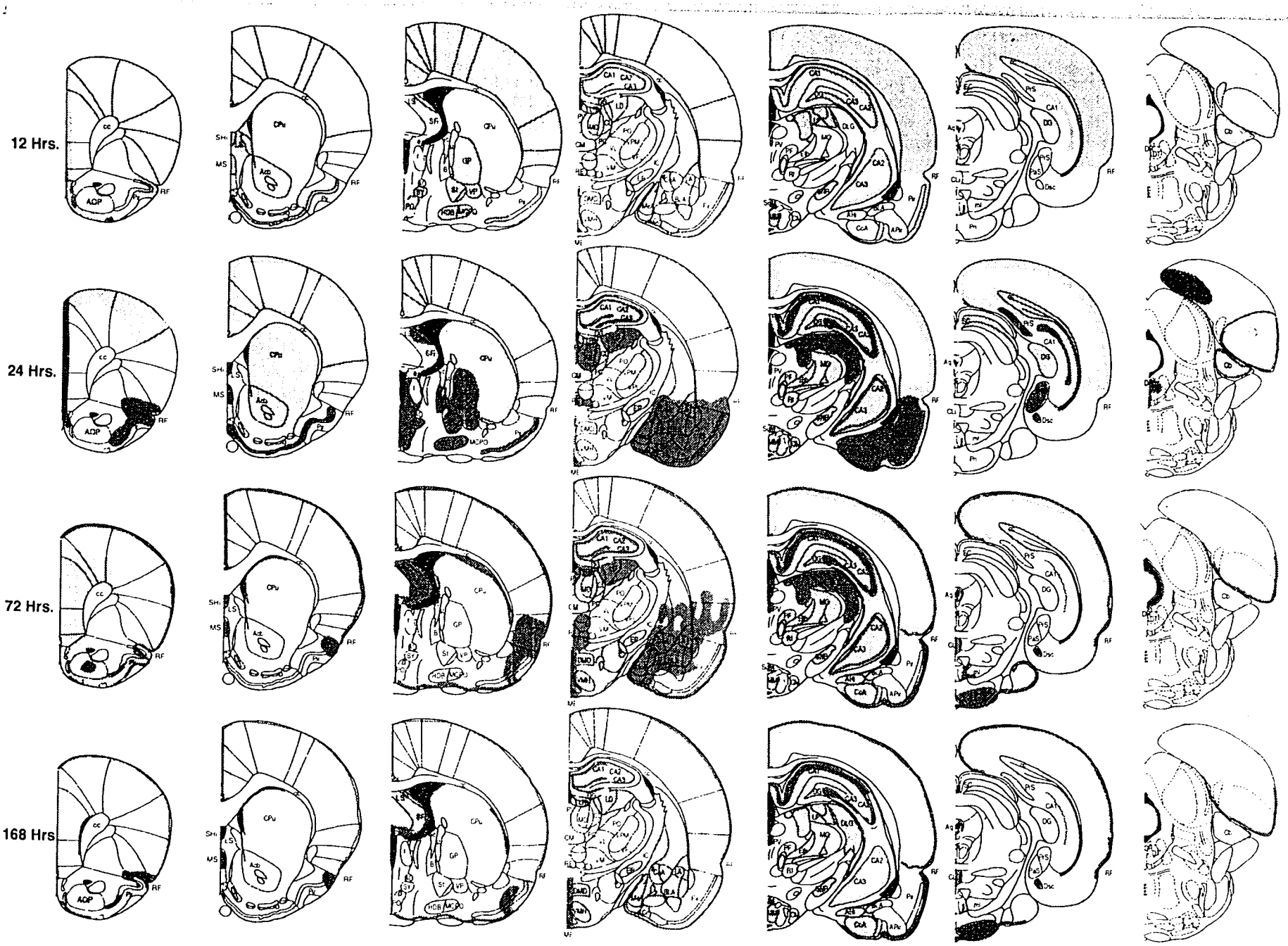
12 Hrs.
24 Hrs.
72 Hrs.
168 Hrs

Table 11. Morphological changes associated with kainic acid induced seizures

	Hyperchromatic, pyknotic cells						Cell fragmentation						Cell loss						Edema, neuropil vacuolization					
Time (hr):	3	5	10	24	72	168	3	5	10	24	72	168	3	5	10	24	72	168	3	5	10	24	72	168
Cortices:																								
Entorhinal cortex	+	++	+++	++++	+	+	-	-	-	+++	+	+	-	-	-	+	+++	++	++	+++	+++	++++	++	+
Piriform cortex	++	+++	+++	++++	++	-	-	-	++	+++	++	+	-	-	-	++	++++	++++	++	+++	+++	++++	++	+
Retrosplenial cortex	+	++	++	++	+	+	-	-	-	+	-	-	-	-	-	-	+	+	+	+	++	++	+	-
Parietal cortex	+	+	+	+	-	-	-	-	-	-	-	-	-	-	-	-	-	-	+	+	+	+	-	-
Perirhinal cortex	+	++	+++	++++	+	+	-	-	-	+++	+	+	-	-	-	+	++	+	++	+++	+++	+++	++	+
Hippocampus:																								
CA1	++	+++	+++	++++	++	+	-	-	++	+++	++	+	-	-	-	++	+++	++++	++	+++	+++	++++	++	+
CA2	++	+++	+++	++++	++	+	-	-	+	++	++	+	-	-	-	++	+++	+++	++	+++	+++	++++	++	+
CA3	++	+++	+++	++++	++	+	-	-	+	++	++	+	-	-	-	++	+++	+++	++	+++	+++	++++	++	+
CA4	++	++	++	+++	+	+	-	-	+	+	+	+	-	-	-	+	++	++	+	++	+++	+++	+	+
Dentate gyrus	+	+	+	++	+	-	-	-	-	-	-	-	-	-	-	-	+	+	+	++	++	+++	-	-
Amygdaloid nuclei:	-	++	+++	++++	++	+	-	-	++	+++	++	+	-	-	-	++	+++	++++	++	+++	+++	++++	++	+
Striatum:	-	-	-	-	-	-	-	-	-	-	-	-	-	-	-	-	-	-	-	-	+	+	-	-
Thalamic nuclei:																								
Medial dorsal	-	+	++	++	+	+	-	-	+	++	+	+	-	-	-	+	++	++	+	++	++	+++	+	-
Lateral dorsal	-	+	++	++	+	+	-	-	+	++	+	+	-	-	-	+	++	++	+	++	++	+++	+	-
Centrolateral	-	-	+	++	+	-	-	-	-	+	-	-	-	-	-	-	-	-	-	+	++	+++	+	-
Centromedial	-	-	+	++	+	-	-	-	-	+	-	-	-	-	-	-	-	-	-	+	++	+++	+	-
Ventrolateral	-	-	+	+	-	-	-	-	-	+	-	-	-	-	-	-	-	-	-	+	++	+++	+	-
Ventromedial	-	-	+	+	-	-	-	-	-	+	-	-	-	-	-	-	-	-	-	+	++	+++	+	-
Reuniens	-	-	+	+	-	-	-	-	-	+	-	-	-	-	-	-	-	-	-	+	++	++	-	-

-, none; + to ++++, denotes increasing frequency/severity

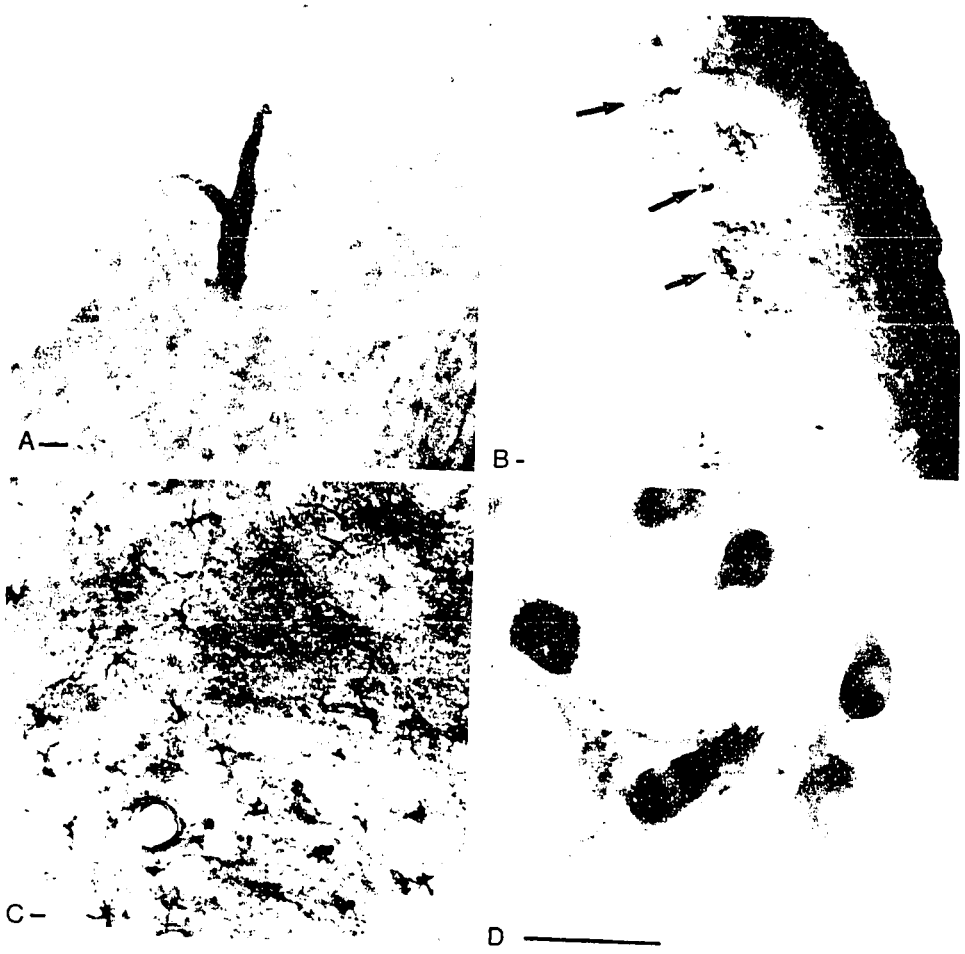

Figure 65. Four different types of PAS-D positive material can be identified in rat brain following kainic acid (10 mg/kg)-induced seizures

(A), **Type 1**-blood vessel-associated staining 24 hr after drug injection. Example taken from entorhinal cortex. (B), **Type 1**-ECM-associated staining of layers I and II of the neocortex and **Type 2**-granular depositions (arrows) 24 hr after drug injection. Example taken from neocortex in the vicinity of the rhinal fissure. (C), **Type 3**-glial labelling 24 hr after drug injection. Example taken from entorhinal cortex. (D), **Type 4**-neuronal labelling 168 hr after drug injection. Example taken from dorsal striatum. Bar 40 μm.

most pronounced at this time point. The second phase of neurodegeneration, 72-168 hr after treatment, was characterized by a reduction in the degree of edema observed, morphological recovery of many affected neurons, and cell death in discrete brain regions. By 168 hr after kainic acid administration, lesions, consisting of small cystic cavities scattered throughout fields of large, hypochromatic neurons, were preferentially localized to discrete regions within the hippocampal formation, entorhinal and piriform cortices, and amygdaloid complex. Pyknotic and hyperchromatic neurons were rarely detected. In areas that had exhibited cell fragmentation, substantial cell loss was noted, most notably in CA1 and CA3 pyramidal cells of the hippocampal formation, throughout the piriform cortex and amygdaloid complex, and within the entorhinal cortex immediately surrounding the piriform cortex as previously reported (4,5,16,34,35,43,46,58,64).

The cellular distribution of PAS-D^+ material varied over time in parallel with the gross morphological alterations accompanying neurodegeneration (Table 11). **Type 1**-staining of blood vessels and ECM components and **Type 3**-positive glia first appeared towards the end of epileptiform activity (12 hr after treatment) and were preferentially localized to edematous tissue. The intensity of **Type 1** and **Type 3** staining peaked 24 hr after kainic acid administration when cerebral edema was most pronounced and morphological alterations were the most extensive. Staining intensity decreased with time until, by 168 hr after treatment, **Type 3**-glial staining could only be observed within areas exhibiting residual edema.

While **Type 1**-labelling of blood vessels and ECM and **Type 3**-glial staining appeared to be correlated with the presence of edema, the appearance of **Type 2**-granules was more indicative of subsequent cell death. PAS-D^+ granular deposits were first observed 24 hr after treatment and were preferentially localized to regions that, at later time points, invariably exhibited cell loss. Staining disappeared prior to gross morphological evidence of necrosis until, by 168 hr after induction of epileptiform activity, **Type 2**-granules were absent from necrotic brain sites and could only be found in conjunction with **Type 1**-ECM material forming a penumbra around damaged tissue.

Type 4-neuronal staining was only observed 168 hr after excitotoxin administration and

Table 12. Changes in PAS-D staining, FLI, anti-GFAP immunoreactivity, and blood-brain barrier breakdown (accumulation of rat Ig immunoreactivity) associated with kainic acid induced seizures

	PAS-D						FLI						Anti- GFAP						Anti rat-IgG					
Time (hr):	3	5	10	24	72	168	3	5	10	24	72	168	3	5	10	24	72	168	3	5	10	24	72	168
Cortices:																								
Entorhinal cortex	-	-	1,3	1,3	1,3	1,3	++	-	-	-	++	++	+	++	+++	++++	++	+	+	+	++	++++	+	-
Piriform cortex	-	-	1,3	1,2,3	1,3	1,3,4	+++	-	-	-	+++	+++	+	++	+++	++++	++	+	+	+	++	++++	++	+
Retrosplenial cortex	-	-	1,3	1,3	1,3	1,3	+	+	+	-	-	-	+	+	++	+++	+	-	+	+	+	++	+	-
Parietal cortex	-	-	1,3	1,3	1	1	+	+	+	-	-	-	+	+	+	++	-	-	+	+	+	++	-	-
Perirhinal cortex	-	-	1,3	1,3	1,2,3	1-4	++++	+	++	-	-		+	+	++	+++	+	+	+	+	++	+++	++	-
Hippocampus:																								
CA1	-	-	1,3	1,2,3	1,3	1,3,4	++	+	+	-	++	++	+	++	+++	++++	++	+	+	+	++	++++	+	+
CA2	-	-	1,3	1,3	1,3	1,3,4	++	-	-	-	+	+	+	++	+++	++++	++	+	+	+	++	++++	-	-
CA3	-	-	1,3	1,2,3	1,3	1,3,4	++	+	+	-	++	++	+	++	+++	++++	++	+	+	+	++	++++	+	+
CA4	-	-	1,3	1,3	1,3	1,3,4	++	-	-	-	+	+	+	++	+++	++++	++	+	+	+	++	++++	-	-
Dentate gyrus	-	-	1,3	1,3	1	1,4	++	+	+	+	-	-	+	+	++	+++	+	+	+	+	++	++++	+	-
Amygdaloid nuclei	-	-	1,3	1,2,3	1,3	1,3,4	++	+	-	-	++	++	+	++	+++	++++	-	-	+	+	++	++++	+	+
Striatum:	-	-	-	1	1	1,4	+	+	+	+	++	++	-	+	+	-	-	-	+	+	+	+	-	-
Thalamic nuclei:																								
Medial dorsal	-	-	1,3	1,3	1,3	1	+	+	+	+	-	-	+	+	++	+++	-	-	+	+	+	-	-	-
Lateral dorsal	-	-	1,3	1,3	1,3	1	+	+	+	+	-	-	+	+	++	+++	-	-	+	+	+	-	-	-
Centrolateral	-	-	1,3	1,3	1	1	+	+	+	+	-	-	+	+	++	+++	-	-	+	+	+	-	-	-
Centromedial	-	-	1,3	1,3	1	1	+	+	+	+	-	-	+	+	++	+++	-	-	+	+	+	-	-	-
Ventrolateral	-	-	1	1,3	1	-	+	+	+	-	-	-	+	+	++	+++	-	-	+	+	+	-	-	-
Ventromedial	-	-	1	1,3	1	-	+	+	+	-	-	-	+	+	++	+++	-	-	+	+	+	-	-	-
Reuniens	-	-	1	1,3	1	-	+	+	+	-	-	-	+	+	++	+++	-	-	+	+	+	-	-	-

1, **Type 1**-ECM or blood vessel associated material; 2, **Type 2**- granular deposits; 3, **Type 3**-glial labelling; 4, **Type 4**-neuronal labelling; + to ++++ denotes increasing intensity/frequency; -, none

was almost exclusively localized to regions of substantial cell loss except for specific staining of striatal neurons in association with **Type 1**-staining of ECM.

FLI and PAS-D$^+$ deposits

Unexpectedly, early induction of the *fos* family of proto-oncogenes was found to be highly predictive not only of subsequent cell death but also of **Type 2**-granular deposits and **Type 4**-neuronal labelling. As indicated in Chapter IV, Section 4, *fos* genes are members of the early response gene family that encodes for transcription factors. During epileptiform seizures and other disorders, their gene products are believed to couple neuronal excitation to changes in target gene expression (11,15,19,22,23,27,32,33,51). Early and long-lasting induction of the *fos* protein (1-5 hr after seizure induction) can be used to determine the degree and extent of prolonged neuronal excitation and, hence, identify neuronal populations most likely to exhibit subsequent cell loss. Renewed expression of c-*fos* mRNA has been demonstrated in apoptotic cell populations 72-168 hr after kainate administration (57). The results of the present study are in accordance with these observations. Epileptiform activity elicited neuronal expression of the *fos* family of proto-oncogenes (Table 12). Control subjects did not exhibit significant immunoreactivity (Figure 63A,B). FLI was observed early in the first phase of neurodegeneration and was highly predictive not only of cell loss but also of later **Type 1**-ECM, **Type 2**-granular, and **Type 4**-neuronal PAS-D staining. Of particular note is the temporal pattern of *fos*-like immunoreactivity observed in the hippocampal formation and piriform cortex. By 3 hr after treatment, FLI was seen in neurons of the pyramidal cell layers of the hippocampal formation and within the dentate gyrus. Neurons in the piriform cortex also demonstrated intense labelling (Figure 63C-D). These areas corresponded to sites of **Type 4**-neuronal labelling observed 168 hr after treatment. By 5 hr after drug injection, FLI was absent from both the CA4 and CA2 cell fields of the hippocampal formation and from the piriform cortex although immunoreactive cells could still be detected in the dentate gyrus, CA1 and CA3 of the hippocampus (Figure 63E-F), the amygdaloid complex, entorhinal cortex, layers I and II of the neocortex and throughout the cortical cell layers in the vicinity of the rhinal fissure, around the third ventricle, surrounding select thalamic nuclei, and, more anteriorly, along the dorsolateral border of the striatum. This distribution corresponded with

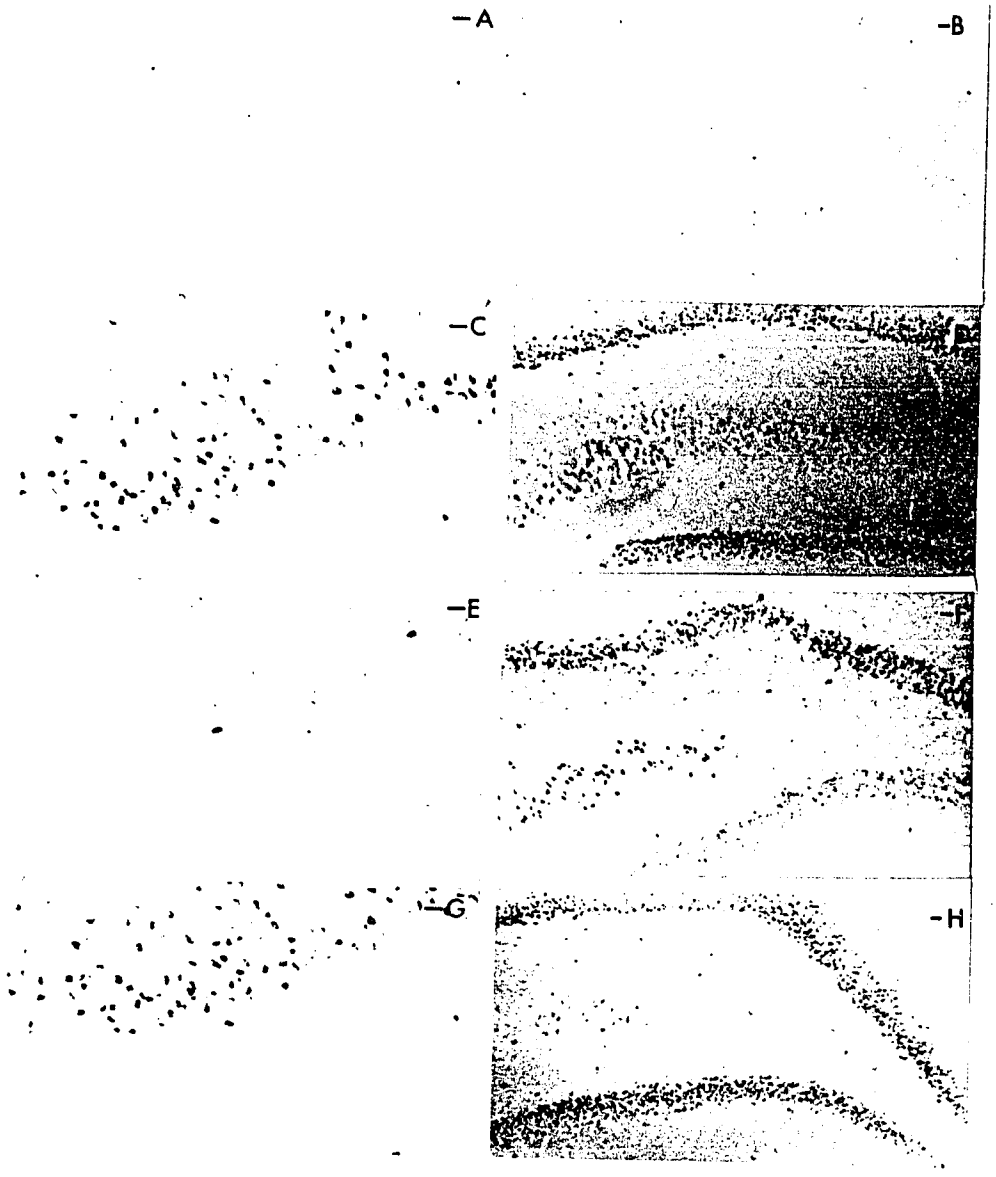

Figure 66. C-*fos*-like immunoreactivity following kainic acid-induced seizures

Control subjects 3 hr after saline injection (A-B). Kainic acid (10 mg/kg)-treated animals 3 hr (C-D), 5 hr (E-F), 24 hr (G), and 168 hr (H) after drug injection. (A), (C), (E), and (G) are taken from the piriform cortex. Panels (B), (D), (F), and (H) are taken from the hippocampal formation. Bar=80 μm.

residual **Type 1**-ECM PAS-D staining observed 72 hr after treatment and accurately predicted long-lasting **Type 2**-granular depositions and **Type 4**-neuronal staining observed 168 hr after treatment. By 24 hr after treatment, FLI expression was no longer detected in the hippocampal formation with the exception of some weak staining in the dentate gyrus (Figure 66H). FLI was absent from the entorhinal and piriform cortices but could be detected in the perirhinal region throughout areas that would express intense **Type 2**-granular deposits 72 hr after kainate administration. FLI reappeared 72 hr after treatment in pyramidal cells of the hippocampal formation (but not in the dentate gyrus) and within neurons of the piriform cortex remaining immunoreactive 168 hr post treatment (Figure 66G). These areas demonstrated considerable cell death and chronic accumulation of **Type 1**-ECM and **Type 4**-neuronal PAS-D staining. Finally, FLI could also be detected 72 hr after kainate injection in a discrete area of the dorsolateral striatum - a region exhibiting intense **Type 4**-neuronal labelling 168 hr after seizure induction without showing any signs of cell loss.

This latter finding was of considerable interest. Evidently, FLI could be used to predict PAS-D neuropathology in addition to cell death. As indicated, FLI labelling was detected 24 hr after treatment in the perirhinal region immediately surrounding damaged portions of the entorhinal cortex as well as 72 hr after treatment in discrete regions of the lateral striatum - areas that do not exhibit cell loss. This distribution accurately predicted the appearance of **Type 2**-granular deposits 72 hr after kainate injection and specific populations of **Type 4**-labelled neurons observed 168 hr after treatment. Therefore, FLI is indicative both of cell loss and accumulation of $PAS\text{-}D^+$ material. FLI may be either a coincident byproduct of the breakdown in cell signalling observed after kainic acid-induced seizures or may actually be a required component in a gene regulation pathway mediating both neuronal death and aberrant carbohydrate accumulation.

GFAP immunoreactivity, blood -brain barrier breakdown, and PAS-D^+ deposits

Acute and chronic neurodegenerative changes were accompanied by two phases of reactive gliosis and blood-brain barrier breakdown (See Table 12 and ref. (29)). In the acute phase, blood-brain barrier breakdown, as assessed by extravasation of rat Ig molecules into brain parenchyma,

was distributed randomly throughout the brain around haemorrhaging blood vessels (medium and fine calibre). In sections from control brain, only vessels in the circumventricular organ such as the arcuate nucleus and the median emminence showed permeability to blood Igs and in these loci there was no associated PAS-D staining (Figure 67A). Within 3-5 hr of kainate administration, rats demonstrated a large number of focal haemorrhages distributed randomly throughout the brain (Figure 67B). By 12 hr after treatment, the distribution of Ig immunoreactivity had changed (Figure 67C). Staining was no longer confined to damaged blood vessels but was also detected throughout the perirhinal, piriform and entorhinal cortices in a pattern congruent with that of **Type 1**-ECM and **Type 3**-glial PAS-D staining observed at the same time point. Blood vessels in areas that had exhibited focal extravasation of rat Igs were **Type 1**-PAS-D positive. Some neurons in the hippocampal formation, centromedial, laterodorsal and reuniens nuclei, piriform cortex, and throughout layers I and II of the neocortex had taken up blood proteins and as such were Ig-immunoreactive (Figure 68A). Many Ig-positive cells were surrounded by PAS-D **Type 2**-granules and **Type 1**-ECM (Figure 68B).

Early reactive gliosis was initially confined to the vicinity of disrupted vasculature. With time, extensive GFAP immunoreactivity could be observed throughout edemic tissue in and around areas of blood-brain barrier breakdown. PAS-D staining was first observed towards the end of the acute phase. **Type 3**-staining of glial cells could be observed throughout edematous tissue (Figure 69A). The majority of these PAS-D positive cells were identified as GFAP-immunoreactive astrocytes while a small subpopulation were GFAP-negative and morphologically characteristic of microglia. The appearance of PAS-D^+ staining correlated with the induction of a diffuse spread of blood proteins throughout specific limbic structures. Initially, labelling (**Type 1**) of the ECM could be observed throughout areas of blood-brain barrier breakdown while specific labelling of haemorrhaging vasculature could be detected around rat Ig-positive capillaries. However, towards the end of the acute phase of neurodegeneration, **Type 1**-ECM staining formed a penumbra around areas exhibiting serum protein accumulation while **Type 2**-granular deposits were localized within Ig-reactive tissue in specific association with Ig-positive neurons. This distribution of **Type 2**-granular deposits was highly predictive of subsequent neuronal death observed in the chronic phase of neurodegeneration. In this later phase of damage, tissue was no

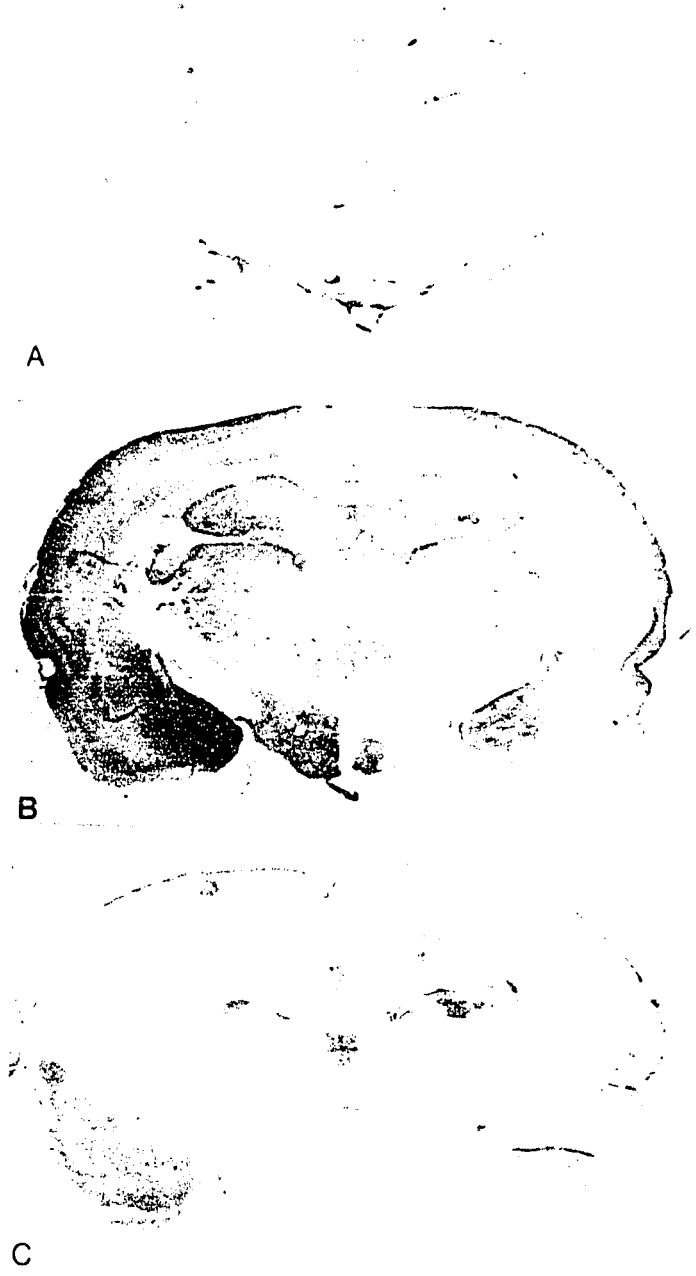

Figure 67. Blood-brain barrier breakdown following kainic acid-induced seizures

Representative photomicrographs illustrate the extent of rat Ig extravasation into brain parenchyma 3, 12, and 24 hr (A-C) after drug injection.

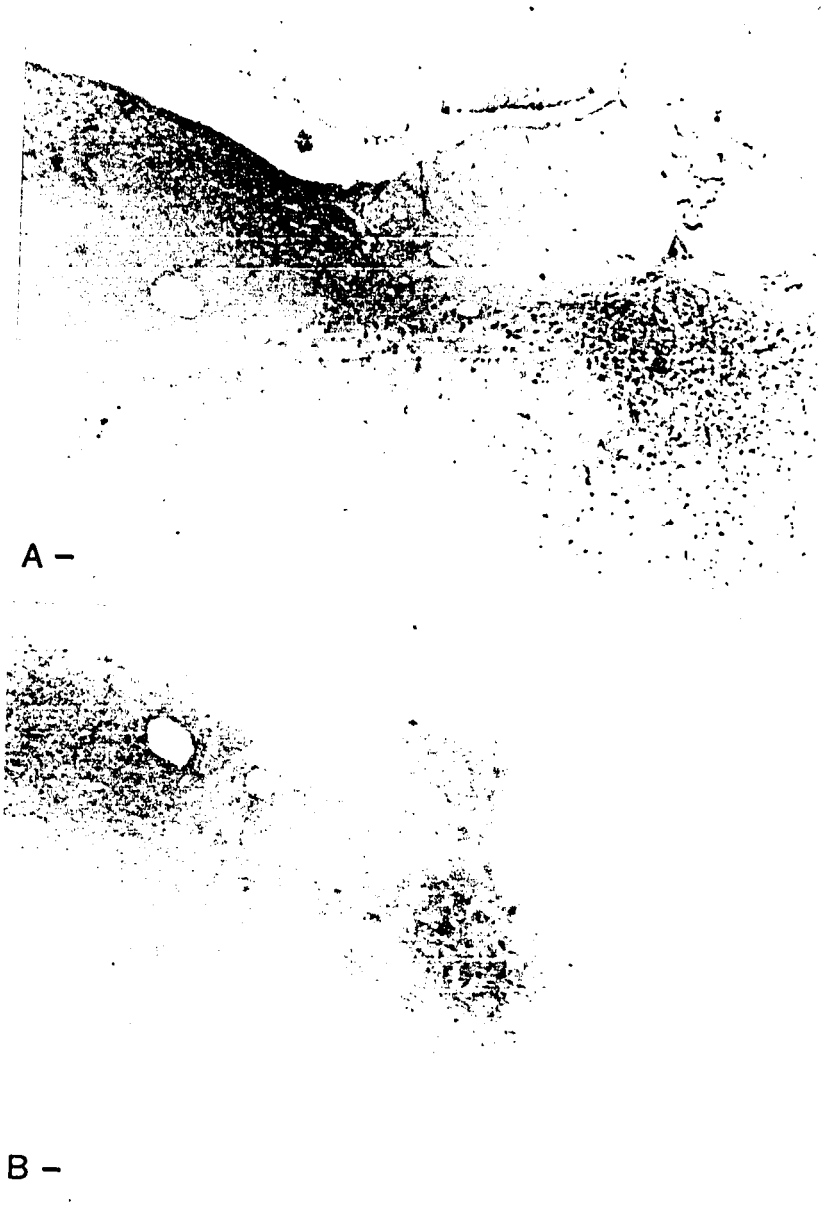

Figure 68. Neuronal accumulation of blood-borne products and PAS-D$^+$ deposits

Relationship between neuronal-labelling of cells with rat Ig (A) and **Type 1**-ECM depositions (B) 24 hr after kainic acid (10 mg/kg) administration. Representative photomicrographs depict a single section double-stained for both rat Ig immunoreactivity and PAS-D staining. Abbreviations as in Figure 64. Scale Bar=200 µm.

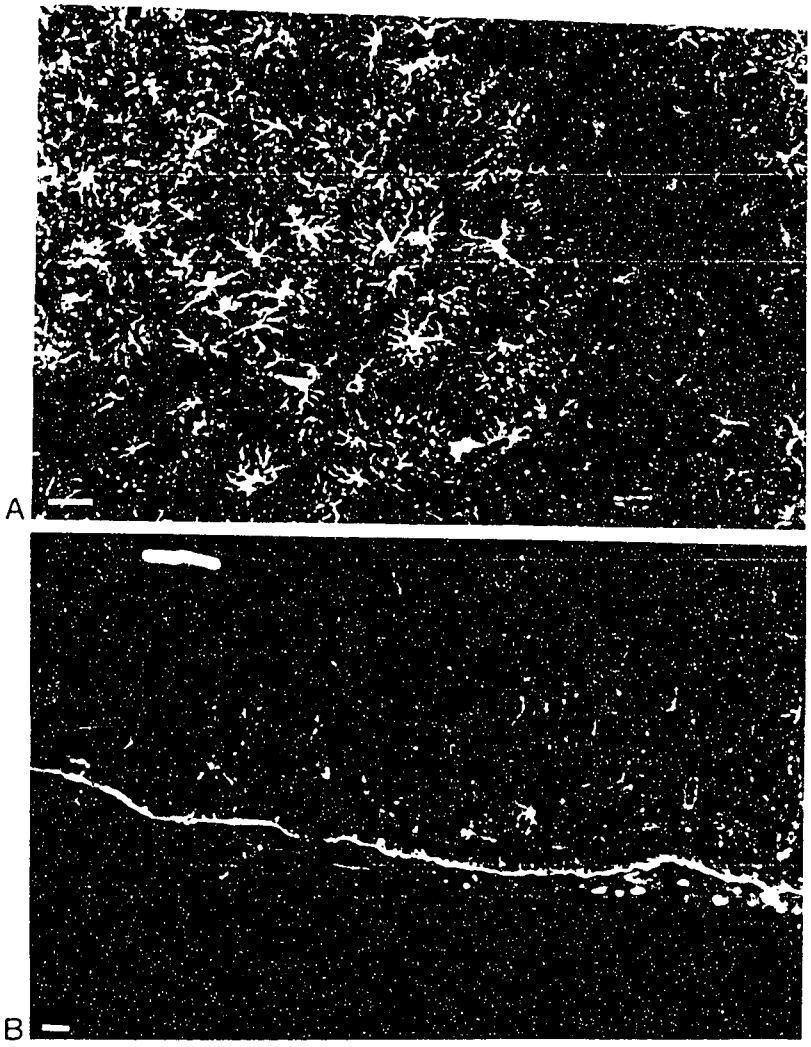

Figure 69. Reactive gliosis following kainic acid-induced seizures

Photomicrographs of anti-GFAP immunoreactive glia after kainic acid (10 mg/kg) administration. (A), staining in the hippocampal formation 24 hr after drug injection. (B), residual labelling in the entorhinal cortex 72 hr after excitotoxin administration. Scale bar=20 μm.

longer grossly edematous. Rat Ig immunoreactivity was minimal and confined to areas of residual edema and **Type 3**-reactive gliosis (Figure 69B). Substantial cell death was noted in areas that had exhibited **Type 2**-granular deposits during the acute phase of neurotoxicity and was surrounded by a penumbra of approximately 100 μm in width of **Type 1**-ECM material. The few remaining cells within these regions were morphologically intact, but were hypochromatic. Many of these neurons were **Type 4**-PAS-D positive.

Relevancy to chronic neurodegenerative disorders

Aberrant PAS-D positive material has been detected in the brain of patients suffering from a variety of chronic neurodegenerative disorders as well as in the brain of senescence accelerated mice (1) and in the CNS of experimental animals following following X- and gamma-irradiation (67) and stab wounding (25). The identity of these PAS-D$^+$ components in diseased brain is ambiguous. The PAS-D stain is known to be specific for highly polymerized carbohydrates such as glycogen or highly sialated glycoproteins and glycolipids (12). In the present model, **Type 2**-granules and **Type 4**-neurons are resistant to amylase digestion (data not shown) suggesting that this material is unlikely to be glycogen. These observations are in accordance with Akiyama et al. (1) who demonstrated that the PAS-D$^+$ granular depositions observed in the brain of senescence-accelerated mice were amylase resistant and histochemically uncharacteristic of glycogen polymers. However, the present study also describes the relationship between PAS-D staining and induction of FLI, neuronal necrosis, reactive gliosis, and blood-brain barrier breakdown in an attempt to establish temporal correlations between the development of PAS-D deposits and several other markers of brain damage using a well-characterized animal model of neuropathology. Four types of aberrant PAS-D material were identified in rat brain following kainic acid induced seizures: **Type 1**-ECM or blood vessel associated-material, **Type 2**-granular deposits, **Type 3**-glial labelling, and **Type 4**-neuronal labelling. Results demonstrate that (1) **Type 1**-ECM staining and **Type 3**-glia are preferentially localized to edematous tissue; (2) the majority of **Type 3**-glia are reactive astrocytes while a minority of PAS-D$^+$ glia appear to be proliferating microglia; (3) **Type 1**-blood vessels identify haemorrhaging vasculature; (4) the early distribution of **Type**

2-granules accurately predicts subsequent cell loss; (5) chronic **Type 2**-granular deposits and **Type 4**-neuronal labelling not associated with cell death are predicted by early changes in FLI; and (6) chronic deposition of all four forms of PAS-D^+ material is confined to areas that exhibited substantial, transient blood-brain barrier compromise. It would appear that the prolonged increase in PAS-D staining could represent the synthesis of heavily glycosylated constituent(s) of the ECM by both neurons and astrocytes as part of an inflammatory response elicited by blood-brain barrier breakdown.

3. Alterations in PAFR Gene Expression in the Hippocampus and Relationship to Morphological and Genetic Markers of Cell Death Following Kainic Acid-Induced Seizures

Abstract

PAFR mRNA was demonstrated for the first time in rat brain by *in situ* hybridization. Expression patterns were mapped in the hippocampal formation. To determine whether PAFR is implicated in progressive neurodegeneration, alterations in PAFR expression were correlated with ACD, induction of clusterin mRNA, reactive gliosis, and PAS-D accumulation using the kainic acid model of myoclonic epilepsy. Each of these neuropathologies is common to chronic neurodegenerative conditions. Induction of epileptiform activity was shown to profoundly alter the pattern of PAFR expression. At the height of the acute phase of neurodegeneration (24 hr after kainate injection), PAFR mRNA levels were reduced in cells throughout the hippocampal formation except for neurons in the CA2 and CA4 cells fields. Given that epileptiform seizures have been shown to induce substantial PAF synthesis and release, these data are in accordance with reports that prolonged stimulation of PAFR with ligand leads to receptor desensitization and reduced mRNA expression (9,44,45,65). Expression of PAFR mRNA was preferentially restricted to neurons and microglia and not to astrocytes. PAFR labelling at 24 hr was predictive of **Type 1**- and **Type 4**-PAS-D accumulation observed 7 days after kainate induction. During the chronic phase of neurodegeneration (3-7 days after kainate administration), substantial increases in PAFR gene expression corresponded with induction of clusterin mRNA expression and ACD. PAS-D **Type 4**-neuronal labelling was correlated with increased PAFR expression. **Type 3**-astrocytic labelling surrounded neurons expressing enhanced levels of PAFR mRNA. These results were confirmed by RT-PCR analysis and morphological evaluation. The possibility that PAF neurotransmission may contribute to the accelerated cell death characteristic of progressive neurodegenerative disorders is discussed.

Introduction

To further explore the involvement of PAF in chronic neuropathology, alterations in PAFR with respect to morphological and genetic indices of long-term degeneration were investigated following kainic acid-induced seizures. As demonstrated in Chapter VI, Section 2, this model of myoclonic epilepsy was chosen because acute induction of severe epileptiform seizures induces many characteristic pathologies common to a variety of neurodegenerative disorders.

Materials and Methods

Induction of epileptiform seizures, histochemical, and immunohistochemical evaluation

Kainic acid (10 mg/kg)-induced seizures (Stage 4) were elicited in 27 male Wistar rats as

described in Chapter VI, Section 2. Rats were perfused at 4, 24, 72, and 168 hr after kainic acid administration. Brain samples were removed and processed for histochemical and immunohistochemical evaluation as described in Chapter VI, Section 2.

In situ hybridization, RT-PCR, and DNA ladder formation

Animals were sacrificed by decapitation and brains were plunged into cold isopentane, flash-frozen in liquid nitrogen, cut into 10 µm cryostat sections, placed in gelatin-coated slides, and stored at -100°C. Frozen sections were fixed for 15 min in 4% paraformaldehyde/PBS (Chapter II, Section 2) and rehydrated for 10 min in PBS containing 5 mM $MgCl_2$. Adjacent sections were treated with RNAse (as a negative control), rinsed briefly in 2x SSC (Chapter V, Section 2) and incubated for 1 hr at 37°C with 100 µl of RNAse A (100 µg/ml; Bohringer Manheim, Que). During RNAse treatment, experimental sections were maintained in PBS containing 5 mM $MgCl_2$. Experimental and negative control slides were rinsed in 70% ethanol (1 min/wash), washed three times in PBS (2 min/wash), rinsed twice in 2x SSC (5 min/wash), and acetylated at room temperature in 16 mM triethanolamine, 0.25% acetic anhydride pH 8.0 (10 min/wash). Sections were rinsed five times in PBS containing 10 mM DTT (5 min/wash), twice in 2x SSC containing 10 mM DTT (5 min/wash), and prehybridized for 1 hr at room temperature in 40 µl of 50% formamide, 2x SSC, 0.4% BSA, 30 mM DTT, 20 mM vanadyl ribonucleoside complex, 10 µg/ml yeast tRNA (heat denatured) and 200 mg/ml salmon testes DNA (heat denatured). Hybridization was performed at 44°C overnight with 40 µl of the prehybridization solutions supplemented with 10% dextran sulfate and labelled probe. Probes were either full-length denatured human PAFR cDNA (Chapter IV, Section 2) kindly provided by Dr. N. and C. Gerard (Harvard Medical School, Harvard) or a full length clusterin cDNA (Chapter IV, Section 4) kindly provided by Dr. M. Tenniswood (Alton Jones Cell Science Centre, Lake Placid). Probes were labelled as described in Chapter IV, Section 4. Slides were washed twice in 50% formamide, 2x SSC, 10 mM DTT (30 min/wash) at 50°C, three times in 50% formamide, 1x SSC, 10 mM DTT (20 min/wash) at 44 °C, and three times in 0.5x SSC, 10 mM DTT (20 min/wash) at room temperature. Sections were dehydrated in an ascending series of ethanol washes. Slides were dipped in nuclear track photographic emulsion, exposed for 3-7 days at 4°C,

and were processed at 15°C for 5 min in Kodak-D19 developer, 30 sec in 2% acetic acid, 5 min in Kodak Rapid Fix, and 30 min in running water. Photographic chemicals were from Kodak, Ont. Sections were lightly counterstained with hematoxylin and eosin and examined under bright- and dark-field illumination using a Zeiss Axioskop microscope.

For RT-PCR analysis, the hippocampal formation was rapidly dissected out of fresh tissue and total RNA extracted after homogenization as described in Chapter IV, Section 2. Primer sequences against the PAFR (Chapter IV, Section 2), clusterin - 5'GCCCTATCATCTATC TACCT3' (forward) and 5'CGGGATAGTAGATAGACT3' (reverse) defining a 1.5 kb fragment of rat mRNA, or GAPDH - 5'CCTCTCTCTTGCTCTCAGTAT3' (forward) and 5'GTATCCGTTGTGGATCTGACA3' (reverse) defining a 742 kb fragment of rat mRNA kindly provided by Dr. M. Tenniswood (Alton Jones Cell Science Centre, Lake Placid) were employed. Analyses were as described in Chapter IV, Section 2

For DNA analysis, DNA was isolated from frozen tissue as described in Chapter III, Section 2 with the exception that tissue blocks were homogenized prior to extraction.

Results and Discussion

PAF has been shown *in vivo* to mediate signal transduction in brain tissue through PAF specific binding sites demonstrated in brain homogenates (3,38). Bazan et al have implicated PAF production in epileptogenesis by providing evidence that synthesis of the phospholipid is enhanced during intense synaptic activity and serves to selectively increase release of excitatory neurotransmitters (3). Prolonged activation of glutamate receptors, as a result of epileptiform activity, results in acute necrosis and long-term apoptotic cell death (57). In keeping with this finding, apoptosis-associated DNA fragmentation has been observed in the hippocampal formation following kainic acid-induced seizures (50,57). While ACD is a natural and necessary process in CNS tissue contributing to the formation and organization of the spinal cord, sympathetic ganglia, retina and corpus callosum (57), inappropriate cell death is characteristic of several neuropathological conditions including the chronic neurodegenerative disorders outlined in Table 3, Chapter II, Section 4. The present experiments were designed to determine whether changes in PAFR expression correlated with increases in the rate of ACD in a kainic acid model of

epileptiform activity.

PAFR gene expression: Relationship to neuropathology

PAFR was expressed at low levels throughout the hippocampal formation (Figure 70). These data represent the first such documentation of PAFR in mammalian brain. RNAse treatment of adjacent sections demonstrated that *in situ* hybridization for PAFR was not the result of non-specific binding (Figure 70). PAFR message was preferentially localized to granule cells within the dentate gyrus and pyramidal neurons within CA1, CA2, CA3 and, to a lesser extent, CA4 hippocampal fields. Interneurons throughout the stratum oriens, radiatum, and moleculaire were PAFR positive with slightly reduced expression in cells of the molecular layer compared to cells in oriens and radiatum (Figure 70). Comparison with hemotoxylin and eosin stained-sections under bright-field microscopy indicated that PAFR expression was predominantly neuronal in origin (Figure 71A).

Induction of epileptiform activity profoundly altered the pattern of PAFR expression. During the acute phase of neurodegeneration, 24 hr following kainic acid-induced seizures, PAFR expression was *reduced* in interneurons in the stratum oriens, radiatum, and moleculaire compared to untreated animals with two notable exceptions (Figure 70). These data are in accordance with reports that prolonged stimulation with PAF leads to receptor desensitization (9,44,45,65) and reduced mRNA expression (9). Mild increases in labelling were observed in and around CA2 and CA4 pyramidal neurons as well as within granule cells of the dentate gyrus proximal to CA4 (Figure 70). However, this latter increase in expression corresponded to an overall decrease in PAFR-labelling throughout the rest of the dentate gyrus. On bright-field examination, both neurons and glial cells (morphologically indicative of microglia) were labelled with silver grains (Figure 71B). Staining of adjacent sections with PAS-D indicated that some **Type 3**-microglia were probably $PAFR^{+}$. Double-labelling of sections processed for *in situ* hybridization with anti-GFAP demonstrated that PAFR reactivity could not be attributed to astrocytic expression despite the large numbers of proliferating astrocytes within the confines of the hippocampal formation (Figure 71C). It was of particular interest to note that those areas expressing PAFR were destined

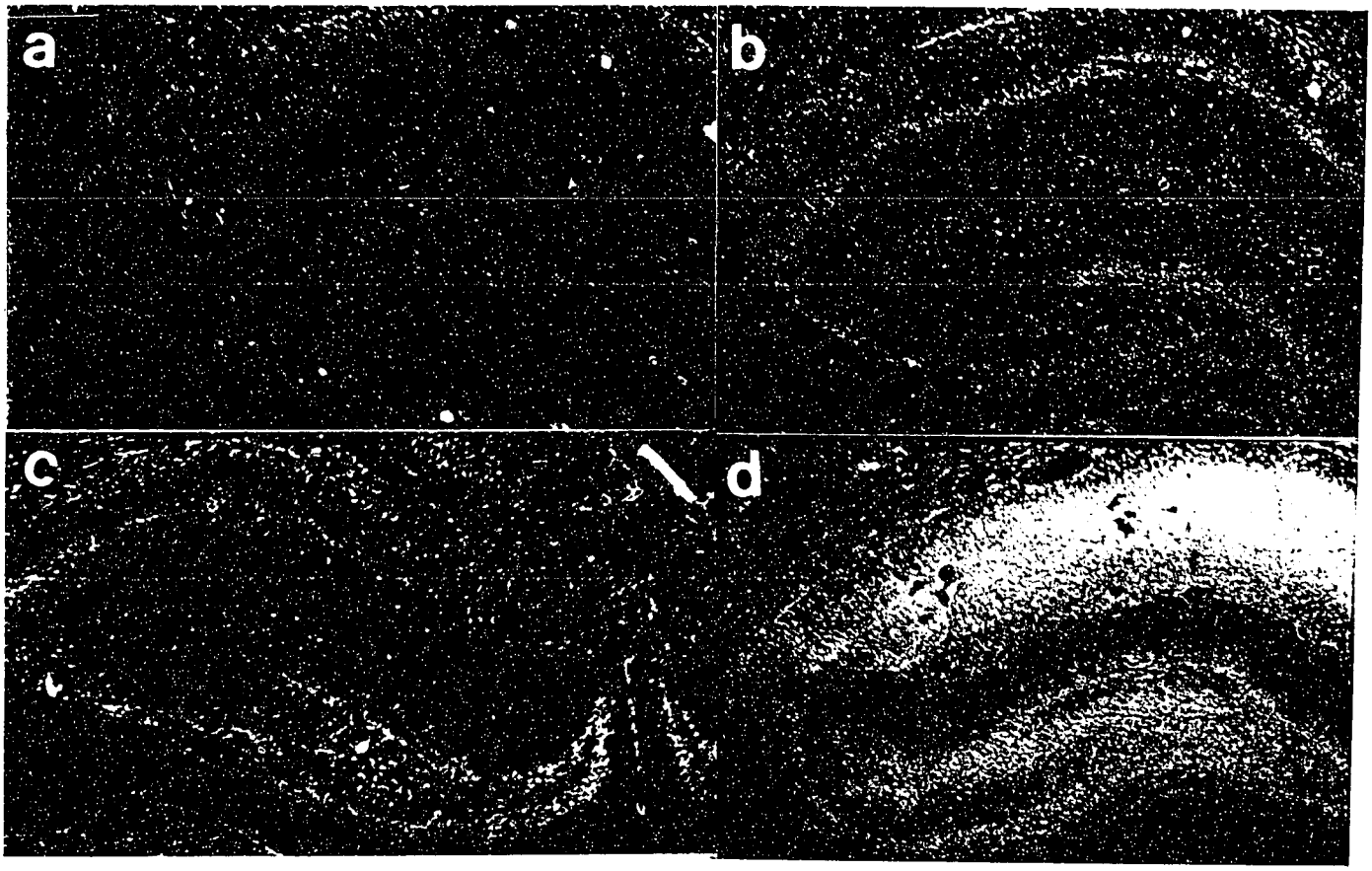

Figure 70. Pattern of PAFR expression in control and kainic acid (10 mg/ml)-treated subjects.

Representative photomicrographs of *in situ* hybridization for PAFR in rat brain hippocampus. Coronal sections (10 μm) were prepared as described in Materials and Methods. (A), RNAse-treated control section. (B), Control. (C), 24 hr after kainic acid treatment. (D), 168 hr after kainic acid treatment. (A) and (B) are adjacent sections. Control animals in this figure were drug-naive subjects. The pattern of PAFR expression in these animals did not differ from that observed in saline-treated subjects (data not shown).

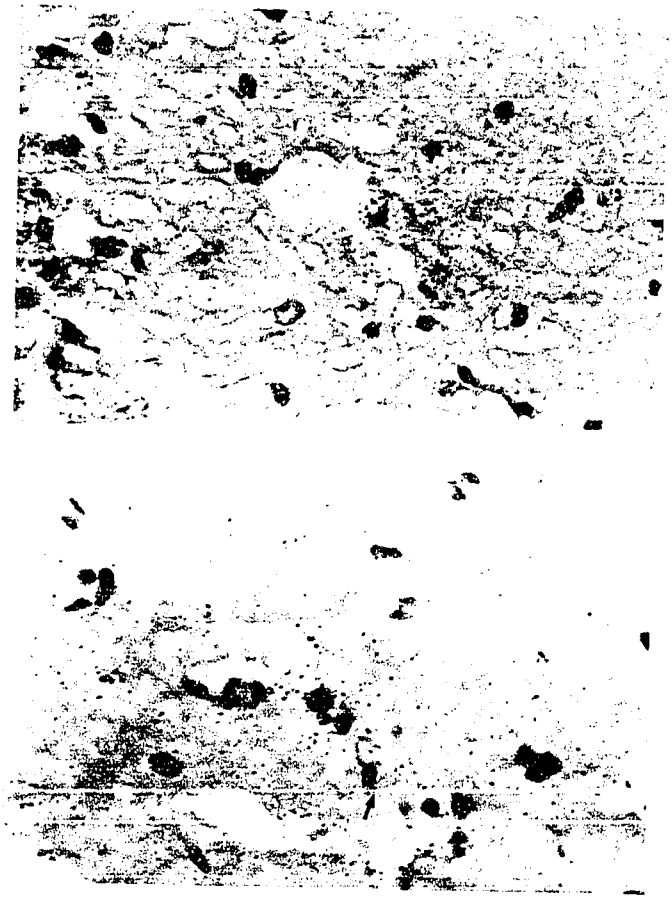

Figure 71. Cellular localization of PAFR expression

Representative photomicrographs of hematoxylin and eosin staining and *in situ* hybridization for PAFR in rat brain hippocampus. (A), control neurons expressing PAFR (CA1). (B), neurons and microglia (arrow) expressing PAFR 24 hr after kainate administration. Double-labelling with anti-GFAP revealed that reactive astrocytes did not express PAFR (data not shown). Scale bar=50 μm.

to exhibit the least amount of cell loss (see Chapter VI, Section 2). However, subsequent examination of sections stained for cresyl violet and PAS-D strongly suggested that PAFR labelling at 24 hr was predictive of other chronic neuropathologies including aberrant process elaboration and **Type 1**- and **Type 4**-PAS-D accumulation observed 7 days after kainate induction (Figure 72AB).

Substantial increases in PAF-R mRNA localized *in situ* were observed 7 days after treatment (Figure 70D). PAFR labelling was evident in vast majority of neurons within CA1 and CA4 of the hippocampal formation, interneurons in the molecular layer of the dentate gyrus, and, to a lesser extent, in granule cells of the dentate gyrus and pyramidal neurons of the CA2 and CA3 hippocampal cell fields. Remarkably, PAFR was strikingly absent from cells in the molecular layer of the hippocampal formation - the only area in the hippocampal formation still grossly edemic and undergoing significant reactive gliosis (Figure 71D). No evidence of glial PAFR expression could be detected either morphologically or in conjunction with anti-GFAP immunoreactivity. The majority of PAF-R expression coincided with chronic PAS-D lesions. However, **Type 1**- and **Type 4**-PAS-D staining were more restricted to the CA cell fields of the hippocampus and was not observed within the stratum oriens or radiatum to the same extent as PAFR expression. PAS-D deposition did exhibit similar specificity for CA1 and CA4 pyramidal cells as did increases in PAFR labelling. No positive correlation was found between **Type 3**-glial labelling 7 days after treatment and localization of PAFR mRNA. In fact, the molecular cell layer, virtually devoid of PAFR expression, was shown to be site of substantial residual reactive gliosis and **Type 1** and **Type 3** PAS-D staining, strongly indicating that activated astrocytes do not express PAFR.

Temporal changes in PAFR expression were confirmed by semi-quantitative RT-PCR of total RNA isolated from whole hippocampi 0, 4, 24, 72, and 168 hr after treatment (Figure 73). A reduction in PAFR mRNA could be observed 24 hr after kainate administration followed by an increase in signal intensity 72-168 hr after seizure induction. No signal was obtained when reactions were carried in the absence of RT indicating that alterations in PCR product intensities were not the result of DNA contamination (data not shown). Furthermore, GAPDH signal intensity was not altered across conditions indicating that equal amounts of mRNA were added to

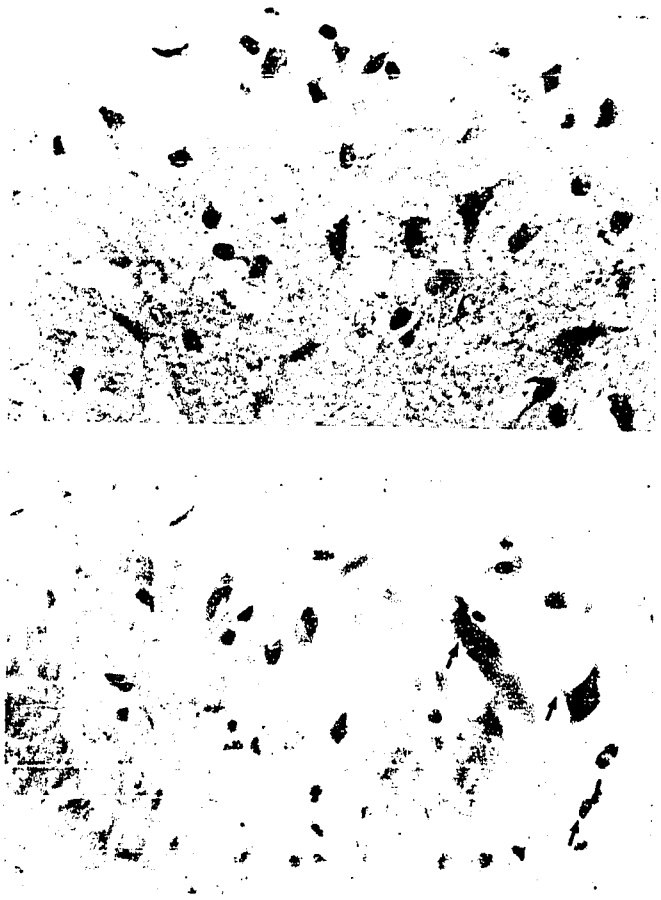

Figure 72. Relationship of seizure-induced changes in PAFR expression to PAS-D pathology

Representative photomicrographs of adjacent sections stained with cresyl violet and PAS-D or processed for *in situ* labelling of PAFR and hematoxylin and eosin counterstaining in rat brain hippocampus. (A), PAFR labelling of neurons in CA2 24 hr after kainate administration. (B) PAS-D accumulation and elaboration of aberrant processes (arrow) in neurons and microglia in the same region as (A) 7 days after treatment. Scale bar=50 μm.

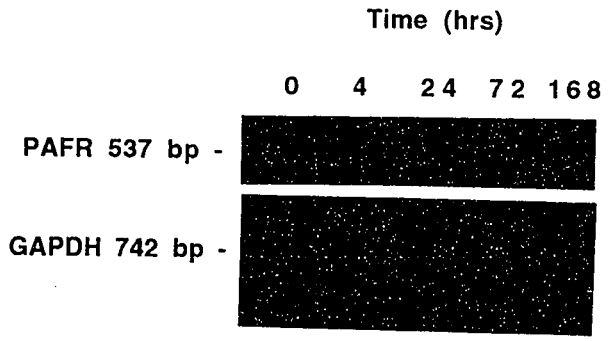

Figure 73. RT-PCR for PAFR in rat hippocampus following kainic acid (10 mg/kg) induced seizures

RT-PCR was performed on total RNA isolated from rat hippocampus 0, 4, 24, 72, and 168 hr after kainate injection as described in Materials and Methods.

each reaction.

Induction of ACD and clusterin gene expression: Relationship to PAFR expression

Epileptiform seizures elicit ACD in CA1 and CA3 pyramidal neurons of the hippocampal formation 72-168 hr after seizure initiation (50,57). Induction is preceded by long-lasting expression of the *fos* gene (50). The apoptotic process is most noticeable in CA3 neurons given that CA1 neurons have been depleted by necrotic changes during the acute phase of neurodegeneration. Similar results were observed in the present experiments. Nucleosome ladder formation was observed in DNA extracts 72 and 168 hr after seizure induction (data not shown). This time course paralleled the reappearance of FLI in CA1 and CA3 fields of the hippocampal formation (Figure 74 and Chapter VI, Section 2). In addition, neurons of CA1 and CA3 were the only cells to exhibit enhanced Ig immunoreactivity 169 hr after treatment. This observation suggests either that neuronally associated blood-borne material entering brain parenchyma during seizure-induced blood-brain barrier compromise had not been cleared or that the blood-brain barrier around regional capillaries was still damaged.

Expression of clusterin is upregulated during ACD presumably as a protective mechanism inhibiting complement-mediated lysis (24,48). Clusterin was originally identified in CNS as the sulfated glycoprotein-2 gene (SGP-2) whose expression was shown to be preferentially located in around Alzheimer's lesions (39). Subsequently, human gliomas and epileptic foci have been demonstrated to exhibit high levels of clusterin mRNA (13). In experimental models of brain damage, seizure activity has been shown to induce clusterin expression (48) in and around tissue undergoing ACD (14). In the present experiments, the temporal expression of clusterin was contrasted to PAFR expression in adjacent sections. Clusterin mRNA was shown to be expressed by untreated animals throughout the hippocampal formation (Figure 75A,B). The specificity of this response was confirmed by RNAse treatment of adjacent sections. Within the acute phase of neurodegeneration, clusterin expression was selectively upregulated in pyramidal cells of the CA2 and CA4 cell fields of the hippocampal formation and interneurons of the stratum radiatum (Figure 75C). This pattern corresponded with localization of PAFR expression. Within the chronic phase of neurodegeneration, substantial increase in clusterin mRNA levels were demonstrated in

Figure 74. FLI and blood-brain barrier breakdown in rat hippocampus 168 h following kainic acid (10 mg/kg)-induced seizures

Immunohistochemistry using an anti-*fos* antibody was performed on coronal rat brain sections 168 hr after kainate injection as described in Materials and Methods. Select enhancement was observed in CA1 and CA3 pyramidal neurons in the hippocampal formation. Data for CA3 is presented (A), Control (*fos* immunoreactivity). (B), 168 hr after kainate treatment (*fos* immunoreactivity). (C), neuronal accumulation of Igs 168 hr after kainate treatment. Scale bar=50 μm.

and around CA1 and CA4 neurons, within interneurons surrounding CA3, and within granule cells of the dentate gyrus, particularly those proximal to CA4 (Figure 75D). Again, this distribution exactly corresponded to the pattern of PAFR expression observed at the same time points. However, examination of counter-stained sections indicated that, unlike PAFR, expression, increases in clusterin mRNA were exclusively confined to neurons. No clusterin expressing microglia could be detected (data not shown).

These data permit speculation into the nature of the correspondence between PAFR and the observed neuropathology. PAF has been shown to elicit increases in the rate of cell death both directly (Chapter III and 5 and ref. (20)) in non-neuronal cells and indirectly by modulating excitatory amino acid transmission in neuronal cultures (3), suggesting that PAF may play a role in the accelerated cell death characteristic of chronic neurodegeneration. The increased PAFR expression observed in regions undergoing apoptosis provides circumstantial evidence to support this hypothesis. In addition, PAF may also influence immune recognition of apoptotic cells by inducing clusterin expression and thus circumventing complement mediated lysis of dying neurons by activated phagocytes (Chapter II, Section 4). Whether these putative effects contribute to chronic neurodegenerative disorders remains to be determined. Certainly, enhanced PAFR expression is associated with **Type 1** and **Type 4** PAS-D deposits characteristic of both epileptigenic lesions and senile dementias. This evidence suggests that PAF plays some role in the endogenous CNS inflammatory response to brain injury and may be associated with many of the aberrant processes seen in progressive neurodegenerative lesions including accelerated cell death, altered gene expression, and deposition of senile plaque materials. Further evaluation is required to elucidate the alleged contribution of PAF to chronic neurodegenerative disorders.

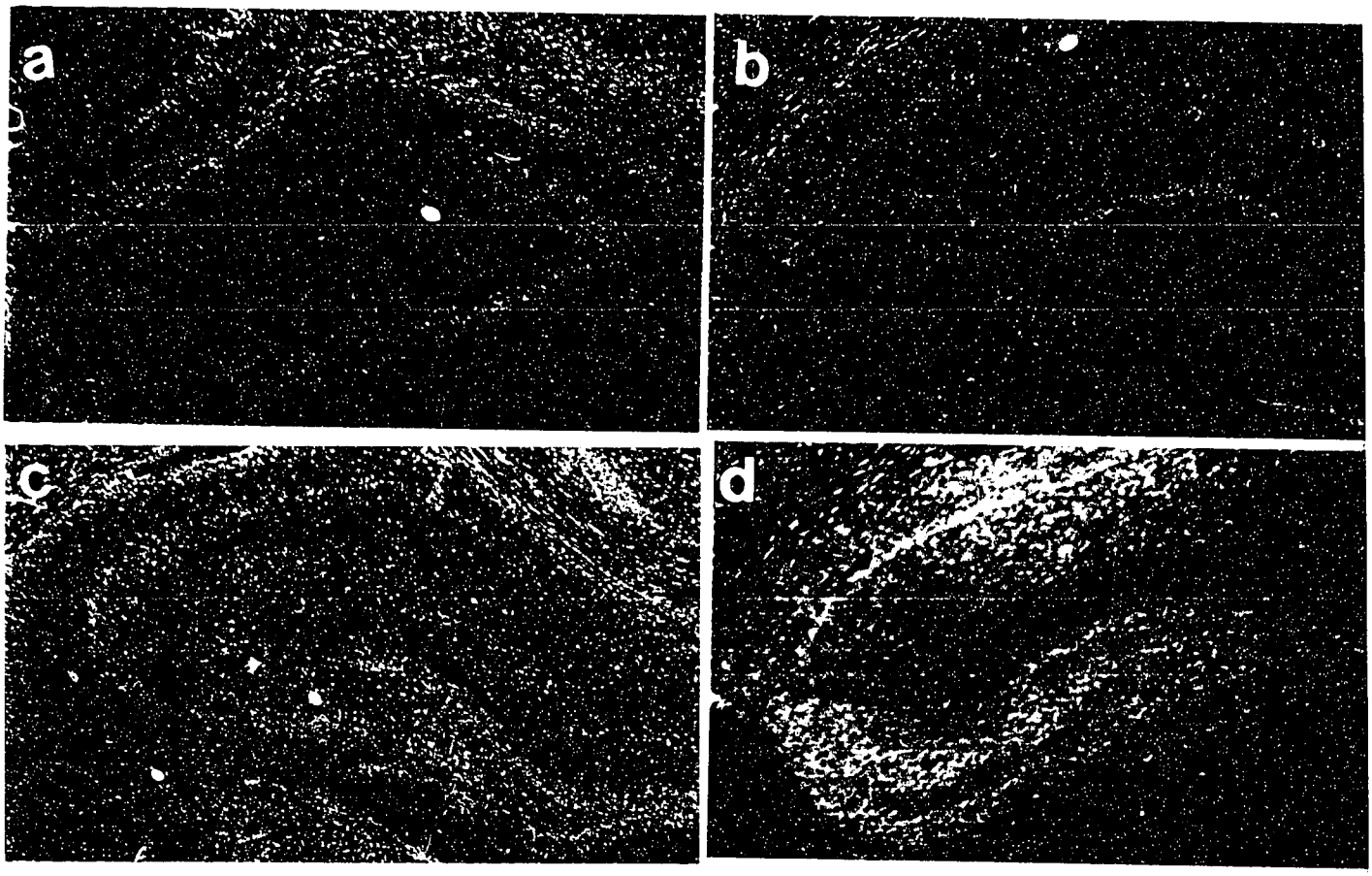

Figure 75. Pattern of clusterin expression in control and kainic acid (10 mg/ml)-treated subjects.

Representative photomicrographs of *in situ* hybridization for clusterin in rat brain hippocampus. Coronal sections (10 μm) were prepared as described in Materials and Methods. (A), RNAse-treated control section. (B), Control. (C), 24 hr after kainic acid treatment. (D), 168 hr after kainic acid treatment. (A) and (B) are adjacent sections. Control animals depicted were drug-naive subjects. The pattern of clusterin expression in these animals did not differ from that observed in saline-treated subjects (data not shown).

4. Overview

The data presented in 'Neurodegeneration' indicate that PAF may play a role in progressive neurodegenerative disorders. Although descriptive in nature, these studies demonstrate that the kainic acid model of myoclonic epilepsy can be used to investigate the relationship between PAF and accelerated cell death, reactive gliosis, blood-brain barrier breakdown, increased clusterin gene expression, and/or PAS-D deposition in senile plaques (see Chapter II, Section 4, Table 3).

The data indicate that temporal changes in PAFR expression following kainic acid-induced epileptiform seizures correspond to both the acute and chronic phases of neurodegeneration. Reductions in PAFR mRNA levels, presumably the result of prolonged receptor activation, were observed at the peak of the acute phase and corresponded exactly with the pattern of clusterin gene expression. These changes in PAFR mRNA localization also preceded the subsequent appearance of long-lasting PAS-D depositions (ie. **Type 1**-ECM accumulation and **Type 4**-neuronal labelling) during the chronic phase of neurodegeneration. PAFR expression was substantially increased during this later phase of neuropathology. The pattern of gene expression corresponded to induction of ACD in PAFR-expressing tissue, the appearance of chronic PAS-D **Type 1** and **Type 4** deposits, and significantly enhanced clusterin expression. Once again, clusterin mRNA was localized to identical brain regions as PAFR mRNA. At each time point, PAFR expression was demonstrated in neurons and some microglia but not astrocytes. These data raise the interesting possibility that stimulation of PAFR selectively mobilized neurons and microglia during the CNS immune/inflammatory response but does not activate astrocytes. Given the data presented in preceding chapters, it is tempting to speculate that PAF directly influences ACD and clusterin expression and contributes to the etiology of PAS-D lesions during epileptiform-induced neurodegeneration. This hypothesis requires further substantiation but does raise the exciting possibility that PAFR antagonists might be used to attenuate seizure-associated damage and/or retard progressive neurodegeneration.

VII

CONCLUSION

Summary

Do endogenous pro-inflammatory agents, specifically PAF, influence tumourigenesis and exacerbate progressive neurodegeneration? Tumours are the result of enhanced cell survival either through *increased* cell proliferation and/or *decreased* cell death. Progressive neurodegenerative disorders are characterized by *accelerated* cell death in the absence of compensatory increases in cell number. These disorders underline the fatal consequences of disrupting the dynamic balance between cell growth, cell differentiation, and cell death. Repeated exposure to pro-inflammatory mediators during chronic inflammatory conditions has been associated with an increased predisposition to malignant tumours as well as with the pathogenesis of the principal lesions characterizing Alzheimer's Disease and related disorders. This thesis describes a series of investigations designed to assess the potential contribution of the pro-inflammatory agent, PAF, to cell regulatory disorders affecting cell number. PAF's ability to perturb the rate of cell growth and/or the rate of cell death in non-inflammatory cells was evaluated *in vitro* using RECs, REC/*ras* cells, and HFs and *in vivo* using an experimental model of myoclonic epilepsy. These systems permitted an appraisal of PAF's effects within both rodent and human models of malignant transformation and chronic neurodegeneration. Four questions are discussed:

(1) Can PAF selectively mediate cell growth and cell death in non-inflammatory cells (Chapter 3: Transformation Potential)?

(2) What signal transduction pathways are responsible for PAF's effects in fibroblasts and epithelial cells (Chapter 4: Signal Transduction)?

(3) Can PAF elicit additional phenotypic alterations in cells already transformed (Chapter 5: Tumour Progression)?

(4) Is PAF implicated in the pathogenesis of chronic lesions in an *in vivo* model of progressive neurodegeneration (Chapter 6: Neurodegeneration)?

PAF's ability to mediate cell function under normal and pathophysiological conditions has been predominantly investigated in inflammatory cell types. Non-inflammatory cell responses to the ligand have only begun to be identified. Figure 77 summarizes the current literature. These studies demonstrate that fibroblasts, epithelial cells, neurons, and tumour cells are capable of responding to PAF in receptor-mediated fashion, synthesizing PAF, and, in the case of secretory epithelial cells, releasing the ligand into the extracellular milieu. Furthermore, other ligands, such as TNFα, are known to depend upon intracellular PAF as an essential signal transduction molecule. In tumour cells, many of PAF's effects are mediated by G-protein activation leading to calcium transients, respiratory burst, cytokine synthesis and release, intracellular PAF accumulation, tyrosine kinase activation, phosphorylation of PLC, phosphoinositide hydrolysis, and gene expression. Functional consequences include cell differentiation, cell death, and/or cell proliferation depending upon the individual cell type and environmental circumstances.

This thesis expands upon such research by demonstrating that PAF has the potential to induce sustained alterations in both the rate of cell growth *and* the rate of cell death depending upon endogenous environmental conditions and specific cellular capabilities. The data demonstrate that these effects are transient but long-lasting and can be observed up to 60-80 days after initial ligand exposure. There is no evidence to suggest that PAF is mutagenic or that PAF elicits heritable changes in target cell genome. Rather, the ligand appears to dose-dependently stimulate cell growth or cell death depending upon the duration of the ligand exposure and the presence or absence of exogenous growth factors. Brief stimulation (<1 hr) appears to activate a variety of signal transduction molecules in the absence of growth enhancement or cytotoxicity. These signalling agents include PAFR, PKC mobilization, phosphorylation of proteins on tyrosine residues, oxyradical production, and *de novo* gene expression of the proto-oncogene c-*fos* and the ACD-related gene clusterin. The results provided in this thesis represent the first such demonstration in normal fibroblasts, epithelial cells, and/or brain tissue. Transient stimulation (1-6 hr) elicits long-term growth enhancement (60-80 days). Phenotypic transformation includes increased focus formation, saturation density, autonomous cell growth (ie. growth in low serum), and AI growth. Long-term increases in cell growth in the absence of further ligand exposure appear to be mediated by increases in intracellular PAF concentrations that trigger the synthesis

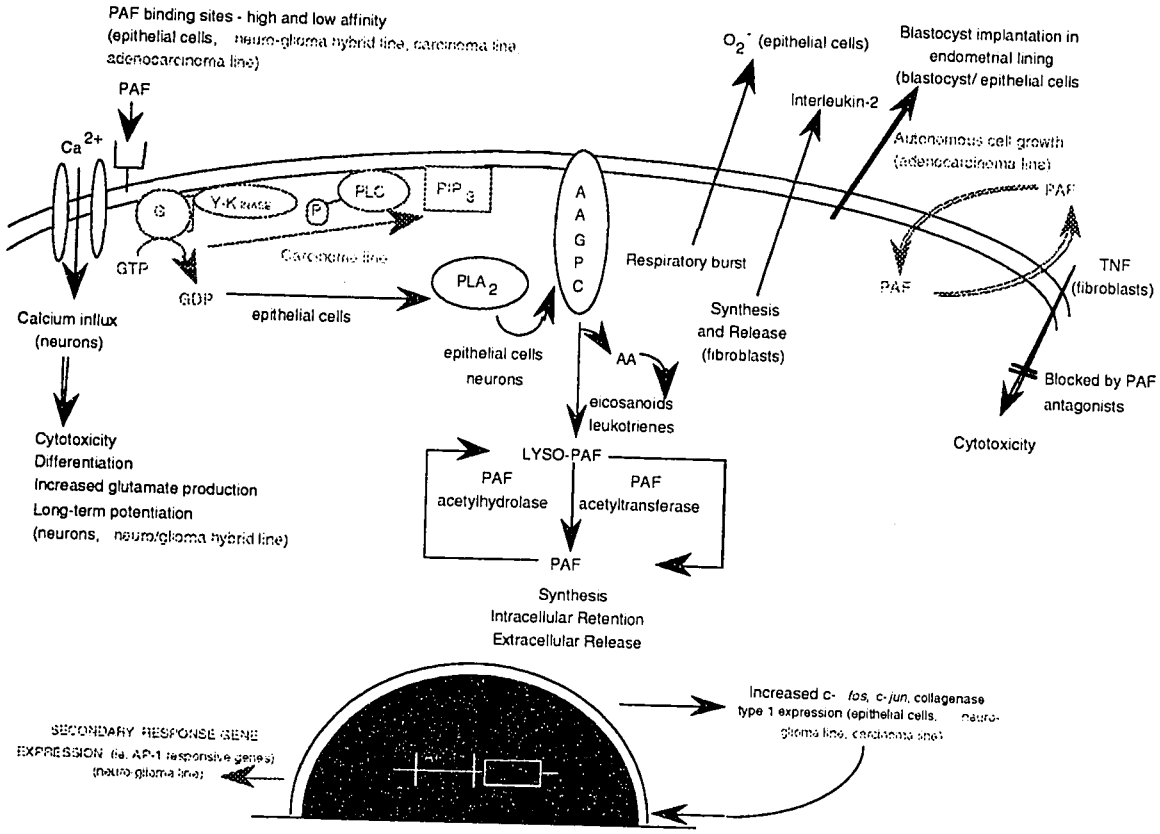

Figure 77. Functional consequences and underlying signal transduction mechanisms resulting from PAF stimulation of non-inflammatory cells

Schematic depicts cell membrane and nucleus. Cell type used to identify the mechanism depicted are illustrated in brackets. Double-lined arrows indicates functional consequences mediated by signal transduction molecules not yet elucidated. Black text/drawing depicts PAF-induced responses in normal cells. Grey text/drawing depicts PAF-induced responses in tumour cells. Abbreviations are as defined in Chapter 1. Drawing is based on references 1-21.

and release of mitogenic factors. Intracellular PAF levels are presumed to remain elevated and mitogenicity is sustained as the result of this autocrine feedback loop. Growth enhancement is accompanied by induction of clusterin and UPA gene expression. These gene products presumably facilitate escape from immune surveillance and extravasation of cells through the ECM. Species differences were noted between human and rodent cells in that HFs demonstrated increased cell proliferation only when cells were grown under suboptimal conditions and RECs exhibited enhanced cell growth under both optimal and suboptimal culture conditions. All of these effects appear to be mediated by PAFR and tyrosine kinase activity. In HFs, activation of PKC was required for growth enhancement. In RECs, PKC did not influence cell growth. None of the observed effects appeared to be mediated by cyclooxygenase metabolites of AA. Lastly, prolonged exposure (72 hr) to PAF dose-dependently elicits ACD in both RECs and HFs when cells are cultured in the absence of excess growth factors. Apoptosis was determined by changes in nuclear and cytoplasmic morphology and DNA analysis. Induction of ACD could be blocked by removing the ligand from the medium or by adding exogenous growth factors to PAF-treated cultures.

In *ras*-transformed cells, transient exposure (1 hr) to PAF elicited an ACD program in target cells followed by a period of prolonged growth enhancement in surviving cells when cultured under suboptimal conditions. In the presence of 10% FCS which supplies exogenous growth factors, 1 hr treatment with PAF initially induced reduced cell growth in lieu of cell death followed by enhanced cell proliferation in the absence of further ligand stimulation. These data suggest a role for $p21^{ras}$ in the PAF-induced apoptotic program but not in PAF-mediated mitogenicity given that RECs and REC/*ras* cells behaved identically 10-50 days after PAF treatment. One interpretation is that the presence of oncogenic *ras* sensitizes cells to undergo PAF-induced ACD since REC/*ras* undergo apoptosis after only brief exposure to the ligand while RECs require continued stimulation to maintain the apoptosis program. Despite this apparent separation in signalling mechanisms, both PAF-mediated increases in the rate of cell growth and the rate of cell death were dependent upon PAFR activation, phosphorylation of proteins on tyrosine residues, and the presences or absence of exogenous growth factors. These data suggest a possible role for PAF in both tumour regression and tumour progression.

Finally, data is presented to implicate PAF in the pathogenesis of neurodegenerative lesions characterized by PAS-D$^+$ depositions and accelerated cell death using a kainic acid model of myoclonic epilepsy. Neuropathology resulting from sustained epileptiform seizures can be divided into two phases: acute (0-24 hr after kainic acid administration) and chronic (3-7 days after kainate injection). The acute phase is characterized by necrosis, edema, profound reactive gliosis, blood-brain barrier breakdown, and accumulation of PAS-D$^+$ lesions around areas exhibiting extravasation of circulating proteins into brain parenchyma. At the height of this damage, PAFR expression is downregulated with residual expression restricted to brain regions demonstrating enhanced clusterin mRNA levels and predictive of areas destined to be spared from subsequent neuronal deterioration. Enhanced *fos* protein immunoreactivity at this early time point predicts (1) subsequent cell death, (2) neuronal accumulation of PAS-D$^+$ material, and (3) chronic expression of PAFR mRNA. At every time point, PAFR expression was confined to neurons and some microglia. Astrocytes did not express PAFR. The chronic phase of neuropathology is initiated 3-7 days after epileptiform seizure induction and lasts anywhere from 3 months to 1 year after injury. Damage is characterized by ACD in select brain regions, accumulation of chronic PAS-D$^+$ lesions, mild, residual gliosis, and restoration of blood-brain barrier integrity. PAFR expression is substantially upregulated during this period and is confined either to areas undergoing cell death in conjunction with increased clusterin gene expression or to areas exhibiting chronic PAS-D$^+$ lesions. Enhanced *fos* immunoreactivity and residual Ig immunoreactivity accompany this increase in PAFR mRNA levels.

A theoretical model, depicted in Figure 77, is proposed to interpret these data. Fibroblasts, epithelial cells, and neurons respond to extracellular PAF stimulation through activation of PAFR. Brief stimulation with PAF under normal physiological conditions (ie. half-life of 2-12 min) elicits signal transduction by stimulating tyrosine phosphorylation of proteins resulting in PKC activation, and transient gene expression (Figure 77, black line schematic). However, during an inflammatory response, cells are most likely chronically exposed to PAF. Subsequent responses depend upon the duration and dose of ligand exposure. Cells transiently exposed to high doses of PAF would undergo delayed growth enhancement. These effects are mediated by prolonged

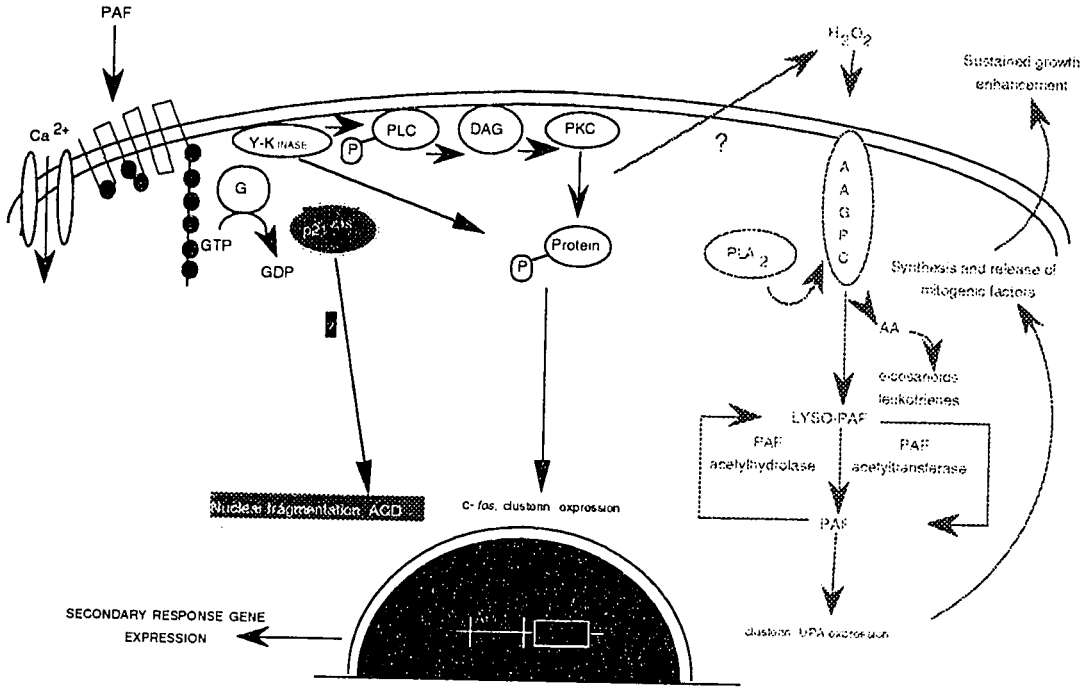

Figure 77. Functional consequences and underlying signal transduction mechanisms resulting from PAF stimulation of non-inflammatory cells

Schematic depicts cell membrane and nucleus. Black text/drawing depicts PAF-induced responses following brief stimulation (<1 hr). Grey text/drawing depicts PAF-induced responses following repeated, transient stimulation and/or chronic exposure to low doses of ligand. White on grey text/drawing depicts PAF-induced responses following chronic exposure to high doses of PAF. See text for further details. Abbreviations are as defined in Chapter 1.

signal transduction leading to exposure of PAF-treated cells to H_2O_2 (Figure 77, gray line schematic). Stimulation with both PAF and H_2O_2 leads to enhanced intracellular PAF synthesis that, in turn, triggers the synthesis and release of mitogenic factors. Intracellular PAF production sets up an autocrine feedback loop by which PAF levels remain elevated signalling sustained mitogenicity. These effects are accompanied by renewed clusterin gene expression and *de novo* UPA expression (Figure 77, gray line schematic). Induction of this loop can be prevented by (1) blocking extracellular PAF receptors during PAF exposure, (2) inhibiting tyrosine kinase (rodent and human cells) or PKC activity (human cells) during ligand stimulation, (3) preventing H_2O_2 accumulation in the presence of PAF, or (4) blocking putative intracellular PAF receptors upon removal of the ligand. Furthermore, cells continually exposed to low does of PAF would undergo enhanced cell proliferation through similar signal transduction mechanisms. This effect probably ensures that non-inflammatory cells, transiently exposed to PAF or chronically exposed to low doses of ligand, undergo sustained cell proliferation in order to facilitate wound healing during an inflammatory responses. Conversely, prolonged exposure to high doses of PAF elicits ACD. The duration of ligand exposure required to stimulate ACD can be abbreviated by introduction of oncogenic *ras* into cells strongly suggesting that PAF works through *ras* or through some common signal transduction pathway to elicit cell death (Figure 77, white on grey schematic). This pathway can be abrogated by administration of exogenous growth factors indicting that PAF is only capable of signalling ACD under sub-optimal growth conditions. Induction of ACD depends upon PAFR activation and phosphorylation of proteins on tyrosine residues. Thus, cells chronically exposed to high doses of inflammatory mediators (ie. at the core of inflamed tissue) are induced to die. Finally, during chronic inflammatory disorders, repeated exposure to PAF could contribute to (1) enhanced cell proliferation of cells within the potentially damaging inflammatory environment, (2) transient induction of a 'metastatic' phenotype in cells already transformed thus facilitating escape from immune surveillance (increased clusterin gene expression) and extravasation of cells through the ECM (increased UPA gene expression), and/or (3) stimulation of ACD.

Within the CNS, PAF appears to mediate cell death and cell differentiation. Since neurons are incapable of further replication, PAF-elicited ACD could contribute to the pathogenesis of

neurodegenerative disorders characterized by enhanced cell loss. This effect was investigated in an experimental model of myoclonic epilepsy. *In vivo*, PAFR levels are down-regulated following acute injury and at the height of the subsequent inflammatory response. This reduction could represent a protective response given that exacerbation of cerebral inflammation would lead to massive cell death. Cells that continue to express low levels of PAFR are also protected from later damage presumably by induction of clusterin gene expression. During the chronic phase of neurodegeneration, PAFR levels are substantially increased in and around areas undergoing either ACD or accumulation of PAS-D^+ lesions. These data indicate that PAF may participate in the exacerbation of neurodegenerative lesions and could play a role in inducing accelerated cell death during chronic cerebral inflammatory conditions.

In summary, the pro-inflammatory agent, PAF, is capable of disrupting the delicate balance between cell growth, cell death, and cell differentiation. In this manner, PAF may participate in tumour progression and contribute to progressive neurodegenerative disorders.

VIII

REFERENCES

Chapter II

1. Akiyama H, Ikeda K, Kondo H, Kato M, McGeer PL (1993) Microglia express the type 2 plasminogen activator inhibitor in the brain of control subjects and patients with Alzheimer's disease. Neurosci Lett 164: 233-235

2. Akiyama H, Nishimura T, Kondo H, Ikeda K, Hayashi Y, McGeer PL (1994) Expression of the receptor for macrophage colony stimulating factor by brain microglia and its upregulation in brains of patients with Alzheimer's disease and amyotrophic lateral sclerosis. Brain Res 639: 171-174

3. Alessi DR, Smythe C, Keyse SM (1993) The human CL100 gene encodes a Tyr/Thr-protein phosphatase which potently and specifically inactivates MAP kinase and suppresses its activation by oncogenic ras in Xenopus oocyte extracts. Oncogene 8: 2015-2020

4. Alexander-Williams J (1976) Inflammatory disease of the bowel. Dis Colon Rectum 19: 579-581

5. Altman J (1994) Microglia emerge from the fog. Trends Neurosci 17: 47-49

6. Altman LC, Ayars GH, Baker C, Luchtel DL (1993) Cytokines and eosinophil-derived cationic proteins upregulate intercellular adhesion molecule-1 on human nasal epithelial cells. J Allergy Clin Immunol 92: 527-536

7. Andrade SP, Vieira LBGB, Bakhle YS, Piper PJ (1994) Effect of platelet activating factor (PAF) on the formation of blood vessels in subcutaneous implants in mice. J Lipid Mediat 9: 117-121

8. Antonopoulou S, Demopoulos CA, Iatrou C, Moustakas G, Zirogiannis P (1994) Platelet-activating factor acetylhydrolase (PAF-AH) in human kidney. Int J Biochem 26: 1157-1162

9. Araki S, Tsuna I, Kaji K, Hayashi H (1994) Programmed cell death in response to alkyllysophospholipids in endothelial cells. J Biochem (Tokyo) 115: 245-247

10. Araujo DM, Lapchak PA (1994) Induction of immune system mediators in the hippocampal formation in Alzheimer's and Parkinson's diseases: Selective effects on specific interleukins and interleukin receptors. Neuroscience 61: 745-754

11. Argyris T, Slaga T (1981) Promotion of carcinomas by repeated abrasion in initiated skin of mouse. Cancer Res 41: 5193-5195

12. Arnould T, Michiels C, Remacle J (1993) Increased PMN adherence on endothelial cells after hypoxia: Involvement of PAF, CD18/CD11b, and ICAM-1. Am J Physiol Cell Physiol 264: C1102-C1110

13. Asmis R, Randriamampita C, Tsien RY, Dennis EA (1994) Intracellular Ca2+, inositol 1,4,5-trisphosphate and additional signalling in the stimulation by platelet-activating factor of prostaglandin E2 formation in P388D1 macrophage-like cells. Biochem J 298: 543-551

14. Au B, Collins PD, Williams TJ (1994) Role of PAF in zymosan-induced IL-8 release from human neutrophils. Agents Actions 41 Suppl C PT 2: C185-C187

15. Badawi AF, Mostafa MH, O'Connor PJ (1992) Involement of alkylating agents in schistosome-associated bladder cancer: the possible basic mechanism of induction. Cancer Lett 63: 171-188

16. Baldi E, Bonaccorsi L, Finetti G, Luconi M, Muratori M, Susini T, Forti G, Serio M, Maggi M (1994) Platelet-activating factor in human endometrium. J Steroid Biochem Mol Biol 49: 359-363

17. Barr RM, Judge M, Mallet AI, Kobza-Black A, Barlow R, Greaves MW (1994) Platelet activating factor (PAF) and lyso-PAF in inflamed human skin. Agents Actions 41 Suppl C PT 2: C260-C261

18. Barthelson RA (1993) Quantitation of IL-4 expression in small numbers of cells from mice. J Immunol Methods 161: 67-76

19. Bates EJ, Harvey DP, Ferrante A (1992) Inhibition of neutrophil respiratory burst and degranulation responses to platelet-activating factor by antagonists WEB 2086, CV 6209 and CV 3988. Int Arch Allergy Appl Immunol 97: 50-56

20. Bazan HEP, Tao Y, Bazan NG (1993) Platelet-activating factor induces collagenase expression in corneal epithelial cells. Proc Natl Acad Sci USA 90: 8678-8682

21. Bazan NG, Zorumski CF, Clark GD (1993) The activation of phospholipase A_2 and release of arachidonic acid and other lipid mediators at the synapse: The role of platelet-activating factor. J Lipid Mediat 6: 421-427

22. Benveniste J, Henson PM, Cochrane CG (1972) Leukocyte-dependent histamine release from rabbit platelets: The role of IgE, basophils, and platelet activating factor. J Exp Med 136: 1356-1377

23. Benveniste J, Tence M, Varenne P, Bidault J, Boullet C, Polonsky J (1979) Semi-synthese et stucture purposee du facteur activant les plaquettes (P.A.F.); PAF-acether, un alkyl ether analogue de la lysophosphatidylcholine. C R Acad Sci [D], (Paris) 289: 1037-1040

24. Berdel WE, Munder PG (1987) Antineoplastic actions of ether lipids related to platelet-activating factor. In: Snyder F (ed) Platelet-Activating Factor and Related Lipid Mediators. Plenum Press, New York, pp 449-468

25. Beusenberg FD, Bonta IL, Van Amsterdam JGC (1994) Cyclic-AMP level and eicosanoid release from alveolar macrophages are differentially affected by high and low dose of platelet activating factor. Biochem Pharmacol 47: 588-590

26. Bito H, Honda Z, Nakamura M, Shimizu T (1994) Cloning, expression and tissue distribution of rat platelet-activating-factor-receptor cDNA. Eur J Biochem 221: 211-218

27. Bittrich H, Matik AK, Kraker I, Appel KE (1993) NO_2-induced DNA single strand breaks are inhibited by antioxidative vitamins in V79 cells. Chem Biol Interact 86: 199-211

28. Blank ML, Snyder F, Byers LW, Brooks B, Muirhead EE (1979) Antihyertensive activty of an alkyl ether analog of phosphatidylcholine. Biochem Biophys Res Commun 90: 1194-1200

29. Bombara MP, Webb DL, Conrad P, Marlor CW, Sarr T, Ranges GE, Aune TM, Greve JM, Blue ML (1993) Cell contact between T cells and synovial fibroblasts causes induction of adhesion molecules and cytokines. J Leukocyte Biol 54: 399-406

30. Borth W (1992) a2-macroglobulin, a multifunctional binding protein with targeting characteristics. FASEB J 6: 3345-3353

31. Braquet P, Paubert-Braquet M, Koltai M, Bourgain R, Bussolino F, Hosford D (1989) Is there a case for PAF antagonists in the treatment of ischemic states? TIPS 10: 23-30

32. Braquet P, Pignol B, Maisonnet T, Mencia-Heurta J (1991) Platelet-activating factor modulates interleukin-2 production by mouse fibroblasts. Int Arch Appl Immunol 94: 165-166

33. Braquet P, Touqui L, Shen T, Vargaftig B (1987) Perspectives in platelet-activating research. Pharmacol Rev 39: 99-145

34. Brass LF, Woolkalis MJ, Manning DR (1988) . J Biol Chem 263: 5348-5355

35. See ref 57

36. Burgers JA, Akkerman J-WN (1993) Regulation of the receptor for platelet-activating factor on human platelets. Biochem J 291: 157-161

37. Busciglio J, Gabuzda DH, Matsudaira P, Yankner BA (1993) Generation of b-amyloid in the secretory pathway in neuronal and nonneuronal cells. Proc Natl Acad Sci USA 90: 2092-2096

38. Cabellos C, MacIntyre DE, Forrest M, Burroughs M, Prasad S, Tuomanen E (1992) Differing roles for platelet-activating factor during inflammation of the lung and subarachnoid space. The special case of *Streptococcus pneumoniae*. J Clin Invest 90: 612-618

39. Carpenter AF, Carpenter PW, Markesbery WR (1993) Morphometric analysis of microglia in Alzheimer's disease. J Neuropathol Exp Neurol 52: 601-608

40. Catalán RE, Martínez AM, Aragonés MD, Garde E, Díaz G (1993) Platelet-activating factor stimulates protein kinase C translocation in cerebral microvessels. Biochem Biophys Res Commun 192: 446-451

41. Catalán RE, Martínez AM, Aragonés MD, Garde E, Lombardía M, Ortega P (1993) PAF and thrombin actions in platelets are selectively affected by a new 1,4-dihydropyridine derivative. J Biochem (Tokyo) 113: 450-455

42. Cerutti P, Trump B (1991) Inflammation and oxidative stress in carcinogenesis. Cancer Cells 3: 1-7

43. Chang SW (1994) Endotoxin-induced pulmonary leukostasis in the rat: Role of platelet-activating factor and tumor necrosis factor. J Lab Clin Med 123: 65-72

44. Chao W, Liu H, Hanahan DJ, Olson MS (1992) Platelet-activating factor-stimulated protein tyrosine phosphorylation and eicosanoid synthesis in rat Kupffer cells. Evidence for calcium-dependent and protein kinase C-dependent and -independent pathways. J Biol Chem 267: 6725-6735

45. Chao W, Olson MS (1993) Platelet-activating factor: Receptors and signal transduction. Biochem J 292: 617-629

46. Chau L-Y, Hu C-Y, Chang W-T, Hsu Y-S (1992) Possible existence of two subsets of platelet-activating factor receptor to mediate polyphosphoinositide breakdown and calcium influx in neuroblastoma x glioma hybrid NG 108- 15 cells. J Neurochem 59: 1090-1098

47. Chen S-C, Redenius D, Young JC, Schwartz RC (1993) Synergy of IL-7 and v-Ha-*ras* in the *in vitro* neoplastic progression of murine pre-B cells. Oncogene 8: 2119-2125

48. Clark GD, Happel LT, Zorumski CF, Bazan NG (1992) Enhancement of hippocampal excitatory synaptic transmission by platelet-activating factor. Neuron 9: 1211-1216

49. Correa P (1992) Human gastric carcinogenesis: a multistep and multifactorial process - first American Cancer Society award lecture on cancer epidemiology and prevention. Cancer Res 52: 6735-6740

50. Coyle JT, Puttfarcken P (1993) Oxidative stress, glutamate, and neurodegenerative disorders. Science 262: 689-695

51. Creasia D, Netteshim P (1975) Particulates and chronic inflammation increase rates of carcinogenesis. In: Karbe E, Parke J (eds) Experimental Lung Cancer. Springer Verlag, New York, pp 234-235

52. Das KM, Squillante L, Robertson FM (1993) Amplified expression of intercellular adhesion molecule- 1 (ICAM-1) and M_R 40K protein by DLD-1 colon tumor cells by interferon-gamma. Cell Immunol 147: 215-221

53. Davis EJ, Foster TD, Thomas WE (1994) Cellular forms and functions of brain microglia. Brain Res Bull 34: 73-78

54. Delbridge LM, Stewart AG, Goulter CM, Morgan TO, Harris PJ (1994) Platelet-activating factor and WEB-2086 directly modulate rat cardiomyocyte contractility. J Mol Cell Cardiol 26: 185-193

55. Dell' Albani P, Condorelli DF, Mudò G, Amico C, Bindoni M, Belluardo N (1993) Platelet-activating factor and its methoxy-analogue ET-18- OCH3 stimulate immediate early gene expression in rat astroglial cultures. Neurochem Int 22: 567-574

56. Demopoulos CA, Pinkard RN, Hanahan DJ (1979) Platelet activating factor. Evidence for 1-O-alkyl-2-acetyl-sn-glyceryl-3-phosphorylcholine as the active component (a new class of lipid chemical mediators). J Biol Chem 254: 9355-9358

57. Denizot Y, Chaussade S (1994) Platelet activating factor and Crohn's disease. Gut 35: 141

58. Denizot Y, Nathan N (1993) Platelet-activating factor antagonists and infected cirrhosis. Gastroenterology 105: 1267

59. Dilon P, Fitzpatrick M, Ritre A, Durna W (1988) Effect of platelet-activating factor on leukocyte adherence to micorvascular endothelium. Inflammation 12: 563-573

60. Dippold W, Wittig B, Schwaeble W, Mayet W, Meyer zum Bueschenfelde KH (1993) Expression of intercellular adhesion molecule 1 (ICAM-1, CD54) in colonic epithelial cells. Gut 34: 1593-1597

60. Doeffier E, Borrel M, Lefort J, Chignard M, Brozuet C, Heyman F, Godfroid J, Vargaftig B (1986) Effects of PAF-acether and structural analogues on platelet activation and bronchoconstriction in guinea pigs. Eur J Pharmacol 131: 179-188

62. Domingo MT, Spinnewyn B, Chabrier PE, Braquet P (1994) Changes in [3H]PAF binding and PAF concentrations in gerbil brain after bilateral common carotid artery occlusion: A quantitative autoradiographic study. Brain Res 640: 268-276

63. Doussis-Anagnostopoulou I, Kaklamanis L, Cordell J, Jones M, Turley H, Pulford K, Simmons D, Mason D, Gatter K (1993) ICAM-3 expression on endothelium in lymphoid malignancy. Am J Pathol 143: 1040-1043

64. Dulioust A, Hilliquin P, Menkes C-J, Benveniste J, Arnoux B (1992) Paf-acether acethylhydrolase activity is increased in patients with rheumatic diseases. Scand J Rheumatol 21: 161-164

65. Eikelenboom P, Hack CE, Rozemuller JM, Stam FC (1989) Complement activation in amyloid plaques in Alzheimer's dementia. Virchows Arch Cell Pathol 56: 259-262

66. El Azzouzi B, Jurgens P, Benveniste J, Thomas Y (1993) Immunoregulatory functions of PAF-acether. IX. Modulation of apoptosis in an immature T cell line. Biochem Biophys Res Commun 190: 320-324

67. Eliakim R, Rachmilewitz D (1994) Platelet activating factor and Crohn's disease. Reply. Gut 35: 141

68. Elstad MR, Parker CJ, Cowley FS, Wilcox LA, McIntyre TM, Prescott SM, Zimmerman GA (1994) CD11b/CD18 integrin and a Beta-glucan receptor act in concert to induce the synthesis of platelet-activating factor by monocytes. J Immunol 152: 220-230

69. Ferraris L, Karmeli F, Eliakim R, Klein J, Fiocchi C, Rachmilewitz D (1993) Intestinal epithelial cells contribute to the enhanced generation of platelet activating factor in ulcerative colitis. Gut 34: 665-668

70. Ferrini S, Sforzini S, Cambiaggi A, Poggi A, Meazza R, Canevari S, Colnaghi MI, Moretta L (1994) The LFA-1/ICAM

cell adhesion pathway is involved in tumor-cell lysis mediated by bispecific monoclonal-antibody-targeted T lymphocytes. Int J Cancer 56: 846-852

71. Forloni G, Chiesa R, Smiroldo S, Verga L, Salmona M, Tagliavini F, Angeretti N (1993) Apoptosis mediated neurotoxicity induced by chronic application of b amyloid fragment 25-35. Neuroreport 4: 523-526

72. Frenkel K (1992) Carcinogen-mediated oxidant formation and oxidative DNA damage. Pharmacol Ther 53: 127-166

73. Fujiki H, Suganuma M (1994) Tumor necrosis factor-Alpha, a new tumor promoter, engendered by biochemical studies of okadaic acid. J Biochem (Tokyo) 115: 1-5

74. Gallin JI (1993) Inflammation. In: Paul WE (ed) Fundamental Immunology. Raven Press, New York, pp 1015-1032

75. Gardner CR, Laskin JD, Laskin DL (1993) Platelet-activating factor-induced calcium mobilization and oxidative metabolism in hepatic macrophages and endothelial cells. J Leukocyte Biol 53: 190-196

76. Gay JC (1993) Mechanism and regulation of neutrophil priming by platelet- activating factor. J Cell Physiol 156: 189-197

77. Gehrmann J, Banati RB, Kreutzberg GW (1993) Microglia in the immune surveillance of the brain: Human microglia constitutively express HLA-DR molecules. J Neuroimmunol 48: 189-198

78. Gelbard HA, Nottet HSLM, Swindells S, Jett M, Dzenko KA, Genis P, White R, Wang L, Choi Y-B, Zhang D, Lipton SA, Tourtellotte WW, Epstein LG, Gendelman HE (1994) Platelet-activating factor: a candidate human immunodeficiency virus type 1-induced neurotoxin. J Virol 68: 4628-4635

79. Gerard C, Gerard NP (1994) The pro-inflammatory seven-transmembrane segment receptors of the leukocyte. Curr Opin Immunol 6: 140-145

80. Gerard NP, Gerard C (1994) Receptor-dependent internalization of platelet-activating factor. J Immunol 152: 793-800

81. Giulian D, Li J, Leara B, Keenen C (1994) Phagocytic microglia release cytokines and cytotoxins that regulate the survival of astrocytes and neurons in culture. Neurochem Int 25: 227-233

82. Gomez-Cambronero J, Wang E, Johnson G, Huang C, Sha'afi R (1991) Platelet-activating factor induces tyrosine phosphorylation in human neutrophils. J Biol Chem 266: 6240-6245

83. Gordon LL, Weitzman S (1988) The respiratory burst and carinogenesis. In: Sbarra AJ, Strauss RR (eds) The Respiratory Burst and Its Physiological Significance. Plenum, New York, pp 277-298

84. Graham RM, Stephens CJ, Silvester W, Leong LLL, Sturm MJ, Taylor RR (1994) Plasma degradation of platelet-activating factor in severely ill patients with clinical sepsis. Crit Care Med 22: 204-212

85. Graham RM, Strahan ME, Norman KW, Watkins DN, Sturm MJ, Taylor RR (1994) Platelet and plasma platelet-activating factor in sepsis and myocardial infarction. J Lipid Mediat 9: 167-182

86. Griffin WST, Sheng JG, Gentleman SM, Graham DI, Mrak RE, Roberts GW (1994) Microglial interleukin-1Alpha expression in human head injury: Correlations with neuronal and neuritic Beta-amyloid precursor protein expression. Neurosci Lett 176: 133-136

87. Grigoriadis G, Lim WH, Stewart AG (1993) Importance of basal and agonist-stimulated intracellular calcium for superoxide anion generation in peritoneal macrophages. Cell Physiol Biochem 3: 117-126

88. Grigoriadis G, Stewart AG (1992) Albumin inhibits platelet-activating factor (PAF)-induced responses in platelets and

macrophages: Implications for the biologically active form of PAF. Br J Pharmacol 107: 73-77

89. Grupe R, Ziska T, Kertscher H-P (1993) New phospholipid-analogous PAF antagonists with mast cell (MC_1 degranulation-inhibiting properties. Agents Actions 38 Suppl. C PT 2: C224-C227

90. Guerrant RL, Fang GD, Thielman NM, Fonteles MC (1994) Role of platelet activating factor in the intestinal epithelial secretory and Chinese hamster ovary cell cytoskeletal responses to cholera toxin. Proc Natl Acad Sci USA 91: 9655-9658

91. Haga S, Ikeda K, Sato M, Ishii T (1993) Synthetic Alzheimer amyloid b/A4 peptides enhance production of complement C3 component by cultured microglial cells. Brain Res 601: 88-94

92. Haglind E, Xia G, Rylander R (1994) Effects of antioxidants and PAF receptor antagonist in intestinal shock in the rat. Circ Shock 42: 83-91

93. Harper MJK, Kudolo G, Alecozay A, Jones M (1989) Platelet-activating factor (PAF) and blastocyst-endometrial interactions. In: Development of Preimplantation Embryos and their Environment. Alan Liss, New York, pp 305-315

94. Haswell-Elkins MR, Satarug S, Elkins DB (1992) *Opisthorchis viverrini* infection in northeast Thailand and its relationship to cholangiocarcinoma. J Gastro Hepatol 7: 538-548

95. Hattori M, Adachi H, Tsujimoto M, Arai H, Inoue K (1994) Miller-Dieker lissencephaly gene encodes a subunit of brain platelet-activating factor acetylhydrolases. Nature 370: 216-218

96. Hattori M, Arai H, Inoue K (1993) Purification and characterization of bovine brain platelet- activating factor acetylhydrolase. J Biol Chem 268: 18748-18753

97. Herbert J-M (1992) Characterization of specific binding sites of ^{3}H-labelled platelet-activating factor ([^{3}H]PAF) and a new antagonist, [^{3}H]SR 27417, on guinea-pig tracheal epithelial cells. Biochem J 284: 201-206

98. Herbert JM, Fraisse L, Bachy A, Valette G, Savi P, Laplace MC, Lassalle J, Roche B, Lale A, Keane PE, Maffrand JP (1993) Biochemical and pharmacological properties of SR 27388, a dual antioxidant and PAF receptor antagonist. J Lipid Mediat 8: 31-51

99. Herbert JM, Laplace M-C, Cailleau C, Maffrand JP (1993) Effect of SR 27417 on the binding of [^{3}H]PAF to rabbit and human platelets and human polymorphonuclear leukocytes. J Lipid Mediat 7: 57-78

100. Hirafuji M, Shinoda H (1993) Roles of prostacyclin, EDRF and active oxygens in leukocyte- dependent platelet adhesion to endothelial cells induced by platelet-activating factor *in vitro*. Br J Pharmacol 109: 524-529

101. Hirashima Y, Endo S, Ohmori T, Kato R, Takaku A (1994) Platelet-activating factor (PAF) concentration and PAF acetylhydrolas activity in cerebrospinal fluid of patients with subarachnoid hemorrhage. J Neurosurg 80: 31-36

102. Honda Z, Nakamura M, Miki I, Minami M, Watanabe T, Seyma Y, Okado H, Toh H, Ito K, Miyamoto M, Shimizu T (1991) Cloning by functional expression of platelet-activating factor receptor from guinea-pig lung. Nature 349: 342-345

103. Honda Z, Takano T, Gotoh Y, Nishida E, Ito K, Shimizu T (1994) Transfected platelet-activating factor receptor activates mitogen-activated protein (MAP) kinase and MAP kinase kinase in Chinese hamster ovary cells. J Biol Chem 269: 2307-2315

104. Hsieh K-H, Ng C-K (1993) Increased plasma platelet-activating factor in children with acute asthmatic attacks and decreased in vivo and in vitro production of platelet-activating factor after immunotherapy. J Allergy Clin Immunol 91: 650-657

105. Hu S, Martella A, Anderson WR, Chao CC (1994) Role of cytokines in lipopolysaccharide-induced functional and structural abnormalities of astrocytes. Glia 10: 227-234

106. Humpel C, Lippoldt A, Chadi G, Ganten D, Olson L, Fuxe K (1993) Fast and widespread increase of basic fibroblast growth factor messenger RNA and protein in the forebrain after kainate-induced seizures. Neuroscience 57: 913-922

107. Hunyadi J, Kenderessy AS, Duda E, Braquet P, Dobozy A (1993) Platelet-activating factor antagonists (BN 52021 and BN 50730) inhibit tumor necrosis factor-alfa-mediated cytotoxicity on murine L929 tumor cells. Mol Immunol 30: 517-519

108. Hurta RAR, Greenberg AH, Wright JA (1993) Transforming growth factor b1 selectively regulates ornithine decarboxylase gene expression in malignant H-*ras* transformed fibrosarcoma cell lines. J Cell Physiol 156: 272-279

109. Hwang S-B, Lam M-H, Pong S-S (1986) . J Biol Chem 261: 532-537

110. Ishii T, Haga S, Yagaishita S, Tareishi J (1984) The presence of complement in amyloid plaques of Creutzfeldt-Jakob disease and Gerstmann-Straussler-Scheinker disease. Appl Pathol 2: 370-379

111. Isola VJ, Hartman TC, Trumble SJ, Ruzek MC, Gentile JM (1993) Metabolism of 2-aminofluorene by human polymorphonuclear leukocytes: More evidence for the association between inflammation and cancer. Environ Health Perspect 101 Suppl 3: 27-31

112. Issekutz TB (1993) Dual inhibition of VLA-4 and LFA-1 maximally inhibits cutaneous delayed-type hypersensitivity-induced inflammation. Am J Pathol 143: 1286-1293

113. Ito Y, Sugatani J, Miki H, Uyama M, Saito K (1993) Corneal PAF acetylhydrolase increases in anterior segment ischemia in rabbits. Exp Eye Res 57: 107-115

114. Jamil KMA, Takano T, Nakao A, Honda Z, Shimizu T, Watanabe T, Kurokawa K (1992) Expression of platelet activating factor receptor in renal tubular cell line (LLC-PK1). Biochem Biophys Res Commun 187: 767-772

115. Janzer RC, Raff MC (1987) Astrocytes induce blood-brain barrier properties in endothelial cell. Nature 325: 253-257

116. Jeanneton O, Delvaux M, Botella A, Frexinos J, Bueno L (1994) Homologous desensitization of PAF receptors via a PGE2-dependent pathway on intestinal smooth muscle. J Lipid Mediat 10: 331-344

117. Johnson SA, Lampert-Etchells M, Pasinetti GM, Rozovsky I, Finch CE (1992) Complement mRNA in the mammalian brain: Responses to Alzheimer's disease and experimental brain lesioning. Neurobiol Aging 13: 642-648

118. Jomary C, Neal MJ, Jones SE (1993) Comparison of clusterin gene expression in normal and dystrophic human retinas. Mol Brain Res 20: 279-284

119. Juncos LA, Ren Y, Arima S, Ito S (1993) Vasodilator and constrictor actions of platelet-activating factor in the isolated microperfused afferent arteriole of the rabbit kidney. Role of endothelium-derived relaxing factor/nitric oxide and cyclooxygenase products. J Clin Invest 91: 1374-1379

120. Kageshita T, Yoshii A, Kimura T, Kuriya N, Ono T, Tsujisaki M, Imai K, Ferrone S (1993) Clinical relevance of ICAM-1 expression in primary lesions and serum of patients with malignant melanoma. Cancer Res 53: 4927-4932

121. Kalaria RN (1993) The immunopathology of Alzheimer's disease and some related disorders. Pathology 13367: 12336-13105

122. Kalaria RN, Galloway PG, Perry G (1991) Widespread amyloid P component immunoreactivity in cortical amyloid plaques of Alzheimer's disease and other degenerative disorders. Neuropathol Appl Neurobiol 17: 189-201

123. Kane DJ, Sarafian TA, Anton R, Hahn H, Gralla EB, Valentine JS, oerd T, Bredesen DE (1993) Bcl-2 inhibition of neural death: Decreased generation of reactive oxygen species. Science 262: 1274-1277

124. Kato K, Clark GD, Bazan NG, Zorumski CF (1994) Platelet-activating factor as a potential retrograde messenger in CA1 hippocampal long-term potentiation. Nature 367: 175-179

125. Kato M, Tokuyama K, Morikawa A, Kuroume T, Barnes PJ (1993) Platelet-activating factor-induced enhancement of superoxide anion generation in guinea-pigs. Eur J Pharmacol 232: 7-12

126. Koh J, Yang LL, Cotman CW (1990) b-Amyloid protein increases the vulnerability of cultured cortical neurons to excitotoxic damage. Brain Res 533: 315-320

127. Kornecki E, Ehrlich YH (1988) Neuroregulatory and neuropathological actions of the ether-phospholipid platelet activating factor. Science 240: 1792-1794

128. Korth R, Bidault J, Palmantier R, Benveniste J, Ninio E (1993) Human platelets release a Paf-acether: Acetylhydrolase similar to that in plasma. Lipids 28: 193-199

129. Kretzschmar HA (1993) Neuropathology of human prion diseases (spongiform encephalopathies). Dev Biol Stand 80: 71-90

130. Kubes P (1993) Polymorphonuclear leukocyte - endothelium interactions: A role for pro-inflammatory and anti-inflammatory molecules. Can J Physiol Pharmacol 71: 88-97

131. Kunievsky B, Yavin E (1992) Platelet-activating factor stimulates arachidonic acid release and enhances thromboxane B_2 production in intact fetal rat brain ex *vivo*. J Pharmacol Exp Ther 263: 562-568

131b. Kunitake ST, Moser AH, Doerrier WT, Rapp JT, Gruenfeld C, Feingold KR (1994) Endotoxin and cytokines increase hepatic messenger RNA levels and serum concentrations of apolipoprotein J (clusterin) in Syrian hamsters. J Clin Invest 94: 1304-1209

132. Kunz D, Gerard NP, Gerard C (1992) The human leukocyte platelet-activating factor receptor. cDNA cloning, cell surface expression, and construction of a novel epitope-bearing analog. J Biol Chem 267: 9101-9106

133. Lepage N, Miron P, Hemmings R, Roberts KD, Langlais J (1993) Distribution of lysophospholipids and metabolism of platelet- activating factor in human follicular and peritoneal fluids. J Reprod Fertil 98: 349-356

134. Levistre R, Masliah J, Bereziat G (1993) Stimulatory and inhibitory guanine-nucleotide-binding regulatory protein involvement in stimulation of arachidonic-acid release by N-formyl-methionyl-leucyl-phenylalanine and platelet-activating factor from guinea-pig alveolar macrophages-- Differential receptor/G-protein interaction assessed by pertussis and cholera toxins. Eur J Biochem 213: 295-303

135. Lianos EA, Zanglis A (1992) Effects of complement activation on platelet-activating factor and eicosanoid synthesis in rat mesangial cells. J Lab Clin Med 120: 459-464

136. Lindsley HB, Smith DD, Cohick CB, Koch AE, Davis LS (1993) Proinflammatory cytokines enhance human synoviocyte expression of functional intercellular adhesion molecule-1 (ICAM-1). Clin Immunol Immunopathol 68: 311-320

137. Lohman IC, Halonen M (1993) The effects of combined histamine and platelet-activating factor antagonism on systemic anaphylaxis induced by immunoglobulin E in the rabbit. Am Rev Respir Dis 147: 1223-1228

138. Lohmeyer M, McNaughton L, Hunt SP, Workman P (1994) Stimulation of intracellular free calcium increases by platelet-activating factor in HT29 colon carcinoma cells. Spectrofluorimetric and preliminary spatio-temporal analysis using confocal laser scanning fluorescence imaging microscopy. Biochem Pharmacol 47: 975-985

139. Lue L-F, Rogers J (1992) Full complement activation fails in difuse plaques of the Alzheimer's disease cerebellum. Dementia 3: 308-313

140. Lustig HS, Chan J, Greenberg DA (1992) Comparative neurotoxic potential of glutamate, endothelins, and platelet-activating factor in cerebral cortical cultures. Neurosci Lett 139: 15-18

141. Maat-Schieman MLC, Rozemuller AJ, Van Duinen SG, Haan J, Eikelenboom P, Roos RAC (1994) Microglia in diffuse plaques in hereditary cerebral hemorrhage with amyloidosis (Dutch). An immunohistochemical study. J Neuropathol Exp Neurol 53: 483-491

142. Mabuchi K, Sugiura T, Ojima-Uchiyama A, Masuzawa Y, Waku K (1992) Differential effects of platelet-activating factor on superoxide anion production in human eosinophils and neutrophils. Biochem Int 26: 1105-1113

143. Maggi M, Bonaccorsi L, Finetti G, Carloni V, Muratori M, Laffi G, Forti G, Serio M, Baldi E (1994) Platelet-activating factor mediates an autocrine proliferative loop in the endometrial adenocarcinoma cell line HEC-1A. Cancer Res 54: 4777-4784

144. Mallat M, Chamak B (1994) Brain macrophages: Neurotoxic or neurotrophic effector cells? J Leukocyte Biol 56: 416-422

145. Mangino MJ, Murphy MK, Weiss A, Anderson CB (1993) Characterization of platelet-activating factor receptors on canine T lymphocytes. J Immunol 151: 5310-5318

146. Marcheselli VL, Bazan NG (1994) Platelet-activating factor is a messenger in the electroconvulsive shock-induced transcriptional activation of c-fos and zif-268 in hippocampus. J Neurosci Res 37: 54-61

147. Matsuzaki M, Ishiguro Y, Tetsumoto T, Tsukada Y, Kayahara H, Tadasa K (1992) PAF acetylhydrolase activities in human systemic lupus erythematosus and lupus-prone mice. Clin Chim Acta 210: 139-144

148. May PC, Lambert-Etchells M, Johnson SA, Poirier J, Masters JN, Finch CE (1990) Dynamics of gene expression for a hippocampal glycoprotein elevated in Alzheimer's disease and in response to experimental lesion in rat. Neuron 5: 831-839

149. Mazer BD, Domenico J, Szepesi A, Lucas JJ, Gelfand EW (1994) Role for Ca2+ in expression of cell cycle regulated genes in PAF-stimulated cells. J Lipid Mediat 10: 269-281

150. McCafferty D-M, Kubes P, Wallace JL (1993) Inhibition of platelet-activating factor-induced leukocyte adhesion in vivo by a leumedin. Eur J Pharmacol 232: 169-172

151. McGeer PL, Akiyama H, Itagaki S, McGeer EG (1989) Immune system response in Alzheimer's Disease. Can J Neurol Sci 16: 516-527

152. McManus LM, Woodard DS, Deavers SI, Pinckard RN (1993) PAF molecular heterogeneity: Pathobiological implications. Lab Invest 69: 639-650

153. McNeill TH, Masters JN, Finch CE (1991) Effect of adrenalectomy on neuron loss and distribution of sulfated glycoprotein-2 in the dentate gyrus of prepubertal rats. Exp Neurol 111: 140-144

154. Miles DW, Happerfield LC, Naylor MS, Bobrow LG, Rubens RD, Balkwill FR (1994) Expression of tumour necrosis factor (TNFAlpha) and its receptors in benign and malignant breast tissue. Int J Cancer 56: 777-782

155. Milhoan KA, Lane TA, Bloor CM (1992) Hypoxia induces endothelial cells to increase their adherence for neutrophils: Role of PAF. Am J Physiol Heart Circ Physiol 263: H956-H962

156. Mitchell J, Sundstrom LE, Wheal HV (1993) Microglial and astrocytic cell responses in the rat hippocampus after an intracerebroventricular kainic acid injection. Exp Neurol 121: 224-230

157. Miyagawa H, Nabe M, Hopp RJ, Okada C, Bewtra AK, Townley G (1992) The effect of WEB 2086 on PAF-induced eosinophil chemotaxis and LTC_4 production from eosinophils. Agents Actions 37: 39-43

158. Mogi M, Harada M, Riederer P, Narabayashi H, Fujita K, Nagatsu T (1994) Tumor necrosis factor-Alpha (TNF-Alpha) increases both in the brain and in the cerebrospinal fluid from parkinsonian patients. Neurosci Lett 165: 208-210

159. Montero A, Rodriguez-Barbero A, Lopez-Novoa JM (1993) A role for platelet-activating factor in endothelin-1-induced rat mesangial cell proliferation. Eur J Pharmacol 243: 235-240

160. Morimoto H, Principe P, Robin J-P, Broquet C, Mencia-Huerta JM, Braquet P, Bonavida B (1993) Cytotoxic properties of a new synthetic demethylpodophyllotoxin derivative, BN 58705, against human tumor cell lines. Cancer Chemother Pharmacol 32: 293-300

161. Muehlematter D, Larson R, Cerutti P (1981) Active oxygen induced DNA strand breakage and polyADP-ribosylation in promotable and non-promotable JB6 mouse epidermal cells. Carcinogenesis 9: 239-245

162. Muirhead EE, Leach BE, Byers LW, Brooks B (1976) Enhanced potency of depressor renomedullary lipid. Circulation 54: II-175

163. Mutoh H, Bito H, Minami M, Nakamura M, Honda Z, Izumi T, Nakata R, Kurachi Y, Terano A, Shimizu T (1993) Two different promoters direct expression of two distinct forms of mRNAs of human platelet-activating factor receptor. FEBS Lett 322: 129-134

164. Nakamura M, Honda Z, Matsumoto T, Noma M, Shimizu T (1993) Isolation and properties of platelet-activating factor receptor cDNAs. J Lipid Mediat 6: 163-168

165. Narahara H, Frenkel RA, Johnston JM (1993) Secretion of platelet-activating factor acetylhydrolase following phorbol ester-stimulated differentiation of HL- 60 cells. Arch Biochem Biophys 301: 275-281

166. Narahara H, Johnston JM (1993) Effects of endotoxins and cytokines on the secretion of platelet-activating factor-acetylhydrolase by human decidual macrophages. Am J Obstet Gynecol 169: 531-537

167. Nathan C (1992) Nitric oxide as a secretory product of mammalian cells. FASEB J 6: 3051-3064

168. Nguyen T, Brunson CL, Crespi CL, Penman BW, Wishnok JS, Tannenbaum SR (1992) DNA damage and mutation in human cells exposed to nitric oxide in vitro. Proc Natl Acad Sci USA 89: 3030-3034

169. Ninio E, Maiza H, Bidault J (1993) Autocrine amplification of PAF-acether formation in immunologically activated murine macrophages. J Leukocyte Biol 54: 296-299

170. Nomura Y, Kitamura Y (1993) Inducible nitric oxide synthase in glial cells. Neurosci Res 18: 103-107

171. O'Flaherty J, Redman J, Jacobson D, Rossi A (1990) Stimulation and priming of protein kinase C translocation by a Ca2+ transient-independent mechanism. J Biochem 265: 21619-21623

172. O'Flaherty JT, Jacobson DP, Redman JF (1992) Regulation of platelet-activating-factor receptors and the desensitization response in polymorphonuclear neutrophils. Biochem J 288: 241-248

173. O'Flaherty JT, Tessner T, Greene D, Redman JR, Wykle RL (1994) Comparison of 1-O-alkyl-, 1-O-alk-1'-enyl-, and 1-O-acyl-2-acetyl-sn- lycero-3-phosphoethanolamines and -3-phosphocholines as agonists of the platelet-activating factor family. Biochim Biophys Acta Lipids Lipid Metab 1210: 209-216

174. Ochi T, Cerutti P (1987) Clastogenic action of hydroperoxy--5,8,11,13-icosatetraenoic acids on the mouse embryo fibroblast C3H/10T1/2. Proc Natl Acad Sci USA 84: 990-994

175. Ohshima H, Bartsch H (1994) Chronic infections and inflammatory processes as cancer risk factors: Possible role of nitric oxide in carcinogenesis. Mutat Res Fundam Mol Mech Mutagen 305: 253-264

176. Okada C, Hopp RJ, Miyagawa H, Sugiyama H, Nair NM, Bewtra AK, Townley RG (1992) Effect of terfenadine on neutrophil and eosinophil chemotactic activities after inhalation of platelet-activating factor in vivo and on neutrophil chemotaxis in vitro. Int Arch Allergy Appl Immunol 97: 181-186

177. Olson NC, Kruse-Elliott KT, Whorton AR, Dodam JR (1993) Pertussis toxin attenuates platelet-activating factor-induced pulmonary hemodynamic alterations in pigs. Am J Physiol Lung Cell Mol Physiol 264: L213-L221

178. Parks JE, Hough SR (1993) Platelet-activating factor acetylhydrolase activity in bovine seminal plasma. J Androl 14: 335-339

179. Patrizio M, Levi G (1994) Glutamate production by cultured microglia: Differences between rat and mouse, enhancement by lipopolysaccharide and lack effect of HIV coat protein gp120 and depolarizing agents. Neurosci Lett 178: 184-188

180. Pellon MI, Fernandez-Gallardo S, Gijon MA, Garcia MC, Liu F-T, Sanchez Crespo M (1993) Effect of immunological stimulation on the production of platelet-activating factor by rat peritoneal cells: Its relevance to anaphylactic reactions. Immunopharmacology 26: 73-82

181. Phenekos C, Siafaka-Kapadai A, Trapali M, Botitsi E, Mavris M (1992) Effect of gliclazide on platelet-activating factor-induced platelet aggregation in patients with non-insulin-dependent diabetes mellitus. Metabolism 41 Suppl. 1: 30-32

182. Piani D, Frei K, Pfister HW, Fontana A (1993) Glutamate uptake by astrocytes is inhibited by reactive oxygen intermediates but not by other macrophage-derived molecules including cytokines, leukotrienes or platelet-activating factor. J Neuroimmunol 48: 99-104

183. Polihronis M, Paizis K, Carter G, Sedal L, Murphy B (1993) Elevation of human cerebrospinal fluid clusterin concentration is associated with acute neuropathology. J Neurological Sci 115: 230-233

184. Powell DW (1992) Epithelial secretory responses to inflammation: Platelet activating factor and reactive oxygen metabolites. Ann NY Acad Sci 664: 232-247

185. Preston-Martin S, Pike SC, Ross RK, Jones PA, Henderson BE (1990) Increased cell division as a cause of human cancers. Cancer Res 50: 7415-7421

186. Principe P, Sidoti C, Braquet P (1992) Tumor cell kinetics following antineoplastic ether phospholipid treatment. Cancer Res 52: 2509-2515

187. Rabinovici R, Yeh CG, Hillegass LM, Griswold DE, DiMartino MJ, Vernick J, Fong K-LL, Feuerstein G (1992) Role of complement in endotoxin/platelet-activating factor- induced lung injury. J Immunol 149: 1744-1750

188. Rediske JJ, Quintavalla JC, Haston WO, Morrissey MM, Seligman B (1992) Platelet activating factor stimulates intracellular calcium transients in human neutrophils: Involvement of endogenous 5-lipoxygenase products. J Leukocyte Biol 51: 484-489

189. Rogers J, Cooper NR, Webester S, Schultz J, McGeer PL, Styren SD, Civin WH, Brachova L, Bradt B, Ward P, Lieberburg I (1992) Complement activation by b amyloid in Alzheimer's disease. Proc Natl Acad Sci USA 89: 10016-10020

190. Rola-Pleszczynski M, Thivierge M, Gagnon N, Lacasse C, Stankova J (1993) Differential regulation of cytokine and cytokine receptor genes by PAF, LTB4 and PGE2. J Lipid Mediat 6: 175-181

191. Rosin MP, Anwar WA, Ward AJ (1994) Inflammation, chromosomal instability, and cancer: The schistosomiasis model. Cancer Res 54 Suppl: 1929s-1933s

192. Rosin MP, Saad El Din Zaki S, Ward AJ, Anwar WA (1994) Involvement of inflammatory reactions and elevated cell proliferation in the development of bladder cancer in schistosomiasis patients. Mutat Res Fundam Mol Mech Mutagen 305: 283-292

193. Rossi AG, Norman KE, Donigi-Gale D, Shoupe TS, Edwards R, Williams TJ (1992) The role of complement, platelet-activating factor and leukotriene B4 in a reversed passive Arthus reaction. Br J Pharmacol 107: 44-49

194. Rothlein R, Mainolfi EA, Kishimoto TK (1993) Treatment of inflammation with anti-ICAM-1. Res Immunol 144: 735-739

195. Sasaki A, Hirato J, Nakazato Y (1993) Immunohistochemical study of microglia in the Creutzfeldt- Jakob diseased brain. Acta Neuropathol 86: 337-344

196. Satoh K, Yoshida H, Imaizumi T, Takamatsu S, Mizuno S (1992) Platelet-activating factor acetylhydrolase in plasma lipoproteins from patients with ischemic stroke. Stroke 23: 1090-1092

197. Schuermann GM, Aber-Bishop AE, Facer P, Lee JC, Rampton DS, Dore CJ, Polak JM (1993) Altered expression of cell adhesion molecules in uninvolved gut in inflammatory bowel disease. Clin Exp Immunol 94: 341-347

198. Schumacher U, Kretzschmar H, Pfueller U (1994) Staining of cerebral amyloid plaque glycoproteins in patients with Alzheimer's disease with the microglia-specific lectin from mistletoe. Acta Neuropathol 87: 422-424

199. Schwinger RHG, Böhm M, La Rosée K, Erdmann E (1992) Existence of PAF receptors in human platelets and human lung tissue but not in the human myocardium. Am Heart J 124: 320-330

200. Shacter E, Beecham EJ, Covey JM, Kohn KW, Potter M (1988) Activated neutrophils induce prolonged DNA damage in neighbouring cells. Carcinogenesis 9: 2297-2304

201. Shea TB, Beermann ML, Honda T, Nixon RA (1994) Secretion of amyloid precursor protein and laminin by cultured astrocytes is influenced by culture conditions. J Neurosci Res 37: 197-207

202. Shukla SD (1992) Platelet-activating factor receptor and signal transduction mechanisms. FASEB J 6: 2296-2301

203. Shukla SD, Paul A, Klachko DM (1992) Hypersensitivity of diabetic human platelets to platelet activating factor. Thromb Res 66: 239-246

204. Sidoti C, Principe P, Vandamme B, Broquet C, Braquet P (1992) Cytostatic activity of new synthetic anti-tumor aza-alkyllysophospholipids. Int J Cancer 51: 712-717

205. Simmonds NJ, Allen RE, Stevens TRJ, Van Someren RNM, Blake DR, Rampton DS (1992) Chemiluminescence assay of mucosal reactive oxygen metabolites in inflammatory bowel disease. Gastroenterology 103: 186-196

206. Sipka S, Koltai M, Braquet P, Szegedi G (1992) Histamine potentiates human platelet aggregation induced by platelet-activating factor. Int Arch Allergy Appl Immunol 97: 89-92

207. Smeyne RJ, Vendrell M, Hayward M, Baker SJ, Miao GG, Schilling K, Robertson LM, Curran T, Morgan JI (1993) Continuous c-fos *expression* precedes programed cell death in *vivo*. Nature 363: 166-169

208. Smith DM, Tran HM, Soo VW, McQuiston SA, Tartaglia LA, Goeddel DV, Epstein LB (1994) Enhanced synthesis of tumor necrosis factor-inducible proteins, plasminogen activator inhibitor-2, manganese superoxide dismutase, and protein 28/5.6, is selectively triggered by the 55-kDa tumor necrosis factor receptor in human melanoma cells. J Biol Chem 269: 9898-9905

209. Snyder F (1990) Platelet activating factor and related acetylated lipids as biologically active cellular mediators. Am J Physiol 259: C697-C708

210. Sobhani I, Hochlaf S, Denizot Y, Vissuzaine C, Rene E, Benveniste J, Lewin MMJ, Mignon M (1992) Raised concentrations of platelet activating factor in colonic mucosa of Crohn's disease patients. Gut 33: 1220-1225

211. Squinto SP, Block AL, Braquet P, Bazan NG (1989) Platelet-activating factor stimulates a fos/jun/AP-1 transcriptional signalling system in human neuroblastoma cells. J Neurosci 24: 558-566

212. Stoll LL, Denning GM, Kasner NA, Hunninghake GW (1994) Platelet-activating factor may stimulate both receptor-dependent and receptor-independent increases in [Ca2+] in human airway epithelial cells. J Biol Chem 269: 4254-4259

213. Sugatani J, Miwa M, Komiyama Y, Murakami T (1993) Quantitative analysis of platelet-activating factor in human plasma. Application to patients with liver cirrhosis and disseminated intravascular coagulation. J Immunol Methods 166: 251-261

214. Sugimoto T, Tsuchimochi H, McGregor CGA, Mutoh H, Shimizu T, Kurachi Y (1992) Molecular cloning and characterization of the platelet-activating factor receptor gene expressed in the human heart. Biochem Biophys Res Commun 189: 617-624

215. Takano T, Honda Z, Sakanaka C, Izumi T, Kameyama K, Haga K, Haga T, Kurokawa K, Shimizu T (1994) Role of cytoplasmic tail phosphorylation sites of platelet-activating factor receptor in agonist-induced desensitization. J Biol Chem 269: 22453-22458

216. Tanaka T, Iimori M, Tsukatani H, Tokumura A (1994) Platelet-aggregating effects of platelet-activating factor-like phospholipids formed by oxidation of phosphatidylcholines containing an sn-2-polyunsaturated fatty acyl group. Biochim Biophys Acta Lipids Lipid Metab 1210: 202-208

217. Tooyama I, Kawamata T, Akiyama H, Moestrup SK, Gliemann J, McGeer PL (1993) Immunohistochemical study of a2-macroglobulin receptor in Alzheimer and control postmortem human brain. Mol Chem Neuropathol 18: 153-157

218. Townsend GC, Scheld WM (1994) Platelet-activating factor augments meningeal inflammation elicited by Haemophilus influenzae lipooligosaccharide in an animal model of meningitis. Infect Immun 62: 3739-3744

219. Tran A, Vanhée D, Capron A, Vorng H, Braquet P, Joseph M (1992) Separate induction of human blood platelet aggregation or cytotoxicity by different concentrations of PAF-acether and thrombin. Agents Actions 36: 39-43

220. Travers JB, Li Q, Sprecher H, Fertel RH (1992) Binding of carbamyl-platelet-activating factor to the Raji lymphoblast

platelet-activating factor receptor. Int J Immunopharmacol 14: 515-523

221. Tripathi Y, Kandala J, Lim R, Shulka S (1991) Platelet activating factor induces expression of early response genes c-fos and TIS-1 in human epidermoid carcinoma A-431 cells. Life Sci 49: 1767-1769

222. Tripathi YB, Lim RW, Fernandez-Gallardo S, Kandala JC, Guntaka RV, Shukla SD (1992) Involvement of tyrosine kinase and protein kinase C in platelet- activating-factor-induced c-*fos* gene expression in A-431 cells. Biochem J 286: 527-533

223. Trochtenberg DS, Lefferts PL, King GA, Hwang YS, Christman BW, Snapper JR (1992) Effects of thromboxane synthase and cyclooxygenase inhibition on PAF-induced changes in lung function and arachidonic acid metabolism. Prostaglandins 44: 555-577

224. Ulvestad E, Williams K, Mork S, Antel J, Nyland H (1994) Phenotypic differences between human monocytes/macrophages and microglial cells studied in situ and in vitro. J Neuropathol Exp Neurol 53: 492-501

225. Vaekevae A, Laurila P, Meri S (1993) Co-deposition of clusterin with the complement membrane attack complex in myocardial infarction. Immunology 80: 177-182

226. Valone F (1987) Platelet-activating factor binding to specific cell membrane receptors. In: Snyder F (ed) Platelet-Activating Factor and Related Lipid Mediators. Plenum Press, New York, pp 137-152

227. Van der Bruggen T, Kok PTM, Raaijmakers JAM, Lammers JWJ, Koenderman L (1994) Cooperation between Fcgamma receptor II and complement receptor type 3 during activation of platelet-activating factor release by cytokine-primed human eosinophils. J Immunol 153: 2729-2737

228. Vedeler C, Ulvestad E, Grundt I, Conti G, Nyland H, Matre R, Pleasure D (1994) Fc receptor for IgG (FcR) on rat microglia. J Neuroimmunol 49: 19-24

229. Verbeek MM, Otte-Hoeller I, Westphal JR, Wesseling P, Ruiter DJ, De Waal RMW (1994) Accumulation of intercellular adhesion molecule-1 in senile plaques in brain tissue of patients with Alzheimer's disease. Am J Pathol 144: 104-116

230. Viac J, Gueniche A, Faure M, Claudy A (1993) Soluble intercellular adhesion molecule 1 (sICAM-1) and malignant melanoma. Cancer Lett 72: 191-194

231. Walker DG, McGeer PL (1992) Complement gene expression in human brain: Comparison between normal and Alzheimer's disease cases. Mol Brain Res 14: 109-116

232. Wang F, Naik UP, Ehrlich YH, Freyberg Z, Osada S, Ohno S, Kuroki T, Suzuki K, Kornecki E (1993) A new protein kinase C, nPKCeta', and nPKCø are expressed in human platelets: Involvement of nPKCeta' and nPKCø in signal transduction stimulated by PAF. Biochem Biophys Res Commun 191: 240-246

233. Warringa RAJ, Mengelers HJJ, Kuijper PHM, Raaijmakers JAM, Bruijnzeel PLB, Koenderman L (1992) In vivo priming of platelet-activating factor-induced eosinophil chemotaxis in allergic asthmatic individuals. Blood 79: 1836-1841

234. Weitzman S, Weitberg A, Clark E, Strossel T (1985) Phagocytes as carcinogens: malignant transformation by human neutrophils. Science 227: 1231-1233

235. Whawell SA, Scott-Coombes DM, Vipond MN, Tebbutt SJ, Thompson JN (1994) Tumour necrosis factor-mediated release of plasminogen activator inhibitor 1 by human peritoneal mesothelial cells. Br J Surg 81: 214-216

236. Williams AE, Lawson LJ, Perry VH, Fraser H (1994) Characterization of the microglial response in murine scrapie. Neuropathol Appl Neurobiol 20: 47-55

237. Yamamoto H, Nagata M, Tabe K, Kimura I, Kiuchi H, Sakamoto Y, Yamamoto K, Dohi Y (1993) The evidence of platelet activation in bronchial asthma. J Allergy Clin Immunol 91: 79-87

238. Yasuhara O, Aimi Y, McGeer EG, McGeer PL (1994) Expression of the complement membrane attack complex and its inhibitors in Pick disease brain. Brain Res 652: 346-349

239. Ye R, Prossnitz E, Zou A, Cochrane C (1991) Characterization of a human cDNA that encodes a functional receptor for platelet-activating factor. Biochem Biophys Res Commun 180: 105-111

240. Yee GM, Squires PM, Cejic SS, Kennedy TG (1993) Lipid mediators of implantation and decidualization. J Lipid Mediat 6: 525-534

241. Yoshida H, Satoh K, Imaizumi T (1992) Activity of platelet-activating factor acetylhydrolase exists in red cell membrane. Am J Hematol 40: 61-63

242. Yue T-L, Gu J-L, Feuerstein G (1992) Protein kinase C activator phorbol 12, 13-dibutyrate inhibits platelet activating factor-stimulated Ca2+ ^{m}obilization and phosphoinositide turnover in neurohybrid NG108-15 cells. Neurochem Res 17: 997-1004

243. Zarco P, Maestre C, Herrero-Beaumont G, González E, Garcia-Hoyo R, Navarro FJ, Braquet P, Egido J (1992) Involvement of platelet-activating factor and tumour necrosis factor in the pathogenesis of joint inflammation in rabbits. Clin Exp Immunol 88: 318-323

244. Zimmerman R, Cerutti P (1984) Active oxygen acts as a promoter of tranformation in mouse embryo C3H/10T1/2/C18 fibroblasts. Proc Natl Acad Sci 81: 2085-2087

Chapter III

1. Alexander-Williams J (1976) Inflammatory disease of the bowel. Dis Colon Rectum 19: 579-581

2. Argyris T, Slaga T (1981) Promotion of carcinomas by repeated abrasion in initiated skin of mouse. Cancer Res 41: 5193-5195

3. Bertrand R, Solary E, O'Connor P, Kohn KW, Pommier Y (1994) Induction of a common pathway of apoptosis by staurosporine. Exp Cell Res 211: 314-321

4. Catalán RE, Martínez AM, Aragonés MD, Garde E, Díaz G (1993) Platelet-activating factor stimulates protein kinase C translocation in cerebral microvessels. Biochem Biophys Res Commun 192: 446-451

5. Cerutti P, Trump B (1991) Inflammation and oxidative stress in carcinogenesis. Cancer Cells 3: 1-7

6. Chao W, Liu H, Hanahan DJ, Olson MS (1992) Platelet-activating factor-stimulated protein tyrosine phosphorylation and eicosanoid synthesis in rat Kupffer cells. Evidence for calcium-dependent and protein kinase C-dependent and -independent pathways. J Biol Chem 267: 6725-6735

7. Compere SJ, Baldacci PA, Sharpe AH, Jaenisch RJ (1989) Retroviral transduction of the human c-Ha-*ras* oncogene into midgestation mouse embryos promotes rapid epithelial hyperplasia. Mol Cell Biol 9: 6-14

8. Creasia D, Netteshim P (1975) Particulates and chronic inflammation increase rates of carcinogenesis. In: Karbe E, Parke J (eds) Experimental Lung Cancer. Springer Verlag, New York, pp 234-235

9. Denizot Y, Chaussade S (1994) Platelet activating factor and Crohn's disease. Gut 35: 141

10. Ferraris L, Karmeli F, Eliakim R, Klein J, Fiocchi C, Rachmilewitz D (1993) Intestinal epithelial cells contribute to the enhanced generation of platelet activating factor in ulcerative colitis. Gut 34: 665-668

11. Floyd R (1990) Role of oxygen free radicals in carcinogenesis and brain ischemia. FASEB 4: 2587-2597

12. Frenkel K (1992) Carcinogen-mediated oxidant formation and oxidative DNA damage. Pharmacol Ther 53: 127-166

13. Gandhi CR, DeBuysere MS, Olson MS (1992) Platelet-activating factor-mediated synthesis of prostaglandins in rat Kupffer cells. Biochim Biophys Acta Mol Cell Res 1136: 68-74

14. Gelbard HA, Nottet HSLM, Swindells S, Jett M, Dzenko KA, Genis P, White R, Wang L, Choi Y-B, Zhang D, Lipton SA, Tourtellotte WW, Epstein LG, Gendelman HE (1994) Platelet-activating factor: a candidate human immunodeficiency virus type 1-induced neurotoxin. J Virol 68: 4628-4635

15. Gomez-Cambronero J, Wang E, Johnson G, Huang C, Sha'afi R (1991) Platelet-activating factor induces tyrosine phosphorylation in human neutrophils. J Biol Chem 266: 6240-6245

16. Guenette RS, Daehlin L, Mooibroek M, Wong K, Tenniswood MPR (1994) Thanatogen expression during involution of the rat ventral prostate after castration. J Androl in press:

17. Haswell-Elkins MR, Satarug S, Elkins DB (1992) *Opisthorchis viverrini* infection in northeast Thailand and its relationship to cholangiocarcinoma. J Gastro Hepatol 7: 538-548

18. Heidelberger C (1977) Chemical oncogenesis in culture. Mutat Res 114: 283-291

19. McKormick, J.J. and Maher, V.M., Measurement of colony-forming ability and mutagenesis in diploid human cells. In E.C. Friedberg and P.C. Hanawalt (Eds.) DNA Repair, A Laboratory Manual of Research Procedures, Marcel Dekker, New York, 1981, pp. 501-522

20. Kerr JFR, Winterford CM, Harmon BV (1994) Apoptosis: Its significance in cancer and cancer therapy. Cancer 73: 2013-2026

21. Kerr JFR, Wyllie AH, Currie AR (1972) Apoptosis: A basic biological phenomenon with wide-ranging implications in tissue kinetics. Br J Cancer 26: 239-257

22. Maggi M, Bonaccorsi L, Finetti G, Carloni V, Muratori M, Laffi G, Forti G, Serio M, Baldi E (1994) Platelet-activating factor mediates an autocrine proliferative loop in the endometrial adenocarcinoma cell line HEC-1A. Cancer Res 54: 4777-4784

23. Montero A, Rodriguez-Barbero A, Lopez-Novoa JM (1993) A role for platelet-activating factor in endothelin-1-induced rat mesangial cell proliferation. Eur J Pharmacol 243: 235-240

24. Nishihira J, Ishibashi T, Takeichi N, Sakamoto W, Nakamura M (1994) A role for oxygen radicals in rat monocytic leukemia cell differentiation under stimulation with platelet-activating factor. Biochim Biophys Acta Mol Cell Res 1220: 286-290

25. O'Flaherty J, Redman J, Jacobson D, Rossi A (1990) Stimulation and priming of protein kinase C translocation by a Ca2+ transient-independent mechanism. J Biochem 265: 21619-21623

26. O'Flaherty J, Redman J, Schmitt J, Ellis J, Surles J, Marx M, Piantadosi C, Wykle R (1987) 1-O-alkyl-2-N-methylcarbamyl-glycerophsophocholine: a biologically potent, non-metabolizable analog of platelet-activating factor. Biochem Biophys Res Commun 147: 18-24

Cancer Res 54 Suppl: 1929s-1933s

31. Rosin MP, Saad El Din Zaki S, Ward AJ, Anwar WA (1994) Involvement of inflammatory reactions and elevated cell proliferation in the development of bladder cancer in schistosomiasis patients. Mutat Res Fundam Mol Mech Mutagen 305: 283-292

32. Shacter E, Beecham EJ, Covey JM, Kohn KW, Potter M (1988) Activated neutrophils induce prolonged DNA damage in neighbouring cells. Carcinogenesis 9: 2297-2304

33. Shukla SD (1992) Platelet-activating factor receptor and signal transduction mechanisms. FASEB J 6: 2296-2301

34. Singletary SE, Ames FC, Buzdar AU (1994) Management of inflammatory breast cancer. World J Surg 18: 87-92

35. Sobhani I, Hochlaf S, Denizot Y, Vissuzaine C, Rene E, Benveniste J, Lewin MMJ, Mignon M (1992) Raised concentrations of platelet activating factor in colonic mucosa of Crohn's disease patients. Gut 33: 1220-1225

36. Templeton AC (1975) Acquired diseases. In: Fraumeni JF (ed) Persons at high risk of cancer: an approach to cancer etiology and control. Academic Press, New York, pp 69-84f

37. Tenniswood MPR, Taillefer D, Latkins J, Guenette RS, Mooibroek M, Daehlin L, Welsh J (1994) Control of gene expression during apoptosis in hormone-dependent tissue. In: Tomei LD, Cope FO (eds) Apoptosis II. The molecular basis of cell death. Cold Spring Harbor Lab. Press, Cold Spring Harbor, NY, pp in press

38. Tripathi YB, Lim RW, Fernandez-Gallardo S, Kandala JC, Guntaka RV, Shukla SD (1992) Involvement of tyrosine kinase and protein kinase C in platelet- activating-factor-induced *c-fos* gene expression in A-431 cells. Biochem J 286: 527-533

39. Weitzman S, Weitberg A, Clark E, Strossel T (1985) Phagocytes as carcinogens: malignant transformation by human neutrophils. Science 227: 1231-1233

40. Wells XE, O'Neill C (1992) Biosynthesis of platelet-activating factor by two-cell mouse embryos. J Reprod Fertil 96: 61-71

41. Wilkinson D, Sandhu JK, Breneman JW, Tucker JD, Birnboim HC (1995) A transplantable murine tumour cell line containing an *hprt* marker gene for detection of *in vivo* clastogenic/mutagenic events. Br J Cancer (in press)

42. Wyllie AH, Kerr JFR, Currie AR (1980) Cell death: the significance of apoptosis . Int Rev Cytol 68: 251-306

43. Zimmerman R, Cerutti P (1984) Active oxygen acts as a promoter of tranformation in mouse embryo C3H/10T1/2/C18 fibroblasts. Proc Natl Acad Sci 81: 2085-2087

Chapter IV

1. Baldi E, Bonaccorsi L, Finetti G, Luconi M, Muratori M, Susini T, Forti G, Serio M, Maggi M (1994) Platelet-activating factor in human endometrium. J Steroid Biochem Mol Biol 49: 359-363

2. Birnboim HC (1988) Rapid extraction of high molecular weight RNA from cultured cells for Northern analysis. Nucleic Acids Res 16: 1487-1490

3. Birnboim HC (1992) Extraction of high molecular weight RNA and DNA from cultured mammalian cells. In: Wu R (ed) Methods in Enzymology. Academic Press Inc, San Diego, pp 154-160

4. Birnboim HC, Motora D, Liteplo RG (1989) Indomethacin shifts the peak of c-fos, EGR-1, and c-myc gene expression in

Chapter IV

1. Baldi E, Bonaccorsi L, Finetti G, Luconi M, Muratori M, Susini T, Forti G, Serio M, Maggi M (1994) Platelet-activating factor in human endometrium. J Steroid Biochem Mol Biol 49: 359-363

2. Birnboim HC (1988) Rapid extraction of high molecular weight RNA from cultured cells for Northern analysis. Nucleic Acids Res 16: 1487-1490

3. Birnboim HC (1992) Extraction of high molecular weight RNA and DNA from cultured mammalian cells. In: Wu R (ed) Methods in Enzymology. Academic Press Inc, San Diego, pp 154-160

4. Birnboim HC, Motora D, Liteplo RG (1989) Indomethacin shifts the peak of c-fos, EGR-1, and c-myc gene expression in confluent fibroblasts induced by phorbol myristate acetate. Biochem Biophys Res Commun 161: 508-513

5. Bito H, Honda Z, Nakamura M, Shimizu T (1994) Cloning, expression and tissue distribution of rat platelet-activating-factor-receptor cDNA. Eur J Biochem 221: 211-218

6. Bradford MM (1976) A rapid and sensitive method for the quantitation of microgram quanties of protein utilizing the principle of protein-dye binding. Anal Biochem 72: 248-254

7. Catalán RE, Martínez AM, Aragonés MD, Garde E, Díaz G (1993) Platelet-activating factor stimulates protein kinase C translocation in cerebral microvessels. Biochem Biophys Res Commun 192: 446-451

8. Chakravarthy B, Bussey A, Whitfield J, Sikorska M, Williams R, Durkin J (1991) The direct measurement of protein kinase C (PKC) activity in isolated membranes using a selective peptide substrate. Anal Biochem 196: 144-150

9. Chao W, Liu H, Hanahan DJ, Olson MS (1992) Protein tyrosine phosphorylation and regulation of the receptor for platelet-activating factor in rat Kupffer cells. Effect of sodium vanadate. Biochem J 288: 777-784

10. Chao W, Liu H, Hanahan DJ, Olson MS (1992) Platelet-activating factor-stimulated protein tyrosine phosphorylation and eicosanoid synthesis in rat Kupffer cells. Evidence for calcium-dependent and protein kinase C-dependent and -independent pathways. J Biol Chem 267: 6725-6735

11. Chen J-H, Birnboim HC (1993) Oligodeoxynucleotides capable of binding to GC-rich regions in DNA are inappropriately synthesized during random hexanucleotide-primed labelling reactions. DNA Cell Biol 12: 177-181

12. Dell' Albani P, Condorelli DF, Mudò G, Amico C, Bindoni M, Belluardo N (1993) Platelet-activating factor and its methoxy-analogue ET-18- OCH_3 stimulate immediate early gene expression in rat astroglial cultures. Neurochem Int 22: 567-574

13. Elstad MR, Parker CJ, Cowley FS, Wilcox LA, McIntyre TM, Prescott SM, Zimmerman GA (1994) CD11b/CD18 integrin and a Beta-glucan receptor act in concert to induce the synthesis of platelet-activating factor by monocytes. J Immunol 152: 220-230

14. Freeman SN, Rennie PS, Chao J, Lund LR, Andreasen PA (1990) Urokinase- and tissue-type plasminogen activators are supressed by cortisol in the involuting prostate of castrated rats. Biochem J 269: 189-194

15. Guenette RS, Daehlin L, Mooibroek M, Wong K, Tenniswood MPR (1994) Thanatogen expression during involution of the rat ventral prostate after castration. J Androl in press:

16. Herbert J-M (1992) Characterization of specific binding sites of ^{3}H-labelled platelet-activating factor ([^{3}H]PAF) and a new antagonist, [^{3}H]SR 27417, on guinea-pig tracheal epithelial cells. Biochem J 284: 201-206

21. Kuruvilla A, Putcha G, Poulos E, Shearer WT (1993) Tyrosine phosphorylation of phospholipase C concomitant with its activation by platelet-activating factor in a human B cell line. J Immunol 151: 637-648

22. Laemmli UK (1970) Cleavage of structural proteins during the assembly of the head of bacteriophage T4. Nature 227: 680-685

23. Maggi M, Bonaccorsi L, Finetti G, Carloni V, Muratori M, Laffi G, Forti G, Serio M, Baldi E (1994) Platelet-activating factor mediates an autocrine proliferative loop in the endometrial adenocarcinoma cell line HEC-1A. Cancer Res 54: 4777-4784

24. Marcheselli VL, Bazan NG (1994) Platelet-activating factor is a messenger in the electroconvulsive shock-induced transcriptional activation of c-fos and zif-268 in hippocampus. J Neurosci Res 37: 54-61

25. Mazer BD, Domenico J, Szepesi A, Lucas JJ, Gelfand EW (1994) Role for Ca2+ in expression of cell cycle regulated genes in PAF-stimulated cells. J Lipid Mediat 10: 269-281

26. Murphy CT, Kellie S, Westwick J (1993) Tyrosine-kinase activity in rabbit platelets stimulated with platelet-activating factor--The effect of inhibiting tyrosine kinase with genistein on platelet-signal-molecule elevation and functional responses. Eur J Biochem 216: 639-651

27. Mutoh H, Bito H, Minami M, Nakamura M, Honda Z, Izumi T, Nakata R, Kurachi Y, Terano A, Shimizu T (1993) Two different promoters direct expression of two distinct forms of mRNAs of human platelet-activating factor receptor. FEBS Lett 322: 129-134

28. Müller E, Dagenais P, Alami N, Rola-Pleszczynski M (1993) Identification and functional characterization of platelet-activating factor receptors in human leukocyte populations using polyclonal anti-peptide antibody. Proc Natl Acad Sci USA 90: 5818-5822

29. Narahara H, Nishioka Y, Johnston JM (1993) Secretion of platelet-activating factor acetylhydrolase by human decidual macrophages. J Clin Endocrinol Metab 77: 1258-1262

30. O'Flaherty J, Redman J, Jacobson D, Rossi A (1990) Stimulation and priming of protein kinase C translocation by a Ca2+ transient-independent mechanism. J Biochem 265: 21619-21623

31. Piechaczyk M, Blanchard JM, Marty L, Dani C, Panabieres F, Sabouty SE, Fort P, Jeanteur P (1984) Post-transcriptional regulation of glyceraldehyde-3-phosphate-dehydrogenase gene expression in rat tissues. Nucleic Acids Res 12: 6951-6963

32. Squinto SP, Block AL, Braquet P, Bazan NG (1989) Platelet-activating factor stimulates a fos/jun/AP-1 transcriptional signalling system in human neuroblastoma cells. J Neurosci 24: 558-566

33. Sugimoto T, Tsuchimochi H, McGregor CGA, Mutoh H, Shimizu T, Kurachi Y (1992) Molecular cloning and characterization of the platelet-activating factor receptor gene expressed in the human heart. Biochem Biophys Res Commun 189: 617-624

34. Thurston AW,Jr., Rhee SG, Shukla SD (1993) Role of guanine nucleotide-binding protein and tyrosine kinase in platelet-activating factor activation of phospholipase C in A431 cells: Proposal for dual mechanisms. J Pharmacol Exp Ther 266: 1106-1112

35. Towbin H, Staehelin T, Gordon J (1979) Electrophoretic transfer of proteins from polyacrylamide gels to nitrocellulose sheets: Procedure and some applications. Proc Natl Acad Sci USA 76: 4350-4354

36. Tripathi YB, Lim RW, Fernandez-Gallardo S, Kandala JC, Guntaka RV, Shukla SD (1992) Involvement of tyrosine

33. Sugimoto T, Tsuchimochi H, McGregor CGA, Mutoh H, Shimizu T, Kurachi Y (1992) Molecular cloning and characterization of the platelet-activating factor receptor gene expressed in the human heart. Biochem Biophys Res Commun 189: 617-624

34. Thurston AW,Jr., Rhee SG, Shukla SD (1993) Role of guanine nucleotide-binding protein and tyrosine kinase in platelet-activating factor activation of phospholipase C in A431 cells: Proposal for dual mechanisms. J Pharmacol Exp Ther 266: 1106-1112

35. Towbin H, Staehelin T, Gordon J (1979) Electrophoretic transfer of proteins from polyacrylamide gels to nitrocellulose sheets: Procedure and some applications. Proc Natl Acad Sci USA 76: 4350-4354

36. Tripathi YB, Lim RW, Fernandez-Gallardo S, Kandala JC, Guntaka RV, Shukla SD (1992) Involvement of tyrosine kinase and protein kinase C in platelet- activating-factor-induced *c-fos* gene expression in A-431 cells. Biochem J 286: 527-533

37. Van der Bruggen T, Kok PTM, Raaijmakers JAM, Lammers JWJ, Koenderman L (1994) Cooperation between Fcgamma receptor II and complement receptor type 3 during activation of platelet-activating factor release by cytokine-primed human eosinophils. J Immunol 153: 2729-2737

38. Wang F, Naik UP, Ehrlich YH, Freyberg Z, Osada S, Ohno S, Kuroki T, Suzuki K, Kornecki E (1993) A new protein kinase C, nPKCeta', and nPKCø are expressed in human platelets: Involvement of nPKCeta' and nPKCø in signal transduction stimulated by PAF. Biochem Biophys Res Commun 191: 240-246

39. Whawell SA, Scott-Coombes DM, Vipond MN, Tebbutt SJ, Thompson JN (1994) Tumour necrosis factor-mediated release of plasminogen activator inhibitor 1 by human peritoneal mesothelial cells. Br J Surg 81: 214-216

40. Wong P, Pineault JM, Taillefer D, Leger JG, Wang C, Tenniswood MPR (1993) Genomic organization and expression of the rat and human TRPN-2 genes. J Biol Chem 268: 5021-5031

41. Ye R, Prossnitz E, Zou A, Cochrane C (1991) Characterization of a human cDNA that encodes a functional receptor for platelet-activating factor. Biochem Biophys Res Commun 180: 105-111

Chapter V

1. Alessi DR, Smythe C, Keyse SM (1993) The human CL100 gene encodes a Tyr/Thr-protein phosphatase which potently and specifically inactivates MAP kinase and suppresses its activation by oncogenic ras in Xenopus oocyte extracts. Oncogene 8: 2015-2020

2. Baron HM, Bobrisheva IV, Varshaver NB (1992) The activated human c-Ha-*ras*-1 oncogene as a mutagen. Cancer Genet Cytogenet 62: 15-20

3. Bazan HEP, Tao Y, Bazan NG (1993) Platelet-activating factor induces collagenase expression in corneal epithelial cells. Proc Natl Acad Sci USA 90: 8678-8682

4. Birnboim HC (1983) A rapid alkaline extraction method for the isolation of plasmid DNA. Methods Enzymol 100B: 243-255

5. Birnboim HC (1992) Extraction of high molecular weight RNA and DNA from cultured mammalian cells. In: Wu R (ed) Methods in Enzymology. Academic Press Inc, San Diego, pp 154-160

6. Bresser J, Doering J, Gillespie D (1983) Quick blot: selective mRNA or DNA imobilization from whole cells. DNA 2: 243-254

7. Cheley S, Anderson R (1984) A reproducible microanalytical method for the detection of specific RNA sequences by dot-

12. Ferraris L, Karmeli F, Eliakim R, Klein J, Fiocchi C, Rachmilewitz D (1993) Intestinal epithelial cells contribute to the enhanced generation of platelet activating factor in ulcerative colitis. Gut 34: 665-668

13. Franklin RA, Mazer B, Sawami H, Mills GB, Terada N, Lucas JJ, Gelfand EW (1993) Platelet-activating factor triggers the phosphorylation and activation of MAP-2 kinase and S6 peptide kinase activity in human B cell lines. J Immunol 151: 1802-1810

14. Fujiwara T, Grimm EA, Mukhopadhyay T, Cai DW, Owen-Schaub LB, Roth JA (1993) A retroviral wild-type p53 expression vector penetrates human lung cancer spheroids and inhibits growth by inducing apoptosis. Cancer Res 53: 4129-4133

15. Gelbard HA, Nottet HSLM, Swindells S, Jett M, Dzenko KA, Genis P, White R, Wang L, Choi Y-B, Zhang D, Lipton SA, Tourtellotte WW, Epstein LG, Gendelman HE (1994) Platelet-activating factor: a candidate human immunodeficiency virus type 1-induced neurotoxin. J Virol 68: 4628-4635

16. Gonen B, Kahana O, Witz IP (1992) In vivo tumorigenicity and in vitro sensitivity to tumor- necrosis-factor† mediated killing of c-Ha-*ras*-transformed cells. Cancer Immunol Immunother 35: 388-394

17. Gonos ES, Spandidos DA (1993) Oncogenes in cellular immortalisation and differentiation (*Review*). Anticancer Res 13: 1117-1122

18. Gordon LL, Weitzman S (1988) The respiratory burst and carinogenesis. In: Sbarra AJ, Strauss RR (eds) The Respiratory Burst and Its Physiological Significance. Plenum, New York, pp 277-298

19. Honda Z, Takano T, Gotoh Y, Nishida E, Ito K, Shimizu T (1994) Transfected platelet-activating factor receptor activates mitogen-activated protein (MAP) kinase and MAP kinase kinase in Chinese hamster ovary cells. J Biol Chem 269: 2307-2315

20. Hunter T (1991) Cooperation between oncogenes. Cell 64: 249-270

21. Iwamoto Y, Reich R, Nemeth G, Yamada Y, Martin GR (1993) Cyclic AMP decreases chemotaxis, invasiveness and lung colonization of H-ras transformed mouse fibroblasts. Clin Exp Metastasis 11: 492-501

22. Khosravi-Far R, Der CJ (1994) The Ras signal transduction pathway. Cancer Metastasis Rev 13: 67-89

23. Maggi M, Bonaccorsi L, Finetti G, Carloni V, Muratori M, Laffi G, Forti G, Serio M, Baldi E (1994) Platelet-activating factor mediates an autocrine proliferative loop in the endometrial adenocarcinoma cell line HEC-1A. Cancer Res 54: 4777-4784

24. Manser T, Gefter ML (1984) Isolation of hybridomas expressing a specific heavy chain variable region gene segment by using a screing technique that detects mRNA sequences in whole cell lysates. Proc Natl Acad Sci USA 81: 2470-2474

25. McCormick F (1993) How receptors turn ras on. Nature 363: 15-16

26. McLachlin JR, Mittereder N, Daucher MB, Kadan M, Eglitis MA (1993) Factors affecting retroviral vector function and structural integrity. Virology 195: 1-5

27. Nishikawa K, Rotbein J, Vijjeswarapu D, Owen-Schaub L, Rosenblum MG, Donato NJ (1994) Positive and negative selection for tumor necrosis factor responsiveness reveals an inhibitory role for EGF receptor in TNF-induced antiproliferation. Lymphokine Cytokine Res 13: 37-45

28. Oldfield EH, Ram Z, Culver kW, Blaese RM, DeVroom HL, Anderson WF (1993) Gene therapy for the treatment of brain tumours using intra-tumoural transduction with thymidine kinase gene and intravenous ganciclovir. Hum Gene Ther

using a screing technique that detects mRNA sequences in whole cell lysates. Proc Natl Acad Sci USA 81: 2470-2474

25. McCormick F (1993) How receptors turn ras on. Nature 363: 15-16

26. McLachlin JR, Mittereder N, Daucher MB, Kadan M, Eglitis MA (1993) Factors affecting retroviral vector function and structural integrity. Virology 195: 1-5

27. Nishikawa K, Rotbein J, Vijjeswarapu D, Owen-Schaub L, Rosenblum MG, Donato NJ (1994) Positive and negative selection for tumor necrosis factor responsiveness reveals an inhibitory role for EGF receptor in TNF-induced antiproliferation. Lymphokine Cytokine Res 13: 37-45

28. Oldfield EH, Ram Z, Culver kW, Blaese RM, DeVroom HL, Anderson WF (1993) Gene therapy for the treatment of brain tumours using intra-tumoural transduction with thymidine kinase gene and intravenous ganciclovir. Hum Gene Ther 4: 39-69

29. Piechaczyk M, Blanchard JM, Marty L, Dani C, Panabieres F, Sabouty SE, Fort P, Jeanteur P (1984) Post-transcriptional regulation of glyceraldehyde-3-phosphate-dehydrogenase gene expression in rat tissues. Nucleic Acids Res 12: 6951-6963

30. Rosin MP, Anwar WA, Ward AJ (1994) Inflammation, chromosomal instability, and cancer: The schistosomiasis model. Cancer Res 54 Suppl: 1929s-1933s

31. Samiei M, Sanghera JS, Pelech SL (1993) Activation of myelin basic protein and S6 peptide kinases in phorbol ester- and PAF-treated sheep platelets. Biochim Biophys Acta Mol Cell Res 1176: 287-298

32. Shih A, Weinberg R (1982) Isolation of a transforming sequence from a human bladder carcinoma cell line. Cell 29: 161-169

33. Sobhani I, Hochlaf S, Denizot Y, Vissuzaine C, Rene E, Benveniste J, Lewin MMJ, Mignon M (1992) Raised concentrations of platelet activating factor in colonic mucosa of Crohn's disease patients. Gut 33: 1220-1225

34. Southern PJ, Berg P, Jeanteur P (1982) Transformation of mammalian cells to antiobiotic resistance with a bacterial gene under control of the SV40 early region promotor. J Molec Appl Genet 1: 327-341

35. Takano T, Honda Z, Sakanaka C, Izumi T, Kameyama K, Haga K, Haga T, Kurokawa K, Shimizu T (1994) Role of cytoplasmic tail phosphorylation sites of platelet-activating factor receptor in agonist-induced desensitization. J Biol Chem 269: 22453-22458

36. Thomas PS (1983) Hybridization of denatured RNA transferred or dotted to nitrocellulose paper. Methods Enzymol 100: 255-266

37. Thompson J, Gillespie D (1987) Molecular hybridization with RNA probes in concentrated solutions of guanidine thiocyanate. Anal Biochem 163: 281-291

38. Tolsma SS, Cohen JD, Ehrlich LS, Bouck NP (1993) Transformation of NIH/3T3 to anchorage independence by H- *ras* is accompanied by loss of suppressor activity. Exp Cell Res 205: 232-239

39. Tordai A, Franklin RA, Johnson C, Mazer BD, Clay KL, Gelfand EW (1994) Autocrine stimulation of B lymphocytes by a platelet-activating factor receptor agonist, 1-palmitoyl-2-acetoyl-sn-glycero-3-phosphoch line. J Immunol 152: 566-573

40. Varela-Echavarria A, Prorock CM, Ron Y, Dougherty JP (1993) High rate of genetic rearrangement during replication of a Moloney murine leukemia virus-based vector. J Virol 67: 6357-6364

Periodic acid Schiff (PAS)-positive granular structures increase in the brain of senescence accelerated mouse (SAM). Acta Neuropathol 72: 124-129

2. Akiyama H, Kawamata T, Yamada T, Tooyama I, Ishii T, McGeer PL (1993) Expression of intercellular adhesion molecule (ICAM)-1 by a subset of astrocytes in Alzheimer disease and some other degenerative neurological disorders. Acta Neuropathol 85: 628-634

3. Bazan NG, Zorumski CF, Clark GD (1993) The activation of phospholipase A_2 and release of arachidonic acid and other lipid mediators at the synapse: The role of platelet-activating factor. J Lipid Mediat 6: 421-427

4. Ben-Ari Y (1983) The role of seizures in kainic acid induced brain damage. In: Fuxe K, Roberts P, Schwartz R (eds) Excitotoxins: Wenner Gren International Symposium. Macmillan Press, London, pp 184-198

5. Ben-Ari Y, Tremblay EP, Ottersen OP, Meldrum BS (1980) The role of epileptic activity in hippocampus and 'remote' cerebral lesions induced by kainic acid. Brain Res 191: 79-97

6. Bito H, Nakamura M, Honda Z, Izumi T, Iwatsubo T, Seyama Y, Ogura A, Kudo Y, Shimizu T (1992) Platelet-activating factor (PAF) receptor in rat brain: PAF mobilizes intracellular Ca^{2+} in hippocampal neurons. Neuron 9: 285-294

7. Cajal RS, Glanes A, Martinez A, Saenz E, Gutierrez M (1974) Lafora's Disease: An ultrastructural and histochemical study. Acta Neuropathol 30: 189-196

8. Chau L-Y, Hu C-Y, Chang W-T, Hsu Y-S (1992) Possible existence of two subsets of platelet-activating factor receptor to mediate polyphosphoinositide breakdown and calcium influx in neuroblastoma x glioma hybrid NG 108- 15 cells. J Neurochem 59: 1090-1098

9. Chau LY, Peck K, Yen HH, Wang JY (1994) Agonist-induced down-regulation of platelet-activating factor receptor gene expression in U937 cells. Biochem J 301: 911-916

10. Clark GD, Happel LT, Zorumski CF, Bazan NG (1992) Enhancement of hippocampal excitatory synaptic transmission by platelet-activating factor. Neuron 9: 1211-1216

11. Clark M, Post RM, Weiss SRB, Nakajima T (1992) Expression of c-fos mRNA in acute and kindled cocaine seizures in rats. Brain Res 582: 101-106

12. Culling, CFA (1974) Handbook of Histopathological Techniques and Histochemistry. Thomas Burton, London

13. Danik M, Chabot J-G, Mercier C, Benabid A-L, Chauvin C, Quirion R, Suh M (1991) Human gliomas and epileptic foci express high levels of a mRNA related to rat testicular sulfated glycoprotein-2, a purported marker of cell death. Proc Natl Acad Sci USA 88: 8577-8581

14. Danik M, Chabot JG, Hassan-Gonzalez D, Suh M, Quirion R (1993) Localization of sulfated glycoprotein-2/clusterin mRNA in the rat brain by in situ hybridization. J Comp Neurol 334: 209-227

15. Daval J-L, Nakajima T, Gleiter CH, Post RM, Marangos PJ (1989) Mouse brain c-fos mRNA distribution following a single electroconvulsive shock. J Neurochem 52: 1954-1957

16. Dawson R,Jr., Wallace DR (1992) Kainic acid-induced seizures in aged rats: Neurochemical correlates. Brain Res Bull 29: 459-468

17. deLeon GA (1974) Bielschowsky bodies: Lafora-like inclusions associated with atrophy of the lateral pallidum. Acta Neuropathol 30: 183-188

express high levels of a mRNA related to rat testicular sulfated glycoprotein-2, a purported marker of cell death. Proc Natl Acad Sci USA 88: 8577-8581

14. Danik M, Chabot JG, Hassan-Gonzalez D, Suh M, Quirion R (1993) Localization of sulfated glycoprotein-2/clusterin mRNA in the rat brain by in situ hybridization. J Comp Neurol 334: 209-227

15. Daval J-L, Nakajima T, Gleiter CH, Post RM, Marangos PJ (1989) Mouse brain c-fos mRNA distribution following a single electroconvulsive shock. J Neurochem 52: 1954-1957

16. Dawson R,Jr., Wallace DR (1992) Kainic acid-induced seizures in aged rats: Neurochemical correlates. Brain Res Bull 29: 459-468

17. deLeon GA (1974) Bielschowsky bodies: Lafora-like inclusions associated with atrophy of the lateral pallidum. Acta Neuropathol 30: 183-188

18. Doly M, Cluzel J, Millerin M, Bonhomme B, Braquet P (1993) Prevention of chloroquine-induced electroretinographic damage by a new platelet-activating factor antagonist, BN 50730. Ophthalmic Res 25: 314-318

19. Duman RS, Craig JS, Winston SM, Deutch AY, Hernandez TD (1992) Amygdala kindling potentiates seizure-stimulated immediate- early gene expression in rat cerebral cortex. J Neurochem 59: 1753-1760

20. El Azzouzi B, Jurgens P, Benveniste J, Thomas Y (1993) Immunoregulatory functions of PAF-acether. IX. Modulation of apoptosis in an immature T cell line. Biochem Biophys Res Commun 190: 320-324

21. Forno LS, Langston JW (1993) Lewy bodies and aging: Relation to Alzheimer's and Parkinson's diseases. Neurodegeneration 2: 19-24

22. Gass P, Herdegen T, Bravo R, Kiessling M (1992) Induction of immediate early gene encoded proteins in the rat hippocampus after bicuculline-induced seizures: Differential expression of KROX-24, FOS and JUN proteins. Neuroscience 48: 315-324

23. Gass P, Herdegen T, Bravo R, Kiessling M (1993) Spatiotemporal induction of immediate early genes in the rat brain after limbic seizures: Effects of NMDA receptor antagonist MK-801. Eur J Neurosci 5: 933-943

24. Guenette RS, Daehlin L, Mooibroek M, Wong K, Tenniswood MPR (1994) Thanatogen expression during involution of the rat ventral prostate after castration. J Androl in press:

25. Guth L, Dempsey PJ (1970) Mechanisms controlling glycogen levels in injured brain, normal brain, liver and heart. Exp Neurol 29: 152-161

26. Hattori M, Adachi H, Tsujimoto M, Arai H, Inoue K (1994) Miller-Dieker lissencephaly gene encodes a subunit of brain platelet-activating factor acetylhydrolases. Nature 370: 216-218

27. Herdegen T, Sandkühler J, Gass P, Kiessling M, Bravo R, Zimmermann M (1993) JUN, FOS, KROX, and CREB transcription factor proteins in the rat cortex: Basal expression and induction by spreading depression and epileptic seizures. J Comp Neurol 333: 271-288

28. Kalaria RN (1993) The immunopathology of Alzheimer's disease and some related disorders. Pathology 13367: 12336-13105

29. Kalaria RN, Grahovac I (1990) Serum amyloid P immunoreactivity in hippocampal tangles, plaques and vessels: Implications for leakage across the blood-brain barrier in Alzheimer's disease. Brain Res 516: 349-353

neuropathological correlates. Brain Res 218: 299-318

36. Lustig HS, Chan J, Greenberg DA (1992) Comparative neurotoxic potential of glutamate, endothelins, and platelet-activating factor in cerebral cortical cultures. Neurosci Lett 139: 15-18

37. Mann DM, Sumpter PQ, Davies CA, Yates PO (1987) Glycogen accumulates in the cerebral cortex in Alzheimer's disease. Acta Neuropathol 73: 181-185

38. Marcheselli VL, Bazan NG (1994) Platelet-activating factor is a messenger in the electroconvulsive shock-induced transcriptional activation of c-fos and zif-268 in hippocampus. J Neurosci Res 37: 54-61

39. May PC, Lambert-Etchells M, Johnson SA, Poirier J, Masters JN, Finch CE (1990) Dynamics of gene expression for a hippocampal glycoprotein elevated in Alzheimer's disease and in response to experimental lesion in rat. Neuron 5: 831-839

40. McGeer PL, Akiyama H, Itagaki S, McGeer EG (1989) Immune system response in Alzheimer's Disease. Can J Neurol Sci 16: 516-527

41. McIntyre D, Nathanson D, Edson N (1982) A new model for partial status epilepticus based on kindling. Brain Res 250: 53-63

42. McKeith I, Fairbairn A, Briel R, Harrison R, Tasker N (1993) Lewy bodies and Alzheimer's disease. Br J Psychiatry 163: 262-263

43. Nadler JV, Cuthbertson GJ (1980) Kainic acid neurotoxicity toward hippocampal formation: Dependence on specific excitatory pathways. Brain Res 195: 47-56

44. Nakamura M, Honda Z, Matsumoto T, Noma M, Shimizu T (1993) Isolation and properties of platelet-activating factor receptor cDNAs. J Lipid Mediat 6: 163-168

45. O'Flaherty JT, Jacobson DP, Redman JF (1992) Regulation of platelet-activating-factor receptors and the desensitization response in polymorphonuclear neutrophils. Biochem J 288: 241-248

46. O'Shaughnessy D, Gerber GJ (1986) Damage induced by systemic kainic acid in rats is dependent upon seizure activity - A behavioral and morphological study. Neurotoxicol 7: 187-202

47. Ogawa M, Araki M, Nagatsu I, Yoshida M (1989) Astroglial cell alteration caused by neurotoxin: Immunohistochemical observations with antibodies to glial fibrillary acidic protein, laminin, and tyrosine hydroxylase. Exp Neurol 106: 187-196

48. Pasinetti GM, Johnson SA, Oda T, Rozovsky I, Finch CE (1994) Clusterin (SGP-2): A multifunctional glycoprotein with regional expression in astrocytes and neurons of the adult rat brain. J Comp Neurol 339: 387-400

49. Paulus W, Jellinger K (1993) Comparison of integrin adhesion molecules expressed by primary brain lymphomas and nodal lymphomas. Acta Neuropathol 86: 360-364

50. Pollard H, Cantagrel S, Charriaut-Marlangue C, Moreau J, Ben-Ari Y (1994) Apoptosis associated DNA fragmentation in epileptic brain damage. Neuroreport 5: 1053-1055

51. Popovici T, Represa A, Crépel V, Barbin G, Beaudoin M, Ben-Ari Y (1990) Effects of kainic acid-induced seizures and ischemia on c-*fos*- like proteins in rat brain. Brain Res 536: 183-194

52. Powell HC, Ward HW, Garrett RS, Orloff MJ, Lampert PW (1979) Glycogen accumulation in the nerves and kidney of chronically diabetic rats. J Neuropath Exp Neurol 38: 114-127

observations with antibodies to glial fibrillary acidic protein, laminin, and tyrosine hydroxylase. Exp Neurol 106: 187-196

48. Pasinetti GM, Johnson SA, Oda T, Rozovsky I, Finch CE (1994) Clusterin (SGP-2): A multifunctional glycoprotein with regional expression in astrocytes and neurons of the adult rat brain. J Comp Neurol 339: 387-400

49. Paulus W, Jellinger K (1993) Comparison of integrin adhesion molecules expressed by primary brain lymphomas and nodal lymphomas. Acta Neuropathol 86: 360-364

50. Pollard H, Cantagrel S, Charriaut-Marlangue C, Moreau J, Ben-Ari Y (1994) Apoptosis associated DNA fragmentation in epileptic brain damage. Neuroreport 5: 1053-1055

51. Popovici T, Represa A, Crépel V, Barbin G, Beaudoin M, Ben-Ari Y (1990) Effects of kainic acid-induced seizures and ischemia on c-*fos*- like proteins in rat brain. Brain Res 536: 183-194

52. Powell HC, Ward HW, Garrett RS, Orloff MJ, Lampert PW (1979) Glycogen accumulation in the nerves and kidney of chronically diabetic rats. J Neuropath Exp Neurol 38: 114-127

53. Prehn JHM, Krieglstein J (1993) Platelet-activating factor antagonists reduce excitotoxic damage in cultured neurons from embryonic chick telencephalon and protect the rat hippocampus and neocortex from ischemic injury in vivo. J Neurosci Res 34: 179-188

54. Rieckmann P, Nünke K, Burchhardt M, Albrecht M, Wiltfang J, Ulrich M, Felgenhauer K (1993) Soluble intercellular adhesion molecule-1 in cerebrospinal fluid: An indicator for the inflammatory impairment of the blood-cerebrospinal fluid barrier. J Neuroimmunol 47: 133-140

55. Schluesener HJ, Meyermann R (1993) Intercrines in brain pathology. Expression of intercrines in a multiple sclerosis and Morbus Creutzfeldt-Jakob lesion. Acta Neuropathol 86: 393-396

56. Schmidt-Kastner R, Meller D, Bellander B-M, Strömberg I, Olson L, Ingvar M (1993) A one-step immunohistochemical method for detection of blood- brain barrier disturbances for immunoglobulins in lesioned rat brain with special reference to false-positive labelling in immunohistochemistry. J Neurosci Methods 46: 121-132

57. Smeyne RJ, Vendrell M, Hayward M, Baker SJ, Miao GG, Schilling K, Robertson LM, Curran T, Morgan JI (1993) Continuous c-*fos* expression precedes programed cell death *in vivo*. Nature 363: 166-169

58. Sperk G, Lassman H, Baran H, Seitelberger F, Hornikiewicz O (1985) Kainic acid-induced seizures: Dose-relationship of behavioural, neurochemical, and histopathological changes. Brain Res 338: 289-295

59. Squinto SP, Block AL, Braquet P, Bazan NG (1989) Platelet-activating factor stimulates a fos/jun/AP-1 transcriptional signalling system in human neuroblastoma cells. J Neurosci 24: 558-566

60. Sugatani J, Miwa M, Komiyama Y, Murakami T (1993) Quantitative analysis of platelet-activating factor in human plasma. Application to patients with liver cirrhosis and disseminated intravascular coagulation. J Immunol Methods 166: 251-261

61. Suzuki K, David E, Kutschman B (1971) Presenile dementia with "Lafora-like" intraneuronal inclusions. Arch Neurol 25: 69-80

62. Suzuki Y, Akiyama K, Suu S (1978) Lafora-like inclusion bodies in the CNS of aged dogs. Acta Neuropathol 44: 217-222

63. Suzuki Y, Kamiya S, Ohta K, Suu S (1979) Lafora-like bodies in a cat. Acta Neuropathol 48: 55-58

Chapter VII

1. Barr RM, Lawlor F, Judge MR, Courtney P, Barlow R, Kobza Black A, Mallet AI, Greaves MW (1993) Platelet activating factor, lyso-platelet activating factor and arachidonic acid release in normal human skin and the influence of topical steroid treatment. Br J Clin Pharmacol 35: 637-641

2. Bazan HEP, Tao Y, Bazan NG (1993) Platelet-activating factor induces collagenase expression in corneal epithelial cells. Proc Natl Acad Sci USA 90: 8678-8682

3. Braquet P, Pignol B, Maisonnet T, Mencia-Heurta J (1991) Platelet-activating factor modulates interleukin-2 production by mouse fibroblasts. Int Arch Appl Immunol 94: 165-166

4. Chau L-Y, Hu C-Y, Chang W-T, Hsu Y-S (1992) Possible existence of two subsets of platelet-activating factor receptor to mediate polyphosphoinositide breakdown and calcium influx in neuroblastoma x glioma hybrid NG 108- 15 cells. J Neurochem 59: 1090-1098

5. Clark GD, Happel LT, Zorumski CF, Bazan NG (1992) Enhancement of hippocampal excitatory synaptic transmission by platelet-activating factor. Neuron 9: 1211-1216

6. Ferraris L, Karmeli F, Eliakim R, Klein J, Fiocchi C, Rachmilewitz D (1993) Intestinal epithelial cells contribute to the enhanced generation of platelet activating factor in ulcerative colitis. Gut 34: 665-668

7. Herbert J-M (1992) Characterization of specific binding sites of ^{3}H-labelled platelet-activating factor ([^{3}H]PAF) and a new antagonist, [^{3}H]SR 27417, on guinea-pig tracheal epithelial cells. Biochem J 284: 201-206

8. Hunyadi J, Kenderessy AS, Duda E, Braquet P, Dobozy A (1993) Platelet-activating factor antagonists (BN 52021 and BN 50730) inhibit tumor necrosis factor-alfa-mediated cytotoxicity on murine L929 tumor cells. Mol Immunol 30: 517-519

9. Inoue H, Ganbo T, Hisamatsu K, Ishida H (1993) Study on the metabolism of lyso-platelet activating factor (lyso-PAF) in human paranasal sinus mucosa. The cultured ciliated epithelium can convert lyso-PAF to PAF. Life Sci 52: PL227-PL232

10. Kald B, Boll RM, Gustafson-Svaerd C, Sjoedahl R, Tagesson C (1994) Phospholipase C from Clostridium perfringens stimulates acetyltransferase-dependent formation of platelet-activating factor in cultured intestinal epithelial cells (INT 407). Scand J Gastroenterol 29: 243-247

11. Kinnula VL, Adler KB, Ackley NJ, Crapo JD (1992) Release of reactive oxygen species by guinea pig tracheal epithelial cells in vitro. Am J Physiol Lung Cell Mol Physiol 262: L708-L712

12. Kornecki E, Ehrlich YH (1988) Neuroregulatory and neuropathological actions of the ether-phospholipid platelet activating factor. Science 240: 1792-1794

13. Lustig HS, Chan J, Greenberg DA (1992) Comparative neurotoxic potential of glutamate, endothelins, and platelet-activating factor in cerebral cortical cultures. Neurosci Lett 139: 15-18

14. Madden MC, Smith JP, Dailey LA, Friedman M (1994) Polarized release of lipid mediators derived from phospholipase A2 activity in a human bronchial cell line. Prostaglandins 48: 197

15. Maggi M, Bonaccorsi L, Finetti G, Carloni V, Muratori M, Laffi G, Forti G, Serio M, Baldi E (1994) Platelet-activating factor mediates an autocrine proliferative loop in the endometrial adenocarcinoma cell line HEC-1A. Cancer Res 54: 4777-4784

11. Kinnula VL, Adler KB, Ackley NJ, Crapo JD (1992) Release of reactive oxygen species by guinea pig tracheal epithelial cells in vitro. Am J Physiol Lung Cell Mol Physiol 262: L708-L712

12. Kornecki E, Ehrlich YH (1988) Neuroregulatory and neuropathological actions of the ether-phospholipid platelet activating factor. Science 240: 1792-1794

13. Lustig HS, Chan J, Greenberg DA (1992) Comparative neurotoxic potential of glutamate, endothelins, and platelet-activating factor in cerebral cortical cultures. Neurosci Lett 139: 15-18

14. Madden MC, Smith JP, Dailey LA, Friedman M (1994) Polarized release of lipid mediators derived from phospholipase A2 activity in a human bronchial cell line. Prostaglandins 48: 197

15. Maggi M, Bonaccorsi L, Finetti G, Carloni V, Muratori M, Laffi G, Forti G, Serio M, Baldi E (1994) Platelet-activating factor mediates an autocrine proliferative loop in the endometrial adenocarcinoma cell line HEC-1A. Cancer Res 54: 4777-4784

16. Powell DW (1992) Epithelial secretory responses to inflammation: Platelet activating factor and reactive oxygen metabolites. Ann NY Acad Sci 664: 232-247

17. Thurston AW,Jr., Rhee SG, Shukla SD (1993) Role of guanine nucleotide-binding protein and tyrosine kinase in platelet-activating factor activation of phospholipase C in A431 cells: Proposal for dual mechanisms. J Pharmacol Exp Ther 266: 1106-1112

18. Tooyama I, Kawamata T, Akiyama H, Moestrup SK, Gliemann J, McGeer PL (1993) Immunohistochemical study of α2-macroglobulin receptor in Alzheimer and control postmortem human brain. Mol Chem Neuropathol 18: 153-157

19. Tripathi YB, Lim RW, Fernandez-Gallardo S, Kandala JC, Guntaka RV, Shukla SD (1992) Involvement of tyrosine kinase and protein kinase C in platelet- activating-factor-induced *c-fos* gene expression in A-431 cells. Biochem J 286: 527-533

20. Wong B, Tang W, Ziboh VA (1992) Identification of a membrane-associated 1-0-alkyl-2-arachidonoyl- *sn*-glycero-3-phosphocholine hydrolyzing phospholipase A_2 in guinea pig 1 epidermis: Implications in the cutaneous biosynthesis of platelet-activating factor. FEBS Lett 305: 213-216

21. Yue T-L, Gu J-L, Feuerstein G (1992) Protein kinase C activator phorbol 12, 13-dibutyrate inhibits platelet activating factor-stimulated Ca^{2+} mobilization and phosphoinositide turnover in neurohybrid NG108-15 cells. Neurochem Res 17: 997-1004

STEFFANY A.L. BENNETT

EDUCATION

B.A. Honours (Psychology)
Carleton University, Ottawa, Ontario, Canada, 1988

M.Sc. (Neuroscience Specialization)
Carleton University, Ottawa, Ontario, Canada, 1989

Ph.D. (Biochemistry)
University of Ottawa, Ottawa, Ontario, Canada, 1995

EMPLOYMENT

Research Assistant, Cognitive Psychology (Lab: Dr. Lise Paquet)
Department of Psychology, Carleton University, Ottawa, Ontario, Canada
1987-1989

Teaching Assistant, Introduction to Psychology (Course: 49:100)
Department of Psychology, Carleton University, Ottawa, Ontario, Canada
1988-1989

Sessional Lecturer, Neuroanatomy/Neurophysiology (Course: PYS5160)
Faculty of Medicine, University of Ottawa, Ottawa, Ontario, Canada
1989-1993

Post-Doctoral Research Fellow (Lab: Dr Martin P.R. Tenniswood)
Molecular Biology and Biochemistry Core Facility, W. Alton Jones Cell
Science Center, Lake Placid, NY, USA, 1995-pres.

PROFESSIONAL TRAINING/ RESEARCH PROJECTS

- 1987-1989 *Investigation of neurochemical and behavioural indices underlying self-administration of drugs of abuse*

  M.Sc. and B.A.Hon. Thesis Research, Supervisor: Dr. D.C.S. Roberts (Life Sciences, Carleton University, Ottawa, Ontario, Canada)

- 1989-1990 *Neuroanatomical and immunohistochemical investigation of the tuberomamillary nucleus in diseased brain*

  Ph.D. Thesis Research, Supervisor: Dr. W. Staines (Dept. of Anatomy and Neurobiology, University of Ottawa, Ottawa, Ontario, Canada)

- 1991 (Dec) *Research Training: Primary Human Cell Explantation*

  Supervisor: Dr. L Germain (Dept. of Surgery, Laval University, Quebec City, Quebec, Canada)

- 1989-1994 *Development of an animal model of progressive neurodegeneration and chronic cerebral inflammation*

  Collaborative research project with Drs. D.C.S. Roberts (Life Sciences, Carleton University, Ottawa, Ontario, Canada) and Dr. W. Staines (Dept. of Anatomy and Neurobiology, University of Ottawa, Ottawa, Ontario, Canada)

- 1990-1995 *The endogenous inflammatory phospholipid, platelet activating factor, mediates tumour progression and neurodegeneration*

  Ph.D. Thesis Research, Supervisor: Dr. H.C. Birnboim (Depts. of Biochemistry and Microbiology, University of Ottawa and Dept. of Exp. Oncology, Ottawa Regional Cancer Centre, Ottawa, Ontario, Canada)

- 1994-pres. *In vivo exposure to chronic inflammation induces a neoplastic phenotype in cell explants derived from patients with Graves Disease. An examination of underlying signal transduction events.*

  Collaborative research project with Dr. T. Smith (Dept. of Biochemistry and Mol. Bio., Albany Medical College, Albany, New York, USA)

- 1995-pres. *Cerebral immune and inflammatory responses in progressive neurodegenerative disorders: Role of endogenous pro-inflammatory phospholipid ligands in the regulation of cerebral complement*

  Post-doctoral fellowship in the laboratory of Dr. M. Tenniswood (W. Alton Jones Cell Science Centre, Lake Placid, New York, USA). Part of a collaborative research project with Dr. D.C.S. Roberts (Life Sciences, Carleton University, Ottawa, Ontario, Canada)

ARGRAVES/Bruce/DAN?

ADMINISTRATIVE EXPERIENCE

- 1988-1989 Designed course requirements for students in the joint University of Ottawa/Carleton University Neuroscience Specialization as a member of the Curriculum Evaluation Committee. Department of Psychology, Carleton University, Ottawa, Ontario, Canada

- 1993-1994 Created 1994-1996 graduate student curriculum requirements and seminar series format as a member of the Curriculum Review Committee. Department of Biochemistry, University of Ottawa, Ottawa, Ontario, Canada

- 1990-1995 Supervised Biochemistry undergraduate and medical students as senior graduate student in laboratory of Dr. H.C. Birnboim. Department of Biochemistry, University of Ottawa, Ottawa, Ontario, Canada

- 1994-1995 Acted as scientific liason between Department of Biochemistry, University of Ottawa and Henry Munro Middle School, Carleton Board of Education designing projects and scientific curriculum and giving seminars in conjunction with staff and students

- 1995-pres Supervised of Biochemistry graduate students as post-doctoral fellow in laboratory of Dr. M. Tenniswood, W. Alton Jones Cell Science Centre, Lake Placid, NY, USA.

- 1995-pres Established protein analysis program and subsequent personnel training in laboratory of Dr. D.C.S. Roberts, Life Sciences, Carleton University, Ottawa, Ontario, Canada

AWARDS

Ontario Scholar, 1984; Award for Excellence, 1984; F.W. Baldwin Scholarship, 1985; Carleton In-Course Scholarship, 1985; Ottawa Ladies College Scholarship, 1985; Dr. F.W.C. Mohr Scholarship, 1986; NSERC Undergraduate Research Scholarship, 1987-1988; R.A. Wendt Book Prize, 1988; Senate Medal for Academic Achievement, 1988; Ontario Graduate Studentship, 1988-1989; Epstein Award for Outstanding Research, 1989; University of Ottawa Research Scholarship, 1989-1994; Medical Research Council Studentship, 1989-1994;

W. Alton Jones Cell Science Center Post-Doctoral Fellowship, 1995-pres.

REFERENCES

Dr. H. Chaim Birnboim, M.Sc., M.D., F.R.C.P.
Dept. of Exp. Oncology, Ottawa Regional Cancer Centre, General Division, 501 Smyth Rd., Ottawa, Ontario, Canada K1H 8L6 tel: (613) 737-6701 fax: (613) 737-6745

Dr. David C.S. Roberts, Ph.D.
Dept. of Life Sciences, Carleton University, 1125 Colonel By Drive, Ottawa, Ontario, Canada, K1S 5B6 tel: (613) 788-2600 ext 7495 fax: (613) 788-4052

Dr. Martin P.R. Tenniswood, Ph.D., Director of Molecular Biology Core Facility
Alton Jones Cell Science Centre, 10 Old Barn Rd., Lake Placid, New York, USA 12946-1099 tel: (518) 523-1273 fax: (518) 523-1849

PUBLICATIONS

Refereed papers, published or in press

Roberts DCS, Bennett SAL, Vickers GJ (1989) The estrous cycle affects cocaine self-administration on a progressive ratio schedule in rats. Psychopharmacol 98: 401-411

Bennett SAL, Birnboim HC (1991) Induction of a novel glycosidase activity in *ras*-transformed rat embryo fibroblasts by treatment with platelet activating factor. J Glycoconjugate 8: 189

Roberts DCS, Bennett SAL (1993) Heroin self-administration in rats under a progressive ratio schedule of reinforcement. Psychopharmacology (Berl) 111: 215-218

Bennett SAL, Leite LCC, Birnboim HC (1993) Platelet activating factor, an endogenous mediator of inflammation, induces phenotypic transformation of rat embryo cells. Carcinogenesis 14: 1289-1296

Bennett SAL, Birnboim HC (1993) Platelet activating factor (PAF) induces phenotypic transformation in RECs but reduces *in vitro* malignant characteristics of *ras*-transformed RECs. FASEB J 7: A1294

De Vouge MW, Yamazaki A, Bennett SAL, Chen JH, Shwed PS, Couture C, Birnboim HC (1994) Immunoselection of GRP94/endoplasmin from a KNRK cell-specific lambdagt11 library using antibodies directed against a putative heparanase amino-terminal peptide. Int J Cancer 56: 286-294

Bennett SAL, Chen JH, Birnboim HC (1994) Recovery of a rare clone from a population of unstable retroviral vector-expressing mammalian cells using a new RNA extraction and slot-blot protocol. J Virol Methods 50:245-255.

Bennett SAL, Birnboim HC (1995) Platelet activating factor induces a transformed phenotype in human fibroblasts. In: Parke J (ed) Advances in Prostaglandin, Thromboxane and Leukotriene Research. Raven Press, New York pp. 467-470.

Bennett SAL, Stevenson B, Staines W, Roberts DCS (1995) Accumulation of pathological periodic acid schiff (PAS)-positive depositions in cerebrum following kainic acid-induced seizures: Relationship to c-fos induction, neuronal necrosis, reactive gliosis, and blood-brain barrier breakdown. Acta Neuropathol 89: 126-138.

Refereed papers, submitted

Bennett SAL, Birnboim HC (1995) Platelet activating factor activates protein kinase C and induces *fos* mRNA expression in rodent embryo cells. J Cell Biol (in review)

Bennett SAL, Birnboim HC (1995) Malignant transformation of human fibroblasts induced by platelet activating factor is mediated by PAF receptor, protein kinase C, and tyrosine kinase. Int. J. Cancer (in review)

Abstracts, published

Bennett SAL, Vickers GJ, Roberts DCS (1988) Gender and estrous cycle affect cocaine self-administration on a progressive ratio schedule of reinforcement. Soc Neurosci Abstr 15: 268.7 (Toronto, Canada, poster presentation)

Roberts DCS, Bennett SAL (1989) Qualitative differences between heroin and cocaine self-administration behaviour revealed by progressive ratio schedules of reinforcement. Soc Neurosci Abstr 16: 253.8 (Phoenix, USA, poster presentation)

Bennett SAL, Staines W, Roberts DCS (1989) Characterization of cell degeneration, blood-brain barrier disruption, and brain glycogen deposition following intraperitoneal administration of kainic acid. Soc Neurosci Abstr 16: 770 (Phoenix, USA, poster presentation)

Roberts DCS, Bennett SAL (1990) Heroin self-administration on a progressive ratio schedule of reinforcement: Effect of dose manipulation, naltrexone pretreatment and saline substitution. Soc Neurosci Abstr 17: 311.22 (Phoenix, USA, poster presentation)

Bennett SAL, Birnboim HC (1991) Treatment of *ras-transfected* rat embryo cells with platelet activating factor induces a novel glycosidase activity. 34th Annual Meeting Canadian Federation of Biological Societies 34: 102 (Kingston, Canada, poster presentation)

Bennett SAL, Birnboim HC (1992) Platelet activating factor induces a transformed phenotype in primary rat embryo cells. 8th International Conference on Prostaglandins and Related Compounds 8: 152 (Montreal, Canada, poster presentation)

Bennett SAL, Birnboim HC (1994) Brief exposure to platelet activating factor induces phenotypic transformation of human fibroblasts. 9th International Conference on Prostaglandins and Related Compounds 9: 8 (Florence, Italy, slide presentation)

Bennett SAL, Staines W, Roberts DCS, Tenniswood MPR (1994) Clusterin expression following

kainic acid-induced seizures: Relationship to progressive neurodegeneration, c-*fos* induction, platelet activating factor receptor expression, and blood-brain barrier breakdown. The Second Clusterin Workshop, p. 40. (Couer D'Alene, USA, slide presentation)

Abstracts, pending

Bennett, SAL, Tenniswood, MPR, and Roberts, DCS. (1995) Chronic upregulation of platelet activating factor is associated with clusterin expression, apoptosis, and neurodegeneration in rat brain following kainic acid-induced seizures. Soc Neurosci Abstr 22 (San Diego, USA, slide presentation)

Invited speaker presentations

Development of a malignant phenotype in rat embryo fibroblasts following treatment with PAF- and TPA- activated granulocytes. National Cancer Institute Annual Oncology Course, McMaster Univ., Hamilton, Canada, June 1990.

Careers in Science, Career Day Seminar, Henry Munro Public School, April 1993

Accumulation of PAS-D-positive aberrant carbohydrates in chronic neurodegeneration. Department of Life Sciences Seminar Series, Carleton Univ., Ottawa, Canada, May 1994.